Implication of mitochondrial dynamics and kynurenine pathway in cardioprotection after myocardial infarction

Rima Kamel

UNIVERSITE BIOLOGIE BRETAGNE SANTE LOIRE

université angers

THESE DE DOCTORAT DE

L'UNIVERSITE D'ANGERS
COMUE UNIVERSITE BRETAGNE LOIRE

ECOLE DOCTORALE N° 605
Biologie Santé
Spécialité : « *Physiologie, Physiopathologie, Biologie Systémique Médicale* »

Par
« Rima KAMEL »

« Implication de la dynamique mitochondriale et de la voie de la kynurénine dans la cardioprotection au cours de l'infarctus du myocarde »

Thèse présentée et soutenue à Angers, le 27 septembre 2019
Unité de recherche : UMR CNRS 6015 Inserm U1083
Thèse N° : 181231

Rapporteurs avant soutenance :

Dr. Stéphanie Barrère-Lemaire, Directeur de Recherche 2 CNRS, IGF UMR 5203, Montpellier, France

Pr. Luc Bertrand, Maître de Recherche FNRS et Professeur Extraordinaire, Louvain, Belgique

Composition du Jury :

Dr. Delphine Baetz, Maîtres de Conférences Universitaire, Inserm U1060 INRA U1397, Lyon, France

Dr. Naig Gueguen, Ingénieur de Recherche, UMR CNRS 6015 Inserm U1083, Angers, France

Pr. Fabrice Prunier, PU-PH, UMR CNRS 6015 Inserm U1083, Angers, France; directeur de thèse

Dr. Sophie Tamareille, Ingénieur d'Etudes, UMR CNRS 6015 Inserm U1083, Angers, France; Co-encadrant de thèse

Invité

Pr. Christian Legros, Professeur des universités, UMR CNRS 6015 Inserm U1083, Angers, France

ENGAGEMENT DE NON PLAGIAT

Je, soussignée Rima Kamel
déclare être pleinement conscient(e) que le plagiat de documents ou d'une partie d'un document publiée sur toutes formes de support, y compris l'internet, constitue une violation des droits d'auteur ainsi qu'une fraude caractérisée.
En conséquence, je m'engage à citer toutes les sources que j'ai utilisées pour écrire ce rapport ou mémoire.

signé par l'étudiante le / /

Cet engagement de non plagiat doit être signé et joint à tous les rapports, dossiers, mémoires.

Présidence de l'université
40 rue de rennes – BP 73532
49035 Angers cedex
Tél. 02 41 96 23 23 | Fax 02 41 96 23 00

université angers

To my Grandmother, whom I lost two years ago and to my Parents…

Acknowledgements

Firstly, I would like to express my sincere appreciation to my thesis director Prof. Fabrice Prunier who provided me with an opportunity to join his team. Without his support, it would not have been possible to obtain this degree.

Secondly, I would like to also express my sincere gratitude to my advisor Dr. Sophie Tamareille for the continuous support of my PhD study, for her patience, motivation, and knowledge. Your guidance helped me in all the time of research and writing of this thesis.

Besides my advisors, I would like to thank my thesis committee members. I look forward to hearing your insightful comments, but also the hard questions which will make me widen my research from various perspectives.

Dr. Stéphanie Barrère-Lemaire, I am honored that a successful scientist like yourself is reporting my thesis work.

Prof. Luc Bertrand, I am also much honored that a renowned researcher with your accomplishments will evaluate my thesis work.

Prof. Christian Legros, I would like to thank you for accepting to being a member of this thesis jury. I look forward to having a fruitful discussion about my work in your presence. And I would also like to thank you for giving me the opportunity to teach. You made me discover another thing that I am passionate about.

Dr. Naig Gueguen, I have always admired the researcher that you are. I am thankful that you accepted my invitation to take part of this committee. I thank you for the patience you have showed me and the knowledge that you taught me.

Dr. Delphine Baetz, I had the pleasure to meet you in person and work in collaboration with you. I am very delighted that you are going to examine my work and surely give me your best insights.

Dr. Daniel Henrion, director of the laboratory, thank you for giving me access to the laboratory and research facilities, for all the discussions and your continuous presence.

Prof. Bijan Ghaleh and Dr. Guy Lenaers, thank you evaluating my progress on a yearly basis. Your helpful insights and comments were extremely appreciated.

Prof. Delphien Prunier, thank you for advising me during my Master 2 and for your continuous help.

My thanks also go to Prof. Laurent Macchi, Prof. Pascal Reynier for all the fruitful discussions and for.

To Sophie, on a less formal note. Even though, you were technically my boss, we never acted on that basis. You were always someone that I would never hesitate in telling them exactly what is on my mind. You always told me that the only reason why you pushed me so far is because you can see all of my potential. Your ways were not always the most pleasant ones, but with a certain recession, they are what made me acknowledge my mistakes, work on my weak points and aspire to be a better researcher. I truly thank you for all the encouragement, all the, exclusively, constructive criticism, and every time you re-assured me that everything was going to be okay and that it is not the end of the world! Sophie, I will truly miss working with you.

To Justine, thank you for all the technical help, correcting my French but most importantly, thank you for all your food recommendations.

To Oussama, thank you for the laughs and fun we had while you were doing your PhD.

To Laura, thank you for advising me during my master 2.

To Aglae, I am truly disappointed that I did not get to work more with you; you are an extremely nice person bringing only positive vibes to this lab.

To Mathilde, Yoan, Emilie, Anne-Laure, Agnes, Louis, Jordan, Abigaelle, Linda, Cyril, Claire, César, Hélène, Céline, Laurent, my fellow lab mates. I thank you for the stimulating discussions and for all the fun we had in the last four years.

To Carole, thank you for being such a kind person and for always being so helpful and available.

To all the members of the SCAHU, especially Jérôme, Pierre, Elodie, Adeline, Laurent, thank you for all your help and your constant availability.

To Elodie, Maeva, Zenouba, Valentine, Joohee, Coralynne, Pauline, you made these years much more pleasant with your presence and your energy.

To Layale, Zaynoun, and Berna, I know that each of us went their separate way, but every time we talk it is like nothing changed. I hope that you will accomplish all your dreams (I can't wait to finally see you defending your thesis) and have the best future I know you deserve.

To Khalil, thank you for always being my friend and for your constant re-assuring calls.

To Michel for all the encouragement especially that we were going through the same rough patch!

To Camélia, your so very positive energy was a real support.

To Laura, my childhood friend, I hope I can be there for you when you will be accomplishing your dreams like you are here for me now.

To Elisia, we consistently talked every day. I always knew your daily problems just like you knew mine. I appreciate our friendship so much and love how well we know each other even with all the distance. You always understood my sad moments and were joyous in my happy ones. I can't wait for all the fun we will have after all of this is done.

To Nay, my Paris and travel friend. Even though, we fought every two minutes each time I saw you (Nescafe always come first, I get it!), I would never forget all the laughs (and sometimes cries) we had in Paris and Italy and Belgium and... Thank you for being my friend and for always being there for me. These years were so much better knowing I had someone who understood me and would never get tired of listening.

To Moe, you were a true friend who stood by me and I wish you nothing but the best in your life.

To Ali, Mirvana, Zaher, and Mirna thank you for all the distracting moments, for all the outings, for all the games, for everytime you made me feel more at home.

To Ahmad, I think we started on the wrong foot with me being a bit too bossy but things became quite well afterwards. I sometimes even laugh at your jokes! I really appreciate the friendship that we have, all the discussions and the laughs. You are a really good person and I am very happy to call you a friend.

To Charbel and Jacynthe, you only came to the lab this year, but with your presence and energy you made me less stressed and we had so much fun together.

To Samar, you are my gym buddy even though gym was no longer a priority in the last couple of months. You were my insta buddy, my foodie lover buddy, shopping buddy, selfie buddy... In fact, you were my buddy in many things, we had so much fun together, and you made these years fly by with your very much appreciated presence in my life.

To Cyrielle, little did I know that my fellow master 2 would become such an important person in my life. It was that summer that we spent in the biochemistry lab that got us so much closer. We had so much fun, and told each other a lot of things (the lab was probably not the best place to discuss such kind of things but why not). You were the person that showed me vulnerability but also strength. You believed in me and never failed to tell me your exact opinion of everything that I did. You always encouraged me to reach my very best potential. Thank you for every time you were there and of being the amazing friend that you are.

To Louwana, you were the ear that would never get sick of hearing me nag about the same thing over and over and over again. You were my shoulder to cry on in hard times. I had so much fun scaring you, staying late in the lab with you, guessing name songs, having some very interesting philosophic existential conversations. You taught me a lot of things and I don't know how these years could have gone by without you. You became family for me here in France. All of these times are precious memories that I could never forget. I truly hope you accomplish all of your dreams and I will always wish you nothing but the best. "la ekher l 3omer"

Cyrielle and Louwana, my desk buddies, I am going to miss you so much…

To Georges, even though things have changed, nothing I say will express my gratitude for your support and the importance you had in the leading to this moment….

To all my family members, my uncles (Joseph, Antoine, Elias, Doumit), my aunts (Dolly, Rita, Patricia, Carina, Malake), thank you all for your support, I love you.

To my cousins: Bouchra, Sam, Jérôme, Gautier, Marilynn and Joe, I look forward to seeing your bright future, I wish you all the luck in the world.

To my cousin Joseph, thank you for all the distracting moments, and your support during the hard times (I promise you I will try my best to not break another leg when I come to live in Paris). To Sarah, technically you are my cousin, but you are my sister, my friend and my family. I am so lucky I grew up having a role model like you. You are smart, funny and compassionate. You never failed to be the one I go to every time missing my family became too much. I love you.

To my grandmother, it was the most devastating news that I heard here. You were the one who taught me how to be kind, gentle, warm hearted, and how to appreciate all the small things in life. I miss you and I know you are always watching over me.

To all the people that I unfortunately could have forgotten to mention…

Last but surely not the least, to my most precious blessing, to my support system, my family: my parents and my brother. Thank you for supporting me throughout this thesis in all its ups and downs and my life in general. I would not be standing here without your presence in my life. I owe you everything that I have accomplished. Thank you for all the video calls, all the pep talks, all the encouragement in all its ways, but most importantly thank you for all the delicious food that surely helped during the writing of this thesis. I truly hope I can make you proud of me as much as I am proud to call you my family. I love you immensely.

Table of Contents

List of figures **1**

List of tables **5**

List of abbreviations **6**

General Introduction **9**

Literature overview **12**

Chapter 1: Myocardial ischemia/reperfusion injury and cardioprotection *13*

1. Myocardial infarction *14*
1.1. Epidemiology and treatment 14

2. Myocardial ischemia/reperfusion injuries *14*
2.1. Definition 14
2.2. Mechanisms 15

3. Cardioprotective strategies *17*
3.1. Definition and classification 17
3.2. Conditioning 19
3.2.1. Ischemic conditioning 20
3.2.2. Pharmacological conditioning 21
3.3. Signaling molecules and pathways 21

Chapter 2:Mitochondria and mitochondrial dynamics *24*

1. The mitochondrion *25*
1.1. Generalities 25
1.2. Main functions 25
1.2.1. Oxidative phosphorylation 26
1.2.2. Oxidative stress 27
1.2.3. Apoptosis and necrosis 29

2. Mitochondrial network *30*
2.1. Definition 30
2.2. Mitochondrial fission 32
2.2.1. Dynamin related protein (DRP1) 32
2.2.2. DRP1 receptors 34
2.2.3. Mechanism of mitochondrial fission 35
2.2.4. Mitochondrial autophagy (mitophagy) 36
2.3. Mitochondrial fusion 39
2.3.1. Mitofusines 1 and 2 (MFN 1, 2) 39
2.3.2. Optic atrophy factor 1 (OPA1) 41
2.3.3. Mechanism of mitochondrial fusion 42

3. Mitochondrial dynamics in the heart *43*
3.1. DRP1 in cardiomyocytes 45
3.2. OPA1 in cardiomyocytes 45
3.3. Mitochondrial dynamics and myocardial ischemia/reperfusion injuries 47
3.3.1. DRP1 and ischemia/reperfusion injuries 47
3.3.2. OPA1 and ischemia/reperfusion injuries 48

Chapter 3:The Kynurenine pathway *50*

1. Tryptophan : an essential amino acid *51*

2. Metabolic pathways of tryptophan ... *51*
2.1. Serotonin pathway ... 51
2.2. Kynurenine pathway ... 52
2.2.1. Characteristics of major enzymes of the kynurenine pathway ... 55
2.2.2. Kynurenine pathway metabolites ... 56
a) Kynurenine ... 56
b) Kynurenic acid ... 57
N-methyl-D-aspartate (NMDA) receptors ... 58
G-protein coupled receptor 35 (GPR35) ... 59
Aryl hydrocarbon receptor (AhR) ... 60
c) Quinolinic acid ... 61
2.2.3. NAD^+ synthesis ... 61
a) NAD^+ and sirtuins ... 62
2.2.4. Kynurenine pathway and mitochondria ... 63
2.2.5. Kynurenine pathway and ischemia/reperfusion injuries ... 64
a) Cerebral ischemia/reperfusion injuries ... 65
b) Myocardial ischemia/reperfusion injuries ... 66

Aim of the thesis ... 68

Materials and methods ... 70

1. Animal Ethics ... *71*

2. Animal experiments ... *71*
2.1. Echocardioghraphy ... 71
2.2. *In vivo* ischemia/reperfusion experiments and infarct size assessment ... 71
2.2.1. Mice model ... 71
2.2.2. Rat model ... 72
2.3. Tissue Sampling and preparation ... 73

3. Protein expression analysis ... *73*
3.1. Protein extraction ... 73
3.2. Western Blot ... 73

4. Gene expression analysis ... *74*
4.1. RNA extraction ... 74
4.2. Reverse transcription ... 74
4.3. qPCR ... 74

5. Mitochondrial morphology analysis by electron microscopy ... *75*

6. Statistics ... *75*

Results ... 76

Part 1:Mitochondrial dynamics and ischemia/reperfusion injuries ... *77*

1. Study N°1: DRP1 haploinsufficiency attenuates cardiac ischemia reperfusion injuries ... *78*
1.1. Scientific background ... 79
1.2. Article N°1 ... 80

2. Study N°2: Cardiac characterization of a $Drp1^{+/-}$ $Opa1^{+/-}$ deficient mouse model ... *100*
2.1. Scientific background ... 101
2.2. Materials and methods ... 102
2.2.1. Mouse model ... 102
2.2.2. Mitochondrial morphology by transmission electron microscopy ... 102
2.2.3. Statistics ... 102
2.3. Results study N°2 ... 103

2.4. Discussion 109

3. Conclusion 113

Part 2:Kynurenine pathway metabolites mediate cardioprotection 114

1. Study N°3: Kynurenic acid reduces myocardial ischemia/reperfusion injuries by activating antioxidant defense and mitophagy 115

1.1. Scientific background 116
1.2. Article N°2 117
1.3. Supplementary results 143

2. Study N°4: Kynurenine mediates cardioprotection in acute myocardial infarction 145

2.1. Scientific background 146
2.2. Materials and methods 147
2.2.1. *In vitro* H9C2 hypoxia/reoxygenation 147
2.2.2. Animal studies 147
2.2.3. Myocardial ischemia/reperfusion rat model 147
2.2.4. Acetylated protein profile 148
2.2.5. Statistics 148
2.3. Results 149
2.4. Discussion 157

3. Conclusion 161

GENERAL discussion 162

Conclusion and perspectives 167

Annexes 169

1. Increase in Cardiac Ischemia-Reperfusion Injuries in Opa1$^{+/-}$ mouse model 170

2. Tryptophane-Kynurenine pathway in the remote ischemic conditioning mechanism 190

References 219

List of figures

Figure 1: Myocardial ischemia/reperfusion injuries in final myocardial infarct size. 15

Figure 2: Mechanisms underlying ischemia/reperfusion injuries in cardiomyocytes 17

Figure 3: Different categories of cardioprotective modalities aiming to reduce myocardial reperfusion injuries 19

Figure 4: Schematic representation of different types of conditioning depending on time and type of application. 20

Figure 5: Schematic representation of mitochondrial function inside of a cell 26

Figure 6: Schematic representation of the mitochondrial respiratory chain complexes 27

Figure 7: Representation of reactions catalyzed by Superoxide dismutase (SOD), catalase (CAT), glutathione peroxidase (GPX) and peroxiredoxin (PRX) enzymes to neutralize the toxic oxygen radical 28

Figure 8: Mitochondria's implication in apoptosis and necrosis pathways. 30

Figure 9: Spectrum of mitochondrial morphologies in fibroblast 31

Figure 10: Role of mitochondrial fusion (MFN1, MFN2, OPA1) and fission (DRP1, hFIS1, MFF, MiD49/51) proteins in cellular mechanisms 32

Figure 11: DRP1 protein structure and post-translational modifications by mentioned proteins 33

Figure 12: Mitochondrial fission regulation in mammals due to DRP1's interaction with its different receptors 35

Figure 13: Mitochondrial fission process in mammals. 36

Figure 14: Schematic representation of autophagy process 37

Figure 15: Different pathways of mitophagy inside a cell. 39

Figure 16: Mitofusins structure and post-translational modification sites with arrows indicating proteins potentially implicated in these modifications in cardiomyocytes 40

Figure 17: Schematic presentation of OPA1 protein structure 41

Figure 18: Schematic Illustration of mammalian mitochondrial fusion 43

Figure 19: Electron microscopy image depicting mitochondrial populations inside a cardiomyocyte. 44

Figure 20: The serotonin pathway to metabolize tryptophan into serotonin and further along into melatonin 52

Figure 21: Tryptophan metabolic pathways 54

Figure 22: Different effects and actions of kynurenic acid inside and outside the nervous system 58

Figure 23: Structure and activation of the N-methyl-D-aspartate (NMDA) receptor formed of two subunits: NR1 and NR2 59

Figure 24: Endogenously ($G_{12/13}$, $G_{i/0}$) used signaling pathways by GPR35 60

Figure 25: NAD^+ synthesis: salvage and *de novo* pathways; and NAD^+ consummers 62

Figure 26: Sirtuins mechanism of action in deacetylating proteins using NAD^+ as a co-factor liberating nicotinamide 63

Figure 27: Graphical abstract of a study depicting mechanism of kynurenic acid-mediated cardioprotection 67

Figure 28: Anatomical characteristics and heart function of 3-month-old *Drp1*$^{+/-}$ *Opa1*$^{+/-}$ (n=8-10) and their wild type littermate (WT) mice (n=5-10). (A) Body weight (BW). (B) Heart weight over body weight (HW/BW) ratio. (C) Left ventricular weight over heart weight (LVW/HW). (D) Cardiac echocardiography, left: Left ventricle end-systolic volume (LVESD), middle: LV end-diastolic volume (LVEDD), right: LV fractional shortening (FS). 103

Figure 29: Mitochondrial morphology. (A) Representative electron microscopy (EM) images of left ventricle longitudinal sections at baseline in WT and mice. Scale bar: 1 µm. (B) Left: mitochondrial frequency represented according to the quartile distribution of the mitochondrial area. Right: the number of mitochondria per field. WT (n=2068) *Drp1*$^{+/-}$ *Opa1*$^{+/-}$ (n=1208). Data are represented as median [min;max]. 104

Figure 30: Mitochondrial dynamics protein expression. OPA1, MFN2, DRP1, and FIS1 expression assessed by means of western blotting (n=9-10/group). Immunoblots and histograms represented quantifications and GAPDH was used as a loading control. Values are expressed as mean ± SEM. ns= not significant, ** p=0.01, ***p<0.001. 105

Figure 31: Mitochondrial respiratory chain complexes and PGC1α protein expression assessed by means of western blotting (n=9-10/group). Immunoblots and histograms represented quantifications and GAPDH was used as a loading control. Values are expressed as mean ± SEM. ns= not significant. 106

Figure 32: Representative immunoblot and quantification of autophagy proteins. Autophagy protein expression levels were assessed by means of western blot in quantitative analysis of LC3-I and LC3-II, p62 and PARK2 in *Drp1*$^{+/-}$ *Opa1*$^{+/-}$ and WT mice. The results are expressed as ratios of protein band densities to GAPDH or ratio of LC3-II/LC3-I (n=9-10 per group). Values are mean ± SEM. ns=not significant, *p<0.05 107

Figure 33: Histograms on the left showing quantification of area at risk (AAR) as a percentage of the total left ventricle (LV) and on the right area necrosis (AN) as a percentage of AAR (n=6-7/group). ns=not significant. 108

Figure 34: Histograms showing (A) relative mortality and (B) percentage of cells with conserved mitochondrial membrane potential of control cells, that did not undergo hypoxia/reoxygenation (H/R), and cells that underwent H/R either vehicle (DMSO) or KYNA-treated (10µM). Treatment was performed either 10 min before hypoxia in DMEM medium (pre), or pre + during hypoxia (per), or pre + per + during reoxygenation (post) (n=3-9); Values are expressed as mean±SEM; * p<0.05, ***p<0.001. 143

Figure 35: Representative immunoblots and histograms quantification of protein expression for p-GSK3β, GSK3β, p-STAT3 and STAT3 in non-ischemic (sham), ischemic + vehicle (MI), and

ischemic + KYNA (MI+KYNA) left ventricle samples after 15 min of reperfusion (n=6-11). GAPDH was used as loading control. Values are expressed as mean ± SEM. *** p<0.001..... 144

Figure 36: Schematic representation of *in vivo* and *in vitro* experiments and groups. (A) *In vitro*: H9C2 control cells underwent no intervention, cells from the hypoxia/reoygenation (H/R) groups were submitted to 4h 50 min of hypoxia followed by 2 hours of reoxygenation and were either treated with vehicle (DMSO) or with KYN (0.1 or 1 μM) 10 min before hypoxia (pre), or before and during hypoxia (pre+per), or before, during and after hypoxia (pre+per+post). Cell death quantification (n=3-8) as well as mitochondrial membrane potential (n=3-9) were performed 2 hours after reoxygenation. (B) *In vivo*: Sham animals underwent no injection and no left anterior descending coronary artery (LAD) ligation, MI group underwent 40 min of ischemia followed by 2 hours of reperfusion. 10 min before coronary artery occlusion vehicle NaOH (1M) or KYN (150mg/Kg) was administrated intraperitoneally. Infarct size assessment using 2,3,5-triphenyltetrazolium chloride (TTC) staining after 2 hours of reperfusion, tissue sampling was performed after either 15 min or 2 hours of reperfusion. 149

Figure 37: Histograms showing (A) relative mortality and (B) percentage of cells with conserved mitochondrial membrane potential of control (CT) cells, that did not undergo hypoxia/reoxygenation (H/R), and cells that underwent H/R either vehicle (DMSO) or KYN (0.1 or 1μM)-treated. Treatment was performed either 10 min before hypoxia in DMEM medium (pre), or pre + during hypoxia (per), or pre + per + during reoxygenation (post) (n=3-9); Values are expressed as mean±SEM; * p<0.05, ***p<0.001. 150

Figure 38: Histograms showing area at risk (AAR) as a percentage of the total left ventricle (LV) and area of necrosis (AN) as a percentage of AAR in left ventricle samples after 2 hours of reperfusion (n=6-8/group); Values are expressed as mean±SEM; * p<0.05. 150

Figure 39: Representative immunoblots of (A) acetylated protein profile after 15 min of reperfusion (B) with histograms showing quantification of Silent information regulator 1 (SIRT1) protein expression after 2 hours of reperfusion in non-ischemic (sham), ischemic + vehicle (MI), and ischemic + KYN (MI+KYN) left ventricle samples (n=6-11). GAPDH was used as loading control. Values are expressed as mean±SEM. 151

Figure 40: Representative immunoblots and histograms showing quantification of protein expression for (A) mitochondrial respiratory chain complex and (B) PGC1α in non-ischemic (sham), ischemic + vehicle (MI), and ischemic + KYN (MI+KYN) left ventricle samples after 2 hours of reperfusion (n=5-10). β-actin was used as loading control. (C) Histograms showing quantification of complex over citrate synthase activity ratio (I/CS, II/CS, III/CS, IV/CS) or complex ratio activity (I/II, III/I, IV/I) assessed by means of spectrophotometry in sham, MI, MI+KYNA left ventricle samples after 2 hours of reperfusion (n=5-11). Values are expressed as mean±SEM; * p<0.05, *** p<0.001..... 152

Figure 41: GPR35 mRNA expression and protein expression of p-ERK1/2, ERK1/2, p-Akt, Akt, p-GSK3β, GSK3β, p-STAT3 and STAT3, respectively by means of quantitative polymerase chain reaction and western blot. (A) GPR35 mRNA expression in sham, (MI), and KYN (MI+KYN) left ventricle samples after 2 hours of reperfusion (n=6-11). (B) Representative immunoblots and histogram quantification of protein expression for p-ERK1/2, ERK1/2, p-Akt, Akt, p-GSK3β, GSK3β, p-STAT3 and STAT3 in sham, MI and MI + KYN groups after 15 min of reperfusion (n=6-11). GAPDH was used as loading control. Data are expressed as mean±SEM. * p<0.05, *** p<0.001. . 153

Figure 42: Representative immunoblots and histograms quantification of protein expression for p-AMPKα, AMPKα, p-FOXO3α and FOXO3α in non-ischemic (sham), ischemic + vehicle (MI), and ischemic + KYN (MI+KYN) left ventricle samples after 15 min of reperfusion (n=6-11). GAPDH was used as loading control. Values are expressed as mean±SEM. * p<0.05. 154

Figure 43: Representative immunoblots and histogram quantification of protein expression for p62, PARK2 and LC3b-II in non-ischemic (sham), ischemic + vehicle (MI), and ischemic + KYN (MI+KYN) left ventricle samples after 2 hours of reperfusion (n=6-7). GAPDH was used as loading control. Values are expressed as mean±SEM. ** $p<0.01$. 154

Figure 44: Anti-oxidant markers gene expression, by means of RT-qPCR. SOD1, 2, 3 and catalase mRNA expression in non-ischemic (sham), ischemic + vehicle (MI), and ischemic + KYN (MI+KYN) left ventricle samples after 2 hours of reperfusion (n=6-11). Values are expressed as mean±SEM. * $p<0.05$, ** $p<0.01$, *** $p<0.001$. 155

Figure 45: Representative immunoblots and histogram quantification of SOD1, 2, 3 and catalase protein expression in non-ischemic (sham), ischemic + vehicle (MI), and ischemic + KYN (MI+KYN) left ventricle samples after 2 hours of reperfusion (n=6-11). GAPDH was used as loading control. Values are expressed as mean±SEM. * $p<0.05$, ** $p<0.01$. 156

List of tables

Table 1: Different types of post-translational modifications of the dynamin related protein 1 (DRP1). 34

Table 2: Effect of mitochondrial fusion and fission proteins ablation *in vivo* models 46

Table 3: Functions of some enzymes of the kynurenine pathway 56

Table 4: Kynurenine pathway enzymes as therapeutic targets in some clinical conditions 65

List of abbreviations

3-OHKYN: 3-Hydroxykynurenine

5-HT: 5-Hydroxytryptamine

5-HTP: 5-Hydroxytryptophan

ADOA: Autosomal Dominant Optic Atrophy

AhR: Aryl hydrocarbon Receptor

AhRR: AhR repressor

Apaf-1: Apoptotic protease activating factor 1

ARNT: Aryl hydrocarbon Receptor Nuclear Transporter

ATP: Adenosine Triphosphate

BNIP3: BCL2 Interacting Protein 3

CL: Cardiolipin

DNA: Deoxyribonucleic Acid

Dnm1l: Dynamin 1 like protein

DRP1: Dynamin Related Protein 1

E1, E2, E3: Ubiquitin ligase enzyme 1,2,3

Egln1: αKG-dependent dioxygenase

ER: Endoplasmic Reticulum

ERK1/2: Extracellular-signal-Regulated Kinase 1/2

FADH2: Flavin Adenine Dinucleotide

FIS1: Mitochondrial fission 1 protein

FUNDC1: FUN14 Domain Containing 1

GED: GTPase Effector Domain

GPR35: G protein coupled receptor 35

GSK3-β: Glycogen Synthase Kinase-3-β

GTP: Guanosine Triphosphate

H/R: Hypoxia/Reoxygenation

HIF: Hypoxia-Inducible Factor

HR2: Heptad Repeated domain 2

Hsp90: Heat shock protein 90

I/R: Ischemia/Reperfusion

IDO: Indoleamine-pyrrole 2,3-dioxygenase

IFN-γ: Interferon gamma

IL-22: Interleukin 22

KAT: Kynurenine Aminotransferase

KMO: Kynurenine 3-monooxygenase

KTR: KYN/TRP ratio

KYN: Kynurenine

KYNA: Kynurenic Acid

LAD: Left Anterior Descending

LC3b: Microtubule-associated proteins light chain 3b

L-OPA1: Long form OPA1

LPS: Lipopolysaccharides

Mdivi-1: Mitochondrial division inhibitor-1

MFF: Mitochondrial Fission Factor

MFN1,2: Mitofusins 1,2

MI: Myocardial Infarction

miAAT: mitochondrial Aspartate Aminotransferase

MIEF1 (MiD51): Mitochondrial Elongation Factor 1

MIEF2 (MiD49): Mitochondrial Elongation Factor 2

MIS: Mitochondrial Import Sequence

MPP: Mitochondrial Processing Peptidase

mPTP: mitochondrial Permeability Transition Pore

mtDNA: mitochondrial DNA

NADH: Nicotinamide adenine dinucleotide

NADPH: Nicotinamide adenine dinucleotide phosphate

Nfk: N-Formyl-Kynurenine

NMDA: N-methyl-D-aspartate

NNP52: Nuclear Dot Protein 52

NO: Nitric oxide

OPA1: Optic Atrophy 1

OPTN: Optineurin

P62: Nucleoporin p62

PARL: Presenilin-Associated Rhomboid-Like Protease

PBS: Phosphate Buffer Saline

PGAM5: Phosphoglycerate Mutase family Member 5

PI3K: Phosphoinositide 3-Kinase (PI3K)

PINK1: PTEN-induced kinase 1

PKA: Protein Kinase A

QPRT: Quinolinate Phosphoribosyl Transferase

RC: Respiratory Control ratio

RISK: Reperfusion Injury Salvage Kinase

RNA: Ribonucleic Acid

ROS: Reactive Oxygen Species

rRNA: ribosomal RNA

SAFE: Survivor Activating Factor Enhancement

SIRT: Sirtuins

SOD: Superoxide Dismutase

S-OPA1: Short form OPA1

SQSTM1: Sequestosome 1

SR: Sarcoplasmic Reticulum

Src: Proto-oncogene tyrosine-protein kinase

STAT3: Signal Transducer and Activator of Transcription 3

TBK1: TANK Binding Kinase 1

TDO: Tryptophan 2,3-dioxygenase

TNF: Tumor Necrosis Factor

TPH: Tryptophan hydroxylase

tRNA: transfer RNA

TRP: Tryptophan

TRPRS: Tryptophanyl-Transfer RNA Synthetase

VDAC: Voltage Dependent Anion Channel

XAP2: hepatitis B virus X-associated protein 2

αKG: Alpha Ketoglutarate

General Introduction

My thesis project took place in the UMR CNRS 6015 Inserm 1083 directed by Dr. Daniel HENRION, a unit in the MitoVasc laboratory. This unit is divided into two teams: Team MitoLab and Team CARME. The first team is mainly interested in studying the role of mitochondria in different pathologies, and the second team, in which my work too place, is mainly dedicated to study the cardiovascular pathologies (Myocardial infarction, cardioprotection, hypertension, obesity…). The main purpose of our research is uncovering cardioprotective strategies to reduce myocardial ischemia/reperfusion injuries. This project was conducted under the supervision of Pr. Fabrice Prunier and Dr. Sophie Tamareille.

The heart is one of the most susceptible organs to ischemia. A lack of adequate irrigation (ischemia) equals to a rupture in oxygen and nutrients supplement, which leads to cell death and organ failure. Huge progress has been made in the last decade when it comes to treating myocardial infarction. However, despite the indispensable beneficial role of reperfusion, researchers found that final infarct size was in part due to ischemia injuries, but also to reperfusion (Benhabbouche et al. 2011). Cells that were once deprived of oxygen and nutrients during a certain amount of time will not be able to properly use these elements once reperfusion takes place. In fact, reperfusion induces the activation of many signaling pathways which eventually lead to mitochondrial swelling, and cell death. Therefore, reperfusion has to be associated to a cardioprotective strategy, which in turn will condition the cells to properly use oxygen and nutrients when reperfusion happens. Numerous cardioprotective modalities were documented: ischemic conditioning, hypothermia, pharmacological conditioning… Each one of these strategies has had a certain amount of success on animal studies, but until now none has been successfully employed in treating myocardial ischemia/reperfusion injuries on a clinical level. Moreover, signaling pathways implicated in cardioprotection seen in animals have yet to be established.

My thesis project was focused on understanding the implication of mitochondrial dynamics and the kynurenine pathway in cardioprotection after myocardial infarction cardioprotection. Regarding the first part; Mitochondria, now known as dynamic organelles, have been shown to being highly implicated in these injuries. In fact, alteration of the mitochondrial network ultrastructure has been shown detrimental to the cell. A study was already performed on a mouse model deficient in mitochondrial fusion protein, OPA1. In this work, we showed exacerbated myocardial injuries after ischemia/reperfusion compared to WT littermates (Le Page et al. 2016) (Cf. Annexes 1). Herein, we sought to investigate the effect of modulating mitochondrial dynamics protein expression on myocardial ischemia/reperfusion injuries. Thus, we worked on a mice model deficient in a mitochondrial fission protein (DRP1) and on a model deficient in both mitochondrial fission and fusion proteins (DRP1 and OPA1 respectively).

Concerning the second part of this project, our previously published work (Chao de la Barca et al. 2016; Kouassi Nzoughet et al. 2017), showed that remote ischemic conditioning of rats significantly increased plasmatic levels of many metabolites, of which kynurenine. The latter is a metabolite of the tryptophan metabolic pathway: the kynurenine pathway. An injection of this molecule, 10 minutes before a myocardial ischemia/reperfusion, was capable of inducing a smaller infarct size compared to vehicle treated group (Chao de la Barca et al. 2016). Moreover, a study published in 2016 showed a cardioprotective role of kynurenic acid, a metabolite deriving of kynurenine (Olenchock et al. 2016). Therefore, the next step was to elucidate underlying signaling pathways of both metabolites-induced cardioprotection.

Literature overview

Chapter 1: Myocardial ischemia/reperfusion injury and cardioprotection

1. Myocardial infarction

1.1. Epidemiology and treatment

Cardiovascular diseases are the leading cause of mortality worldwide. In fact, 3.8 million men and 3.4 million women die of coronary heart disease each year. This makes myocardial infarction (MI) a major public health problem. One year after an acute MI and in optimal myocardial reperfusion, the rate of death is 10% and, cardiac failure accounts for 25% (Yellon and Hausenloy 2007).

The myocardium's function is essentially ensured by an adequate supply in oxygen and nutrients. MI is the result of a total or partial abrupt occlusion of a coronary artery. The myocardium distal to the occlusion becomes ischemic and is deprived of nutrients and oxygen. Coronary occlusion usually occurs after the rupture of a pre-existing atheroma plaque (Ibanez et al. 2015) and leads to many physiological, biochemical, mechanical, morphological, and molecular consequences. Infarct size is dependent on several factors: the surface of the ischemic myocardium, the duration of ischemia, and the presence of a collateral circulation corresponding to the blood flow remaining in the ischemic area despite the coronary occlusion (Benhabbouche et al. 2011).

Unrelieved ischemia leads to irreversible injuries, cell death, and a myocardial dysfunction. Thus, establishing coronary-artery patency is of extreme importance since myocardial viability/ infarct size is a key factor in patient's prognostic and development of heart failure (Varma and Brecker 2001). The treatment is salvaging the ischemic myocardium by reperfusion in order to limit final infarct size. Reperfusion consists in re-establishing the blood flow by either thrombolysis or primary angioplasty coupled with a preventive treatment of re-occlusion. The rapidity of this procedure determines infarct size and patient's prognostic (Benhabbouche et al. 2011).

2. Myocardial ischemia/reperfusion injuries

2.1. Definition

In human, reperfusion occurring during the golden hour (60-90 minutes after coronary artery blockage), averts death by acute myocardial infarction (Balamurugan et al. 2018). Reimer et al. showed that myocardial necrosis progressed with prolonged ischemia in a 'wavefront' pattern confirming the concept of early reperfusion being crucial to salvage the ischemic myocardium and reducing infarct size (Reimer et al. 1977; Ovize et al. 2010; Maroko et al. 1972).

Final infarct size is due to two components: Ischemia injuries and reperfusion injuries. Even though timely reperfusion is of paramount importance to salvage the ischemic myocardium, it leads to what is called reperfusion injuries. These injuries were first described by Jennings et al in 1960 (Jennings et al. 1960). They are defined as myocardial injuries due to the restoration of the coronary blood flow

and animal studies showed that reperfusion injuries can account up to 50% of final infarct size (Fig.1) (Yellon and Hausenloy 2007).

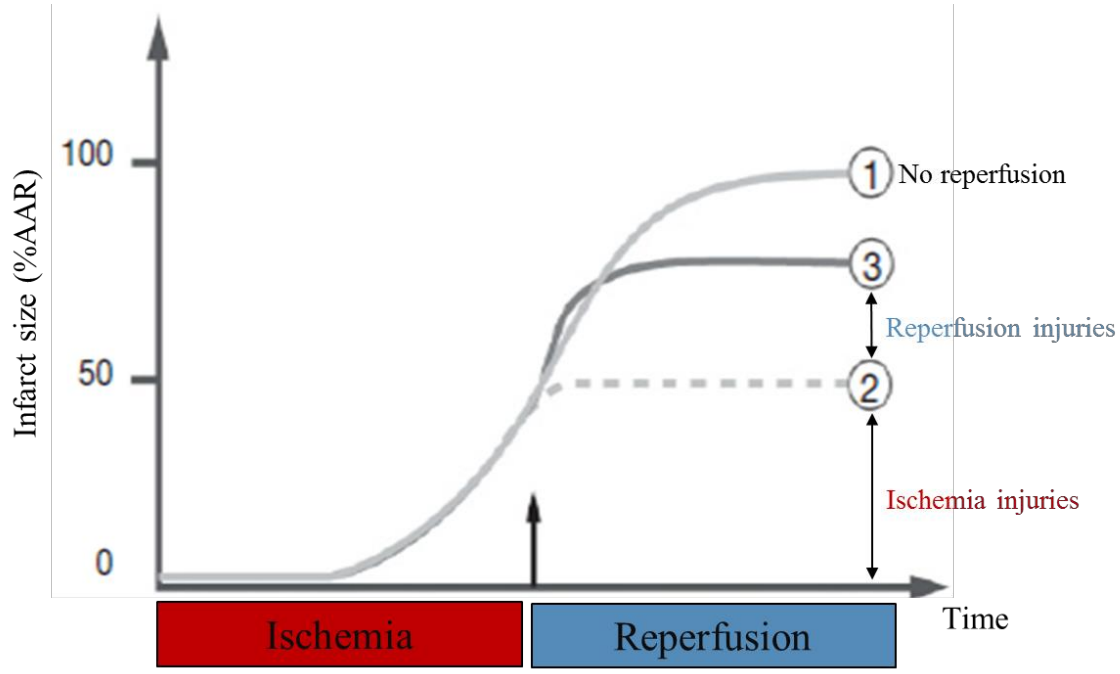

Figure 1: Myocardial ischemia/reperfusion injuries in final myocardial infarct size. Infarct size was expressed as a percentage of the area at risk (ARR). In (1) is shown final infarct size if the ischemic myocardium is not reperfused, in (2) is shown expected infarct size after reperfusion due mainly to ischemia injuries and in (3) is shown actual infarct size due to both ischemia and reperfusion injuries. Adapted by (Benhabbouche et al. 2011).

2.2. Mechanisms

Mechanisms underlying ischemia/reperfusion (I/R) injuries have been studied for more than 45 years now. Ischemia-induced by an interrupted coronary flow leads to a rapid decrease of oxygen pressure in tissues, and a cease of oxidative phosphorylation. To compensate reduction in ATP, cardiomyocytes switch to anaerobic respiration. This leads to the formation of lactate, and a decrease in pH. This decrease induces the extrusion of H^+ by the Na^+/H^+ exchanger and results in intracellular Na^+ overload. The latter activates the Na^+/Ca^{2+} exchanger that functions in reverse mode, extruding Na^+ and leading to intracellular Ca^{2+} overload. Moreover, pH decrease inhibits mitochondrial permeability transition pore (mPTP) opening and myofibril contracture (Fig. 2) (Avkiran and Marber 2002).

Reperfusion, a double-edged weapon, allows the re-establishment of blood flow, meaning oxygen and nutrients. However, as mentioned beforehand, reperfusion is also responsible for what is now known as reperfusion injuries. After reperfusion, 4 physiological responses, with different

degrees of detrimental consequences on the myocardium, are distinguished (Benhabbouche et al. 2011):

- Myocardial stunning, defined as: "a mechanical dysfunction that persists after reperfusion despite the absence of irreversible damage and despite restoration of normal or near-normal coronary flow". This form of injury is due simultaneously to a calcium overload and reactive oxygen species (ROS) toxicity. It is usually reversible in a couple of days or weeks (Braunwald and Kloner 1982).
- Cardiac dysfunction is the no-reflow phenomenon. It is the inability to reperfuse the ischemic zone due to the impedance of the microvascular blood flow during the opening of the coronary artery (Krug, Du Mesnil de, and Korb 1966). This is usually due to capillary damage with impaired vasodilatation, cardiomyocyte swelling, platelet micro- thrombi and neutrophil plugging (Heusch et al. 2009; Ito 2006).
- Reperfusion arrhythmias have been proven to exist in all studied animal species. Mechanisms of these injuries are not well understood (Hearse and Tosaki 1987).
- Lethal reperfusion injury meaning that reperfusion, distinct from ischemia, is solely responsible for the death of cells that were still viable at the end of the ischemic event (Piper, Garcia-Dorado, and Ovize 1998).

Mediators of lethal reperfusion injuries have been well studied in literature. Major contributory factors are oxidative stress, calcium overload, mPTP opening, and hypercontracture (Yellon and Hausenloy 2007). During reperfusion, a burst of oxidative stress is produced. ROS are generated due to the re-activation of the electron transport chain. Other sources of ROS include xanthine oxidase (endothelial cells) and the nicotinamide adenine dinucleotide (phosphate) (NADPH) oxidase (neutrophils). ROS induce the opening of the mPTP, and mediate dysfunction of the sarcoplasmic reticulum (SR). This leads to calcium overload, lipid peroxidation, enzyme denaturation, and direct oxidative damage to DNA. Reperfusion results in the rapid restoration of physiological pH, after activation of the Na^+/H^+ exchanger (NHE) and Na^+/HCO_3^- co-transporter (NBC) and the washout of lactic acid, which releases the inhibitory effect on mPTP opening and cardiomyocyte contracture. The restoration of the mitochondrial membrane potential drives calcium into the mitochondria, which can also induce mPTP opening. Several hours after the onset of myocardial reperfusion, neutrophils accumulate in the infarcted myocardial tissue in response to the release of the ROS (chemoattractants) (Hausenloy and Yellon 2013) (Fig. 2).

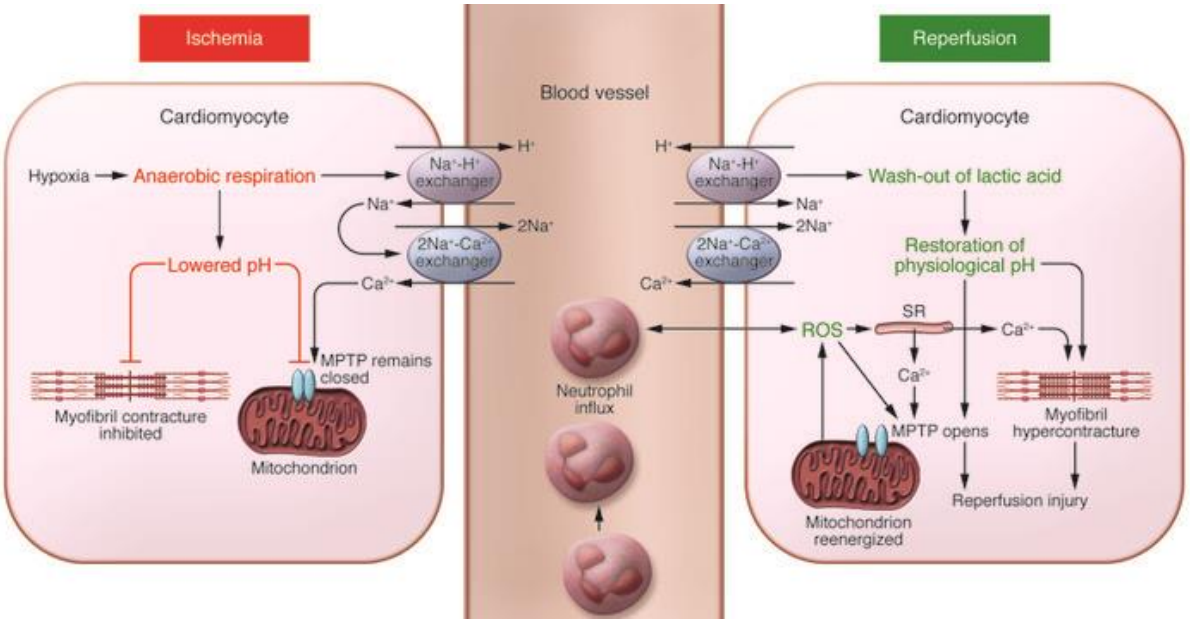

Figure 2: Mechanisms underlying ischemia/reperfusion injuries in cardiomyocytes (Hausenloy and Yellon 2013).

Thus, when speaking of reperfusion injuries, we are speaking of paradoxes (Benhabbouche et al. 2011; Yellon and Hausenloy 2007). The **oxygen paradox** is one of the first described paradoxes. In fact, when re-oxygenating the ischemic myocardium, the same oxygen that was once indispensable for the salvage of the myocardium becomes the cause of oxidative stress which generates a degree of myocardial injury that greatly exceeds the injury induced by its absence (ischemia) alone. Oxidative stress also reduces the bioavailability of nitric oxide (NO) limiting its cardioprotective effect (inhibition of neutrophil accumulation, inactivation of superoxide radicals, and improvement of coronary blood flow). The second paradox is the **calcium paradox**, reperfusion causes an intracellular and a mitochondrial calcium overload which causes a hypercontracture of heart cells and mPTP opening leading to cardiomyocyte death. The third and last paradox is the **pH paradox**. Reperfusion allows rapid restoration of physiological pH after the washout of lactic acid and the activation of the sodium-hydrogen exchanger, and the sodium-bicarbonate symporter. This rapid and excessive activation leads to reperfusion injuries.

3. Cardioprotective strategies

3.1. Definition and classification

Cardioprotection results from the activation of endogenous mechanisms in cardiomyocytes when submitted to stress. Since identifying the part played by reperfusion in the final infarct size, scientists have been trying to couple reperfusion with cardioprotective techniques in order to improve

the patient's prognostic. Treatments that protect from reperfusion injury should generally be applied as early as possible during reperfusion because most cell death occurs during the first minutes of reflow. Many treatments have been identified to confer robust cardioprotection in experimental animal models of acute myocardial I/R injuries. However, translation of these cardioprotective techniques into the clinical stage of acute MI for the patient benefit has been disappointing (Ibanez et al. 2015).

Cardioprotective strategies can be classified based on different criteria (Fig. 3) (Davidson et al. 2019):

A. Firstly, we can distinguish 3 types of cardioprotective strategies based on the modality of their application: ischemic conditioning, pharmacological conditioning, and physical intervention. The first one consists in conditioning the heart to the brutal increase in oxygen and nutrients upon reperfusion by submitting the heart (local) or another organ (remote) to brief episodes of I/R. The pharmacological protection is done by administrating different kind of molecules like anti-oxidants, anti-coagulants, anti-apoptotic agents... And, physical intervention is treating I/R injuries, mainly, with hypothermia or electrical nerve stimulation.
B. Secondly, we can classify cardioprotection modalities according to the time of application, meaning, applied before ischemia during ischemia, at reperfusion, or late into reperfusion.
C. Thirdly, cardioprotective strategies can be differentiated based on cellular and intracellular targets. In fact, different types of cells can be targeted to diminish I/R injuries: cardiomyocytes, circulating cells like neutrophils or platelets, or cells implicated in microvascular obstruction. Moreover, different pathways can be targeted within the same cell like inhibiting cell death pathways (necrosis, apoptosis…) or activating endogenous pro-survival pathways.

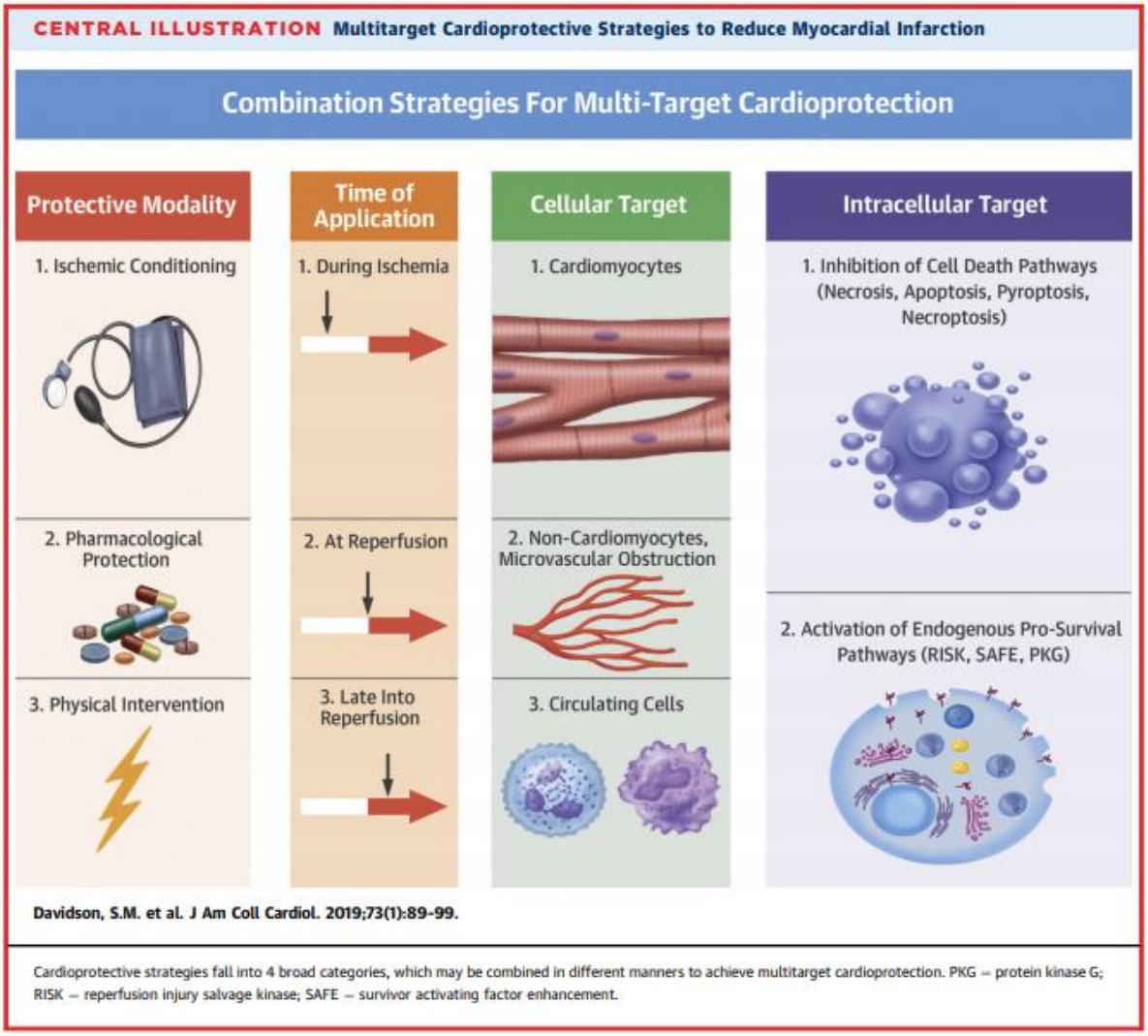

Figure 3: Different categories of cardioprotective modalities aiming to reduce myocardial reperfusion injuries; PKG: protein kinase G, RISK: reperfusion injury salvage kinase, SAFE: survivor activating factor enhancement (Davidson et al. 2019).

3.2. Conditioning

As mentioned beforehand, conditioning is a type of cardioprotective strategy and can be applied at different times of acute myocardial I/R (Fig. 4). We can distinguish two types of conditioning: ischemic and pharmacological conditioning.

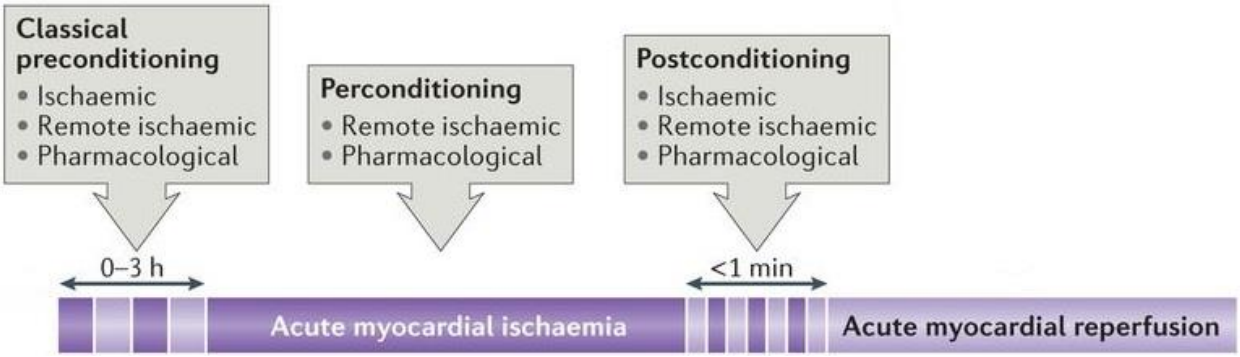

Figure 4: Schematic representation of different types of conditioning depending on time and type of application. Dark purple represents ischemia period whereas purple represents reperfusion .Adapted by (Hausenloy and Yellon 2016).

3.2.1. Ischemic conditioning

In 1986, Murry et al. were the first to describe a cardioprotective strategy. It consisted of performing brief occlusion episodes on a coronary artery, before realizing a MI on that same artery. This is the definition of local Ischemic pre-conditioning. They stated that minor stress can activate endogenous mechanisms that can confer protection when affronted with more important stress. Four cycles of 5 minutes ischemia and reperfusion prior to a more sustained episode of 40 min ischemia was capable of reducing the final infarct size by 75% in a "conditioned" canine model. However, infarct size was not reduced when the sustained coronary occlusion was of 3 hours duration, emphasizing the need for timely reperfusion (Murry, Jennings, and Reimer 1986). 30 years after ischemic conditioning discovery, it has been applied in different species and on different types of organs and has been shown to be effective in reducing the final infarct size after MI (Hausenloy and Yellon 2016).

To test the effectiveness of this strategy and to facilitate its translation in clinical studies, different studies were conducted where the onset of ischemic conditioning was a criteria and subsequent cardioprotection was studied. We can distinguish different types of ischemic conditioning. It can be dependent on two criteria, time of application and the distance between the conditioned organ and the ischemic one. Subsequently, we find **local** (Murry, Jennings, and Reimer 1986) and **remote** (Przyklenk et al. 1993) ischemic conditioning. Local conditioning, is applying the brief episodes of I/R on the future ischemic coronary, or on a coronary adjacent to the ischemic one. Remote conditioning, is applying the brief episodes of I/R on a distant organ, for example the kidney (McClanahan 1993) or the mesentery (Gho et al. 1996). According to the window during which these episodes are applied (Heusch et al. 2015), we can distinguish, **pre-conditioning** (Kharbanda et al. 2002), which precedes ischemia, **per-conditioning** (Szijarto et al. 2012), meaning during the ischemia period of the MI, and the **post-conditioning** (Zhao et al. 2003), that is applied once reperfusion takes place.

In the clinical setting, ischemic pre-conditioning cannot be used in patients with a MI. However, ischemic post-conditioning, and remote ischemic conditioning, could actually be applied and the majority of clinical studies showed a reduction of infarct size using biomarkers (Yang et al. 2007; Staat et al. 2005; Thibault et al. 2008; Ma et al. 2006; Laskey et al. 2008) or imaging. Remote ischemic conditioning even showed an improved clinical outcome (Sloth et al. 2014).

3.2.2. Pharmacological conditioning

Pharmacological conditioning is the administration of a pharmacologically active molecule, with the same aim as ischemic conditioning: to activate endogenous protective signaling pathways.

In the past 10 years, scientists tried to find pharmacological agents that are capable of triggering similar pathways to that activated during ischemic conditioning. Many phase II clinical trials have been performed to find co-adjuvant pharmacological interventions to ameliorate the myocardial I/R injuries (Ibanez et al. 2015; Davidson et al. 2019).

One of the most promising molecules is **cyclosporine-A**. The latter acts as an mPTP opening inhibitor, a known contributing event to lethal reperfusion injuries (Monassier et al. 2016). However, cyclosporine-A produced inconsistent preclinical results and failed in large clinical trials (Lim, Messow, and Berry 2012; Yingzhong, Lin, and Chunbin 2016).

Another well-studied pharmacological agent is a β-blocker, more known as **Metoprolol**. In fact, chronic β-adrenergic receptor stimulation induces cardiac apoptosis and aggravates myocardial I/R injury. In clinical trials, metoprolol was capable of reducing infarct size and relative mortality. However, increased mortality rate was observed with patients who are hemodynamically compromised (Ibanez et al. 2013).

During a MI, energy depletion is observed in cardiomyocytes. Therefore, the possible therapeutic use of glucose was discussed to prevent this energy depletion. **Glucose modulators** or a mix of glucose/insulin/potassium were tested in several clinical trials during MI with some encouraging results (Nishino et al. 2004; Ji et al. 2013).

3.3. Signaling molecules and pathways

Thousands of studies reported several cell components (organelles and proteins) playing a role in reperfusion injuries. Each cardioprotective treatment, more precisely conditioning, targeted one or more of the identified components. Each strategy had one ultimate end point of protection: reduction of infarct size. The following is a non-exhaustive enumeration of some of the implicated players in I/R injuries and cardioprotection.

One of the most described pathways are the reperfusion injury salvage kinase (**RISK**) pathway and the survival activating factor enhancement (**SAFE**) pathway (Heusch 2015):

-RISK pathway refers to a group of protein and lipid kinases (phosphoinositide-dependent kinase (PI3K), Akt and ERK1/2…) that when specifically activated (phosphorylation) confer cardioprotection by inhibiting mPTP opening (Davidson et al. 2006), improving uptake of calcium in the sarcoplasmic reticulum (Abdallah et al. 2006), and activating anti-apoptotic pathways (Yellon and Baxter 1999). In fact, one of the downstream points of convergence of the RISK pathway is GSK3β, which when phosphorylated is activated and responsible for cardioprotection (Juhaszova et al. 2004).

-The conception of the SAFE pathway began while deciphering signaling pathways implicated in tumor necrosis factor (TNF) reduction of myocardial I/R injury (Lecour et al. 2002). Indeed TNF and its receptor (TNFR2) can activate kinases responsible for the cardioprotection (Hadebe, Cour, and Lecour 2018). A key downstream kinase in the SAFE pathway is signal transducer and activator of transcription 3 (STAT3) is a transcription factor implicated in several physiological and pathological processes in cardiomyocytes. It is located in the cytosol and has been recently identified having a location in the matrix of mitochondria. STAT3 is being seen as a target or as an effector in conditioning because it has been shown to increase complex 1 respiration, to attenuate mPTP opening, and to reduce ROS formation (Boengler et al. 2013). Both of these pathways have been shown activated by remote limb ischemic preconditioning and local ischemic postonditioning(Tamareille et al. 2011; Smith et al. 2004)

It is now known that **mitochondria** have a central role in reperfusion injuries and are the most important effector of conditioning's protection where all of the above signaling pathways converge. They are the main source of intracellular **ROS** that are possibly implicated in reperfusion injuries. Experimental studies showed that reperfusion generates oxidative stress but clinical studies were not capable of proving the beneficial role of antioxidants in treating I/R injuries (Zweier 1988; Downey 1990; Flaherty et al. 1994). Another major component in reperfusion injury that was targeted is the **mPTP**. This mitochondrial pore is a large conductance megachannel in the inner mitochondrial membrane which, once opened for a prolonged period, induce a matrix swelling, rupture of the outer mitochondrial membrane and the release of cytochrome C from the intermembrane space into the cytosol where it activates proteolytic processes and initiates cellular disintegration (Briston et al. 2017).

Another organelle playing a role in reperfusion injuries and considered as an effector of cardioprotective strategies is the **sarcoplasmic reticulum**. In fact, calcium fluxes play an important role in reperfusion injuries. Excessive calcium oscillations during early reperfusion contribute to uncoordinated contracture and eventual cellular disruption. Moreover, there is a tight connexion between sarcoplasmic reticulum, mPTP and calcium fluxes: calcium fluxes contribute to mPTP opening and vice versa (Abdallah et al. 2011). On another note, **sarcoplasmic reticulum stress response and autophagy** are important processes that remove dysfunctional and defective proteins (Doroudgar and Glembotski 2013). During IR, there is an abundance of structurally and functionally defective proteins that should be eliminated, because if not they can jeopardize normal cellular

function. Specific proteins exist that can detect unfolded proteins and induce the transcription of genes coding for chaperones and degrading enzymes. Several proteins are implicated in this process like Light chain 3-phosphatidyl ethanolamine (LC3b), beclin1 among others activated by ROS, calcium and mPTP opening. Endoplasmic reticulum stress response has been shown to be enhanced by postconditioning (Grall et al. 2013) and autophagy has been shown involved in remote postconditioning (Han et al. 2014).

Chapter 2: Mitochondria and mitochondrial dynamics

1. The mitochondrion

1.1. Generalities

Mitochondria are semi-autonomous membrane-bound organelles found in the cytoplasm of eukaryotic cells. Depending on the cell type, the number of mitochondria per cell may differ and hundreds to thousands of mitochondria can be found. Their size (length) is also affected by cell type and can vary from 0.5 µm to 10µm.

Mitochondria have their own genome (mtDNA), replication, transcription and translation machinery. Most mitochondrial proteins are encoded by nuclear genes, and are, once translated, imported into the mitochondria. However, some genes coding for proteins implicated in the respiratory activity are still encoded by the mitochondrial genome.

Because of the double-membrane organization, there are four distinct parts to a mitochondrion: the outer membrane, the intermembrane space, the inner mitochondrial membrane, and the matrix (Low 1956).

The outer membrane is composed of 40% lipids and 60% of proteins. It is characterized by the presence of voltage-dependent anion channel (VDAC) which makes it very permeable to ions and small molecules.

The inner membrane has a very dense protein composition (80%) making it highly impermeable. It is 3 to 5 times longer than the outer membrane but is convoluted into structures called cristae where the mitochondrial respiratory chain complexes are located. Several of the proteins localized in the inner membrane are transporters of the mitochondrial electron transport chain.

In the matrix, extranuclear DNA encoding for rRNAs, tRNAs, and proteins is found.

1.2. Main functions

Mitochondria play a central role in cellular bioenergetics and signaling transduction. They are famed as the energy factory or the powerhouse of eukaryotic cells. In fact, mitochondria harbor two of the most important metabolic pathways, in the matrix the Krebs cycle, and in the cristae, the oxidative phosphorylation. To summarize, the main mitochondrial functions are: (Fig. 5) (Dorn 2015b)

-β -oxidation of fatty acids

-Oxidative phosphorylation: synthesis of Adenosine Triphosphate (ATP) (responsible for 90% of total cellular ATP)

-Oxidative stress: generation of ROS

-Ion homeostasis

-Calcium signaling

-Apoptosis and necrosis

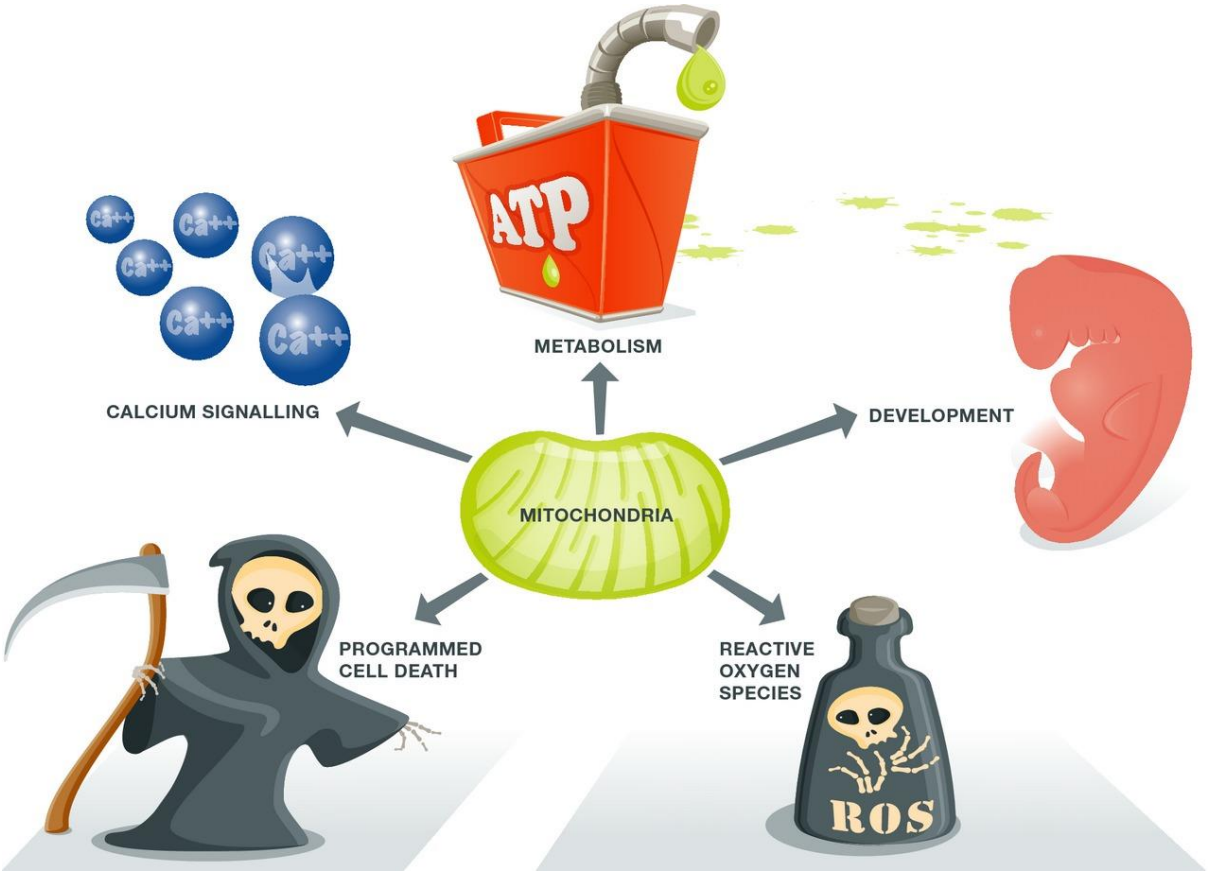

Figure 5: Schematic representation of mitochondrial function inside of a cell (Dorn 2015b).

1.2.1. Oxidative phosphorylation

In the inner membrane of mitochondria, more precisely in the cristae, is found the electron transport chain, the main actor in cellular respiration. This chain is formed by a series of proteins and organic molecules where electrons are passed from one member of the transport chain to another in a series of redox reactions. The energy released in these reactions is captured as a proton gradient used to generate ATP by chemiosmosis. This process is called oxidative phosphorylation and is the main reaction during which most of cellular ATP is produced in aerobic organisms. The concept of oxidative phosphorylation is to use energy-rich molecules such as Nicotinamide adenine dinucleotide (NADH) and flavin adenine dinucleotide ($FADH_2$) to phosphorylate ADP into ATP. ATP, the energy molecule of the cell, can also be produced by glycolysis and beta-oxidation. For example, the oxidation of one molecule of glucose into CO_2 and H_2O is capable of generating about 30 ATP molecules, of which 26 are produced by oxidative phosphorylation.

NADH and $FADH_2$ are considered reduced electron carriers. In fact, NADH and $FADH_2$ are oxidized by the mitochondrial respiratory chain complex I and complex II respectively. In this process, they turn back into NAD+ and FAD+ and are re-used in other steps of cellular respiration. Afterwards, generated electrons are transported along the mitochondrial respiratory chain complex. As they are passed down the electron transport chain, they move from a higher to a lower energy level until

arriving to the complex IV where oxygen is reduced into H_2O molecules. All of these transports couple energy liberated from electrons with extrusion of protons from the mitochondrial matrix into the intermembrane space. This proton gradient creates a protomotive force by generating a mitochondrial membrane potential difference. The energy released upon the passage of the protons *via* the complex V (H^+ transporting ATP-synthase complex) is used to phosphorylate ADP into ATP.

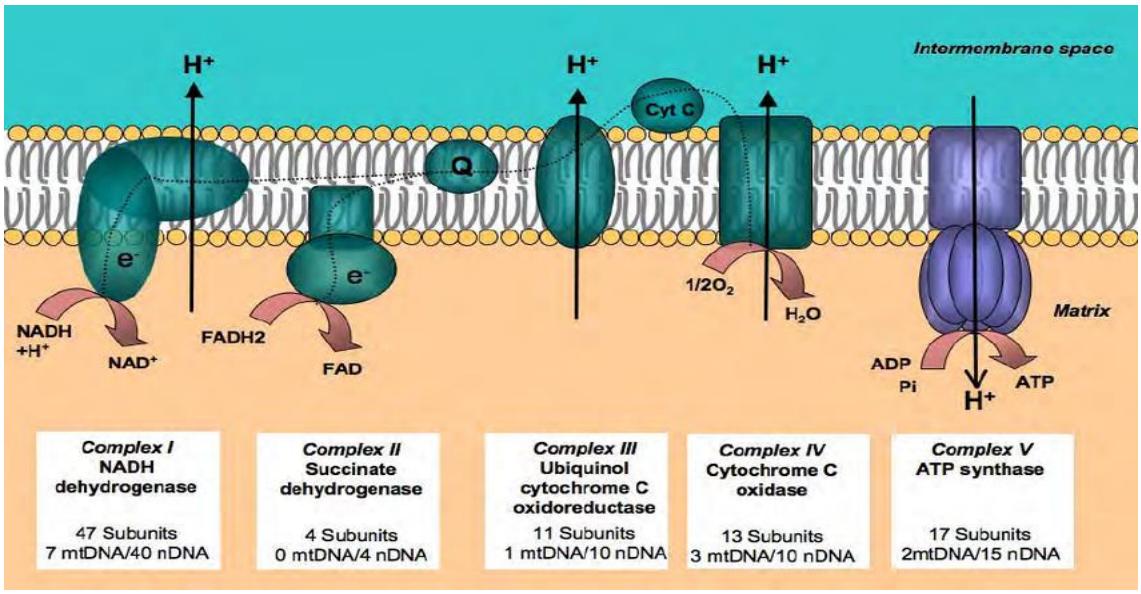

Figure 6: Schematic representation of the mitochondrial respiratory chain complexes. Respiratory chain is located on the inner mitochondrial membrane and consists of five complexes, each formed from subunits coded by either mitochondrial or nuclear DNA (complexes I – V), and two intermediate substrates (coenzyme Q and cytochrome c) (Bellance, Lestienne, and Rossignol 2009).

While oxidative phosphorylation is essential to ATP synthesis, it is also a main source of free radicals, more precisely of ROS (Superoxide anion, hydrogen peroxide, and hydroxyl radical). They are molecules deriving from activation of molecular oxygen. These molecules are unstable and are formed after some electrons evade the mitochondrial respiratory chain and react with molecular oxygen. They are essential molecules in some signaling pathways but can become extremely toxic to the cell when produced excessively. This is why it is essential to have a balance between ROS molecules (pro-oxidant molecules) and anti-oxidant ones like catalase and superoxide dismutase 1, 2, 3 (SOD 1, 2, 3) (Jeremy M Berg 2002).

1.2.2. Oxidative stress

Oxidative stress occurs after favoring the formation of oxidant molecules on that of anti-oxidant enzymes. This means that antioxidants enzymes are overwhelmed by the levels of free radicals. The main actors in the complex antioxidant defense grid, are SODs and Catalases (Dieterich et al. 2000).

SODs are universal enzymes found in all organisms living in the presence of oxygen. They are detoxification metalloproteins and the most powerful antioxidants in the cell. They control the levels

of ROS. Their activity is essential to control the levels of these species inside the cell, limiting their cellular toxicity and regulating their implication in different signaling pathways. Several types of SODs coded by different genes are found in each compartment of the cell and outside the cell. This compartmentalization of these enzymes shows the importance of fine regulation of ROS levels inside the cell. We can distinguish SOD1 or Cu/Zn-SOD mainly localized in the cytosol of the cells, SOD2 or MnSOD, the mitochondrial form, and SOD3 or Cu-Zn SOD, an extracellular SOD present in all tissue fluids (Ighodaro and Akinloye 2018).

Catalase is a 240 kDa tetrameric protein with four similar subunits that use either iron or manganese as a co-factor. It continues the detoxification process initiated by SOD by reducing hydrogen peroxide (H_2O_2) to water and molecular oxygen. This activity is also done by glutathione peroxidases (GPXs), and peroxiredoxins (PRXs) (Zhang et al. 2016).

Superoxide anion ($O_2^{\bullet-}$) is constantly being generated in the cell through endogenous processes and has an important role in cellular signaling pathways. It can be transformed into several other reactive species. SOD enzymes catalyze the dismutation of superoxide ($O_2^{\bullet-}$) and generate hydrogen peroxide (H_2O_2). H_2O_2 can react with iron (Fe^{2+}) to generate the hydroxyl radical ($OH^{\bullet}$). The reaction between $O_2^{\bullet-}$ and nitric oxide ($NO^{\bullet}$) produces ONOO−, whose decomposition in turn gives rise to some highly oxidizing intermediates including $NO_2^{\bullet}$, $OH^{\bullet}$, and $CO_3^{\bullet-}$ and the stable radical NO_3^- (Fig. 7) (Wang et al. 2018).

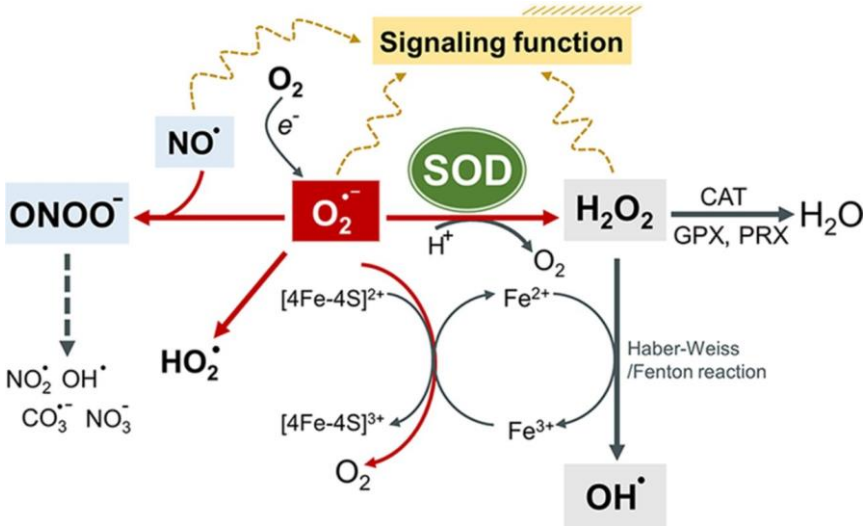

Figure 7: Representation of reactions catalyzed by Superoxide dismutase (SOD), catalase (CAT), glutathione peroxidase (GPX) and peroxiredoxin (PRX) enzymes to neutralize the toxic oxygen radical (Wang et al. 2018).

1.2.3. Apoptosis and necrosis

Cell death is an important and a key event in a cell cycle. Several modes of cell death have been described in the literature, each presenting various forms: apoptosis, necrosis, autophagy…(Galluzzi et al. 2007). In this section, focus will be on the two modes: apoptosis and necrosis. Apoptosis or cell suicide is a programmed cell death in order to remove damaged cells. It is an indispensable physiological process for normal homeostasis and compensates mitosis. Necrosis was initially defined as an accidental cell death but now, various forms of necrosis have been described (e.g. necroptosis, parthanatos, pyroptosis…) (Galluzzi et al. 2018). Necrosis is usually associated with a pathological process and is the outcome of severe injury e.g. abrupt ischemia (Konstantinidis, Whelan, and Kitsis 2012). In both modes, mitochondria are a key player in the implicated signaling pathways leading to either type of cell death. In fact, mitochondria store numerous cell components (e.g. cytochrome C) that once liberated, induce either apoptosis or necrosis (Kroemer, Dallaporta, and Resche-Rigon 1998).

During apoptosis, cell membranes are usually kept intact. And apoptosis activation is usually induced by pro-caspases. These proteins are found under an inactive form inside the cell and are tightly regulated. They are activated once cleaved and in their turn cleave downstream proteins after an aspartic residue. In fact, cytochrome C once liberated binds to Apaf-1 (Apoptosis Protease Activating Factor 1) and forms an apoptosome. This apoptosome binds and activates caspase 9. This protein in its turn activates other procaspases proteins like caspase 3, 6, and 7 and leads to the activation of a very selective pattern of protein degradation. Another class of proteins implicated in apoptosis regulation is the Bcl-2-related proteins. Proteins belonging to this class of gene products can be either anti-apoptotic (Bcl-2, Bcl-X_L, Bcl-w) or pro-apoptotic proteins (Bax, Bak, Bcl-X_S, Bad) (Fig 8A) (Kubli and Gustafsson 2012).

After a necrotic signal, Bcl2 proteins no longer inhibit the mPTP opening. BAX bound to mPTP enhances its opening leading to a rapid influx of solutes and water, since the latter is permeable to all molecules less than 1,5 kDa. This causes dissipation of the mitochondrial membrane potential, inner membrane swelling, and subsequent outer membrane rupture. Destruction of the outer membrane releases cytotoxic proteins into the cytosol and leads to necrotic cell death (Fig. 8B) (Kubli and Gustafsson 2012).

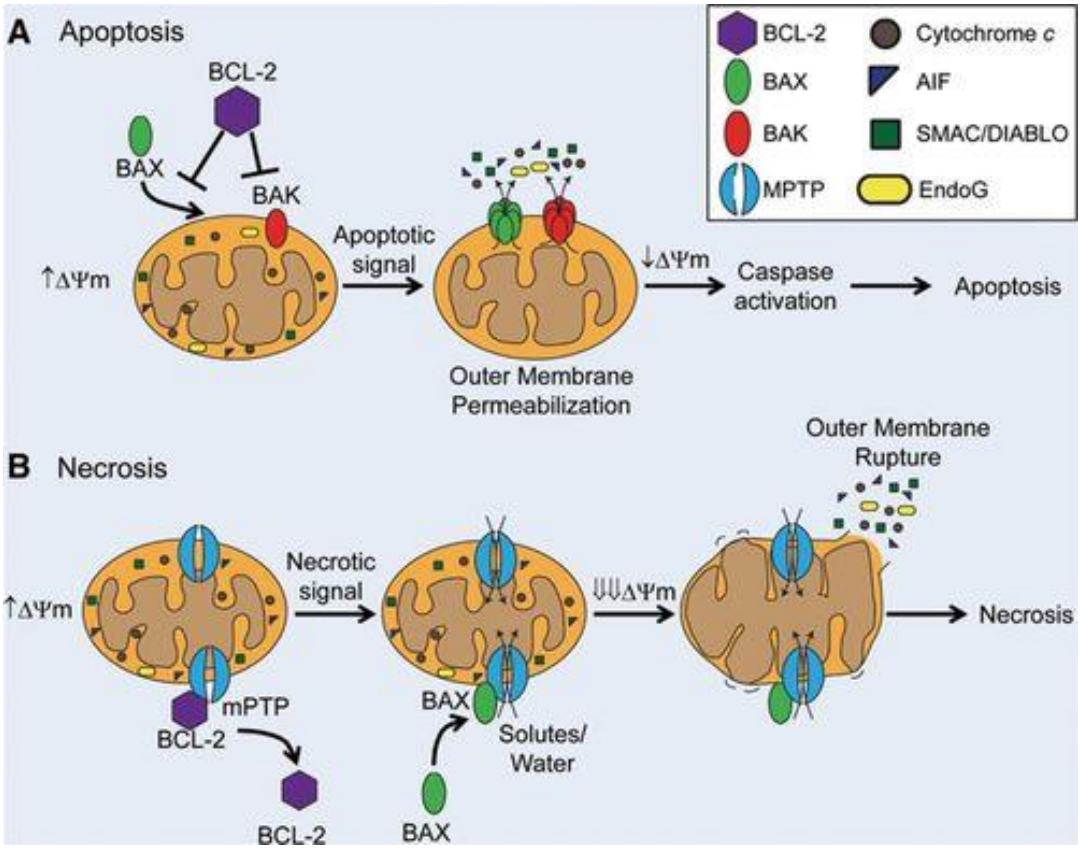

Figure 8: Mitochondria's implication in apoptosis and necrosis pathways (Kubli and Gustafsson 2012).

2. Mitochondrial network

2.1. Definition

For a long time, mitochondria have been depicted as static organelles. They have been pictured as single units existing in the cell, but in fact mitochondria form a well-organized filamentous network inside the cell where they can divide, combine and move along the cytoskeleton to interact with other organelles to always ensure cellular metabolic needs (Dorn 2019). As a matter of fact, the structure of this network can highly affect the wellbeing of a cell. Two types of events maintain the mitochondrial network morphology: mitochondrial fission and mitochondrial fusion. The main components of the mammalian machineries regulating these events are protein members of the dynamin family of large GTPases. These proteins can bind and hydrolyze guanosine triphosphate (GTP) to provide the necessary energy. A proper interplay between these dynamic transitions is crucial to respond to cellular needs depending on nutrient availability and the metabolic state of the cell (Liesa, Palacin, and Zorzano 2009). A deregulation thereof will lead to either a fragmentation or a hyper fusion of this network, and consequences can be severe depending on the cell type and state (Fig. 9) (Wai and Langer 2016).

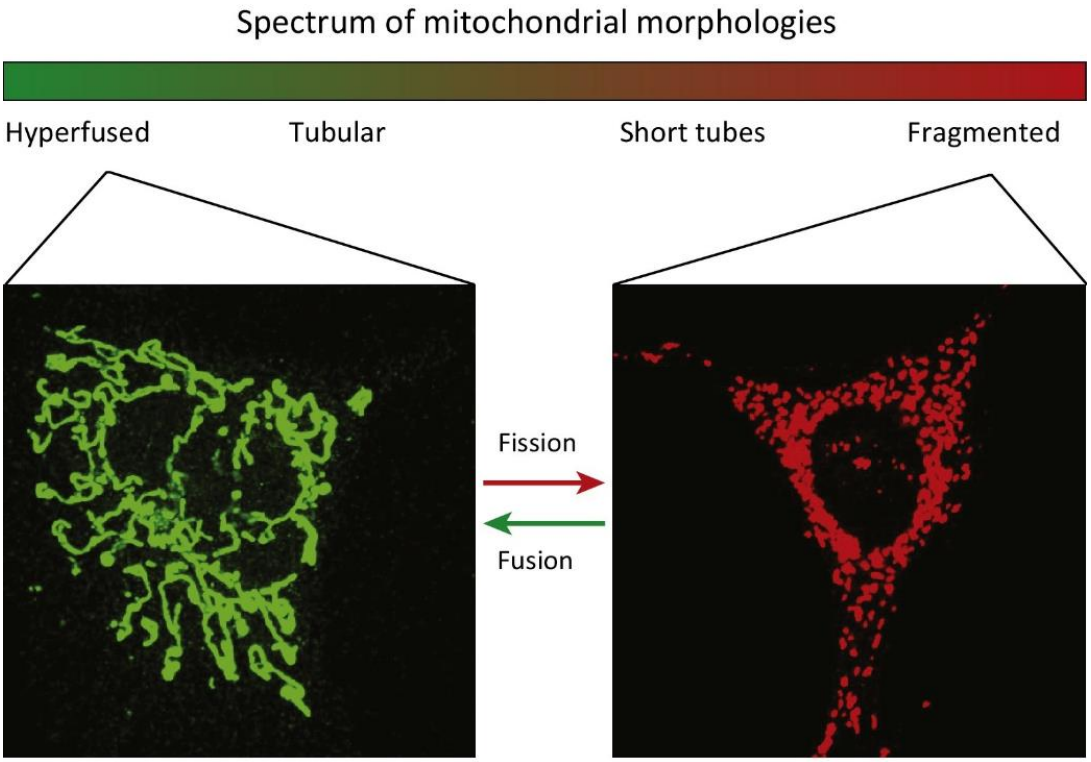

Figure 9: Spectrum of mitochondrial morphologies in fibroblast. Under normal conditions, mitochondrial network is maintained by a balance between mitochondrial fusion and fission. However, under stressful conditions such as nutrient excess, an increase of mitochondrial fission can be observed accompanied by cell death and impaired function of the mitochondrial respiratory chain complexes. In Nutrient Withdrawal, a mild stress, excessive fusion is seen with an increase activity of the mitochondrial respiratory chain complexes (Wai and Langer 2016).

Mitochondrial fission and fusion are orchestrated by different types of proteins and are an essential step in other processes. For example, mitophagy (a selective mitochondrial autophagy) requires both mitochondrial fission but also proteins implicated in mitochondrial fusion. Other proteins implicated in mitochondrial fusion have a role in preventing apoptosis, ensuring the alignment of the respiratory supercomplexes, and in the endoplasmic reticulum/mitochondria tethering (Fig. 10) (Ong et al. 2017).

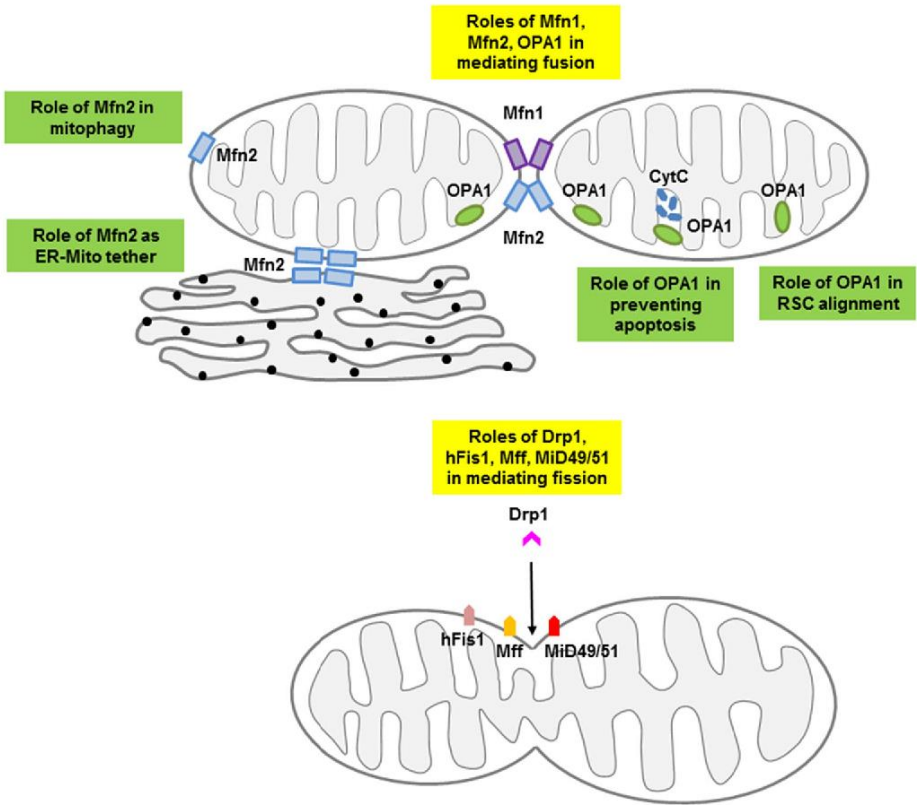

Figure 10: Role of mitochondrial fusion (MFN1, MFN2, OPA1) and fission (DRP1, hFIS1, MFF, MiD49/51) proteins in cellular mechanisms. CytC: cytochrome C, ER: endoplasmic reticulum, RSC: respiratory supercomplex (Ong et al. 2017).

2.2. Mitochondrial fission

Mitochondrial fission is an important process by which mitochondria control their number and size. In a simple symmetrical model, one large mitochondrion is divided into two small mitochondria. Excessively, this will lead to a fragmented discrete phenotype of the mitochondrial network. Several proteins control mitochondrial fission. Essentially, it is due to the interaction between: dynamin-related protein 1 (DRP1) and its receptors: mitochondrial fission protein 1 (FIS1), mitochondrial fission factor (MFF) and mitochondrial Dynamics Proteins or Mitochondrial Elongation Factor (MiD49 or MIEF2 and MiD51 or MIEF1) (Youle and van der Bliek 2012).

2.2.1. Dynamin related protein (DRP1)

It was in 1998 that several independent groups identified the mammalian homologue of a protein capable of inducing mitochondrial division: DRP1, an 80 kDa cytosolic GTPase protein, member of the dynamin superfamily. This protein is coded by the dynamin 1 like (*dnm1l)* nuclear gene. DRP1 is an ubiquitously expressed protein, highly present in the brain, skeletal muscle and the heart (Smirnova et al. 1998).

Structurally, DRP1 consists of four domains: a highly conserved NH_2-terminal GTPase domain, a central domain, an insert B domain and a C-terminal GTPase effector domain (GED) or the assembly domain (Fig.11). The latter interacts with the NH_2-terminal domains to regulate GTPase activity (Haun, Nakamura, and Lipton 2013).

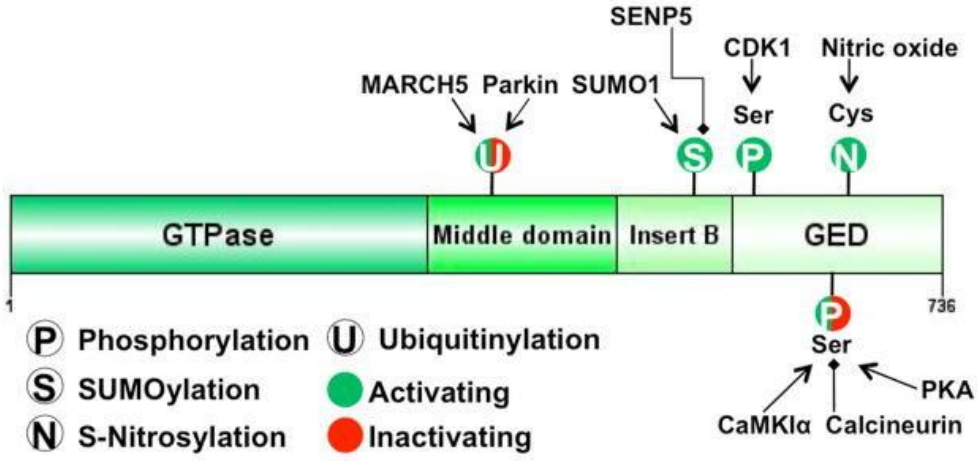

Figure 11: DRP1 protein structure and post-translational modifications by mentioned proteins. P (phosphorylation), N (S-nitrosylation), S (SUMOylation), and U (ubiquitination). CaMKIα: calcium/calmodulin-dependent protein kinase I α, CDK1: Cyclin Dependent Kinase 1, Cys: cysteine, GED: GTPase effector domain, MARCH5: Mitochondrial E3 ubiquitin-protein ligase, PKA: protein kinase A, SENP5: SUMO Specific Peptidase 5, SER: serine, SUMO1: Small Ubiquitin Like Modifier 1; (Haun, Nakamura, and Lipton 2013).

DRP1 is a cytosolic protein that has to be translocated to the mitochondria to induce mitochondrial fission. DRP1's GTPase activity, subcellular localization, protein-protein interactions, protein stability, is regulated by post-translational modifications that can occur in the middle domain, the insert B domain or the GED domain. The modifications within the sites, the upstream effectors and the effects of post-translational modifications are detailed in (Table 1) (Cho et al. 2013).

The most known post-translational modification is phosphorylation. A phosphorylation on the Serine in position 616 by Cdk1/cycline B increases mitochondrial fragmentation by promoting DRP1's translocation to mitochondria (Taguchi et al. 2007; Marsboom et al. 2012). Whereas, a phosphorylation on the Serine in position 637 by protein Kinase A (PKA) will inhibit mitochondrial fission by suppressing Drp1's translocation to mitochondria (Chang and Blackstone 2007b, 2007a). After a calcium overload, calcineurine, a phosphatase, can dephosphorylate DRP1 at S637, promoting mitochondial fission (Cereghetti et al. 2008). Other less known post-translational modifications are SUMOylation (Braschi, Zunino, and McBride 2009), ubiquitination (Yonashiro et al. 2006; Nakamura et al. 2006) and S-nitrosylation (Cho et al. 2009). Briefly, Ubiquitination is linking ubiquitin (small proteins of 76 amino acids) to DRP1 by ubiquitine ligase enzyme (E1, E2, E3). This modification can either increase mitochondrial fragmentation or enhance DRP1 degradation to maintain normal cellular levels. SUMOylation is a reversible post-translational modification where small ubiquitin-like

proteins called SUMO bind to DRP1 to govern its cellular localization. For example, SUMO-1 increase its translocation to mitochondria (Harder, Zunino, and McBride 2004), whereas SUMO2/3 inhibits it (Guo et al. 2013). Finally, S-nitrosylation, is a covalent attachment of a nitric oxide group to cysteine thiol which, in consequence, increases mitochondrial fission (Cho et al. 2009).

Modifications	Sites	Upstream regulators	Effects	References
Phosphorylation	S616	CDK1	Activation	Taguchi et al., 2007
		Erk1/2	Activation	Yu et al., 2011
		PKCδ	Activation	Qi et al., 2011
	S637	PKA	Inactivation	Chang and Blackstone, 2007; Cribbs and Strack, 2007b
		CaMK1α	Activation	Han et al., 2008a
		ROCK1	Activation	Wang et al., 2012c
Dephosphorylation	S637	Calcineurin (PP2B)	Activation	Cereghetti et al., 2008
S-nitrosylation	C644	Nitric oxide	Activation	Cho et al., 2009
SUMOylation	Multi-sites in variable domain	MAPL	Activation	Braschi et al., 2009
DeSUMOylation		SENP5	Inactivation	Zunino et al., 2007b
Ubiquitination		MARCH5	Inactivation	Nakamura et al., 2006a; Yonashiro et al., 2006b
		Parkin	Inactivation	Wang et al., 2011b
O-GlcNAcylation	T585, T586	O-GlcNAc-transferase	Activation	Gawlowski et al., 2012b

Table 1: Different types of post-translational modifications of the dynamin related protein 1 (DRP1). C Cysteine, CaMKIα: calcium/calmodulin-dependent protein kinase I α, CDK1: Cyclin Dependent Kinase 1, ERK1/2: extracellular signal-regulated kinases 1/2, MAPL: mitochondria-associated protein ligase, MARCH5: Mitochondrial E3 ubiquitin-protein ligase, PKA: protein kinase A, PKCδ: protein kinase C δ, ROCK1: Rho Associated Coiled-Coil Containing Protein Kinase 1, Calcineurin or PP2B : protein phosphatase 2B, S: Serine, SENP5: SUMO Specific Peptidase 5, T: threonine; (Cho et al. 2013).

2.2.2. DRP1 receptors

While DRP1's translocation to mitochondria is well regulated by its post-translational modifications, consequence of its translocation is related to the receptor with which it interacts. In fact, many receptors exist on the outer mitochondrial membrane. DRP1's interaction with these receptors leads to fission complexes.

Classically, mitochondrial fission was thought to be only induced by the interaction between DRP1 and FIS1. However, in a study by Otera et al. in 2010, a conventional knockout of FIS1 did not cause a mitochondrial fission deficiency leading to think that other factors could compensate FIS1's role and that the latter is not an essential member of the fission machinery (Otera et al. 2010). Of these other factors, in the same study, the MFF factor was identified. It can form complexes with DRP1 and lead to mitochondrial fission. Afterwards, Palmer et al. in 2011 (Palmer et al. 2011; Liu et al. 2013) identified and characterized MiD49 and MiD51. These two proteins share 45% of amino acids identity. Furthermore, Zhao et al. discovered MIEF1, a protein identical to MiD51. Effectively, these proteins can form complexes with DRP1 on the outer mitochondrial membrane. In contrast, they block mitochondrial fission by sequestrating DRP1. Another way for these receptors to block mitochondrial fission is by sequestrating FIS1; therefore it can no longer interact with DRP1. This

was indeed proven by overexpressing FIS1, which partially reduced the inhibitory effect of MIEF1/MiD51 on DRP1. These findings led to the discovery of the extended model of mitochondrial fission regulation illustrated in (Fig. 12) (Dikov and Reichert 2011).

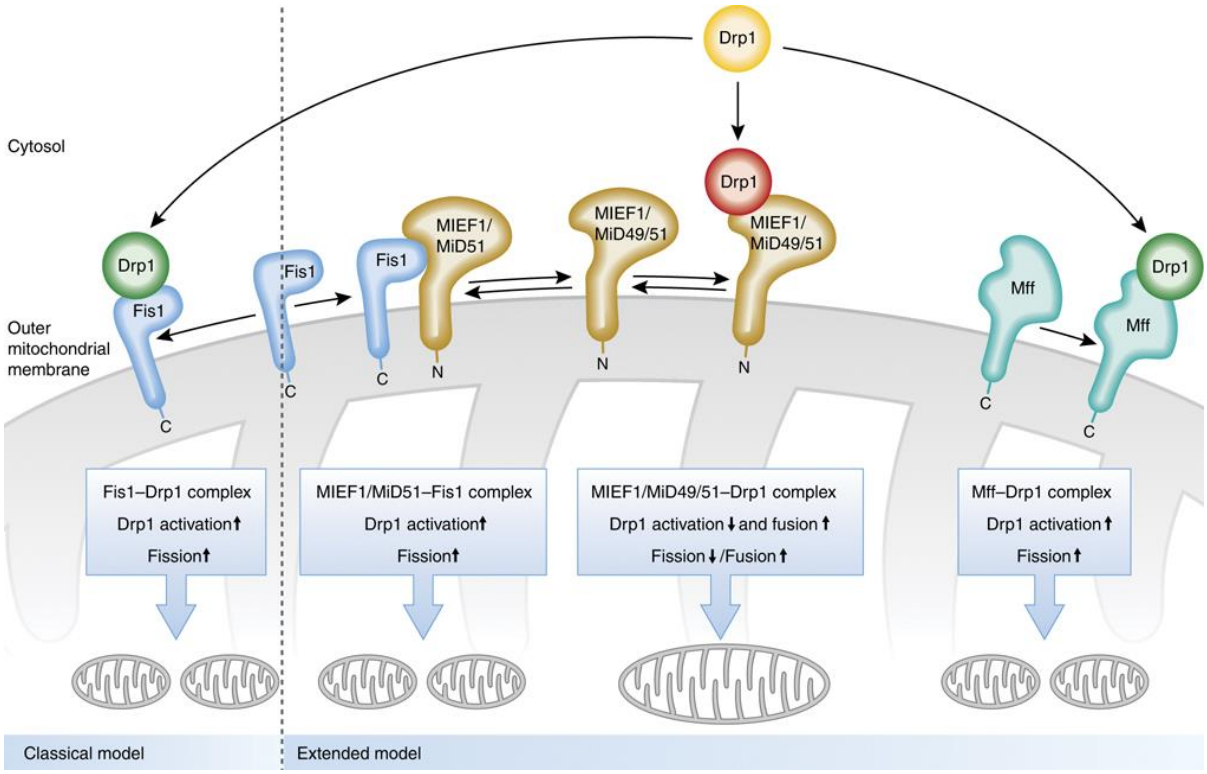

Figure 12: Mitochondrial fission regulation in mammals due to DRP1's interaction with its different receptors. Drp1: Dynamin related protein 1, Fis1: Mitochondrial fission 1 protein, MIEF/MiD: Mitochondrial Elongation Factor, Mff: mitochondrial fission factor; (Dikov and Reichert 2011).

2.2.3. Mechanism of mitochondrial fission

Mitochondrial fission is a multistep process illustrated in Figure 13 (Fig. 13). Mitochondrial division requires a step of pre-constriction ensured by the endoplasmic reticulum (ER). In fact, replication of the mtDNA marks the site for ER recruitment. Afterwards, and since DRP1 is a cytosolic protein, this mechano-enzyme has to be dynamically recruited to mitochondria. DRP1 monomers or dimers are in constant balance between the cytosol and mitochondria. They assemble into spiral/rings shaped oligomers with an outer diameter of 30 nm and an inner diameter of 20 nm at the mitochondria-ER contacts in a Ca^{2+} dependent process. Interestingly, a mutation in the central domain inhibits DRP1 oligomerization (Haun, Nakamura, and Lipton 2013). This shows the importance of this domain in allowing Drp1 to form ring-like oligomer structures at the outer membrane of mitochondria. It is worth noting that many factors are involved in the recruitment of actin and myosin to fission sites, essential actors in the fission inducing machinery.

At future fission sites, DRP1 interacts with MFF, FIS1 and its other receptors. GTP hydrolysis enhances the ring like structure by inducing conformational changes. Here, another protein is recruited, Dynamin 2 (Dnm2). The latter assembles and terminates membrane scission mediated by the DRP1 mitochondrial constriction neck forming two daughter mitochondria.

The mechanisms by which the two mitochondria get rid of the fission machinery are still unclear. Nevertheless, studies proved the existence of both DRP1 and its receptors on both mitochondrial tips after division (Tilokani et al. 2018).

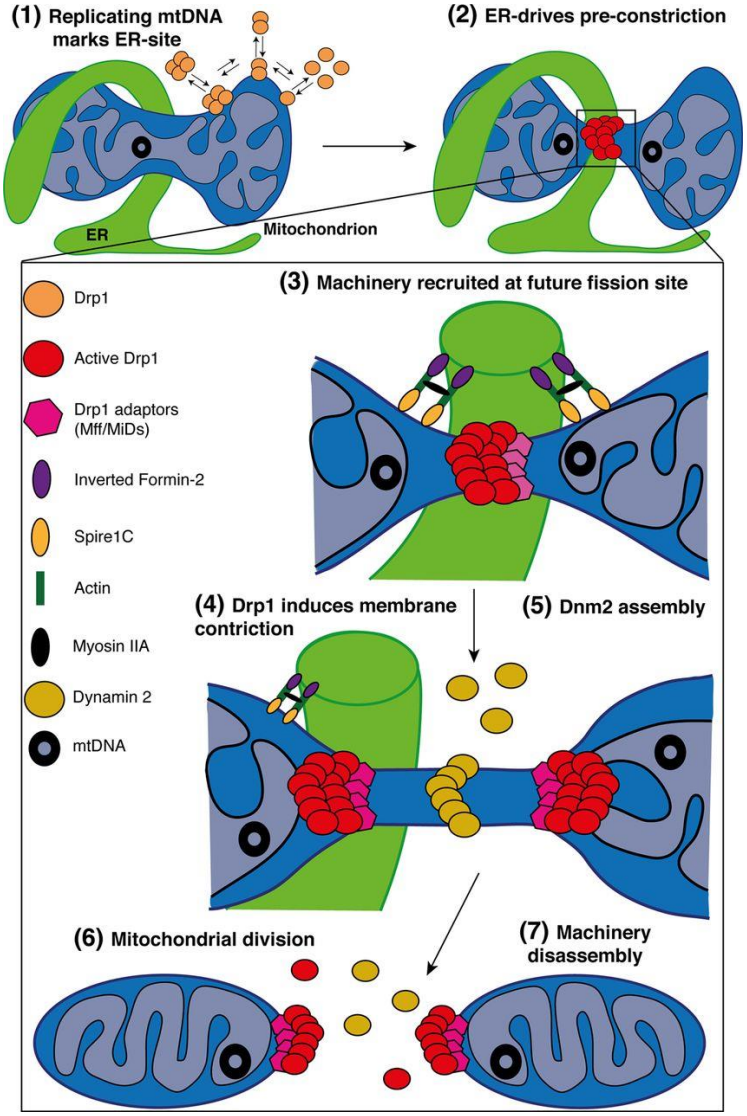

Figure 13: Mitochondrial fission process in mammals (Tilokani et al. 2018).

2.2.4. Mitochondrial autophagy (mitophagy)

Before damaged organelles trigger apoptosis or necrosis, a cell can eliminate them selectively via autophagy. The latter is a highly regulated process used to eliminate defective cell components like macromolecules, organelles, even mitochondria. Mitochondria have a crucial role inside a cell and stringent quality control is necessary to ensure the preservation of a healthy mitochondrial

network. When mitochondria are found defective or containing too much mitochondrial DNA mutations, they are eliminated via a more selective autophagy process called mitophagy (Cadete et al. 2019).

4 different phases are carried out in autophagy: nucleation, elongation, sequestration, and degradation. The mechanism is initiated by formation of the phagophore (**nucleation**). This requires the Unc-51 Like Autophagy Activating Kinase 1 (ULK1) complex and the class III phosphoinositide 3-kinase (PI3K) complex. Afterwards, microtubule-associated protein light chain 3 (LC3I), initially located in the cytoplasm is lipidated and forms LC3II. The latter promotes the **elongation** of the phagophore and the double-membrane structure autophagosome is formed. Nucleoporin p62 (p62) is a protein bound to ubiquitinated proteins (ubiquitination labeling marks proteins that are targeted for degradation) and it binds to LC3II during the formation of the autophagosome as intracellular materials are engulfed into the forming autophagosome (**sequestration**). Subsequently, the autophagosome fuses with a lysosome, which contains hydrolytic enzymes indispensable for the **degradation** of the dysfunctional intracellular material (Fig. 14). During myocardial I/R, autophagy is activated. As a matter of fact, the autophagy-related proteins, beclin 1, and LC3I are activated by ROS, calcium, and MPTP opening (Ndoye and Weeraratna 2016).

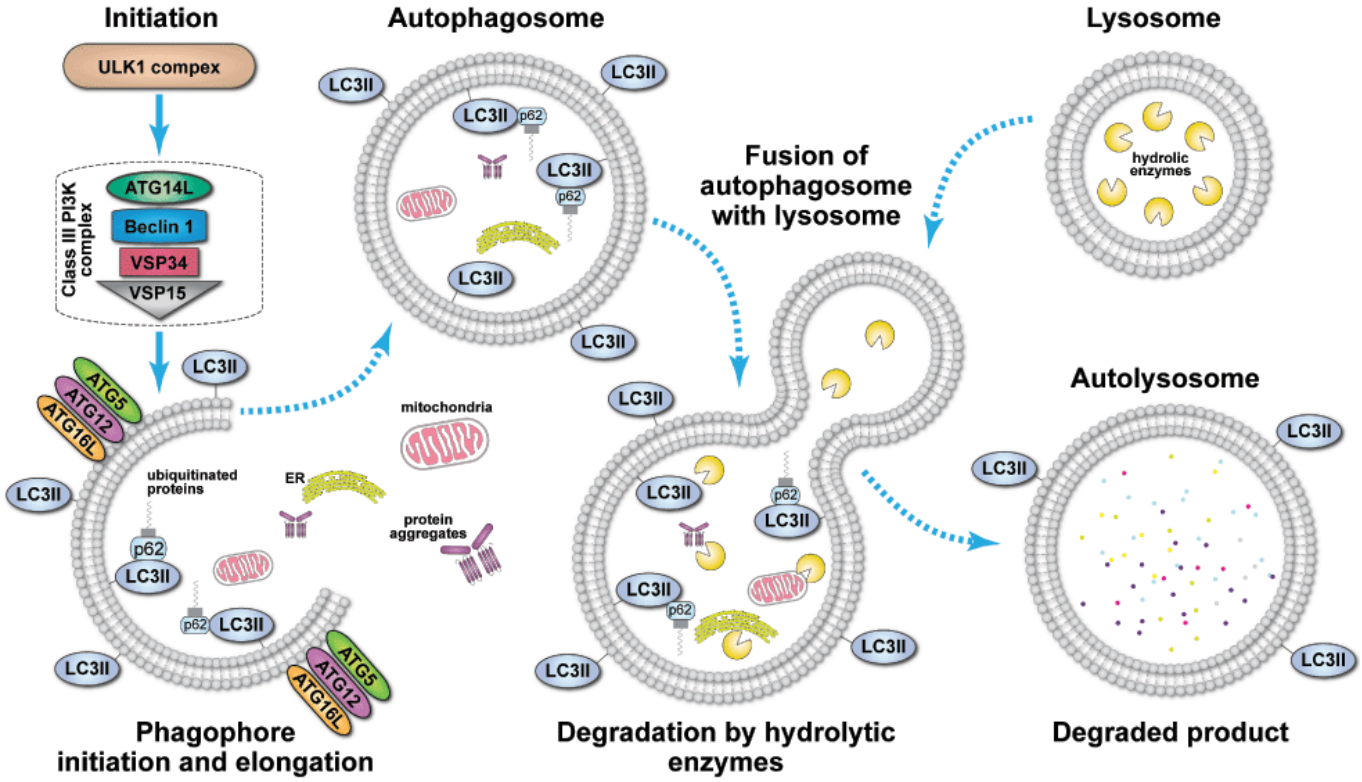

Figure 14: Schematic representation of autophagy process. PI3K: phosphoinositide 3-kinase, ULK1: Unc-51 Like Autophagy Activating Kinase 1, ATG: autophagy related, LC3: microtubule-associated protein light chain 3, p62: Nucleoporin p62 (Ndoye and Weeraratna 2016).

Mitochondrial fission is an essential step in dissociating damaged mitochondria from the rest of the mitochondrial network. However, in this process, fission is called asymmetrical because one mitochondrion is left with a high membrane potential and the defective one is left with a low membrane potential unable to re-fuse with other mitochondria. Once the defective mitochondrion is isolated, mitophagy, the specific autophagy of mitochondria, can take place. Four pathways have been identified that detect dysfunctional mitochondria and recruit autophagosomes for degradation. The most well-known pathway is PTEN-induced kinase (PINK1)/Parkin-mediated mitophagy (Anzell et al. 2018).

PINK1 is a protein containing a mitochondrial targeting domain and, once translated, is translocated into the intermembrane space through the translocase of the outer mitochondrial membrane. In healthy mitochondria, PINK1 mitochondrial concentrations are kept low (Truban et al. 2017). PINK1 integrates the inner mitochondrial membrane via insertion into the translocase of the inner mitochondrial membrane and is rapidly degraded by the mitochondrial membrane peptidase and presenilin-associated rhomboid-like protease (PARL) (Matsuda, Kitagishi, and Kobayashi 2013). However, the import of proteins through the inner mitochondrial membrane relies on steady mitochondrial membrane potential. During ischemia, for example, a decrease in mitochondrial membrane potential is observed. Therefore, PINK1 is no longer inserted into the mitochondria, is no longer degraded and accumulates on depolarized mitochondria. Subsequently, it will phosphorylate and activate different types of proteins like Parkin (Iguchi et al. 2013), an E3 ubiquitin ligase, ubiquitin, and TANK-binding kinase 1 (TBK1). When activated, Parkin will ubiquitinate many outer mitochondrial membrane proteins including mitofusins and VDAC. In fact, PINK1 can phosphorylate MFN2, the mitochondrial fusion protein, transforming it into a receptor for Parkin, which will in turn promote mitophagy furthermore. Moreover, PINK1 can phosphorylate TBK1 which promotes the phosphorylation of three different autophagy adaptor proteins: p62 or the Sequestosome 1 (SQSTM1), optineurin (OPTN), and nuclear dot protein (NDP52). p62 ensures the aggregation of dysfunctional mitochondria. OPTN and NDP52 serve as receptors for the phagophore via ubiquitin and LC3 binding domain (Anzell et al. 2018; Chen and Dorn 2013).

Other pathways that can be utilized to ensure the integrity of the mitochondrial network but will not be detailed in this manuscript are: BCL2 Interacting Protein 3 (BNIP3)/Nix, FUN14 Domain Containing 1 (FUNDC1) and cardiolipin dependent mitophagy. In all cases, these proteins serve as an anchor for the binding of the LC3 present on phagophores and therefore ensure the degradation of damaged mitochondria (Fig.15) (Anzell et al. 2018).

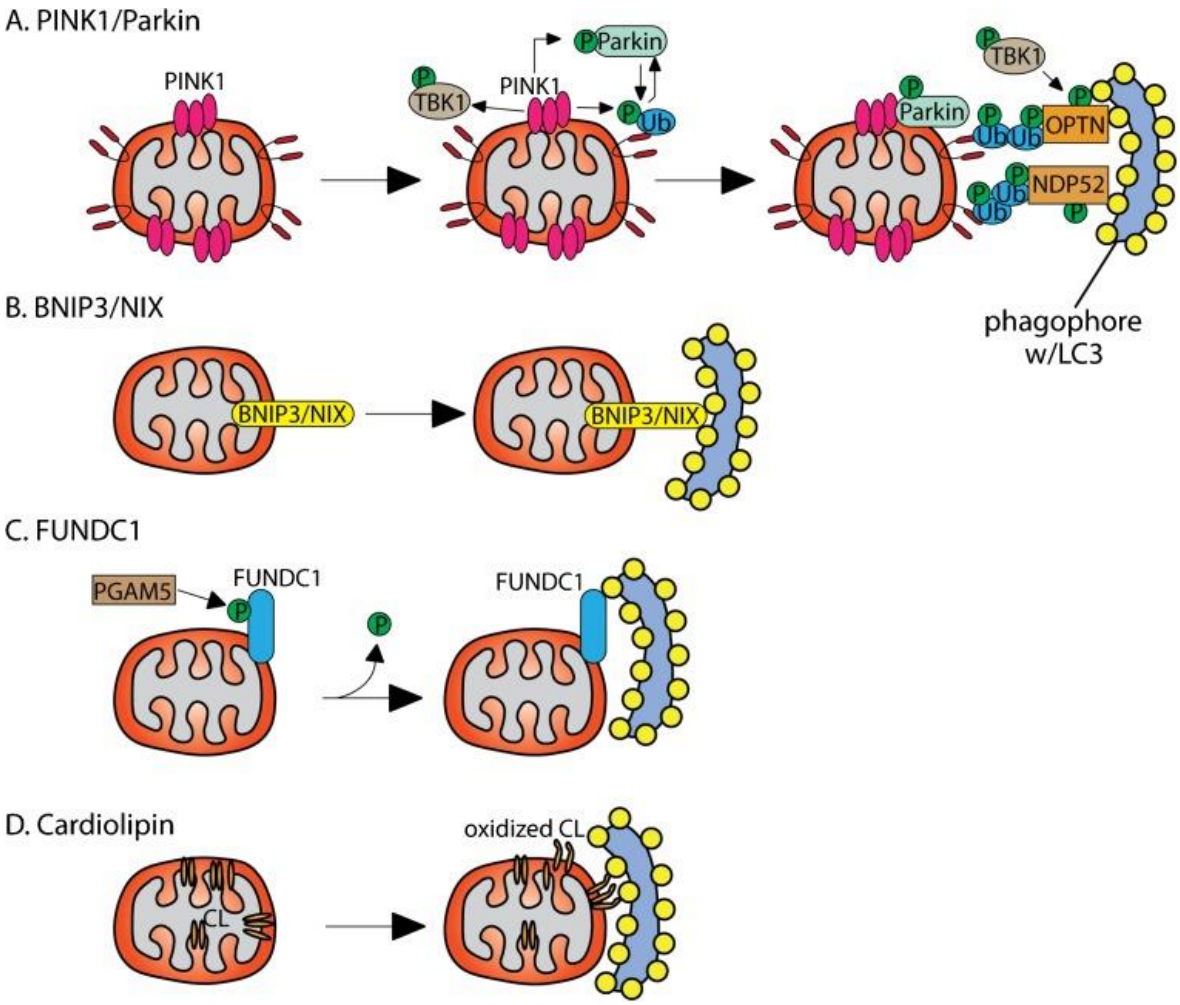

Figure 15: Different pathways of mitophagy inside a cell. PINK1: PTEN-induced kinase 1, TBK1: TANK binding kinase 1, OPTN: optineurin, NDP52: nuclear dot protein 52, LC3: Microtubule-associated proteins light chain 3, BNIP3: BCL2 Interacting Protein 3, FUNDC1: FUN14 Domain Containing 1, CL: Cardiolipin, P: Phosphorylation, Ub: ubiquitination (Anzell et al. 2018).

2.3. Mitochondrial fusion

Mitochondrial fusion is the union of two mitochondria to form one larger mitochondrion. This process requires a coordinated fusion of both outer and inner mitochondrial membranes accompanied by GTP hydrolysis. OPA1 governs the mitochondrial inner membranes fusion. And, the mitofusins 1 and 2 (MFN1 and MFN2) are responsible for the fusion of external mitochondrial membranes. It is a process that allows the transfer and mixing of the components (including mitochondrial DNA) of two mitochondria, an event that can salvage function in damaged mitochondria (Hoppins and Nunnari 2009).

2.3.1. Mitofusines 1 and 2 (MFN 1, 2)

MFN1 and 2 are 85 kDa transmembrane GTPases proteins coded by nuclear genes, belonging to the dynamin superfamily and sharing 80% of sequence homology in humans. Mammalian mitofusins were first discovered by Santel and Fuller in 2001 (Santel and Fuller 2001). They comprise

a COOH-terminal, two transmembrane domains, and a coiled-coil domain 2 (also called heptad repeated domain or HR2). Both of these proteins are regulated by post-translational modifications, mainly phosphorylations and acetylations (Fig.15) (Adaniya et al. 2019). They are located on the outer mitochondrial membrane with a special structure where they span the outer mitochondrial membrane twice, leaving a loop in the intermembrane space and exposing both of the GTPase domain and the HR2 domain to the cytosol. Furthermore, between the HR1 and the TM domain in MFN2 but not in MFN1 a proline rich zone exist, presumably assumed essential for MFN2-specific protein-protein interactions. These GTPases accumulate at contact areas between two adjacent mitochondria, establish homo (MFN1-MFN1 or MFN2-MFN2) or heterotypic (MFN1-MFN2) complexes, and lead to mitochondrial fusion (Hoppins and Nunnari 2009; Hales 2004).

Other than their role in ensuring mitochondrial fusion, MFN2 has reportedly more functions than MFN1. It is also localized at the ER where it plays a role in regulating its structure, function and calcium uptake. It can tether mitochondria to the ER and therefore regulate mitochondrial calcium uptake released by the ER (Merkwirth and Langer 2008).

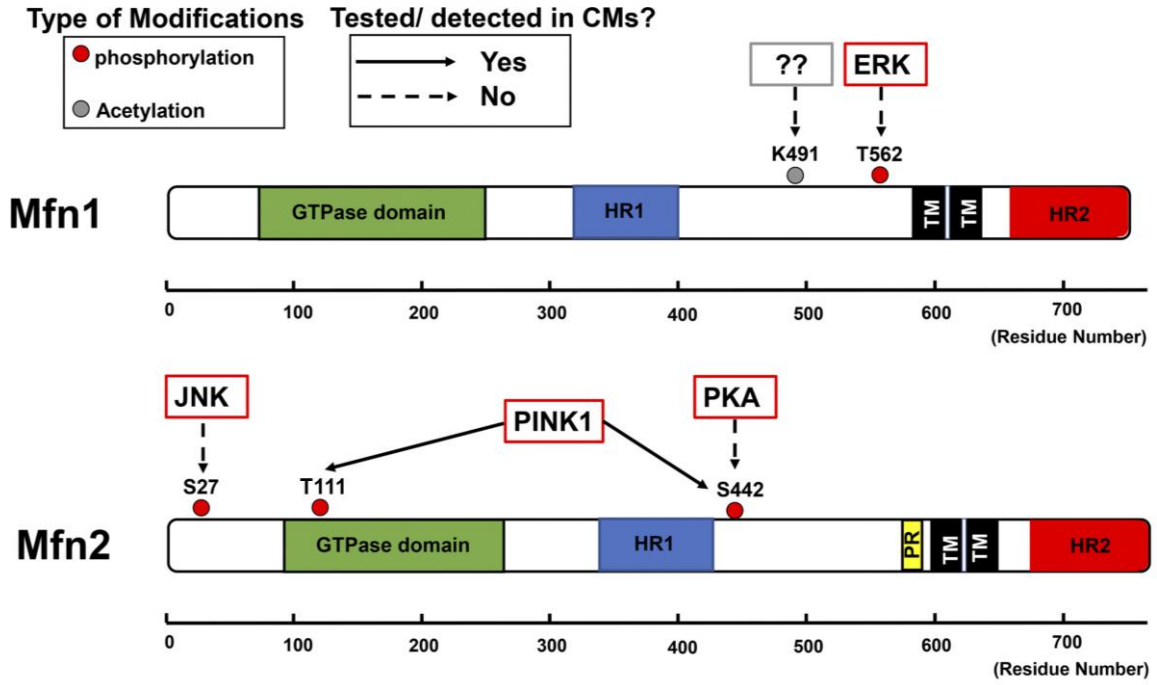

Figure 16: Mitofusins structure and post-translational modification sites with arrows indicating proteins potentially implicated in these modifications in cardiomyocytes. ERK: extracellular signal-regulated kinases, HR: heptad-repeat domain, K: Lysine, Mfn1, 2: Mitofusin 1 and 2 respectively, PINK1: phosphatase and tensin homolog (PTEN)-induced putative kinase 1, PKA: protein kinase A, PR: proline-rich domain, S: serine, T: Threonine, TM: transmembrane domain; (Adaniya et al. 2019).

2.3.2. Optic atrophy factor 1 (OPA1)

OPA1 is an approximately 100kDa dynamin GTPase protein coded by the *opa1* nuclear gene. Alternative splicing of exons 4, 4b, and 5b leads to the formation of 8 different isoforms in humans and 5 different ones in mice. Their expression is tissue-dependent (Delettre et al. 2001). All isoforms primarily present the same structure shown in figure 17 (Fig. 17). OPA1 has the classical structure of a dynamin protein. It is inserted in the inner mitochondrial membrane via an approximately 100 residues NH_2-terminal matrix targeting signal (mitochondrial import sequence: MIS). Following the targeting sequence, a transmembrane domain is found, leaving the rest of the protein exposed to intermembrane space. The rest of the protein is formed by a GTPase domain, a middle domain, and a GTPase effector domain containing a coiled-coil region (Belenguer and Pellegrini 2013).

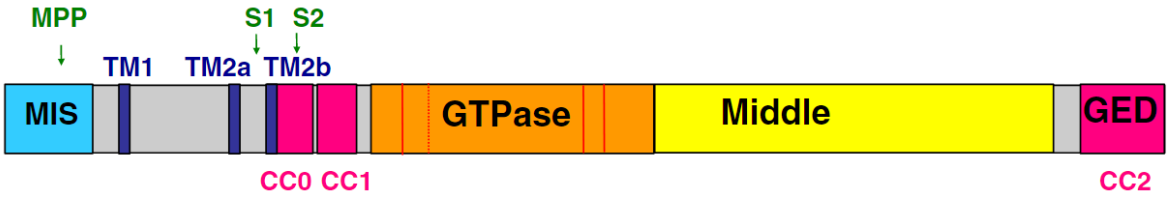

Figure 17: Schematic presentation of OPA1 protein structure. GED: GTPase effector domain, MIS: mitochondrial import sequence, MPP: mitochondrial processing peptidase, S1/S2: sites for proteolytic cleavage, TM: Transmembrane, CC: coiled-coil region (Belenguer and Pellegrini 2013).

Once OPA1 is imported to the mitochondria, a mitochondrial processing peptidase (MPP) removes the MIS. Furthermore, OPA1 harbors at least two sites for proteolytic cleavage (S1 and S2) by membrane bound metalloproteases. Therefore, two isoforms are found: L-OPA1 (Long form) and S-OPA1 (short Form). In an immunoblot, 5 different OPA1 bands are distinguished. The first two bands with a higher molecular weight are long forms of L-OPA1, and the three other fragments correspond to the short isoform S-OPA1. In healthy conditions, the 5 different bands are expressed in an equitable manner. However, stress conditions leading to mitochondrial dysfunction are characterized by a decrease in the long form expression (Adaniya et al. 2019).

Initially it was assumed that both isoforms are necessary to induce mitochondrial fusion since L-OPA1 alone and S-OPA1 alone have little fusion activity. However recent studies showed that S-OPA1 alone is not capable of inducing mitochondrial fusion, whereas L-OPA1 alone can ensure inner mitochondrial fusion (Tilokani et al. 2018).

Post-translational modifications can occur on specific residues regulating OPA1's activity. For instance, an O-GlcNAcylation of OPA1 can inhibit its activity and lead to mitochondrial fragmentation (Makino et al. 2011).Moreover, during stress conditions, a hyperacetylation of lysine residues 926 and 931 can decrease OPA1's GTPase activity (Samant et al. 2014).

Other than its essential and indispensable role in ensuring inner mitochondrial membrane, OPA1 is implicated in cristae remodeling and regulating their function. As a matter of fact, cytochrome C, an important molecule inducing apoptosis, is localized in the cristae (Varanita et al. 2015). Therefore, OPA1 by keeping cristae tightly closed, inhibits its release in the cytosol during apoptosis. Moreover, as mentioned beforehand, the mitochondrial respiratory chain complexes form supercomplexes and are localized in the cristae. The layout of the cristae can highly affect the efficiency of electron transfer and ATP production. Hence, if cristae's closed structure is lost, the supercomplexes assembly is lost and mitochondrial respiration is altered leading to mitochondrial dysfunction (Chen et al. 2009).

2.3.3. Mechanism of mitochondrial fusion

Mitochondrial fusion illustrated in figure 18 (Fig. 18) debuts with a Trans-interaction between either HR2 or GTPase domains of MFN1 and MfN2 proteins. Once dimers are formed, GTP is hydrolyzed, inducing MFNs conformational changes. The latter event leads to mitochondrial docking and to an increase in membrane contact sites. Subsequently, a GTPase-dependent power stroke pulls outer mitochondrial membrane together and induces their fusion.

OPA1 and cardiolipin (CL) drive the mitochondrial inner membrane fusion, downstream the union of the outer membranes. It is worthy to note that OPA1 localization in the intermembrane space allows it to interact with the MFNs proteins to coordinate mitochondrial fusion. Indeed, OPA1-CL complex tether the two inner mitochondrial membranes. Thereof fusion happens after OPA1-dependent GTP hydrolysis allowing mixing of mitochondrial components.

All components of the mitochondrial fusion machinery remain expressed on the outer and inner mitochondrial membrane, however in a dissembled form (Tilokani et al. 2018).

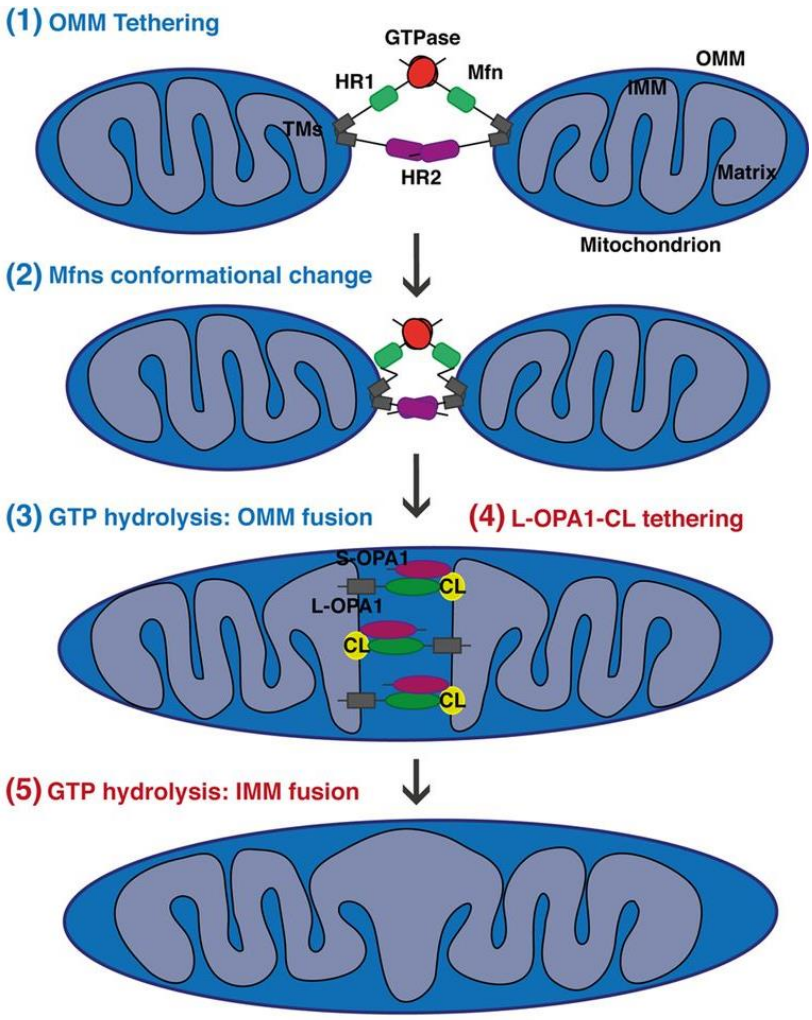

Figure 18: Schematic Illustration of mammalian mitochondrial fusion. CL: cardiolipin, IMM: inner mitochondrial membrane, HR: heptade repeat, OMM: outer mitochondrial membrane, TM : transmembrane ; (Tilokani et al. 2018).

3. Mitochondrial dynamics in the heart

The aforementioned importance of mitochondria is even greater in cardiomyocytes, where they occupy 30% of cell volume and produce ATP through oxidative phosphorylation, an indispensable molecule to cardiomyocyte contractility. In fact, the heart is the most mitochondrial-rich mammalian organ and is exquisitely dependent on these double-membrane organelles. It is called an oxidative muscle since 90% of the produced energy is generated by the mitochondrial oxidative phosphorylation (Schaper, Meiser, and Stammler 1985; Vasquez-Trincado et al. 2016).

Inside a cardiomyocyte we can find 3 populations of mitochondria with different functions depending on their localization (Fig. 19) (Ong et al. 2017):

-Subsarcolemmal mitochondria localized right underneath the sarcolemma are responsible for providing the energy for ion channel function and are involved in cell signaling.

-Perinuclear mitochondria are clustered next to the nucleus and are required to provide energy for transcription.

-Interfibrillar mitochondria (constituting the majority of myocardial mitochondria), are aligned next to the myofibrils. These mitochondria are implicated in calcium signaling between the sarcoplasmic reticulum and mitochondria and are also responsible for generating ATP essential for the myofibrils contraction.

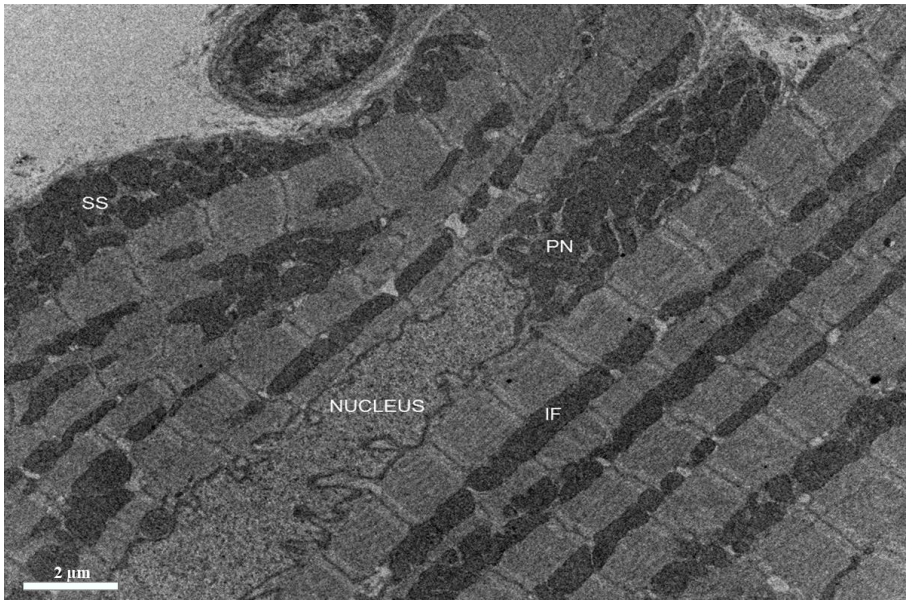

Figure 19: Electron microscopy image depicting mitochondrial populations inside a cardiomyocyte. SS: Subsarcolemmal, PN: Perinuclear, IF: Interfibrillar; (Source: SCIAM, Angers).

Taking into consideration all of the functions maintained by mitochondria, it is not surprising that mitochondria are considered key players in cardiomyocyte cell death after stress like a myocardial ischemia. Mitochondria can drive cellular dysfunction and cell death actively and passively, actively through apoptosis and programmed necrosis, and passively through the generation of ROS responsible of cell toxicity (Murphy, Marsh, and Smith 1987; Kane et al. 1975). Hence, maintenance of mitochondrial function and structure integrity is indispensable in cells with high energy demands.

In the heart, as mitochondria become tightly packed into myofibrils bundles, they do not form networks as seen in other cell types. They are relatively static, constrained in their ability to move and in close contact. Of course they still would be active but at a much slower rate (Piquereau et al. 2013). Despite the fact that they exhibit less frequent dynamic changes, an inhibition of fission leads to enlarged mitochondria and an inhibition of fusion leads to fragmented mitochondria, both of which having functional consequences on the myocardial function (Papanicolaou et al. 2011; Papanicolaou et al. 2012; Ong et al. 2010; Chen and Knowlton 2011). Moreover, the expression of the

mitochondrial dynamics proteins are essential to mammalian life as already proven by many authors. In fact, a homozygous genetic deletion of OPA1 (Piquereau et al. 2012), MFN1, 2 (Song et al. 2015) or DRP1 (Ikeda et al. 2015) leads to prenatal death.

3.1. DRP1 in cardiomyocytes

DRP1 knockout mouse is embryonically lethal at embryonic day 11.5 (Wakabayashi et al. 2009). This shows the importance of DRP1 in embryonic development. Unlike OPA1, heterozygous DRP1 knockout mice, do not show phenotypical differences compared to their wildtype littermates. Moreover and even if knockout is induced directly after birth or at a later stage, it has been shown that a cardiac specific homozygous knockout of DRP1 ($Drp1^{-/-}$) is lethal due to dilated cardiomyopathy associated to a cardiac dysfunction. However heterozygous knockout $Drp1^{+/-}$ mice are viable (Ishihara et al. 2009). Nevertheless, DRP1's localization is of greater importance than its quantity in ensuring apoptosis, mitophagy and mitochondrial fission. Indeed, the high demand on oxidative phosphorylation in the heart requires an adequate removal of damaged mitochondria to maintain both integrity and function of the mitochondrial network. When DRP1 is inhibited, asymmetrical fission is interrupted retaining impaired mitochondria that fuse with similarly impaired mitochondria instead of being eliminated. This could lead to either a widespread activation of mitophagy evoking mitochondrial loss, or stimulate mitophagy that is interrupted before lysosomal fusion (Ikeda et al. 2015; Kageyama et al. 2014). Moreover an alteration in mitochondrial respiration as well as acceleration in mPTP opening has been linked to DRP1's inhibition. DRP1's homozygous inhibition leads to altered cardiac function which ultimately leads to lethality. In human, only one case of *Drp1* mutation was reported (Waterham et al. 2007) until 2016, where three new heterozygous mutations were documented. In all of the aforementioned cases, these mutations lead to severe lethal dysfunctions.

3.2. OPA1 in cardiomyocytes

Mice with a homozygous deficiency in OPA1 die *in* utero (Piquereau et al. 2012). This confirms the importance of OPA1 in embryonic development. In order to investigate the role of OPA1 in mice adult heart, heterozygously deficient mice were generated ($OPA1^{+/-}$). The myocardial characterization of this genetically modified model, showed a decrease in OPA1's expression, an enlargement in mitochondria, and a disruption in cristae. This dysregulation in mitochondria's function and organization led to a mild cardiac phenotype at 3 and 6 months. This phenotype worsened at 12 months, leading to heart failure. Otherwise, only one model showed the opposite effect of OPA1 inhibition, meaning an overexpression of OPA1 (*opa1* gene knocked in after actin β promoter). These mice, even though being viable, developed a cardiac hypertrophy at 9 months without a left ventricular dysfunction (Alavi et al. 2007; Piquereau et al. 2012).

In human, OPA1 was first discovered associated to autosomal dominant optic atrophy (ADOA) (Delettre et al. 2000). Later on, Spiegel et al. (Spiegel et al. 2016), described a homozygous mutation in *Opa1* gene in two young sisters. This mutation provoked a multisystem impairment of which hypertrophic cardiomyopathy.

Taking into consideration all that has been mentioned, it can be concluded that mitochondrial dynamics proteins are crucial actors in fetal development, fetal cardiac development, and in maintaining mitochondrial function in the heart. For review, table 2 recapitulates studies describing the effects of inhibiting mitochondrial fusion and fission proteins in the heart *in vivo* (Table 2) (Adaniya et al. 2019).

Reference	Targeted Protein	Model	Cardiac Phenotype	Mitochondrial Morphology	Mitochondrial Function	Other Notes
Kageyama et al. (94); Song et al. (179)	Drp1	CM-specific (*Myh6* nuclear-directed Cre) KO after birth	Neonatal cardiomyopathy (94); modestly enlarged hearts (179)	Connected or enlarged mitochondria (94)	Mitochondrial respiration ↓ (94); Parkin-independent mitophagy signaling ↑ (94)	Died at 1–1.5 wk (94); died by 6 wk (179)
Song et al. (179)	Drp1	Inducible CM-specific (*Myh6* MER-Cre-MER) KO (132)	At 6–7 wk after Drp1 deletion, DCM, CM necrosis, cardiac fibrosis, and HF	Elongated and enlarged mitochondria	mPTP opening ↑; Parkin-dependent mitophagy signaling ↑	
Ikeda et al. (82)	Drp1	Inducible CM-specific (α-MHC-MER-Cre-MER) homozygous KO	At 4–8 wk after Drp1 deletion, cardiac hypertrophy, CM apoptosis, cardiac fibrosis, and HF	Elongated mitochondria	ATP ↓; mPTP opening ↑; ROS ↑; autophagic flux ↓	Died at 8–13 wk after Drp1 deletion
Ikeda et al. (82); Shirakabe et al. (176)	Drp1	CM-specific (α-MHC) heterozygous KO	Cardiac function at 12 wk →; cardiac hypertrophy at 5 days after TAC ↑; HF at ~4 wk after TAC	Elongated mitochondria; after TAC, enlarged mitochondria at ~24 h and ~4 wk and fragmented mitochondria at 3–5 days	Susceptibility to I/R injury ↑; after 3–5 days of TAC, mitophagy ↑, ATP ↓, and mitochondrial respiration ↓	Homozygous mice: embryonic lethal
Ishihara et al. (85)	Drp1	Muscle-specific (*Mck*) KO	Neonatal cardiomyopathy	Connected or enlarged mitochondria	Mitochondrial respiration ↓	Died at 1–1.5 wk
Piquereau et al. (153)	OPA1	Heterozygous mutation (329–355del, $OPA1^{+/-}$)	Cardiac function at 6 mo →; LV hypertrophy after TAC ↑	Enlarged mitochondria; cristae disorganization	Mitochondrial respiration →; time to reach Ca^{2+}-induced mPTP opening ↑	
Chen et al. (27)	OPA1	Heterozygous mutation (Q285 Stop, $OPA1^{+/-}$)	Cardiomyopathy and HF at 12 mo	Disorganized and fragmented mitochondria ↑; cristae structure ↓	Mitochondrial respiration ↓; ATP ↓; ROS ↑	No apoptotic CM death; homozygous mice: embryonic lethal

Table 2: Effect of mitochondrial fusion and fission proteins ablation *in vivo* models. CM: cardiomyocyte, DCM: dilated cardiomyopathy, DKO: double knockout, DRP1: dynamin-related protein-1, E9.5:embryonic day 9.5, HF: heart failure, I/R: ischemia-reperfusion, KO: knockout, LV: left ventricular, Mck: muscle creatine kinase, MER: modified estrogen receptor, Mff: mitochondrial fission factor, Mfn1 and Mfn2: mitofusin 1 and 2 respectively, MHC: myosin heavy chain, mPTP: mitochondrial permeability transition pore, Myh6: myosin, heavy polypeptide 6 cardiac muscle, Nkx2.5: NK2 homeobox 5, OPA1: optic atrophy protein-1, ROS: reactive oxygen species, SR: sarcoplasmic reticulum, TAC: transverse aortic constriction (Adaniya et al. 2019).

3.3. Mitochondrial dynamics and myocardial ischemia/reperfusion injuries

Mitochondria are highly abundant and sensitive organelles in the heart. And by playing their dual role in being both primary sources of ATP but also of ROS, they have a leading role in I/R injuries since mitochondrial shape tightly regulates its function. They are an important modulator of bioenergetics, ROS production, cell death, calcium signaling… all of which are important events in myocardial I/R injuries (Neubauer 2007).

It was Brady et al. (Brady, Hamacher-Brady, and Gottlieb 2006) that first studied the morphology of mitochondria in the heart after I/R and found extensive fragmentation of mitochondria in HL-1 cells during a sustained episode of simulated ischemia and the simulated reperfusion afterwards. HL-1 cells are a murine atrial derived cardiac cell line. In this study, the link between DRP1, mitochondrial fragmentation and I/R injuries was not made. It was in 2010 that Ong et al. used a dominant negative construct of DRP1 also in a HL-1 cell line to demonstrate that inhibiting mitochondrial fission was cardioprotective and maintained the integrity of the mitochondrial network. Mechanisms underlying excessive mitochondrial fission during ischemia are still unclear. Nonetheless, a calcium overload and an excessive ROS production can be causal factors (Ong et al. 2010).

Therefore, the conventional notion has always been that small mitochondria are 'bad' and large mitochondria are 'good'. Thus, a genetic or a pharmacological interruption of DRP1 meaning, respectively, its expression or activity should decrease I/R injuries. Likewise, an overexpression of mitochondrial fusion proteins such as MFN1, MFN2, or OPA1 should protect cells or the heart from I/R injuries. Nonetheless, a lot of discrepancies in this subject exist which will be detailed in the following segment.

3.3.1. DRP1 and ischemia/reperfusion injuries

DRP1, a pivotal protein in mitochondrial fission, became a therapeutic target in treating myocardial I/R injuries after noticing DRP1's translocation to mitochondria and inducing mitochondrial fission following a sequence of ischemia. Numerous studies were conducted on models where DRP1 was pharmacologically or genetically inhibited in order to understand its role in I/R injuries. Many reviews extensively explain all the different findings in DRP1 inhibition models (Dorn 2015a; Hall et al. 2014).

In 2010, Ong et al. were one of the first to study the effect of DRP1 inhibition. When overexpressing a dominant negative mutant of DRP1 in HL-1 cell line (*Drp1K38A*) the mitochondrial network was less fragmented after a simulated hypoxia/reoxygenation (H/R). The use of a pharmacologically active molecule named mitochondrial division inhibitor-1 (Mdivi-1) also decreased mitochondrial fragmentation (Ong et al. 2010). Mdivi-1 is a molecule discovered in 2008 that was reported to inhibit DRP1 assembly on the outer mitochondrial membrane (Cassidy-Stone et al. 2008). Treating adult

cardiomyocytes with mdivi-1 reduced cell death and inhibited mitochondrial permeability transition pore opening after simulated I/R injury. Mdivi-1 also reduced myocardial infarct size in mice subjected to *in vivo* myocardial I/R by coronary artery occlusion. Similar results were reported by Din et al. in neonatal rat cardiomyocytes and by Sharp et al. in neonatal murine cardiomyocytes and adult rat hearts, where mdivi-1 was used before ischemia (Din et al. 2013; Sharp et al. 2014). On the contrary, in 2016 Dong el al. reported that an administration of mdivi-1 at reperfusion was not capable of reproducing its beneficial effects aforementioned (Dong, Undyala, and Przyklenk 2016). In addition, inhibiting mitochondrial fission using mdivi-1 in heart specific $Drp1^{+/-}$ deficient mice protected these mice of myocardial I/R injuries (Ikeda et al. 2015). This makes mdivi-1 specificity and clinical application quite controversial.

Other pharmacological inhibitors were also used and reported results were somewhat concordant. Dynasore is a dynamin inhibitor. Pre-treating isolated mice heart with the latter reduced myocardial infarct size and mitochondrial fragmentation after 30 minutes ischemia followed by one hour of reperfusion (Gao et al. 2013). P110, an inhibitor of DRP1-FIS1 interaction, administrated at reperfusion decreased myocardial infarct size in rat. This was was explained by a decrease in mitochondrial fragmentation, an improvement of mitochondrial function, and of left ventricular function (Disatnik et al. 2013). FK506 is an inhibitor of a phosphatase calcium and calmodulin-dependent, calcineurin, The latter, by dephosphorylating DRP1 on S637 increases its mitochondrial translocation and induces subsequently mitochondrial fission. FK506 was administrated 10 minutes before a sequence of 30 minutes ischemia and 20 minutes of reperfusion and was capable of decreasing fission and preserving cardiac hemodynamics *ex vivo* (Sharp et al. 2014).

Genetically inhibiting DRP1 specifically in the heart homozygously or heterozygously, increased these mice susceptibility to myocardial I/R injuries. This result was explained by a decrease in mitophagy (Ikeda et al. 2015).

One of many explanations to the differences seen in all the conducted studies is the time lapse of DRP1 inhibition. Indeed, an acute DRP1 inhibition using pharmacologically active molecules seems to be beneficial in reducing myocardial I/R injuries, whereas a genetically chronic inhibition of DRP1 leads to cardiac dysfunction, hence in these genetically modified models, speaking of myocardial I/R injuries becomes obsolete.

3.3.2. OPA1 and ischemia/reperfusion injuries

OPA1's role in non-fusion mechanism made it a target for cardioprotection. Chen et al. conducted two studies in 2009 and 2012. In both cases, they highlighted cells increase of sensitization to H/R injuries when OPA1 was downregulated. In fact, a simulated ischemia on a cardiomyoblast cell line (H9C2), increased mitochondrial fragmentation, cytochrome C release and apoptosis in cells treated with OPA1 siRNA (Chen et al. 2009). In 2012, an increase of ROS production was observed

after one hour of hypoxia and one hour of reoxygenation in $OPA1^{+/-}$ cardiomyocytes (Chen et al. 2012).

Overexpressing Opa1 in H9C2 cells did not reduce H/R injuries. Different results were found when another group of scientists studied OPA1 overexpression's effect. Mice overexpressing OPA1 were more resistant to an ischemia of 40 minutes followed by 15 minutes of reperfusion when compared to their wildtype littermates *ex vivo*. This protection was associated with a stabilization of OPA1 long isoform (L-OPA1) (Varanita et al. 2015).

Since OPA1 KO mice are not viable, studies were conducted on a heterozygous deficient mouse model $OPA1^{+/-}$. Piquereau et al. showed that even though, at baseline, cardiac function of $OPA1^{+/-}$ was comparable to that of WT, altered morphology of the $Opa1^{+/-}$ mice mitochondrial network was observed with larger mitochondria and altered cristae as well as a decreased sensitivity to mitochondrial calcium accumulation and eventual mPTP opening. When challenged with transversal aortic constriction, $Opa1^{+/-}$ hearts demonstrated a greater hypertrophy than in wild-type mice with an altered ejection fraction 6 weeks later (Piquereau et al. 2012). In our lab, we studied cardiac morphology and function as well as mitochondrial function at baseline and OPA1's implication in myocardial I/R injuries in $OPA1^{+/-}$ (Le Page et al. 2016). Cardiac left-ventricular systolic function was not altered after OPA1 downregulation. However after myocardial I/R, $OPA1^{+/-}$ exhibited a greater infarct size compared to WT. A lower sarcoplasmic reticulum Ca^{2+} uptake, and an increased cytosolic Ca^{2+} removal by the Na^{+}/Ca^{2+} exchanger could have been causal.

Chapter 3:
The Kynurenine pathway

1. Tryptophan : an essential amino acid

Tryptophan (TRP) is the least abundant of all essential amino acids. It is plant-derived and one of the 9 essential amino acids for the human body. This means that the human body is unable to synthetize it, but have to obtain it through diet. It accounts for approximately 1% of total amino acids in cellular proteins. Its serum concentration is maintained at 50-100µM by a liver metabolism. Like most other amino acids, it can be present under two stereoisomers, L-tryptophan and D-tryptophan (Wang et al. 2015).

TRP, once absorbed by the body, travels around the periphery circulation under two forms: a free form or bound to albumin. The two states exist in equilibrium with the bound form accounting for 90% of circulating TRP. To cross over the blood-brain barrier, TRP has to be transported in its free form by the competitive and non-specific L-type amino acid transporter (Chen and Guillemin 2009).

TRP is necessary for animal protein synthesis. Its incorporation into proteins is initiated by tryptophanyl-transfer RNA synthetase (TRPRS). It is a building block for numerous life-giving biomolecules, like enzymes, structural proteins, serotonin, melatonin, and neurotransmitters. Moreover, TRP is, sometimes, also the sole source of bioactive molecules that facilitate the generation of a range of crucial molecules. In addition, TRP residues play special roles in anchoring membrane proteins within the cell membrane. It plays a role in many diseases and conditions in the animal and human health. TRP is recognized for being involved in the body's regulation of sleep. Therefore, it is widely used in alternative medicine as treatment for insomnia by normalizing sleep patterns since. It is also used as treatment for anxiety, and depression. TRP is capable of enhancing relaxation and sleep, by soothing nerves and anxiety (Jenkins et al. 2016).

2. Metabolic pathways of tryptophan

During the course of its degradation, TRP is the precursor of many physiologically important molecules. It can be catabolized along 4 different pathways: (a) decarboxylation (Tryptamine); (b) transamination (indolepyruvic acid); (c) hydroxylation (serotonin and 5-hydroxytryptamine in the brain, and melatonin in the pineal gland); (d) oxidation (the kynurenine (KYN) pathway). The two most known and most studied catabolic routes are the serotonin and the kynurenine pathway (Drsata 2003; Le Floc'h, Otten, and Merlot 2011).

2.1. Serotonin pathway

The serotonin pathway is the transformation of TRP into serotonin. The rate-limiting enzyme of this pathway is the tryptophan hydroxylase (TPH). It catalyzes the conversion of tryptophan into 5-hydroxytryptophan (5-HTP), the immediate precursor of serotonin (5-hydroxytryptamine or 5-HT). Afterwards, within the pineal gland, serotonin is acetylated and then methylated to yield melatonin.

Serotonin is produced in platelets and neurons whereas melatonin is mainly produced within the gut (Fig.20) (Fouquet et al. 2019).

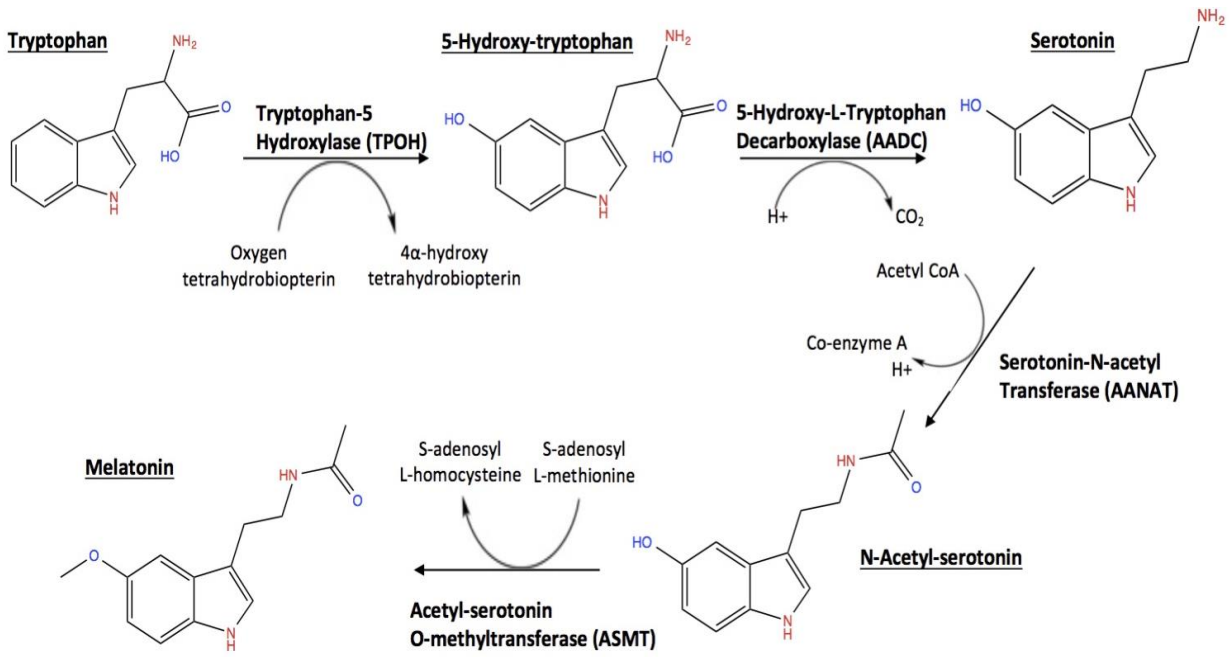

Figure 20: The serotonin pathway to metabolize tryptophan into serotonin and further along into melatonin. Adapted from (Bubenik and Konturek 2011).

Serotonin or 5-hydroxytryptamine (5-HT) is a monoamine neurotransmitter, with approximately 14 variants of serotonin receptors in human. 10% of total serotonin is synthesized in serotonergic neurons of the central nervous system where it is widely recognized as a substance primarily involved in regulating the mood. In fact, low serotonin levels have been linked to depression (the reason why sometimes serotonin is called the happy chemical). Other biological functions include modulating cognition, reward, learning, memory, anxiety, sleep, temperature, eating behavior, sexual behavior, movements, gastrointestinal motility and numerous physiological processes. In fact, approximately 90% of the human body's total serotonin is located in gastrointestinal tract cells, where it regulates intestinal motility. Last but not least, serotonin contributes to the formation of blood clots. It is released by platelets resulting in vasoconstriction, reducing blood flow and facilitating coagulation (Jenkins et al. 2016).

2.2. Kynurenine pathway

The less well known but the main alternative route for TRP metabolism is the kynurenine pathway. In fact, 95% of TRP is converted into KYN and its breakdown products (Wang et al. 2015). Research studies addressing this pathway started around 50 years ago, initially to try to understand its role in the biosynthesis of the nicotinamide adenine dinucleotide (NAD^+), and $NADP^+$, both of which

are co-factors participating in basic cellular reactions (Nath and Shastri 1970). In the past couple of years, it became an area of growing interest where the kynurenine pathway enzymes became target of several drug discovery efforts. Recent evidence suggests that the kynurenine pathway is implicated in modulation of inflammation, immune function. In fact, its enzymes are activated by these immune-inflammatory responses (Wang et al. 2015).

This route exists mainly in the liver, which contains all the enzymes necessary for nicotinic acid synthesis from TRP and accounts for more than 90% of TRP metabolism in human and animals. We can also find the kynurenine pathway extra-hepatically, although only the hepatic pathway includes all the enzymes required for nicotinic acid synthesis. The extrahepatic pathway however is only responsible for 5%–15% of TRP degradation compared to the hepatic one (Badawy 2017). The kynurenine pathway produces many metabolites, and co-factors: $NAD^+(P)^+$ and the reduced form NAD(P)H; nicotinamide and nicotinic acid or vitamin B_3; N-methyl-D-aspartate agonist and antagonist, respectively known as quinolinic acid (QA) and kynurenic acid (KYNA); and many other biologically active molecules. An outline of the kynurenine pathway is given in figure 21 (Fig. 21).

TRP availability, enzyme activities and other factors control the fate and the metabolism of TRP. Once it has been ingested, it is oxidized to N-Formyl-kynurenine (Nfk) by either tryptophan 2,3-dioxygenase (TDO) or indoleamine-pyrrole 2,3-dioxygenase IDO 1, 2. This is the first and the rate limiting reaction of the KYN pathway in mammals. TDO is a liver specific isoform of the enzyme, known as tryptophan oxygenase and L-Tryptophan pyrrolase. IDO is present in other cell types as an alternative inducible enzyme. Both TDO and IDO belong to the family of oxidoreductases. The expression of TDO is induced by TRP and by steroids, whereas IDO's expression is induced by inflammatory cytokines such as interferon (IFN)-γ, tumor necrosis factor (TNF)-α, Lipopolysaccharides (LPS) (Wang et al. 2015)

The next step is a spontaneous reaction, the decomposition of Nfk into formic acid and KYN. Afterwards, KYN can me metabolized into two main branches by various enzymes. This leads to the production of at least two neuroactive metabolites namely KYNA and QA.

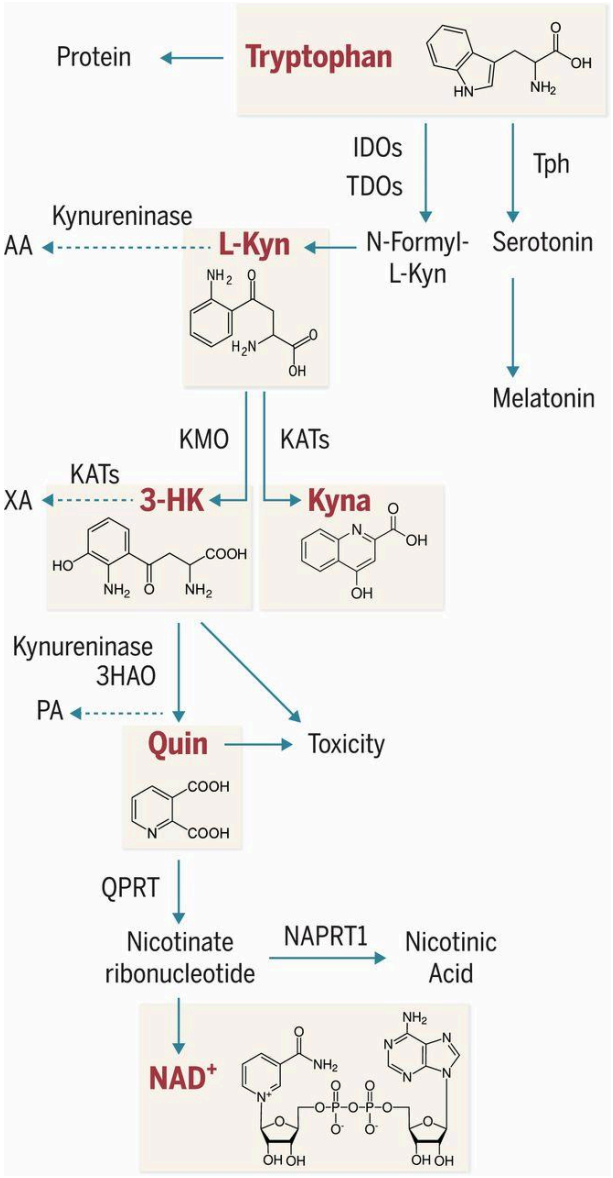

Figure 21: Tryptophan metabolic pathways. TRP metabolism can either lead to protein synthesis, serotonin and melatonin synthesis, or degradation into the kynurenine pathway which leads to the formation of kynurenic acid or nicotinamid adenosine dinucletotide (NAD^+). 3HAO: 3-hydroxyanthranilic acid oxygenase, NAPRT1: nicotinate phosphoribosyltransferase, AA: anthranilic acid; (Cervenka, Agudelo, and Ruas 2017).

Kynureninase produces anthranilic acid from KYN, and KYN-3-hydroxylase (KYN-3-monooxygenase (KMO)) transforms KYN into 3-hydroxykynurenine (3-OHKYN). Both of these products are then converted to 3-hydroxy-anthranilic acid. The latter is then metabolized to form the neurotoxic compound: QA. Quinolinate phosphoribosyl transferase (QPRT) catalyzes several additional biochemical reactions to produce niacin and subsequently to NAD^+ as end product. NAD^+ can be reversibly converted to NADH by the addition of two electrons and one proton to the nicotinamide ring. NAD^+ and NADH are both co-enzyme indispensable for a large number of biochemical cellular reactions (Sas, Szabo, and Vecsei 2018).

Another less occurring metabolizing route of KYN is its transformation into KYNA by the KYN aminotransferases (KAT). KYNA production can be catalyzed by three types of KAT: KAT I, KAT II, KAT III, and mitochondrial aspartate aminotransferase (miAAT) (KAT IV) (Stone and Darlington 2002).

TRP, KYN, and 3-OHkyn readily cross the blood-brain barrier. Therefore the effects of systemic TRP on the brain's kynurenine pathway are in part dependent on its conversion into KYN and 3-OHKYN, and the subsequent entry of these metabolites into the brain. However, due to the polar nature and the lack of efficient transport processes, KYNA and QA penetrate the blood-brain barrier poorly and must be formed within the brain directly (Gobaille et al. 2008; Fukui et al. 1991).

2.2.1. Characteristics of major enzymes of the kynurenine pathway

TDO is exclusively present in the liver and is specific for L-TRP. **IDO**, however, is extrahepatic and can oxidize D-TRP, but also other substrates like indoles, and indoleamines. IDO is localized in a specific manner to serve two main functions. The first one is to ensure a depletion of TRP in an enclosed environment to prevent bacterial and viral infection mediating an antiproliferative effect especially on infectious microorganism that may rely on TRP for growth. The second one is to produce TRP catabolites that suppress immune responses against self-antigens, fetal antigens, or allogenic antigens. Therefore, IDO is thought to be part of the innate immune system (Gupta et al. 1994). Furthermore, it has been shown that IDO inhibition reduces NAD^+ synthesis and promotes cell death, showing the importance of the kynurenine pathway in NAD^+ homeostasis. Additionally IDO expression is upregulated by pro-inflammatory cytokines which shunts the metabolism of TRP towards KYN. It is worthy to note that this enzyme in its inactive form lacks in species like cat, gerbil, golden hamster, and guinea pig. Therefore, they suffer from a toxicity of excessive TRP. Subsequently, rats and mice are the most common animal models in TRP-related studies (Sas, Szabo, and Vecsei 2018).

KMO is a β-nicotinamide adenine dinucleotide 2'-phosphate (NADPH)-dependent flavin monooxygenase, localized in the outer mitochondrial membrane. KMO possesses a high affinity for its substrate, meaning that KYN is usually metabolized into 3-OHKYN. This affinity and its position make it a target in treating neurodegenerative disorders where the kynurenine pathway is implicated (Thevandavakkam et al. 2010).

KAT produce irreversibly, from L-KYN, the only endogenous antagonist of the NMDA receptor, KYNA. KAT I and KAT III have been reported to be expressed in different type of tissues including, the kidney, liver, heart, lung… KAT II is more studied in the rat and human brain, and mitKAT (KAT IV) in the mouse brain (Han et al. 2010).

QPRT belongs to the phosphoribosyltransferase (PRT) family and is an essential enzyme in the synthesis of NAD^+ using QA as a precursor in both prokaryotes and eukaryotes. QPRT plays a prominent role in ensuring QA homeostasis in the brain. Hence, a dysregulation of the QPRT enzyme activity increases QA levels. This have been proved to be strongly involved in several severe neurodegenerative disorders including Huntington's disease, Alzheimer's disease, and Epilepsy… (Youn et al. 2016)

The main functions of the kynurenine pathway and the enzymes responsible for each task are summarized in Table 3. These functions take place in the liver but in other tissues and body fluids. One more activity should be added to this table which is the role of the KAT in KYNA synthesis (Badawy 2017).

FUNCTION	ENZYME(S) RESPONSIBLE
1. Detoxification of excess Trp	TDO
2. Control of hepatic heme biosynthesis	TDO
3. Control of plasma Trp availability	TDO (physiological conditions)
	IDO (immune activation)
4. Production of kynurenines	TDO/IDO → 3-HAAO
5. Production of picolinic acid	ACMSD
6. Production of NAD^+	QPRT → NAD synthetase
7. Production of niacin	QPRT → NADase and PARP

Table 3: Functions of some enzymes of the kynurenine pathway. ACMSD: 2-amino-3-carboxymuconate-6-semialdehyde decarboxylase or picolinate carboxylase, HAAO: hydroxyanthranilic acid oxygenase, IDO: indoleamine 2,3-dioxygenase, NAD^+: oxidized nicotinamide adenine dinucleotide, NADase: NAD^+ glycohydrolase, PARP: poly-(ADP-ribose) polymerase, QPRT: quinolinate phosphoribosyl transferase, TRP: tryptophan, TDO: TRP 2,3-dioxygenase; (Badawy 2017).

2.2.2. Kynurenine pathway metabolites

a) Kynurenine

KYN is the first metabolite produced in the kynurenine pathway of tryptophan degradation. It contains an aromatic cycle that gives it a hydrophobic characteristic. It has pro-oxidant effects: an aerobic irradiation of KYN produces superoxide radicals. In fact, ROS-induced cell death of natural killer cells, has been linked to increased levels of KYN: KYN availability in the brain depends on TRP metabolism but even more on KYN being transported from the periphery (Goda, Hisaoka, and Ueda 1987).

b) Kynurenic acid

Generation of KYNA has been described in the following cell types: endothelial cells (Stazka et al. 2002), fibroblasts (Asp et al. 2011), skeletal muscle cells (Agudelo et al. 2014)... In general, and under physiological conditions, KATs catalyze the irreversible transamination of KYN to form KYNA. It is also worth to note, that in the presence of ROS, KYN is catalyzed to generate KYNA (Baran et al. 1997).

Kessler and co-workers identified KYNA as an endogenous antagonist of the NMDA receptors (and, to date, is the sole known one) at the glycine co-agonist site (Kessler et al. 1989). It is also a noncompetitive inhibitor of the α-7 nicotinic acetylcholine receptor (Anderson and Maes 2017). Accordingly, dysregulation in endogenous KYNA concentration contributes to the pathophysiology of many disorders, mostly documented in the brain (Fujigaki, Yamamoto, and Saito 2017).

Unlike KYN, KYNA is unable to cross the blood-brain barrier, and has to be formed locally within the brain (Fukui et al. 1991). KYNA is not only found in brain tissue, but also in periphery and is a ligand to other receptors like the G protein-coupled receptor 35 (GPR35) (Wang et al. 2006) and the aryl hydrocarbon receptor (AhR) (DiNatale et al. 2010). When bound to GPR35, KYNA can modulate cAMP production and inhibit the N-type Ca^{2+} channels of sympathetic neurons and astrocytes (Guo et al. 2008). Concerning the AhR receptor signaling, KYNA has immunomodulatory effects where it plays an important role in terminating cytokine release in several cell types like macrophages (Baglole et al. 2008). The NMDA receptor antagonist also exerts antioxidants properties (Lugo-Huitron et al. 2011). Overall, KYNA is an important neuromodulator and an endogenous antioxidant due to its activity on receptors and to its redox characteristics as a ROS scavenger (Fig. 22). Authors like Rozsa et al. and Wirthgten et al. (Wirthgen et al. 2017; Rozsa et al. 2008) have called it a Janus-faced compound in brain physiology. This was in reference to Janus, a god in Greek mythology, usually depicted as having two faces, since he looks to the past and to the future. Same thing is said when it comes to KYNA. Because, even though it is essential to limit the neurotoxicity of excitatory amino acids, and to scavenge ROS, high levels of KYNA are associated to cases like schizophrenia and other neurological and psychiatric diseases implicating cognitive deficits due to impairment in glutamergic and/or cholinergic neurotransmission (Schwarcz et al. 2012).

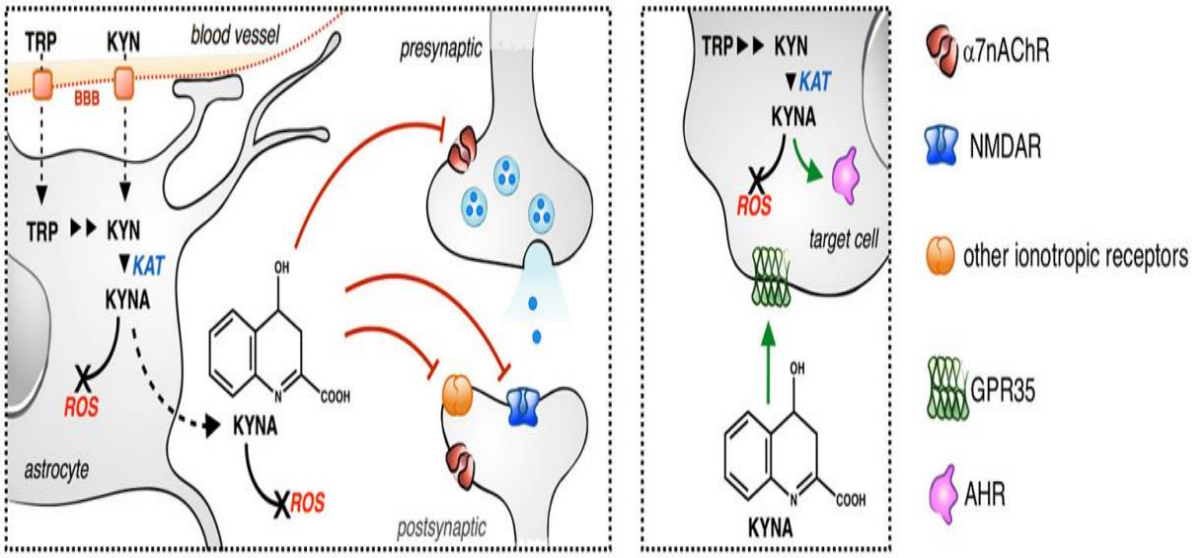

Figure 22: Different effects and actions of kynurenic acid inside and outside the nervous system. AHR: aryl hydrocarbon receptor, BBB: blood brain barrier, GPR35: G protein-coupled receptor 35, KAT: kynurenine aminotransferase, KYN: kynurenine, KYNA: kynurenic acid, NMDAR: N-methyl-D-aspartate receptor, ROS: reactive oxygen species, TRP: tryptophan; (Rossi et al. 2019).

N-methyl-D-aspartate (NMDA) receptors

Most of the excitatory neurotransmission is mediated by a vesicular glutamate release. The NMDA receptors belong to the glutamate receptors. They are ligand-gated ion channels that mediate a Ca^{2+}-permeable component of excitatory neurotransmission in the central nervous system. Glycine, a co-agonist, is essential to ensure the glutamate neurotransmission (Fig. 23) (Hansen et al. 2018). These receptors are expressed in the central nervous system, and have been proven to exist in the heart as well (Leung et al. 2002). They have been shown implicated in both cerebral and myocardial I/R injuries. As a matter of fact, the calcium increase caused by these receptors can be detrimental to the cell. It can induce an increase in ROS levels, cytochrome C release, and a depolarization of the mitochondrial membrane, all of which leading to cell apoptosis (Gao et al. 2007). Therefore an antagonism as well as an agonism should be well regulated to ensure an adequate excitatory neurotransmission

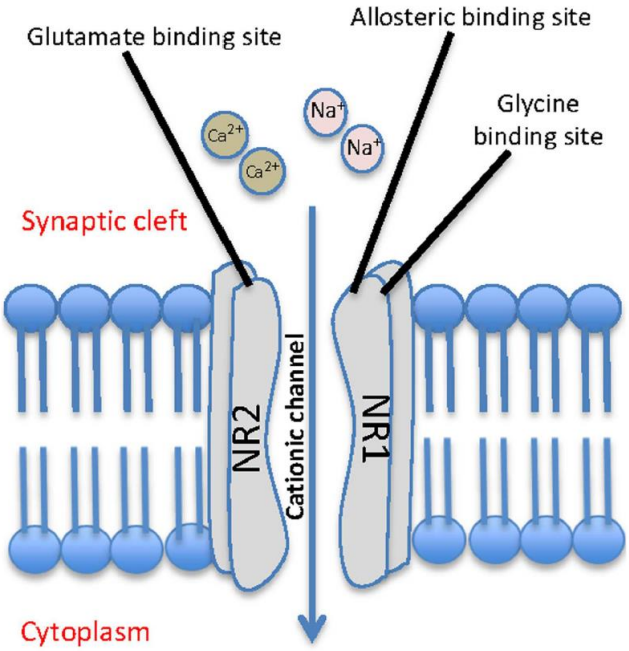

Figure 23: Structure and activation of the N-methyl-D-aspartate (NMDA) receptor formed of two subunits: NR1 and NR2. NMDA cationic channel opening leads to an inward flow of positively charged ions (Lakhan, Caro, and Hadzimichalis 2013).

G-protein coupled receptor 35 (GPR35)

G protein coupled receptor 35 (GPR35) is, as it is mentioned by its name, a receptor coupled to a G-protein. It has long been considered as an orphan receptor meaning that no endogenously produced ligand has been associated with activating it. It was first discovered in 1998 (O'Dowd et al. 1998) and was not, until recently, de-orphanized (Civelli et al. 2013). Using calcium mobilization assays, synthetic and endogenous ligands for GPR35 were found (Oka et al. 2010; Wang et al. 2006) of which, as previously mentioned, KYNA. A Gα-dependent signaling was associated with GPR35 (Fig. 24) (Mackenzie et al. 2011). In fact, using p-ERK1/2 immunoblotting, a kinase that phosphorylates threonine and tyrosine residues, ligand activation of GPR35 was demonstrated. For instance, 2-oleoyl lysophosphatidic acid (Oka et al. 2010) and tyrphostin-51 (Deng, Hu, and Fang 2011) were recognized as GPR35 agonists using this type of experiment.

A study performed both *in vitro* (neonatal mouse cardiomyocytes) and *in vivo* (left anterior descending (LAD) coronary artery ligation mouse model, and a transversal aortic constriction mouse model) showed that hypoxia (a feature of most chronic cardiac pathologies) was capable of inducing a HIF-1 dependent GPR35 gene expression. An overexpression of the latter can modulate cardiomyocyte morphology. The study also showed that GPR35 expression is an early marker of progressive myocardial remodeling in mice and concluded that GPR35 could be used as a novel predictive marker of cardiac failure (Ronkainen et al. 2014). No differences in cardiac phenotype were found when a group of researchers characterized a GPR35 deficient mouse model comparing it to its wild-type littermate. However, this strain of mice was resistant to an increase in systolic,

diastolic and mean arterial blood pressure in contrast to their wild-type littermate (Divorty et al. 2018). GPR35 expression was upregulated in myocardial tissue from hearts of patients suffering of cardiac failure, compared to healthy controls. In addition, GPR35 was selected with eleven other genes for follow up analysis in patients suffering of heart failure (Min et al. 2010). Putting all these data together from different studies, the importance of GPR35 in cardiovascular diseases emerges.

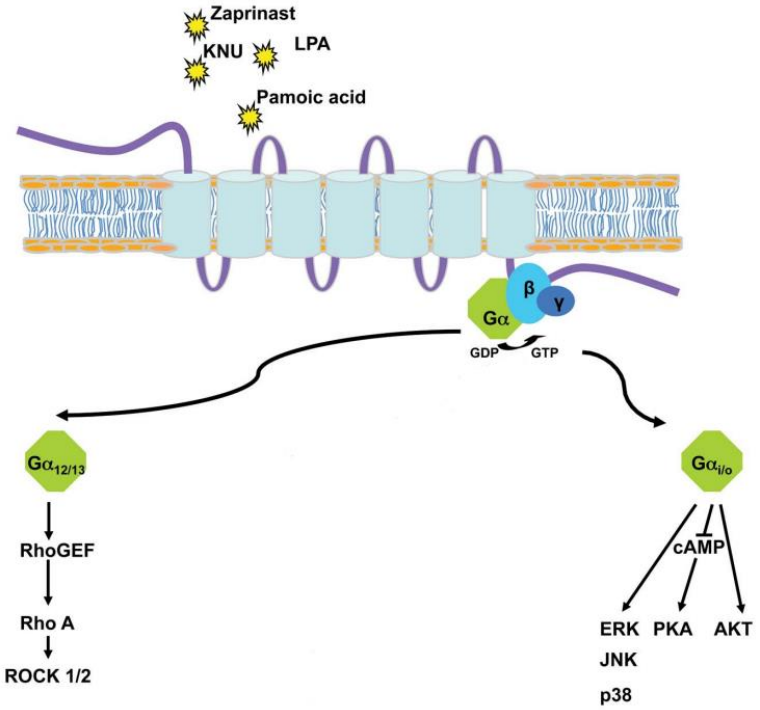

Figure 24: Endogenously ($G_{12/13}$, $G_{i/0}$) used signaling pathways by GPR35. KNU: kynurenic acid, LPA: lysophosphatidic acid; Adapted by (Mackenzie et al. 2011).

Aryl hydrocarbon receptor (AhR)

The aryl hydrocarbon receptor (AhR) is a ligand dependent transcriptional factor widely expressed in many cell types like immune, endothelial, epithelial... (Carlstedt-Duke 1979). This receptor exists in the cytoplasm in an inactive form within a heat shock protein 90 (Hsp90):p23:hepatitis B virus X-associated protein 2 (XAP2): Proto-oncogene tyrosine-protein kinase (Src) chaperone multiprotein complex. Once the ligand binds to this receptor, the complex dissociates and AhR heterodimerizes to the aryl hydrocarbon receptor nuclear transporter (ARNT) in order to promote the transcription of many genes, for example: the cytochrome P450-dependent monooxygenase Cyp1a1, the AhR repressor (AhRR), and interleukin 22 (IL-22) (Larigot et al. 2018). KYNA dimerization with the AhR receptor stimulates the generation of many inflammatory cytokines. In addition, AhR activation upregulates IDO suggesting the existence of a positive feedback loophole (Noakes 2015).

c) Quinolinic acid

QA is the precursor of the *de novo* (main) pathway of NAD^+ and nicotinic acid synthesis (Yang and Sauve 2016). QA is an agonist of the NMDA receptors. It has the same potency as glutamate bound to the NMDA receptor, can persist in the synaptic cleft for a longer period due to less efficient reuptake, which can increase its neurotoxic effects (Guillemin 2012). Moreover, it can disrupt the blood brain barrier, induce a deregulation of the oxidant/antioxidant balance, increase oxidative stress and produce mitochondrial dysfunction, all of which eventually result in cell death (Bordelon et al. 1997; Santamaria et al. 2001; Guillemin 2012). Therefore, QA is considered as a high potency neurotoxin *in vivo*. A deregulation in the oxidant/antioxidant ratio is generated by several mechanisms: QA can affect the ratio of reduced glutathione: oxidized glutathione (Glutathione is an antioxidant enzyme) (Leipnitz et al. 2005), it can also deplete the activity of the copper-and zinc-dependent SOD activity (Rodriguez-Martinez et al. 2000), and can also contribute to lipid peroxidation (Rodriguez et al. 1999).

2.2.3. NAD^+ synthesis

Two main NAD^+ synthesis pathways exist in the cell: The *de novo* pathway and the salvage pathway (Fig. 25) (Walker and Tian 2018). The salvage pathway, which will not be detailed in this manuscript, is the synthesis of NAD^+ from a nicotinic acid or nicotinamide turnover. The *de novo* pathway is the synthesis of NAD^+ from QA (Yang and Sauve 2016).

As a matter of fact, the main hepatic function of the kynurenine pathway is to generate redox factors such as NAD^+ and $NADP^+$. The latter is formed by the action of NAD^+ kinase. Both forms, oxidized and reduced, of these dinucleotides have important roles in cellular signaling pathways and are therefore essential to cell function (Goody and Henry 2018). In the kynurenine pathway, QA formation is favored on KYNA formation. Hence, NAD^+ synthesis from QA or TRP is quantitatively more important than that from nicotinamide or nicotinic acid. In fact, findings show that dietary TRP is more effective than dietary nicotinamide or nicotinic acid in elevating liver nicotinamide dinucleotides (Badawy 2017).

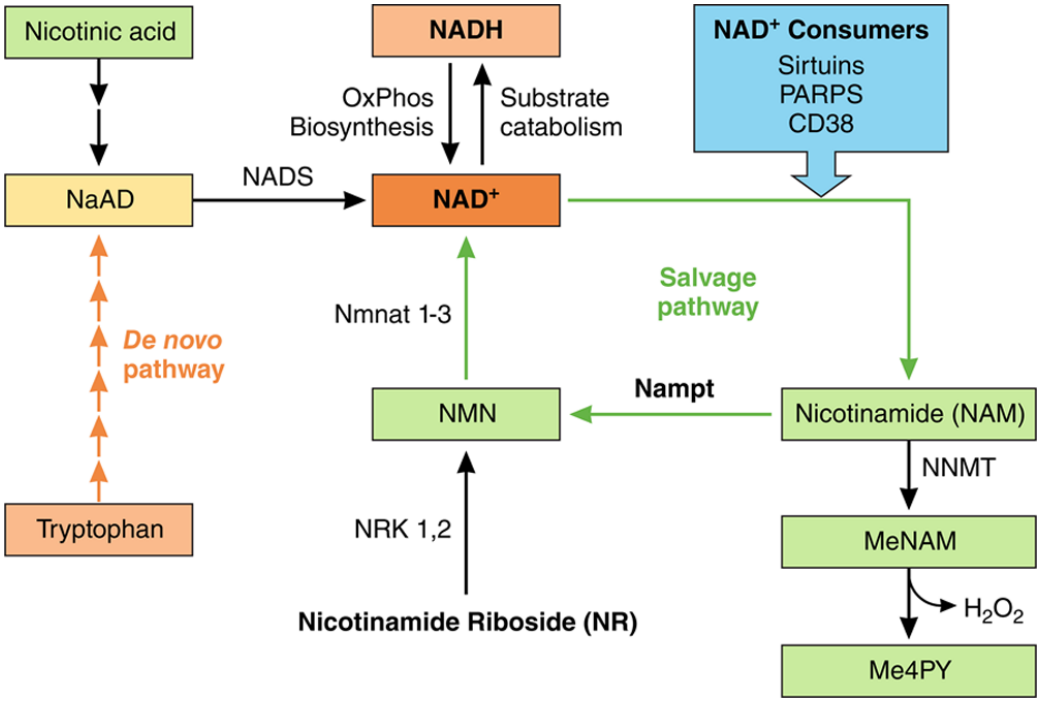

Figure 25: NAD^+ synthesis: salvage and *de novo* pathways; and NAD^+ consummers. NAM: nicotinamide, NMN: nicotinamide mononucleotide, Nampt: nicotinamide phosphoribosyltransferase, NR: nicotinamide riboside, Nrk: nicotinamide riboside kinase, Me4PY: N1-methyl-4-pyridone-5-carboxamide, MeNAM: methyl-nicotinamide, NaAD: nicotinic acid adenine dinucleotide, NADS: NAD synthase, Nmnat: nicotinamide mononucleotide adenyltransferases, NNMT: nicotinamide N-methyltransferase, OxPhos: oxidative phosphorylation, PARPS: poly(ADP-ribose) polymerases (Walker and Tian 2018).

Few data are found in the literature about NAD^+ synthesis quantification and the KYN pathway. Brady et al. conducted an investigation that studied the effect of KYN pathway metabolites on intracellular NAD^+ synthesis and cell apoptosis in a human primary astrocytes and neurons cell models. They found that TRP was capable of increasing NAD^+ intracellular levels. Other kynurenine pathway metabolites (QA, 3-hydroyKYN, 3-hydroyanthranilic acid) were capable of increasing the co-factor levels but decreasing at higher concentrations. In fact, at these concentrations of the kynurenine pathway metabolites, cytotoxicity is observed explaining the decrease in NAD^+ levels (Braidy et al. 2009). The same team conducted a study to evaluate the effect of a kynurenine pathway inhibition on NAD^+ synthesis in the same previously used cell models. Concordantly, a 1-methyl-L-tryptophan (1-MT), IDO inhibitor, treatment decreased NAD^+ synthesis and increased cell death (Braidy, Guillemin, and Grant 2011). All of this shows the importance of the kynurenine pathway in NAD^+ synthesis and cell survival.

a) NAD^+ and sirtuins

Sirtuins (SIRT) are a class of proteins, enzymes, catalyzing the deacetylation of proteins on their lysine residue while using NAD^+ as a co-factor. They belong to the class III of histone deacetylases and their activity is highly affected by NAD^+ availability (Fig. 26) (Li et al. 2015).

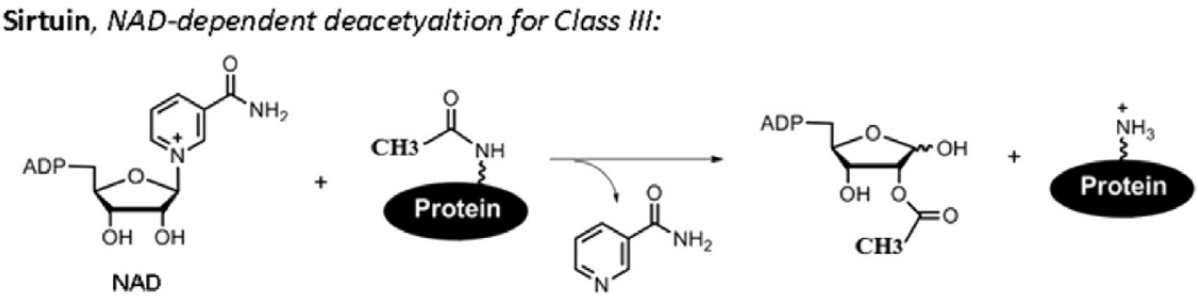

Figure 26: Sirtuins mechanism of action in deacetylating proteins using NAD^+ as a co-factor liberating nicotinamide, O-acyl-ADP-ribose, and a deacylated protein (Li et al. 2015).

There are 7 types of sirtuins, each one of them possessing its proper cellular localization according to its function. They are involved in many important signaling pathways and assure diverse biological functions such as protein secretin, metabolism, genome stability (Frye 2000)… SIRT3 is mainly mitochondrial but can also be found in the cytoplasm and the nucleus. It is also highly expressed in the heart. SIRT3 identified targets include MnSOD or SOD2, complex I, isocitrate dehydrogenase 2, glutamate dehydrogenase. This means that SIRT3 plays an important role in activating mitochondrial metabolic pathways and ROS detoxification (Bugger, Witt, and Bode 2016). SIRT1 is present in the cytoplasm and the nucleus, and can change cellular localization depending on cell type. SIRT6 is mainly found in the nucleus (Matsushima and Sadoshima 2015).

In the past decade, sirtuins have been in the spotlight as potential drug targets in cardiovascular diseases (Matsushima and Sadoshima 2015). For example, SIRT3 protects cardiomyocytes from oxidative stress and like SIRT6 is capable of attenuating cardiac hypertrophy (Sundaresan et al. 2009). The main conclusion of numerous studies (Pillai et al. 2010; Shalwala et al. 2014; Wang et al. 2016) is that sirtuins (SIRT1, 3, 6) are capable of reducing myocardial I/R injuries and cardiac hypertrophy.

The same article that showed the importance of the kynurenine pathway in NAD^+ synthesis in human brain cells, demonstrated a reduction in SIRT1 activity after a 1-MT treatment (Braidy, Guillemin, and Grant 2011). This proves the importance of the kynurenine pathway in ensuring NAD^+ synthesis but more importantly the importance of NAD^+ availability in SIRT1's function.

2.2.4. Kynurenine pathway and mitochondria

Taking into consideration reported kynurenine pathway metabolites properties, a group of researchers in Austria published 3 studies describing effects of kynurenines on respiratory parameters of mitochondria. The first study was conducted on mitochondria isolated from rat heart (Baran et al. 2001). They found that KYN's presence in the medium was capable of reducing the state III respiration, and subsequently the respiratory control ratio (RC) using glutamate/malate or NADH as substrates compared to control. They also found that KYNA reduced the RC by increasing state IV

respiration using glutamate/malate as substrates compared to control. In addition, QA did not influence mitochondrial respiratory parameters with all substrates. Putting together their data, the analysis of the results was the following: mitochondrial KAT could have an influence on the bioenergetics function of mitochondria by catalyzing the transformation of KYN into KYNA, and the latter is able to influence the biochemical mitochondrial function. The second and third studies were of a more extensive type (Baran et al. 2016; Baran et al. 2003). Other metabolites on brain, heart and liver tissues were studied. The summary of these studies study confirmed previous founding, showed that kynurenine pathway metabolites do not significantly influence brain and liver mitochondrial respiratory parameters, and that anthranilic acid had an influence on heart mitochondrial bioenergetics. The conclusion of these studies is that KYNA could act as an endogenous uncoupler of mitochondrial respiration by decreasing ATP synthesis. This phenomenon is of importance for the maintenance of the mammalian cell function during its life span under physiological and pathophysiological conditions.

2.2.5. Kynurenine pathway and ischemia/reperfusion injuries

Taking into consideration the importance of the kynurenine pathway function, it is no wonder that a malfunction in one if its enzyme could be detrimental to the physiology of the body. Actually, the kynurenine pathway has been shown implicated in many diseases and disorders. In Table 4 are mentioned some of the clinical conditions. Thus, modulating the kynurenine pathway metabolism and its enzyme activity, by either decreasing or increasing it, holds therapeutic potential (Badawy 2017).

ENZYME	IDENTIFIED CLINICAL CONDITION(S) FOR TARGETING
TDO	Cancer, major depressive disorder, porphyria
IDO	Cancer, immune diseases, neurological disorders, neurodegenerative diseases
KAT	Schizophrenia,
KMO	Schizophrenia, drug dependence, infectious diseases
Kynase	Neurodegenerative conditions
3-HAAO	Neurological disorders
QPRT	Inflammatory diseases
NMPRT	Cancer
NNMT	Cancer, diabetes, schizophrenia
NADase	Infectious diseases
PARP	Cancer, inflammatory, metabolic, and neurological disorders

Table 4: Kynurenine pathway enzymes as therapeutic targets in some clinical conditions. 3-HAAO: 3-hydroxyanthranilic acid, oxygenase, IDO: indoleamine2,3-dioxygenase, KAT: kynurenine aminotransferase, KMO: kynurenine monooxygenase or kynurenine hydroxylase, Kynase: kynureninase, NADase: NAD+ glycohydrolase, NMPRT: nicotinamide phosphoribosyltransferase, NNMT: nicotinamide N-methyltransferase, QPRT: quinolinate phosphoribosyltransferase, PARP: poly-(ADP-ribose) polymerase, TDO: Trp 2,3-dioxygenase (Badawy 2017).

The kynurenine pathway has been firstly and extensively studied in the brain and in neurodegenerative disorders because disequilibrium between the KYNA and the QA routes, can have major consequences (Stone and Darlington 2013). As mentioned beforehand, KYNA and QA have two opposite roles, the first one being an antagonist of the excitatory NMDA receptors, and the other one being an agonist, an activator of these receptors.

a) Cerebral ischemia/reperfusion injuries

In cerebral I/R injuries and in neurodegenerative disorders, NMDA activation has been highlighted. Therefore, a proper balance in the kynurenine pathway bioactive products is crucial to ensure a proper excitatory nervous transmission.

KYNA, 3-OHKYN, and QA are commonly referred to as neuroactive kynurenines (Wang et al. 2015). The study of their function mainly started at a cerebral level, more precisely, neurodegenerative disorders (Sas, Szabo, and Vecsei 2018). In order to improve injuries, studies were conducted to shift the balance in the kynurenine pathway towards a certain route. In these studies, either KYNA or KYN were administrated in cerebral I/R animal model. Since KYNA cannot cross the blood brain barrier, it was either administrated at a very high concentration, or KYN was injected. Actually, it has been proven that KYN can be metabolized into KYNA in the brain (Turski et al. 1989; Fukui et al. 1991).

KYNA has been shown to confer neuroprotection in a hypoxic-ischemia neonatal rat model (Andine et al. 1988). By inhibiting cell excitation, KYNA decreased stroke size in a middle cerebral artery occlusion rat model (Germano et al. 1987). Moreover, KYN administration (precursor of KYNA) before a focal cerebral ischemia in mice and before a global cerebral ischemia in gerbils decreased ischemic score, proving its neuroprotective role (Gigler et al. 2007). Furthermore, inhibiting KYN hydroxylase (enzyme responsible for QA formation) has also been shown neuroprotective since it increases KYNA production. In a bilateral carotid occlusion in gerbils and in a middle cerebral artery occlusion in rats, treatment with KYN hydroxylase decreased the percentage of pyramidal neurons lesions in hippocampal CA1 region of gerbils and cerebral infarct volumes in rats. Another study showed that 2 days after a simple administration of QA neurons survival decreased, proving QA neurotoxicity (Harris et al. 1998).

b) Myocardial ischemia/reperfusion injuries

Heart diseases are usually associated with inflammation (Heymans et al. 2009). As already mentioned, IDO is an enzyme that is highly regulated by inflammation (Cuffy et al. 2007). Many multi-center prospective studies showed a relationship between IDO activity and coronary heart disease. IDO activity is expressed by KYN/TRP ratio (KTR). This activity was positively correlated with early atherosclerosis and increases carotid artery intima-media thickness in both men and women (Niinisalo et al. 2008) suggesting that IDO activity is a sensitive marker of atherosclerosis. Another study showed that KTR (IDO activity) is higher in patients suffering of a MI compared to control, after an oral load with TRP (Pedersen et al. 2013).

After a cardiac arrest in rats, pigs and humans, kynurenine pathway molecular products concentrations were measured. Kynurenine pathway was activated after cardiac arrest, TRP levels decreased accompanied with an increase in its metabolites in all species (Ristagno et al. 2013).

These studies show the importance of kynurenine pathway and its modulation in heart diseases. Nevertheless, only one study describes kynurenine pathway metabolites on myocardial I/R. KYNA intraperitoneal administration 2 hours before and 2 hours after ischemia reduced infarct size in a mouse myocardial I/R injury. Briefly, alpha-ketoglutarate (αKG)-dependent dioxygenase (Egln1) (a sensor of oxygen regulating hypoxia-inducible factor (HIF)) was inhibited either pharmacologically or using somatic gene deletion specifically in skeletal muscle specifically, in a mice model. These mice were protected against myocardial I/R injuries. Egln1's inhibition caused an accumulation of αKG, a co-factor in the transformation of KYN into KYNA, leading to an increase in the latter's concentration, hence the cardioprotective effect (Graphical abstract shown in Fig. 27) (Olenchock et al. 2016).

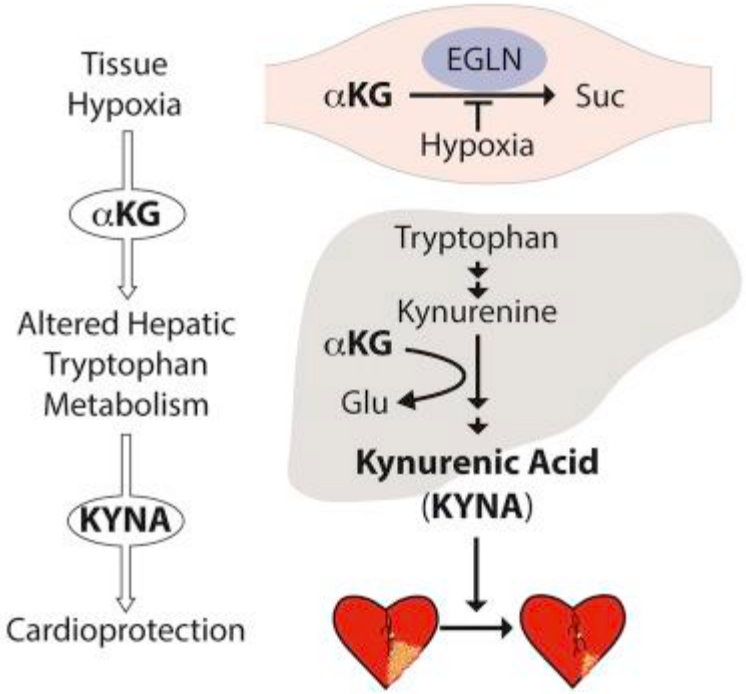

Figure 27: Graphical abstract of a study depicting mechanism of kynurenic acid-mediated cardioprotection (Olenchock et al. 2016).

Recently, a metabolic study was conducted in our laboratory in order to identify metabolites potentially implicated in remote ischemic conditioning. Plasma samples of rats submitted or no to 5 cycles of limb I/R (remote ischemic conditioning) were analyzed using a targeted metabolomics approach. In parallel, plasma samples of 50 patients before and after 3 cycles of I/R were also analyzed to confirm results found in rats. Interestingly, in both plasma samples from rats and humans, remote ischemic conditioning was capable of increasing plasmatic concentration of KYN. Additionally, a KYN injection to rats 10 minutes before a myocardial I/R, decreased infarct size in KYN-treated group compared to vehicle treated group (Chao de la Barca et al. 2016).

Aim of the thesis

The main topic of research in the laboratory is to find cardioptotective strategies to reduce myocardial I/R injuries. That was also the topic of this thesis. More precisely, this work had two main objectives.

The first one was to study the implication of mitochondrial dynamics in I/R injuries. Previous work on a model deficient in mitochondrial fusion protein OPA1, found that decreasing fusion was somewhat making I/R injuries more deleterious to cardiomyocytes. Moreover, discrepancies exist around the role that mitochondrial dynamics proteins play during I/R and around their importance. Therefore, a mouse model hetereozygously deficient in DRP1, a mitochondrial fission protein, was used to explore the importance of mitochondrial fission in a myocardial I/R model, and a model heterozygously deficient in OPA1 and DRP1 was used to determine compensation mechanisms and their impact on infarct size.

The second one was to study KYN and KYNA mediated cardioprotection. In a previous study, in order to better understand underlying mechanisms of ischemic conditioning, plasma samples of rats undergoing or no 4 cycles of limb I/R and plasma samples of human before and after 3 cycles of I/R to the arm, were analyzed for discriminating metabolites. Indeed, KYN was found increased after ischemic conditioning. This metabolite was re-injected to rats 10 minutes before myocardial I/R and was found cardioprotetective. Similar results concerning KYNA were found in a study published by Olenchock et al. in 2017. These data taken together lead to the second objective of this thesis, which was, firstly, to prove again both KYN and KYNA-mediated cardioprotection, and, secondly, to decipher cardioprotection underlying mechanisms.

Materials and methods

Most of the detailed materials and methods were described in the manuscripts presented in the Results section of the document.

1. Animal Ethics

Mice and rats were kept in the "*Service Commun d'Animalerie Hospitalo Universitaire*" (SCAHU). Housing rooms were equipped with standard light cycles (12h light/12h dark), with food and water available *ad libitum*. Female and male mice were used depending on the project at 3, 6, 12 months of age. Male rats were used at 8 to 10 weeks of age, weighing 250-300g. All animal work was performed according to the European Union and French Guiding Principles on the protection of animals used for scientific purposes (Directive 2010/63/UE; French Decree no. 2013–118). Authorizations to conduct animal experiments were obtained from the MENESR, *Ministère de l'Education Nationale de l'Enseignement Supérieur et de la Recherche* (APAFIS#4514-2016031415098201 v2 for Study N°1 (*Drp1*$^{+/-}$ project), APAFIS#15931-2018061815475007 v2 for Study N° 2 (*Drp1*$^{+/-}$ *Opa1*$^{+/-}$ project), APAFIS#8668-20 170 12417473589 v3 for study N°3 and N°4 (KYNA and KYN project)).

2. Animal experiments

2.1. Echocardioghraphy

Echocardiography was performed by a cardiologist (Fabrice Prunier) using a commercially available echocardiograph (ultrasound system viviD7, GE Medical systems). Mice were sedated intraperitoneally with ketamine (60-70 mg/Kg). The left ventricle (LV) was imaged in parasternal short-axis views. LV end-diastolic and end-systolic diameters, ejection fraction, fractional shortening were measured on M-mode view as recommended by the American Society of Echocardiography.

2.2. *In vivo* ischemia/reperfusion experiments and infarct size assessment

2.2.1. Mice model

Myocardial I/R mouse model was performed by a lab technician (Justine Beaumont) and a PhD student (Laura Cellier).

Mice were anesthetized by means of intraperitoneal sodium pentobarbital injection (90mg/kg; Céva Santé Animale) prior to endotracheal intubation and mechanical ventilation using MiniVent 845® (Hugo-Sachs Elektronik—Harvard Apparatus GmbH, March, Germany). Prior to thoracotomy, the mice received an injection of heparin (1,000 IU/kg, Heparineb Choay®, Sanofi). Temperature was monitored and maintained during the procedure at 36.5° to 38°C. The thorax was opened via a left

lateral thoracotomy, and the pericardium was removed to expose the heart. Coronary ligation was performed on the left coronary artery using a monofilament (PROLENE 7.0®, Ethicon, LLC, Cincinnati, Ohio, USA), placed in a polyethylene tube to create a reversible snare. Ischemia was induced by clamping the tube above the coronary artery and confirmed through observations of dyskinesia and cyanosis of the myocardial region below the ligation. It was maintained for 45 minutes, followed by 24 hours of reperfusion by loosening the snare. Afterwards, thorax was closed and mice were injected with buprenorphine (0.1 mg/Kg) for analgesia and kept overnight in their cage with access to water and food.

To delimit the ischemic area-at-risk (AAR) and area of necrosis (AN), mice were anesthetized by means of intraperitoneal sodium pentobarbital injection (90mg/kg) prior to endotracheal intubation and mechanical ventilation. Afterwards, 400 µl of Evans Blue 4% (Sigma-Aldrich Co®) was injected through the left ventricular apex after repeating coronary ligation, coloring the perfused (non-ischemic) myocardium blue. Thereafter, the left ventricle was cut into six to seven slices and sections were incubated with 2,3,5-triphenyltetrazolium chloride (TTC) (Sigma-Aldrich Co®) in phosphate buffer at pH 7.4 and 37°C and fixed in 4% formaldehyde for 24 hours, thereby delimiting the viable myocardium in red and area of necrosis (AN) in white. Quantification was performed using the ImageJ 1.47 software. AAR itself as a percentage of the total left ventricular weight (AAR%LV) and infarct size was expressed as a percentage of the AAR (AN%AAR).

2.2.2. Rat model

Rats were anesthetized by means of intraperitoneal injection of sodium pentobarbital (Exagon®, Axience) (60mg/Kg) and their chest was shaved. Prior to median sternotomy, rats were intubated and ventilated with a small animal ventilator (SAR-830 A/P, CWE). Body core temperature was maintained at 36.5°C-38°C (HB101/2 RS; Bioseb). The pericardium was removed. Ligature was performed on the left anterior descending coronary artery by passing a 7.0 monofilament suture (Premio 7.0, Peters Surgical) through a short length of tubing (PE50) realizing a reversible snare. The latter was clamped onto the epicardial surface directly above the coronary artery. The appearance of epicardial cyanosis and dyskinesia of the ischemic region confirmed ischemia. Following 40 min of occlusion, reperfusion was achieved by loosening the snare, but keeping it in place, and confirmed by observing an epicardial hyperemic response. During reperfusion, anesthesia was verified every 15 min by pinching of the toe and eventually re-injecting sodium pentobarbital (20mg/Kg).

Following 120 min of reperfusion, heart was excised; the snare was re-occluded, and heart was retrogradely perfused with Evans Blue 1%. This permits the outlining of the area at risk. After left ventricle isolation, the latter was cut into six slices, each one weighed and incubated with a 1% solution of TTC, in phosphate buffer at pH 7.4 and 37°C. TTC staining allows the distinction between infarcted myocardium (pale) and viable myocardium (brick red). After 2 hours of incubation with 4% formaldehyde, the slices were photographed. Infarct size was quantified using Image J software. Area

of necrosis (AN) was expressed as a percentage of the AAR (AN%AAR) and the AAR itself as a percentage of the total left ventricular area (AAR%LV).

2.3. Tissue Sampling and preparation

Depending on preceding following manipulation, mice were sacrificed by cervical dislocation or by excising the heart under deep anesthesia. Hearts were harvested rapidly, left ventricle isolated and rapidly freeze clamped in liquid nitrogen.

In study N°1, in case of respirometric investigation of mitochondrial function, mice were sacrified by cervical dislocation, the heart excised, and the fibers of the left ventricle were isolated. To prepare the tissues, for mitochondrial respiration assessment, fibers were kept, dissected and shredded in buffer TP (*transport, perméablisation*) (K_2EGTA 7.23mM, CaK_2EGTA 2.77mM, Imidazole 20 mM, DTT 0.5mM, KH_2PO_4 3mM, $MgCl_2$ 6.56mM, BSA 0.2%, MES 53.3 mM, Taurine 20mM, ATP 5.3mM, PhosphoCreatine 15mM, pH=7.1). After adding saponin (3mg/ml) to buffer TP, fibers were kept at 4°C with gentle agitation. After 30 min, fibers were washed 3 times (10 min) in buffer LR (*Lavage, respiration*) (Imidazole 20mM, DTT 0.5mM, KH_2PO_4 3mM, $MgCl_2$ 4mM, BSA 0.2%, MES 109mM, Taurine 20mM, K_2EGTA 10mM, pH=7.1).

3. Protein expression analysis

3.1. Protein extraction

After reducing the freeze clamped left ventricle samples into powder, 500 µl of extraction buffer was added (Hepes 30mM, EGTA 2.5mM, EDTA 2.5mM, KCl 20mM, β-glycerophosphate 40mM,NaF 40mM, NaPPi 4mM, Glycerol 10%, Nonidet P40 0,1%, protease and phosphatase inhibitor). After 30 seconds of homogenizing using a Polytron® PT2100, the mix was centrifugated at 13000 rpm for 1 hour at 4°C and the pellet was discarded.

3.2. Western Blot

Samples were prepared with, either 40 µg or 100 µg (Lysine-acetylated protein), 4X loading buffer (BioRad), and H_2O. Samples were denatured (for mitochondrial respiratory chain complex proteins were not heated) with heat (95◦C) for 5 min and then separated by SDS-PAGE (10%, 12%, 15% or 4-20% acrylamide gel). After migration, proteins were transferred to a nitrocellulose or PVDF membrane. To limit background noise and non-specific antibodies fixation, membranes were saturated with 5% non-fat dried milk diluted in Tris Base buffer Tween 0.1% (TBST) or with Odyssey buffer (Li-Cor®) diluted in phosphate buffer saline (PBS) 1X for 1 to 3 hours. Afterwards, Membranes were incubated, overnight at 4°C, with antibodies diluted in TBST buffer containing 5% non-fat dried milk or in Odyssey buffer (Li-Cor®) diluted in PBS 1X, against corresponding protein to be revealed. GAPDH (1/10000; Sigma-Aldrich) or β-actin (1/1000; Sigma-Aldrich) or VDAC

(1/1000, abcam), were used as loading controls. Membranes were incubated with appropriate (rabbit or mouse) secondary antibodies (1/5000, Thermo Fisher Scientific) conjugated to horseradish peroxidase. Blots were developed using the enhanced chemi-luminescence method. The band densities were analyzed using Image Lab (BioRad).

4. Gene expression analysis

4.1. RNA extraction

RNA was extracted from approximately 30mg of left ventricle samples using a RNeasy MiniKit reagent (Quiagen) according to the manufacturer's instructions.

Samples were homogenized in qiazol using a Polytron (PRO scientific). After adding 200µl of chloroform, extracts were centrifuged 15min at 12000g, 4°C. Aqueous phase is collected, mixed with 700µl of ethanol, and filtered on RNA mini spin column. Repeated washes and centrifuges eliminate DNA and proteins residues. Finally, spin column is washed with 50µl of RNAase free H_2O and centrifuged 1 min at 10000g to collect RNA.

4.2. Reverse transcription

cDNA was synthesized from 500 ng of mRNA using Quantitect Reverse Transcription kit (Quiagen) following the manufacturer's instructions. DNA was eliminated by heating 2 min at 42°C with gDNA wipeout mix. Reverse transcription reaction was set like the following; 30 min at 42°C, 3 min at 92°C.

4.3. qPCR

In a total volume of 20µl reaction system (10ng of cDNA), SYBR™ Select Master Mix (Applied biosystems) was used to perform qPCR. Thermal cycling reaction performed in Lightcycler® 480 II thermocycler (Roche) consisted of: 95°C for 3 min, 40 cycles of 15 sec at 95°C and 60°C for 1 min. Genes coding for hypoxanthine phosphoribosyltransferase (*hprt*) and glucuronidase beta (*gusb)* were used as reference genes in analyzing target genes mRNA expression. Results of target genes mRNA were normalized on the average of the Ct value of the 2 reference genes mRNA and expressed as $2^{\Delta Ct}$ where ΔCt is the difference between Ct of reference genes and that of target genes.

5. Mitochondrial morphology analysis by electron microscopy

Mitochondrial morphology was examined by means of electron microscopy. After cervical dislocation, hearts were isolated from mice and retrogradely perfused with 2% glutaraldehyde in cacodylate buffer (100mM sodium cacodylate and 2 mM $MgCl_2$; pH 7.3). Afterwards, papillary muscle was isolated and postfixed in the same glutaraldehyde-cacodylate buffer for 30 min.

The following steps were perfomed by the "*Service commun d'imagerie et d'analyses microscopiques*" (SCIAM platform).:Tissue samples were postfixed in cacodylate buffer with 1% osmium tetroxide, contrasted with 1% uranyl acetate in H2O, dehydrated, and embedded in Durcupan. Ultra-thin longitudinal sections of 60 nm were cut and examined using an electron microscope. 20,000x-magnified images were used in the software Image J to assess the number and area of mitochondria. A mean of 60 fields were analyzed per group for mitochondrial morphology.

6. Statistics

Data is expressed as mean±standard error of the mean (SEM) or as median [IQR=Interquartile range: min;max] when appropriate. Statistical significance of the difference between groups was estimated using the Student's *t*-test when normality is verified, using non-parametric Mann-Whitney test when normality was not verified, or one-way ANOVA followed by a LSD (post hoc) test for multi-groups comparisons. p-values <0.05 were considered statistically significant. Statistical analyses were performed using SPSS Statistics v.17.0 software (SPSS Inc.).

Results

Part 1:
Mitochondrial dynamics and ischemia/reperfusion injuries

Study N°1: DRP1 happloinsufficiency attenuates cardiac ischemia reperfusion injuries

Study N°2: Cardiac characterization of *Drp1*$^{+/-}$ *Opa1*$^{+/-}$ deficient mouse model

1. Study N°1: DRP1 haploinsufficiency attenuates cardiac ischemia reperfusion injuries

Manuscript to be submitted to American journal of Physiology

1.1. Scientific background

MI is the main cause of mortality in industrialized countries (Montrief et al. 2019). Albeit timely reperfusion being the main treatment for myocardial ischemia, it still induces damages called reperfusion injuries. Actually, final observed infarct size is due to two components: Ischemia injuries and reperfusion injuries (Benhabbouche et al. 2011). Many experimental and clinical studies were conducted in order to identify strategies capable of activating endogenous cardioprotective signaling pathways and to decipher key players in these pathways.

In all of the examined pathways, mitochondrion is one major component or organelle seemed to always have a role in myocardial I/R injuries. Therefore, a majority of the studies revolved mainly around mitochondrial function and structure. In the past decade, mitochondrial dynamics implication in myocardial I/R injuries has started to intrigue scientists. Brady et al. were one of the first to notice the role of mitochondrial fission in I/R injuries by conducting a study on HL-1 cells. Findings showed that I/R injuries induced mitochondrial fission. Moreover, inhibiting mitochondrial fission proteins allowed re-fusion and lessened injuries (Brady, Hamacher-Brady, and Gottlieb 2006). Ever since, more experiments were conducted where mitochondrial dynamics proteins were inhibited *in vitro* or *in vivo*. The outcome of the studies was different depending on the model used (chronic or acute inhibition of fusion or fission proteins), and type of inhibition (homozygous or heterozygous somatic gene deletion, pharmacological inhibition…) (Cf. Chapter 2: 3.3).

To try to circumvent these discrepancies, we opted to characterize the cardiac phenotype of a model heterozygously deficient for mitochondrial fission protein, DRP1 at baseline and after myocardial I/R.

1.2. Article N°1

DRP1 haploinsufficiency attenuates cardiac ischemia reperfusion injuries

Laura Cellier[1]*, PhD; Rima Kamel[1]*, MS; Sophie Tamareille[1], PhD; Gabriel Garcia[1,2], MD; Camille Villedieu[3], PhD; Bruno Pillot[3], PhD; Naïg Gueguen[1,4], PhD; Ahmad Chehaitly[1], MS; Juan Manuel Chao de la Barca[1,4], MD, PhD; Justine Beaumont[1], Delphine Baetz[3], PhD; Michel Ovize[3,5], MD, PhD; Hiromi Sesaki[6], PhD; Daniel Henrion[1], PhD; Pascal Reynier[1,4], MD, PhD; Guy Lenaers[1], PhD; Fabrice Prunier[1,2], MD, PhD; Delphine Mirebeau-Prunier[1,4], MD, PhD

[1]Institut MITOVASC, CNRS UMR 6015 INSERM U1083, Université d'Angers, Angers, France.
[2]Service de Cardiologie, CHU Angers, Angers, France
[3]Univ Lyon, CarMeN Laboratory, INSERM, Université Claude Bernard Lyon 1, 69500, Bron France
[4]Département de Biochimie et Génétique, CHU Angers, Angers, France
[5]Service d'Explorations Fonctionnelles Cardiovasculaires & CIC de Lyons, Hôpital Louis Pradel, Hospices Civils de Lyon, Lyon, France
[6] Department of Cell Biology, Johns Hopkins University School of Medicine Hunterian 111, 725 N. Wolfe Street, Baltimore, MD 21205, USA

*** Co-first-authors**

Corresponding author:
Prof. Fabrice Prunier, Laboratoire MITOVASC, Bâtiment IRIS 2, 3 rue Roger Amsler, 49100 Angers France
Tel: +33 (0)241 355 147, fax: +33 (0)241 354 004; email: FaPrunier@chu-angers.fr

ABSTRACT

Background: Mitochondrial dynamics is a possible modulator of myocardial ischemia/reperfusion injuries (IRI). We previously reported that mice partially deficient in the fusion protein OPA1 exhibited higher IRI. Therefore, we investigated whether deficiency in the fission protein DRP1 would affect IRI in *Drp1*$^{+/-}$ mouse.

Methods and Results: After baseline characterization of the *Drp1*$^{+/-}$ mice heart, using echocardiography, electron microscopy, and oxygraphy, 3-month-old *Drp1*$^{+/-}$ and wild type (WT) mice were exposed to myocardial ischemia/reperfusion (I/R). The ischemic area-at-risk (AAR) and area of necrosis (AN) were delimited, and the infarct size was expressed by AN/AAR. Proteins involved in mitochondrial dynamics and autophagy were analyzed before and after I/R. Mitochondrial permeability transition pore (mPTP) opening sensitivity was assessed after I/R. Heart weight and left ventricular function were not significantly different in 3-, 6- and 12-month-old *Drp1*$^{+/-}$ mice than in WT. The cardiac DRP1 protein expression levels were 60% lower, whereas mitochondrial area and lipid degradation were significantly higher ($p=0.03$) in *Drp1*$^{+/-}$ mice than in WT, though mitochondrial respiratory parameters and mPTP opening did not significantly differ. Following I/R, the infarct size was significantly smaller in *Drp1*$^{+/-}$ mice than in WT (34.6±3.1% *vs*. 44.5±3.3%, respectively; $p<0.05$) and autophagic markers MFN2 and LC3 II were increased.

Conclusion: Increasing mitochondrial fusion through DRP1 deficiency is associated with protection against IRI, without alteration of basal cardiac and mitochondrial functions. The mechanism of cardioprotection may be related to the increased mitophagy process.

Keywords: ischemia-reperfusion injuries, mitochondrial dynamics, mitochondrial fission, DRP1

INTRODUCTION

Ischemic heart disease, and more specifically myocardial infarction (MI), is still the leading cause of morbidity and mortality in developed countries (Nichols et al. 2014). Timely reperfusion during myocardial infarction is crucial for the salvage of the ischemic myocardium, but paradoxically leads to ischemia-reperfusion injuries (IRI) that account for the final myocardial damage (Yellon and Hausenloy 2007). Due to their major cell functions, such as ATP synthesis, calcium homeostasis, and cell death/survival mechanisms, mitochondria are critical structures involved in IRI (Hausenloy and Yellon 2013; Ong, Hall, and Hausenloy 2013). Mitochondria are dynamic structures changing morphology by fission and fusion mechanisms under the action of proteins anchored in the inner or outer mitochondrial membranes (Youle and van der Bliek 2012). This mitochondrial dynamics proves essential to maintaining the mitochondrial network integrity and appears of great relevance in IRI (Ong, Hall, and Hausenloy 2013; Le Page et al. 2016). Mitochondrial fusion orchestrated by optic atrophy 1 protein (OPA1) and mitofusin 1 and 2 (MFN1, 2) leads to elongated mitochondria, enabling exchanges of mitochondrial matrix proteins and mitochondrial DNA. In contrast, mitochondrial fission results in smaller and fragmented mitochondria and is orchestrated by the GTPase dynamin related protein-1 (DRP1). DRP1 is a cytosolic protein that translocates to the mitochondrial outer membrane following post-translational modifications. By means of oligomerization and constriction, DRP1 leads to mitochondrial fission through its interaction with outer mitochondrial membrane receptors, such as the human fission protein factor 1 (hFIS1), mitochondrial fission factor (Mff), and mitochondrial dynamics proteins of 49 and 51KDa (MiD49 and MiD51). Fission is an essential step in the mitophagy mechanism, enabling the segregation of unrecoverable mitochondria to initiate their elimination (Dorn 2015b).

Myocardial IRI are associated with an imbalance in mitochondrial dynamics in favor of fission (Brady, Hamacher-Brady, and Gottlieb 2006; Ong et al. 2010). Thus, modulating mitochondrial dynamics is a topic of intense research designed to limit IRI. In previous *in vivo* experiments, we observed a larger infarct size in mice with partial deficiency of the fusion protein Opa1 exposed to myocardial I/R than in that of wild-type (Le Page et al. 2016). This finding was consistent with an *in vitro* study in which simulated ischemia of the cardiomyoblast cell line H9C2 cells with Opa1 *shRNA* increased mitochondrial fragmentation and cell death(Chen et al. 2009). Moreover, a mild Opa1 overexpression was found to protect the mice hearts from ischemic damage (Varanita et al. 2015). The opposite approach, consisting of inhibiting fission by pharmacologically targeting DRP1's activity or *Drp1*'s expression (Ikeda et al. 2015; Song et al. 2015), provided controversial results. A cardioprotective effect has been observed in a few studies and attributed to the inhibition of mitochondrial permeability transition pore (mPTP) opening (Ong et al. 2010; Disatnik et al. 2013). Other studies reported increased IRI, which were attributed to mitochondrial autophagy inhibition (Ikeda et al. 2015).

Therefore, this study sought to investigate whether DRP1 deficiency influences myocardial IRI *in vivo* in a deficient *Drp1* mice model.

METHODS

Mouse model

Heterozygous *Drp1* knockout (*Drp1*$^{+/-}$) mice, as previously described (Wakabayashi et al. 2009), were obtained from Professor Hiromi Sesaki at the Johns Hopkins University. Mice were kept using standard light cycles, with food and water available ad libitum. All animal work was performed according to the European Community Guiding Principles in the care and use of animals (Directive 2010/63/UE; Décret n°2013-118). Authorizations to conduct animal experiments were obtained from the MENESR, *Ministère de l'Education Nationale de l'Enseignement Supérieur et de la Recherche* (APAFIS#4514-2016031415098201 v2).

Echocardiography

Transthoracic echocardiography (TTE) was performed using an ultrasound system (Vivid 7 Pro, General Electric Medical Systems) on anesthetized mice (ketamine 60-70mg/Kg, intraperitoneally), as previously described (Prunier et al. 2002). Left ventricular end diastolic diameter (LVEDD), left ventricular end systolic diameter (LVESD), and fractional shortening (FS) were determined using two-dimensional (2D) M-mode echocardiography.

Mitochondrial morphology by transmission electron microscopy

Samples of left ventricular (LV) papillary muscle were prepared for EM, as previously described (Wilding et al. 2006). Briefly, the hearts were fixed using a retrograde perfusion with 2% glutaraldehyde in cacodylate buffer (100mM sodium cacodylate and 2mM $MgCl_2$; pH 7.3). Ultra-thin longitudinal sections of 60nm were cut and examined using an electron microscope, with 20,000x-magnified images by means of the software Image J, designed to assess mitochondrial number and area. In total, 60 fields on average were analyzed per group for mitochondrial morphology.

Respirometric investigation of mitochondrial function

Preparation of permeabilized cardiac fibers, previously described (Saks et al. 1998), was conducted in order to study mitochondrial function *in situ*. The respiratory rates were recorded at 30°C in 2mL glass chambers using a high-resolution Oxygraph respirometer equipped with a Clark oxygen sensor (Oroboros, Innsbruck, Austria) and analyzed by means of DATLAB Analysis software (OROBOROS, Austria).

Respiration was initiated with complex I-dependent substrates (5mM malate/ 2.5mM pyruvate). Complex I-coupled state 3 respiration was measured by adding saturating ADP (1mM), followed by 10mM succinate, enabling the full TCA cycle operation to occur, with maximal coupled respiration sustained by both complexes I+II. Next, 2.5µM rotenone was injected in order to obtain the complex II-coupled state 3 respiration. Oligomycin (8µg/mL) was then added to determine the uncoupled state 4 respiration. Finally, FCCP (1 µM) was added to further control the fiber permeabilization.

The second experiment was initiated with malate and palmitoylCoA/carnitine as substrates (2.5mM malate/ 40µM PalmitoylCoA/ 1mM carnitine), following which 1mM ADP was added in order to investigate the beta-oxidation under phosphorylating condition. Next, antimycin (2µg/mL) was added to inhibit complex III. The experiment was continued to assess complex IV-coupled state 3 respiration, following which complex IV inhibitors (1 mM KCN/ 2 mM azide) were added.

The last experiment was conducted in order to evaluate the coupling of oxidative phosphorylation with mitochondrial creatine kinase. Fibers were exposed to increasing ADP concentrations, either in the presence or absence of creatine (20mM), in order to stimulate the creatine kinase system; the ADP-stimulated respiration was plotted above basal oxygen consumption (V_0) in order to determine the maximal respiration rate (V_{max}).

In vivo ischemia-reperfusion experiments and infarct size assessment

Overall, 3-month-old male *Drp1*$^{+/-}$ mice and their littermates were submitted to myocardial I/R *in vivo*. *Dpr1*$^{+/-}$ and WT mice were anesthetized by means of intraperitoneal sodium pentobarbital injections (80mg/Kg; Ceva Santé Animale) and received an injection of heparin (100IU/Kg, Heparine Choay®, Sanofi aventis, Paris, France) prior to thoracotomy. Myocardial I/R was achieved by temporarily occluding the left coronary artery, then releasing the occlusion as previously described(Le Page et al. 2016). The duration of ischemia was 30 minutes, and that of reperfusion 24 hours.

To delimit the ischemic area-at-risk (AAR) and area of necrosis (AN), Evans Blue 4% (Sigma-Aldrich Co®, *Missouri, USA*) was injected through the left-ventricular apex. Thereafter, the heart sections were incubated with 2,3,5-triphenyltetrazolium chloride (TTC) (Sigma-Aldrich Co®, *Missouri, USA)* and fixed in 4% paraformaldehyde for 24 hours, as previously described(Le Page et al. 2016). The AN (white), AAR (not blue), and total left-ventricular (LV) areas from both sides of each section were measured using the software ImageJ 1.47. AAR/LV and AN/AAR were expressed as percentages, as previously reported (Le Page et al. 2016).

Western Blot Analysis

Three-month-old male and female *Drp1*$^{+/-}$ mice and their littermates were employed. The methods applied for immunoblot preparation were previously described (Kalakech et al. 2014). Protein expression was assessed at basal condition and after the *in vivo* I/R procedure. Overall, 30-50µg of total proteins was separated by SDS-PAGE and transferred to a nitrocellulose or PVDF membrane. The membranes were incubated overnight at 4°C with primary antibodies, and thereafter, with appropriate secondary antibodies conjugated to horseradish peroxidase (Santa Cruz Biotechnology®, *Texas, USA*). The antibodies used consisted of OPA1, DRP1 (BD Transduction Laboratories®; 1/1000), MFN2 (Sigma-Aldrich®; 1/2000), FIS1 (Santa Cruz Biotechnology®; 1/500), LC3B (Enzo Life Sciences; 1/1000), p62 (Enzo Life Sciences; 1/1000), and GAPDH (Sigma-Aldrich®; 1/20000) was employed as a loading control.

Metabolomic Analysis

We applied a targeted, quantitative metabolomic approach to heart tissue extracts by using the Biocrates AbsoluteIDQ p180 Kit (Biocrates Life Sciences AG, *Innsbruck, Austria*), as previously described (Chao de la Barca et al. 2017). The ratio of short-chain acylcarnitines to free carnitine (C2+C3/C0) as a measure of overall beta-oxidation activity, and the ratio of long-chain acylcarnitines to free carnitine (C16+C18/C0) as activity of carnitine palmitoyltransferase 1 (CPT1) were quantified.

Calcium Retention Capacity (CRC)

The mitochondrial permeability transition pore (mPTP) opening was assessed by mean CRC, as previously described (Bochaton et al. 2015). In brief, extra-mitochondrial Ca^{2+} concentration was estimated using Calcium Green™-5N (Life Technologies). Measurements were carried out on isolated cardiac mitochondria from *Drp1*$^{+/-}$ after I/R were performed with or without the adjunction of cyclosporine A (1µM). CRC was expressed as nmoles Ca^{2+}/mg of proteins.

Statistical analysis

Data have been expressed as mean±standard error of the mean (SEM). The statistical significance of the difference between the *Drp1*$^{+/-}$ and WT mice groups was estimated using the Student's *t*-test or non-parametric Mann-Whitney test, as appropriate, with *p*-values <0.05 considered statistically significant.

RESULTS

Anatomical characteristics and heart function of Drp1$^{+/-}$ mice

We characterized the cardiac weight, LV size, and LV function in 3- 6- and 12-month-old *Drp1*$^{+/-}$ and WT mice. The heart rate recorded at the time of echocardiography was not significantly different between groups of the same age (591±30 bpm in WT *vs*. 574±15 bpm in *Drp1*$^{+/-}$ at 3 months; 570±15 bpm in WT *vs*. 585±16 bpm in *Drp1*$^{+/-}$ at 6 months; 579±13 bpm in WT *vs*. 576±8 bpm in *Drp1*$^{+/-}$ at 12 months). Body, heart weights, and LV size were not significantly different between WT and *Drp1*$^{+/-}$ mice of the same age (Figures 1A and 1B), nor were LVEDD and LVESD. Likewise, cardiac function represented by FS did not significantly differ at any time (55±2 % in WT *vs*. 58±1 % in *Drp1*$^{+/-}$ at 3 months; 53±1 % in WT *vs*. 54±1 % in *Drp1*$^{+/-}$ at 6 months; 54±2 % in WT *vs*. 54±1 % in *Drp1*$^{+/-}$ at 12 months) (Figure 1C).

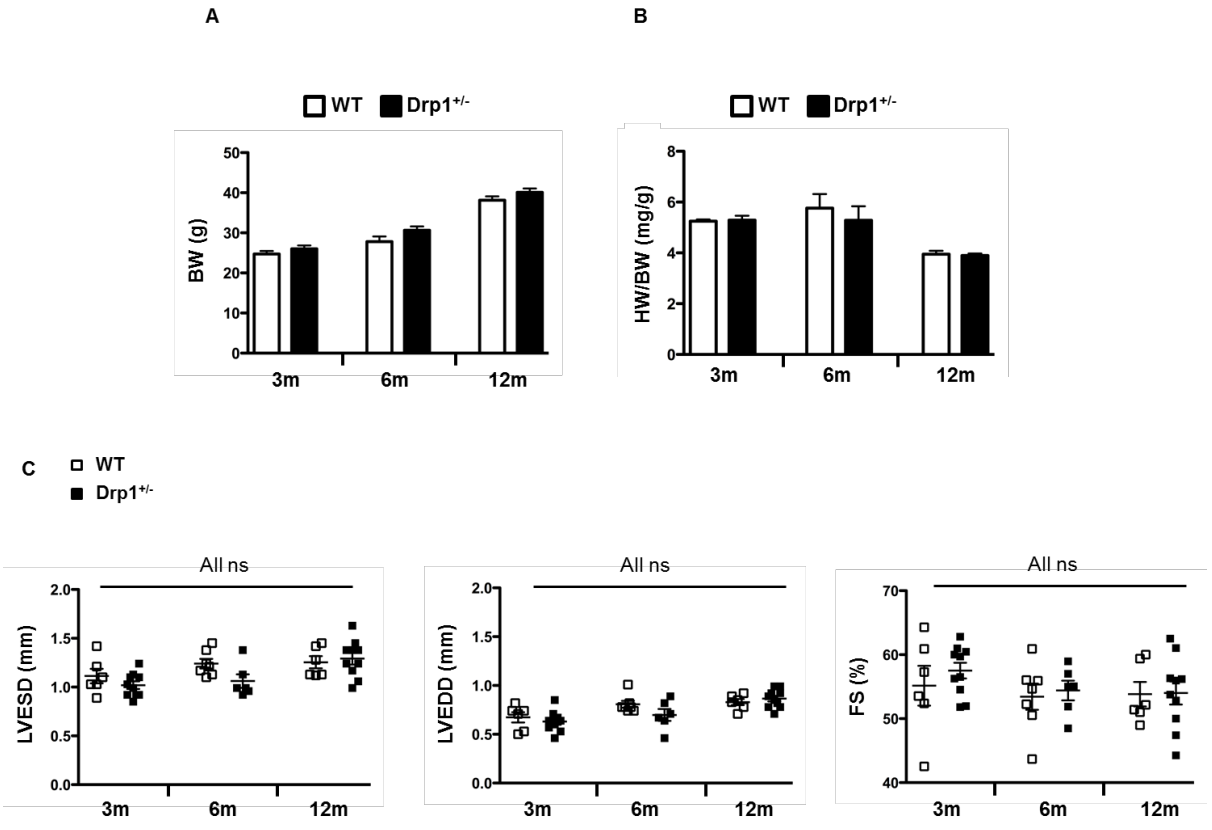

Figure 1 Anatomical characteristics and heart function of 3-, 6- and 12-month-old *Drp1*$^{+/-}$ and their wild type littermate (WT) mice. (A) Body weight (BW). (B) Heart weight to body weight (HW/BW) ratio. (C) Cardiac echocardiography, left: Left ventricle end-systolic volume (LVESD), middle: LV end-diastolic volume (LVEDD), right: LV fractional shortening (FS). Three months: n=6-10 WT and n=10 *Drp1*$^{+/-}$; 6 months: n=7-10 WT and n=6-8 *Drp1*$^{+/-}$; 12 months: n=6-8 WT and n=10 *Drp1*$^{+/-}$.

In vivo I/R injury

The 3-month-old *Drp1*$^{+/-}$ and WT mice were subjected to 30-min myocardial ischemia followed by 24-hour reperfusion (Figure 2). The AN/AAR after I/R, evaluated using Evans Blue and TTC staining, was significantly lower in *Drp1*$^{+/-}$ mice than in WT (34.6±3.1% *vs*. 44.5±3.3%, respectively; $p<0.05$), whereas AAR/LV did not significantly differ between the two groups.

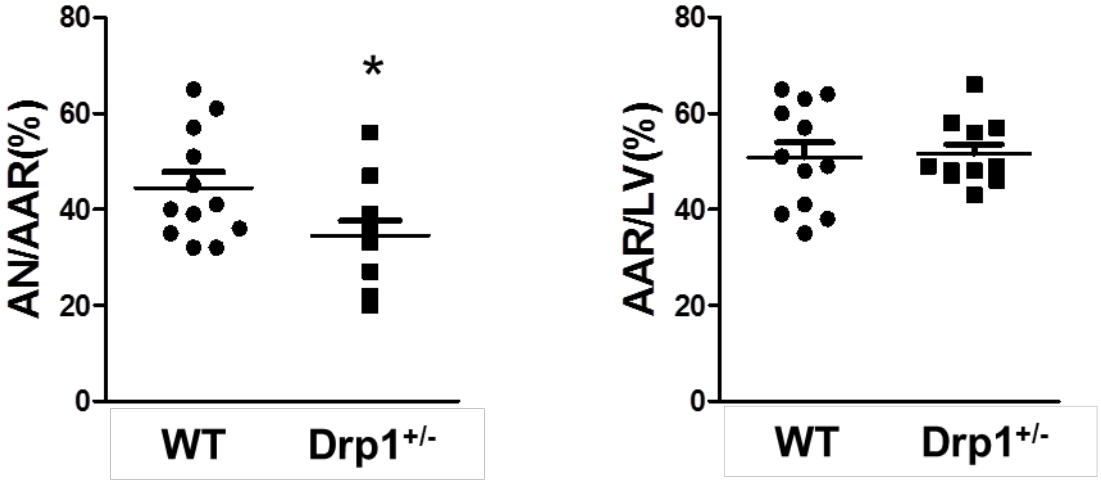

Figure 2 Scatter dot plot showing area necrosis (AN) as a percentage of area at risk (AAR) or AAR as a percentage of the total left ventricle (LV) area (n=11-12/group) * $p<0.05$.

Mitochondrial dynamics protein expression

Immunoblot analyses confirmed that cardiac Drp1 levels were 60% lower in 3-month-old *Drp1*$^{+/-}$ mice than in WT (Figure 3). At baseline, cardiac levels of other proteins involved in mitochondrial dynamics, such as MFN 2, OPA1, and FIS1, were unaltered in *Drp1*$^{+/-}$ mice compared to WT.

After a 30-min ischemia followed by a 24-hour reperfusion, Drp1 levels tended to be lower in *Drp1*$^{+/-}$ mice, though the difference did not achieve statistical significance (3.7±0.5 in WT *vs*. 2.5±0.4 in *Drp1*$^{+/-}$), whereas Mfn2 levels were significantly increased in *Drp1*$^{+/-}$ mice compared to WT (2.2±0.2 in WT *vs*. 2.8±0.1 in *Drp1*$^{+/-}$). Furthermore, Opa1 and FIS1 were not significantly different in WT and *Drp1*$^{+/-}$ mice (OPA1: 2.5±0.3 in WT *vs*. 3.0±0.3 in *Drp1*$^{+/-}$; FIS1: 1.5±0.6 in WT *vs*. 1.4±0.4 in *Drp1*$^{+/-}$) (Figure 3).

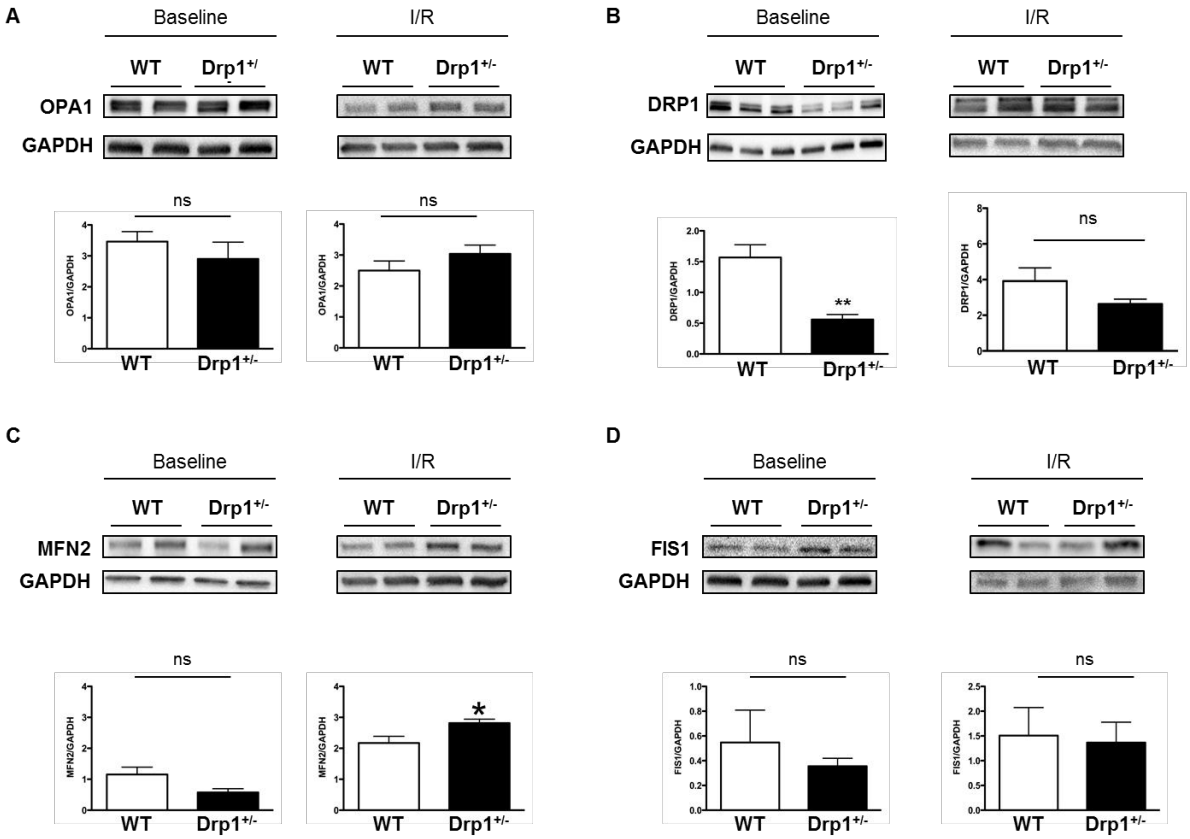

Figure 3 Baseline and post-ischemia/reperfusion (I/R) mitochondrial dynamics protein expression. OPA1 (A), DRP1 (B), MFN2 (C), and FIS1 (D) expression assessed by means of western blotting at baseline (n=8-10/group) and after I/R (n=4-10/group). Representative immunoblots and histograms showing quantifications are represented. GAPDH was used as a loading control. Values are expressed as mean ± SEM. * $p<0.05$.

Mitochondrial morphology

Electron microscopy (EM) analyses of cardiac papillary muscle were performed at 3 month. At baseline, the number of mitochondria in hearts per field was not significantly different between *Drp1*$^{+/-}$ and WT mice, though the mitochondria were enlarged in *Drp1*$^{+/-}$ (Figure 4B). The number of mitochondria per quartile of mitochondrial areas was analyzed (Q1=small, Q2=medium, Q3= small to large, Q4=Large). Quantitative analyses revealed that the mitochondrial area was significantly increased due to the higher frequency of medium-to-large mitochondria in *Drp1*$^{+/-}$ mice.

Following I/R, EM revealed tissue sections of the papillary muscle to exhibit a disruption in the mitochondrial network in *Drp1*$^{+/-}$ and WT mice (Figure 4A).

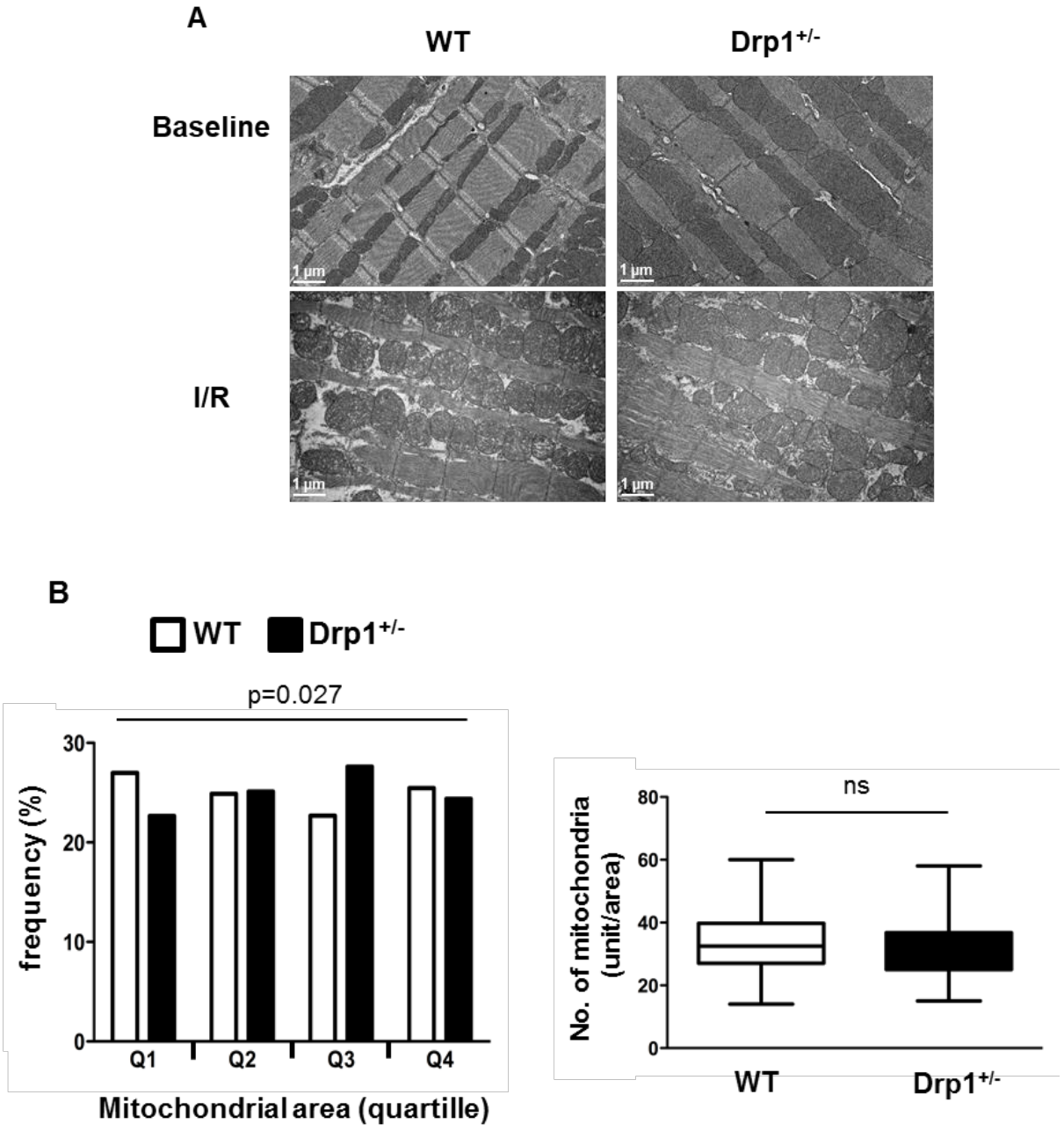

Figure 4 Mitochondrial morphology. (A) Representative electron microscopy (EM) images of left ventricle longitudinal sections at baseline and after 30 minutes of ischemia and 24 hours of reperfusion in 3-month-old *Drp1*$^{+/-}$ and WT mice. Scale bar: 1 µm. (B) Left: mitochondrial frequency represented according to the quartile distribution of the mitochondrial area. Right: the number of mitochondria per field. Counting was performed on 60 representative EM fields per group (n=4 per group). Data are represented as median [min;max].

Mitophagy

In the heart, we quantified the mitophagy protein levels, microtubule-associated proteins 1A/1B light chain 3B (LC3), and sequestosome-1 or ubiquitin-binding protein p62 from *Drp1*$^{+/-}$ mice and WT, under basal conditions and after I/R. Under basal conditions, there was no significant difference in the protein level expression between the two groups (Figure 5). After IR, p62 levels were not significantly different (0.39+/-0.08 in WT *vs*. 0.36+/-0.05 in *Drp1*$^{+/-}$), though LC3 II protein levels were significantly increased in *Drp1*$^{+/-}$ mice compared to WT (0.43+/-0.05 in WT *vs*. 0.96+/-0.16 in *Drp1*$^{+/-}$). LC3-II, a cleaved and lipid-bound form of the LC3 protein, is an integral part of the autophagosomal membrane and serves as a marker of autophagosomes.

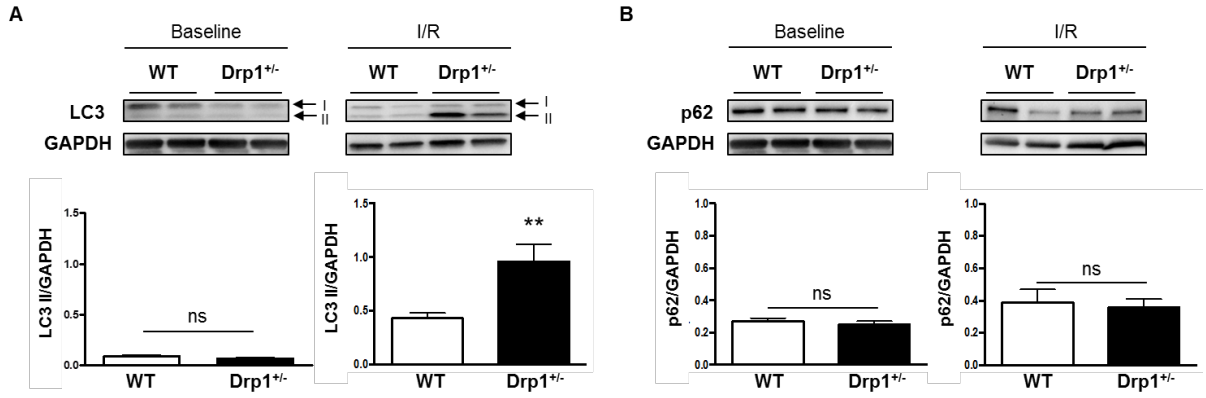

Figure 5 Representative immunoblot of autophagic response proteins. Autophagy levels were assessed by quantitative analysis of autophagy markers LC3-II (A) and p62 (B) in *Drp1*$^{+/-}$ and WT mice at baseline and after ischemia/reperfusion (I/R). The results are expressed as ratios of protein band densities of LC3-II and p62, (n=6-10 per group). GAPDH was used as a loading control. Values are mean ± SEM.

Mitochondrial function

Cardiac energy metabolism of Drp1$^{+/-}$ *mice*

Next, we investigated whether any change in oxidative capacity at baseline could explain the protection in *Drp1*$^{+/-}$ mice after I/R stress. Basal and maximal phosphorylating mitochondrial respirations were not significantly different between the two groups (Figure 6A). None of the complex I, complex II, or complex I+II (full operating TCA) substrates indicated that the respiratory chain capacity was changed. However, when using palmitoylcoA/carnitine as substrate, the maximal respiration was higher in mitochondria from *Drp1*$^{+/-}$mice than in those from WT (37.5±3.8nmol O2/min/mg in WT *vs*. 52.3±3.0nmolO2/min/mg in *Drp1*$^{+/-}$ (Figure 6C)), supporting a higher fatty acid

oxidation capacity in *Drp1*$^{+/-}$. Therefore, we performed metabolomic analysis on *Drp1*$^{+/-}$ and WT heart tissues. There was no significant difference between the two groups in either beta oxidation activity (0.80±0.04 in WT *vs*. 0.76±0.05 in *Drp1*$^{+/-}$) or CPT1 activity (0.08±0.01 in WT *vs*. 0.07±0.01 in *Drp1*$^{+/-}$) (Figure 6D).

The sensitivity of mitochondrial respiration to ADP was estimated with and without creatine to study the coupling of oxidative phosphorylation with mitochondrial creatine kinase. The ratio K_m for ADP without (K_{mADP}) and with creatine ($K_{mADP+creat}$) was assessed with no significant difference found between the two groups (8.2 ±2.3 in WT *vs*. 3.1±0.6 in *Drp1*$^{+/-}$; p=0.14) (data not shown).

Cardiac mPTP function of Drp1$^{+/-}$ *mice*

CRC is taken as an indicator of susceptibility to mPTP opening following calcium overload. We measured CRC on mitochondria isolated from the area at risk of *Drp1*$^{+/-}$ and WT mice. Following IR, CRC was not altered in either group. CsA, a selective mPTP inhibitor, tended to increase the CRC value in WT and Drp1$^{+/-}$ mitochondria after I/R, though not significantly (Figure 6B).

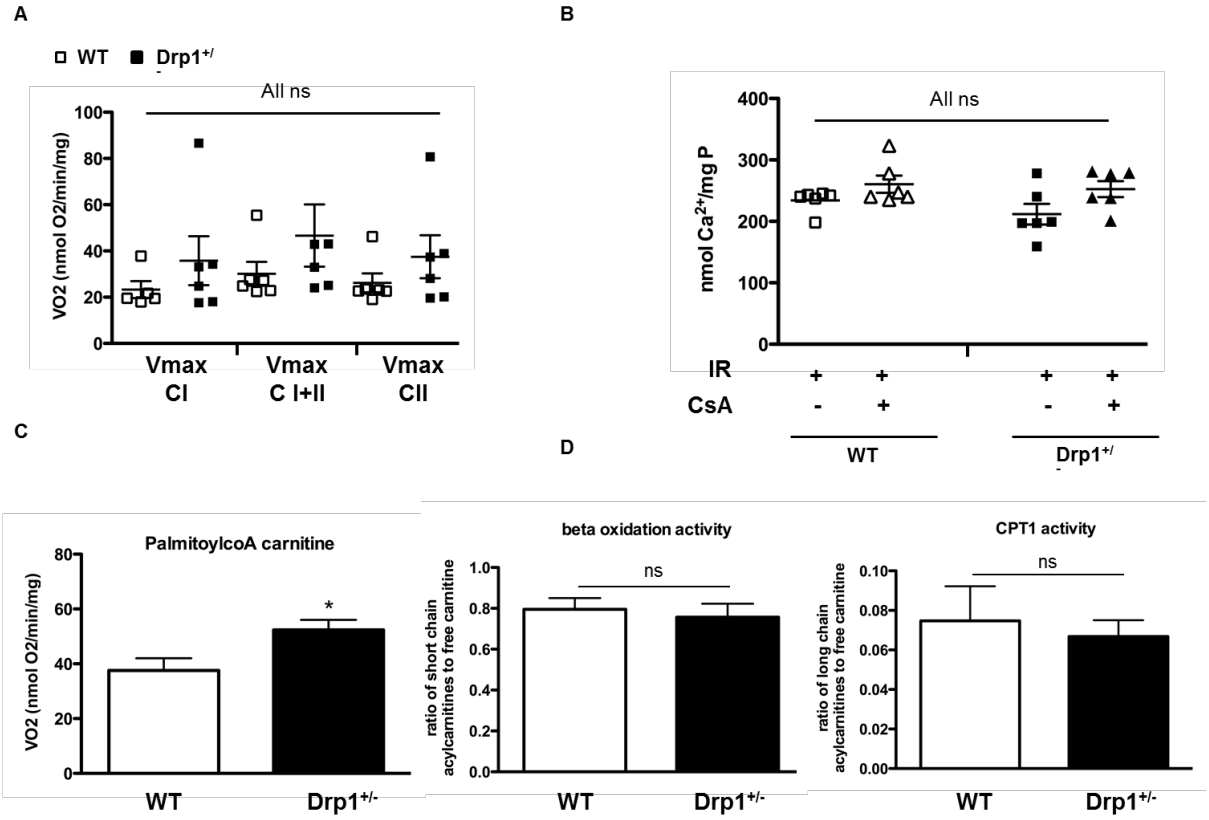

Figure 6 (A) Cardiac energy metabolism and mPTP function. (A) Oxygen consumption rate of permeabilized left ventricular fibers in the presence of 1mM ADP (V_{max}) with 5 mMmalate and 2.5mM pyruvate (complex I, CI), 10mM succinate (both CI and complex II CI + II), and after complex I inhibition with 2.5µM rotenone (CII). Values are expressed as mean ± SEM, (n=5-6 per group). (B) CRC was measured in mitochondria isolated from the areas at risk after a 45-min ischemia followed by a 15-min reperfusion. CRC measurement represented the Ca^{2+} level required for mitochondrial permeability transition pore (mPTP) opening. Extra-mitochondrial Ca^{2+} was detected using Calcium Green^{TM}-5N (Life Technologies). Results were expressed as mean ± SEM nmol Ca^{2+} mg protein -1. (n=6 per group). Mitochondria were isolated from 3-month-old *Drp1*$^{+/-}$ and WT mice. (C) Oxygen consumption rate with 1mM ADP and 2.5mM malate and 40µM palmitoylCoA/1mM carnitine. Values are expressed as mean ± SEM, n=7-8 per group; * $p<0.05$. (D) Metabolomic analysis of the cardiac tissue in 3-month-old *Drp1*$^{+/-}$ and control WT mice. n=10 per group. Left: ratio of short chain acylcarnitines to free carnitine (C2+C3/C0) represents a measure of overall beta-oxidation activity. Right: ratio of long chain acylcarnitines to free carnitine (C16+C18/C0) represents the activity of carnitine palmitoyltransferase 1 (CPT1).

DISCUSSION

Mitochondrial dynamics and myocardial IRI are thought to be closely related. Mitochondrial fission is observed during myocardial ischemia, and mice partially deficient in the fusion protein Opa1 were shown to exhibit higher IRI (Le Page et al. 2016), while mild Opa1 overexpression has previously been revealed to be protective (Varanita et al. 2015). Given this context, targeting the mitochondrial fission protein DRP1 appears to be an attractive therapeutic strategy to limit IRI. Herein, we have reported that heterozygous deficient *Drp1* mice exhibited a lower IRI degree when exposed to myocardial ischemia-reperfusion *in vivo*.

Because complete KO *Drp1* was shown to induce embryonic death by Day E11.5 (Wakabayashi et al. 2009), we investigated a heterozygous deficient *Drp1* model ($Drp1^{+/-}$) (Wakabayashi et al. 2009). In these mice, we observed a 60%-decreased Drp1 cardiac expression, without any change in the other main proteins involved in mitochondrial dynamics. Importantly, no alteration of either cardiac morphology or function was found at the ages of 3, 6, and 12 months. In a conditional cardiac KO *Drp1* mice model, the Drp1 downregulation induced at the age of 15 weeks provoked a lethal dilated cardiomyopathy 8 weeks later through altered mitochondrial respiration (Ikeda et al. 2015; Song et al. 2015). The mitochondrial respiratory chain capacity, evaluated with either complex I, II, or with full operating TCA substrates in permeabilized cardiac fibers, was not found to be altered in our $Drp1^{+/-}$ model, although the mitochondria capacity to oxidize free fatty acids, as evaluated using palmytoylCoA/carnitine as substrates, was found increased. The mechanism responsible for this alteration is still unclear. Alteration in the transport of long chain fatty acids through mitochondrial membrane does not appear to be involved, because the CPT1 activity remained unchanged. Interestingly, opposite results were found in $Opa1^{+/-}$ mice, where cardiac mitochondria were revealed to be less able to oxidize lipids than those of their WT littermates. Mitochondrial fission, induced by stress, is known to be associated with a predominant glycolytic metabolism shift aimed to preserve the energy level (Wai et al. 2015). Hence, one could suggest that the protective effect of increasing mitochondrial fusion is partly related to its association with increased mitochondrial lipid oxidation occurring at the time of reperfusion. More research is necessary to further understand the Drp1's role in lipid oxidation regulation.

Due to its crucial role in cardiomyocyte death in the I/R setting, mPTP opening sensitivity appears to be a credible target that could be modulated by mitochondrial dynamics (24). To date, there are discordant data regarding this potential interaction (Ong et al. 2010; Ikeda et al. 2015; Zhang et al. 2017). In cardiomyocytes with *Drp1* silencing using shRNA and in *Drp1*-KO mice hearts 4 weeks after tamoxifen injection, the mPTP opening was found to be accelerated by *Drp1* downregulation. Nevertheless, since all experiments were performed without I/R, their extrapolation to IRI was limited

(Ikeda et al. 2015). On the contrary, pre-treatment of HL-1 cells or adult rat cardiomyocytes with the DRP1 inhibitor *Mdivi-1* delayed mPTP opening after simulated I/R (Ong et al. 2010). Similarly, a recent study reported that genetic and pharmacological DRP1 inhibition in adult cardiomyocytes reduced transient mPTP opening (Zhang et al. 2017). In our model of partial *Drp1* expression downregulation, mPTP opening sensitivity was found to be unaltered, as evaluated by mean *Calcium Retention Capacity* values. Therefore, the relationship between cardioprotection through DRP1 deficiency and mPTP opening sensitivity was not assumed.

Previous studies have shown pharmacological DRP1 inhibition to be able to protect the heart from IRI (Ong et al. 2010; Ikeda et al. 2015; Zhang et al. 2017; Din et al. 2013). In this respect, *Mdivi-1*, an inhibitor of DRP1's activity, was able to prevent IRI in cellular and animal models, when administered as a pretreatment. On the contrary, a recent study revealed that partial or total cardiac downregulation of *Drp1* exacerbated myocardial IRI (Ikeda et al. 2015). In a later study, the lack of *Drp1* impaired autophagy, with accumulation of abnormal mitochondria and increased cardiomyocyte deaths, was suggested to figure as a consequence. Surprisingly, other authors reported that *Drp1* ablation in adult mice cardiomyocytes resulted in hyper-mitophagy with mitochondrial-associated p62 and LC3 protein level upregulation (Song et al. 2015). Indeed, mitochondrial autophagy proves to be an essential regulator that contributes to strict quality control by maintaining intracellular homeostasis in cardiomyocytes. Both fission and fusion exert an impact on mitochondrial autophagy, with fusion allowing for mitochondrial content exchange and functional complementation, and fission enabling mitochondria enriched with damaged constituents to be isolated, thereby facilitating their degradation. During this process, DRP1 facilitates the degradation of small mitochondria enriched with damaged constituents (Cadete et al. 2019), while Mfn2 plays a crucial role in the fusion of autophagosomes with lysosomes, a critical step in autophagic degradation. Hence, *Mfn2* deficiency in the heart was found to result in impaired mitophagy, mitochondrial dysfunction, and cardiac dysfunction (Zhao et al. 2012; Sebastian et al. 2016). In our work, we have observed no difference between $Drp1^{+/-}$ and WT mice under basal condition regarding LC3 and p62, two markers of mitophagy, which suggests that Drp1 protein level is high enough to maintain mitochondrial autophagy. After I/R, Haploinsufficiency observed under basal conditions disappears and DRP1 protein level becomes comparable to that of WT littermates; suggesting that DRP1 protein levels increased after I/R compared to basal conditions. Moreover, proteins involved in mitohagy such as LC3 and MFN2, increased more in $Drp1^{+/-}$ mice than in their WT littermates. Subsequently, partil DRP1 deficiency conditions these heterozygous mice $Drp1^{+/-}$ to be more able to regulate autophagy in the I/R setting. Indeed, an increase in DRP1 protein level could stimulate mitophagy.

Limits

We have used a constitutive heterozygous deficient *Drp1* mice model designed to assess *in vivo* Drp1's role in the development of IRI. As a consequence of this chronic *Drp1* deficiency, several unsuspected compensation mechanisms may have come into play, such as increased mitochondrial autophagy and lipid oxidation. Moreover, the results pertaining to the absence of effect on mPTP opening sensitivity must be interpreted with caution, as CsA used as a positive control did not affect mPTP opening under our experimental condition. Finally, cardioprotection was only investigated at 24 hours after I/R. It would be of interest to assess whether *Drp1* deficiency would similarly affect post-infarct cardiac remodeling at a more advanced timepoint.

Conclusion

Increasing fusion by means of *Drp1* deficiency is associated with protection against IRI, without alteration in cardiac or mitochondrial functions at basal conditions. This cardioprotection mechanism appears to be related to an increased mitophagy process.

Acknowledgments

The authors would like to thank the university hospital's Joint Animal Care Department (*Service commun d'animalerie hospitalo-universitaire*), as well as the Joint Imaging Department of the University of Angers (*Service commun d'imagerie et d'analyses microscopiques*). Furthermore, the authors are grateful to Morgane Le Mao for mice genotyping, and to Renée Ventura-Clapier for advices concerning cardiac mitochondrial imaging.

Sources of funding

None

Disclosure

None

References

1. Nichols M, Townsend N, Scarborough P, Rayner M. Cardiovascular disease in europe 2014: Epidemiological update. *Eur Heart J*. 2014;35:2950-2959

2. Yellon DM, Hausenloy DJ. Myocardial reperfusion injury. *N Engl J Med*. 2007;357:1121-1135

3. Hausenloy DJ, Yellon DM. Myocardial ischemia-reperfusion injury: A neglected therapeutic target. *J Clin Invest*. 2013;123:92-100

4. Ong SB, Hall AR, Hausenloy DJ. Mitochondrial dynamics in cardiovascular health and disease. *Antioxid Redox Signal*. 2013;19:400-414

5. Youle RJ, van der Bliek AM. Mitochondrial fission, fusion, and stress. *Science*. 2012;337:1062-1065

6. Le Page S, Niro M, Fauconnier J, Cellier L, Tamareille S, Gharib A, Chevrollier A, Loufrani L, Grenier C, Kamel R, Sarzi E, Lacampagne A, Ovize M, Henrion D, Reynier P, Lenaers G, Mirebeau-Prunier D, Prunier F. Increase in cardiac ischemia-reperfusion injuries in opa1+/- mouse model. *PLoS One*. 2016;11:e0164066

7. Dorn GW, 2nd. Mitochondrial dynamism and heart disease: Changing shape and shaping change. *EMBO Mol Med*. 2015;7:865-877

8. Brady NR, Hamacher-Brady A, Gottlieb RA. Proapoptotic bcl-2 family members and mitochondrial dysfunction during ischemia/reperfusion injury, a study employing cardiac hl-1 cells and gfp biosensors. *Biochim Biophys Acta*. 2006;1757:667-678

9. Ong SB, Subrayan S, Lim SY, Yellon DM, Davidson SM, Hausenloy DJ. Inhibiting mitochondrial fission protects the heart against ischemia/reperfusion injury. *Circulation*. 2010;121:2012-2022

10. Chen L, Gong Q, Stice JP, Knowlton AA. Mitochondrial opa1, apoptosis, and heart failure. *Cardiovasc Res*. 2009;84:91-99

11. Varanita T, Soriano ME, Romanello V, Zaglia T, Quintana-Cabrera R, Semenzato M, Menabo R, Costa V, Civiletto G, Pesce P, Viscomi C, Zeviani M, Di Lisa F, Mongillo M, Sandri M, Scorrano L. The opa1-dependent mitochondrial cristae remodeling pathway controls atrophic, apoptotic, and ischemic tissue damage. *Cell Metab*. 2015;21:834-844

12. Ikeda Y, Shirakabe A, Maejima Y, Zhai P, Sciarretta S, Toli J, Nomura M, Mihara K, Egashira K, Ohishi M, Abdellatif M, Sadoshima J. Endogenous drp1 mediates mitochondrial autophagy and protects the heart against energy stress. *Circ Res*. 2015;116:264-278

13. Song M, Mihara K, Chen Y, Scorrano L, Dorn GW, 2nd. Mitochondrial fission and fusion factors reciprocally orchestrate mitophagic culling in mouse hearts and cultured fibroblasts. *Cell Metab*. 2015;21:273-286

14. Disatnik MH, Ferreira JC, Campos JC, Gomes KS, Dourado PM, Qi X, Mochly-Rosen D. Acute inhibition of excessive mitochondrial fission after myocardial infarction prevents long-term cardiac dysfunction. *J Am Heart Assoc*. 2013;2:e000461

15. Wakabayashi J, Zhang Z, Wakabayashi N, Tamura Y, Fukaya M, Kensler TW, Iijima M, Sesaki H. The dynamin-related gtpase drp1 is required for embryonic and brain development in mice. *J Cell Biol*. 2009;186:805-816

16. Prunier F, Gaertner R, Louedec L, Michel JB, Mercadier JJ, Escoubet B. Doppler echocardiographic estimation of left ventricular end-diastolic pressure after mi in rats. *Am J Physiol Heart Circ Physiol*. 2002;283:H346-352

17. Wilding JR, Joubert F, de Araujo C, Fortin D, Novotova M, Veksler V, Ventura-Clapier R. Altered energy transfer from mitochondria to sarcoplasmic reticulum after cytoarchitectural perturbations in mice hearts. *J Physiol*. 2006;575:191-200

18. Saks VA, Veksler VI, Kuznetsov AV, Kay L, Sikk P, Tiivel T, Tranqui L, Olivares J, Winkler K, Wiedemann F, Kunz WS. Permeabilized cell and skinned fiber techniques in studies of mitochondrial function in vivo. *Mol Cell Biochem*. 1998;184:81-100

19. Kalakech H, Hibert P, Prunier-Mirebeau D, Tamareille S, Letournel F, Macchi L, Pinet F, Furber A, Prunier F. Risk and safe signaling pathway involvement in apolipoprotein a-i-induced cardioprotection. *PLoS One*. 2014;9:e107950

20. Chao de la Barca JM, Simard G, Sarzi E, Chaumette T, Rousseau G, Chupin S, Gadras C, Tessier L, Ferre M, Chevrollier A, Desquiret-Dumas V, Gueguen N, Leruez S, Verny C, Milea D, Bonneau D, Amati-Bonneau P, Procaccio V, Hamel C, Lenaers G, Reynier P, Prunier-Mirebeau D. Targeted metabolomics reveals early dominant optic atrophy signature in optic nerves of opa1delttag/+ mice. *Invest Ophthalmol Vis Sci*. 2017;58:812-820

21. Bochaton T, Crola-Da-Silva C, Pillot B, Villedieu C, Ferreras L, Alam MR, Thibault H, Strina M, Gharib A, Ovize M, Baetz D. Inhibition of myocardial reperfusion injury by

ischemic postconditioning requires sirtuin 3-mediated deacetylation of cyclophilin d. *J Mol Cell Cardiol*. 2015;84:61-69

22. Wai T, Garcia-Prieto J, Baker MJ, Merkwirth C, Benit P, Rustin P, Ruperez FJ, Barbas C, Ibanez B, Langer T. Imbalanced opa1 processing and mitochondrial fragmentation cause heart failure in mice. *Science*. 2015;350:aad0116

23. Zhang H, Wang P, Bisetto S, Yoon Y, Chen Q, Sheu SS, Wang W. A novel fission-independent role of dynamin-related protein 1 in cardiac mitochondrial respiration. *Cardiovasc Res*. 2017;113:160-170

24. Din S, Mason M, Volkers M, Johnson B, Cottage CT, Wang Z, Joyo AY, Quijada P, Erhardt P, Magnuson NS, Konstandin MH, Sussman MA. Pim-1 preserves mitochondrial morphology by inhibiting dynamin-related protein 1 translocation. *Proc Natl Acad Sci U S A*. 2013;110:5969-5974

25. Cadete VJJ, Vasam G, Menzies KJ, Burelle Y. Mitochondrial quality control in the cardiac system: An integrative view. *Biochim Biophys Acta Mol Basis Dis*. 2019;1865:782-796

26. Zhao T, Huang X, Han L, Wang X, Cheng H, Zhao Y, Chen Q, Chen J, Cheng H, Xiao R, Zheng M. Central role of mitofusin 2 in autophagosome-lysosome fusion in cardiomyocytes. *J Biol Chem*. 2012;287:23615-23625

27. Sebastian D, Sorianello E, Segales J, Irazoki A, Ruiz-Bonilla V, Sala D, Planet E, Berenguer-Llergo A, Munoz JP, Sanchez-Feutrie M, Plana N, Hernandez-Alvarez MI, Serrano AL, Palacin M, Zorzano A. Mfn2 deficiency links age-related sarcopenia and impaired autophagy to activation of an adaptive mitophagy pathway. *EMBO J*. 2016;35:1677-1693

2. Study N°2: Cardiac characterization of a *Drp1*$^{+/-}$ *Opa1*$^{+/-}$ deficient mouse model

Work in progress

2.1. Scientific background

Mitochondria are double membrane organelles present in hundreds to thousands of copies inside the cell. They are particularly important in cardiomyocytes, where they are the main source of ATP, an essential molecule in ensuring the excitation/contraction coupling. Other than being the major fuel source of the cell, mitochondria have many other functions: they are a main source of ROS, implicated in apoptosis and calcium signaling, and are one of the main actors in regulating cellular metabolism (Ong et al. 2015).

Mitochondrial function is tightly associated to its structure. In fact, mitochondria undergo continuous processes called mitochondrial fusion and fission. GTPase dynamin related protein-1 (DRP1) and human fission protein factor 1's (hFIS1) interaction results in smaller and fragmented mitochondria (mitochondrial fission). In contrast, mitochondrial fusion, mechanism responsible for longer and more elongated mitochondria, is coordinated by optic atrophy 1 protein (OPA1) and by mitofusin 1 and 2 (MFN1,2). A well balance between mitochondrial fusion and mitochondrial fission is essential to preserve the mitochondrial network integrity. This inter-organelle connectivity ensures the mixing of mitochondrial proteins and the replacement of damaged mtDNA (fusion) on one hand, and the elimination of damaged mitochondria by mitophagy (fission) on the other hand (Dorn 2015b).

In the past decade, mitochondrial dynamics became one of the most discussed topics in myocardial I/R injuries. Initially, it was stated that an ischemia leads to mitochondrial fragmentation, which is deleterious and implicated in apoptosis (Ong et al. 2010). Experiments trying to modulate mitochondrial dynamics proteins in order to improve myocardial I/R injuries showed many discrepancies. Some studies showed an improvement of cardiac function and a cardioprotective effect when inhibiting excessive fission (Din et al. 2013; Disatnik et al. 2013). Other studies showed cardiomyopathy in a cardiac homozygously deficient DRP1 mouse model linking it to a downregulation of mitophagy flux (Ikeda et al. 2015), and improved cell death outcome in Mfn2 deficient mice model (Papanicolaou et al. 2011).

To try to evade these contradictions, we conducted experiments on three different types of mouse model. We have already shown that a heterozygously Opa1 deficiency aggravates myocardial I/R injuries (Le Page et al. 2016) and that increasing fusion by means of DRP1 deficiency was associated with protection against I/R injuries (Cf study N°1). In this study, we sought to study the effect of a double heterozygous DRP1 and OPA1 deficiency in vivo on a basal level and in a myocardial I/R mice model.

2.2. Materials and methods

2.2.1. Mouse model

Heterozygous DRP1 and OPA1 knockout (*Drp1*$^{+/-}$ *Opa1*$^{+/-}$) mice were generated by crossing *Drp1*$^{+/-}$ mice previously described (Wakabayashi et al. 2009) and *Opa1*$^{+/-}$ mice previously described (Le Page et al. 2016). Mice were kept using standard light cycles, with food and water available ad libitum. All animal work was performed according to the European Community Guiding Principles in the care and use of animals (Directive 2010/63/UE; Décret n°2013-118). Authorizations to conduct animal experiments were obtained from the MENESR, *Ministère de l'Education Nationale de l'Enseignement Supérieur et de la Recherche* (APAFIS#15931-2018061815475007 v2).

2.2.2. Mitochondrial morphology by transmission electron microscopy

Samples of left ventricular (LV) papillary muscle were prepared for EM, as previously described (Wilding et al. 2006). Briefly, the hearts were fixed using a retrograde perfusion with 2% glutaraldehyde in cacodylate buffer (100mM sodium cacodylate and 2mM $MgCl_2$; pH 7.3). Ultra-thin longitudinal sections of 60nm were cut and examined using an electron microscope, with 20,000x-magnified images by means of the software Image J, designed to assess mitochondrial number and area. In total, 115 fields were analyzed from 4 *Drp1*$^{+/-}$ *Opa1*$^{+/-}$ mice (10 photos/mice) and 4 WT mice (19 photos/mice) for mitochondrial morphology at baseline.

2.2.3. Statistics

When normal distribution is verified, data is expressed as mean±standard error of the mean (SEM) and statistical significance of the difference between groups was estimated using the Student's *t*-test. When normal distribution is not verified, data is expressed as median [IQR=Interquartile range: min;max], and statistical significance between groups was estimated using non-parametric Mann-Whitney. Statistical analyses were performed using SPSS Statistics v.17.0 software (SPSS Inc.).

We chose to characterize Drp1$^{+/-}$ *Opa1*$^{+/-}$ *since Drp1*$^{-/-}$ *Opa1*$^{-/-}$ *mice are not viable, while comparing them to their WT littermates Drp1*$^{+/+}$ *Opa1*$^{+/+}$*. Furthermore, cardiac morphology and function, as well as protein expression in 3-month-old Drp1*$^{+/-}$ *Opa1*$^{+/-}$ *and WT mice were evaluated at baseline as previously mentioned in study N°1. Myocardial I/R was performed on 3-month-old Drp1*$^{+/-}$ *Opa1*$^{+/-}$ *and WT mice as previously detailed in study N°1.*

2.3. Results study N°2

We started by characterizing cardiac morphology by analyzing body weight (BW), heart weight/body weight ratio (HW/BW), Left ventricular (LV) weight/HW (LVW/HW) and LV function in 3-month-old *Drp1*$^{+/-}$ *Opa1*$^{+/-}$ and WT mice by echocardiography. BW (19.7±0.44g in WT vs. 22.8±0.61g in *Drp1*$^{+/-}$ *Opa1*$^{+/-}$), HW/BW ratio (5±0.05mg/g in WT vs. 4.4±0.11g in *Drp1*$^{+/-}$ *Opa1*$^{+/-}$) and LVW/HW (0.6±0.1mg/mg in WT vs. 0.7±0.01mg/mg in *Drp1*$^{+/-}$ *Opa1*$^{+/-}$) were not significantly different between the two groups (Fig. 28A, 28B, 28C). The heart rate recorded at the time of echocardiography was not significantly different between groups (591±29 bpm in WT vs. 594±18 bpm in *Drp1*$^{+/-}$ *Opa1*$^{+/-}$). Left ventricular end diastolic diameter (LVEDD), left ventricular end systolic diameter (LVESD) and fraction shortening (FS) (58±2 % in WT vs. 59±1 % in *Drp1*$^{+/-}$ *Opa1*$^{+/-}$) (Fig. 28D) were not significantly different between WT and *Drp1*$^{+/-}$ *Opa1*$^{+/-}$ mice.

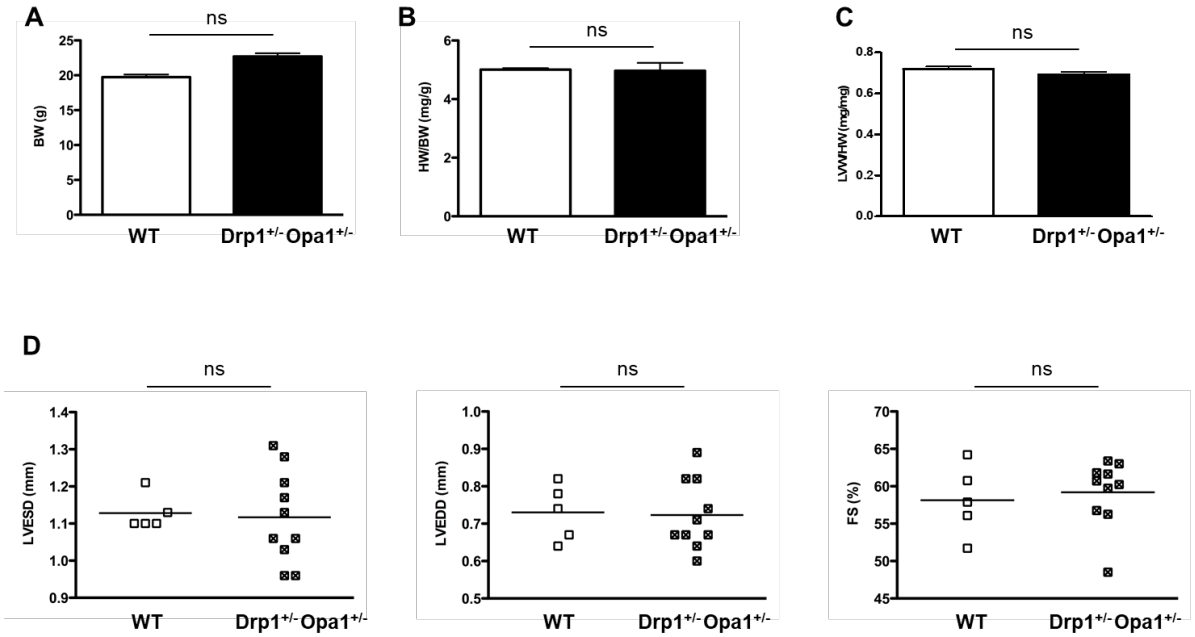

Figure 28: Anatomical characteristics and heart function of 3-month-old *Drp1*$^{+/-}$ *Opa1*$^{+/-}$ (n=8-10) and their wild type littermate (WT) mice (n=5-10). (A) Body weight (BW). (B) Heart weight over body weight (HW/BW) ratio. (C) Left ventricular weight over heart weight (LVW/HW). (D) Cardiac echocardiography, left: Left ventricle end-systolic volume (LVESD), middle: LV end-diastolic volume (LVEDD), right: LV fractional shortening (FS).

Electron microscopy (EM) analyses of cardiac papillary muscle were performed to study the influence of this double haploinsufficiency on mitochondrial morphology. The number of mitochondria per quartile of mitochondrial areas (Q1=small, Q2= medium, Q3= medium to large, Q4= large mitochondria) was analyzed. The number of mitochondria in cardiomyocytes per field was not significantly different between *Drp1*$^{+/-}$ *Opa1*$^{+/-}$ and WT mice (28 [IQR 26; 31] in *Drp1*$^{+/-}$ *Opa1*$^{+/-}$ vs. 32 [IQR 31; 36] in WT (p=0.2). However *Drp1*$^{+/-}$ *Opa1*$^{+/-}$ had significantly higher frequency of large mitochondria (Q4) and less small mitochondria (Q1) than WT (median of mitochondrial area:

0.483 µm^2 [IQR 0.293; 0.715] in *Drp1*$^{+/-}$ *Opa1*$^{+/-}$ vs. 0.368 µm^2 [IQR 0.206; 0.597] in WT) (p<0.001) (Fig. 29).

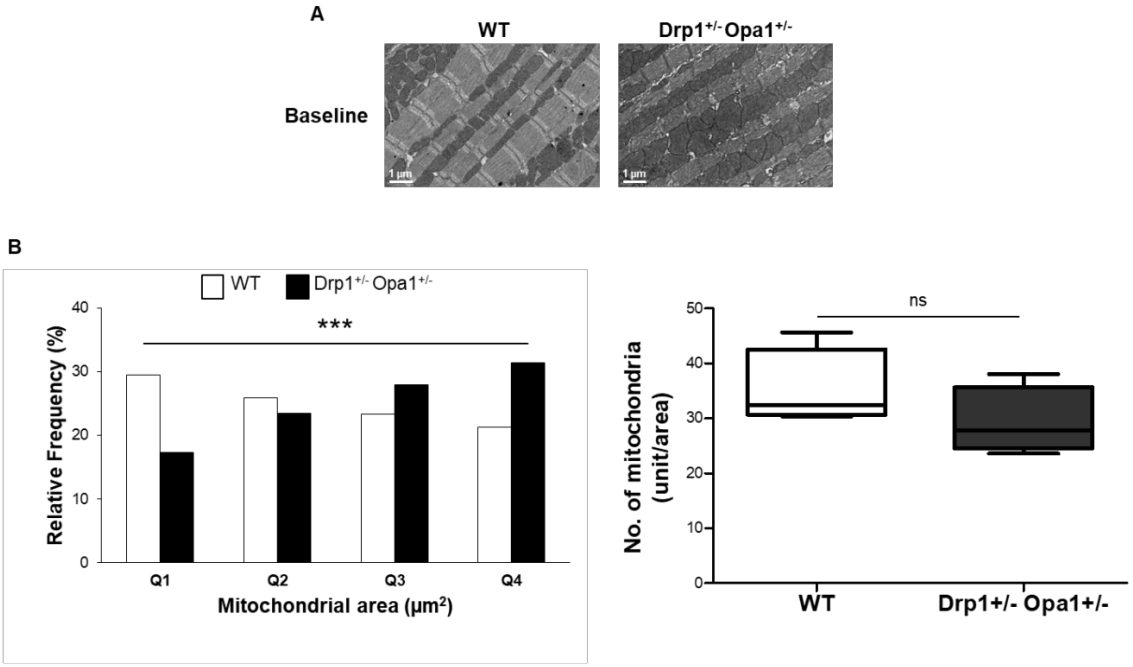

Figure 29: Mitochondrial morphology. (A) Representative electron microscopy (EM) images of left ventricle longitudinal sections at baseline in WT and mice. Scale bar: 1 µm. (B) Left: mitochondrial frequency represented according to the quartile distribution of the mitochondrial area. Right: the number of mitochondria per field. WT (n=2068) *Drp1*$^{+/-}$ *Opa1*$^{+/-}$ (n=1208). Data are represented as median [min;max].

DRP1 and OPA1 haploinsufficiency was confirmed by western blot. DRP1 (0.35±0.07 in *Drp1*$^{+/-}$ *Opa1*$^{+/-}$ vs. 0.81±0.05 in WT) and OPA1 protein cardiac levels (1.11±0.12 in *Drp1*$^{+/-}$ *Opa1*$^{+/-}$ vs. 2.00±0.27 in WT) were significantly lower in *Drp1*$^{+/-}$ *Opa1*$^{+/-}$ compared to their WT littermates (p<0.001 and p=0.01 respectively). Other mitochondrial proteins such as MFN2 and FIS1 were unaltered in *Drp1*$^{+/-}$ *Opa1*$^{+/-}$ compared to their WT littermates (Fig. 30).

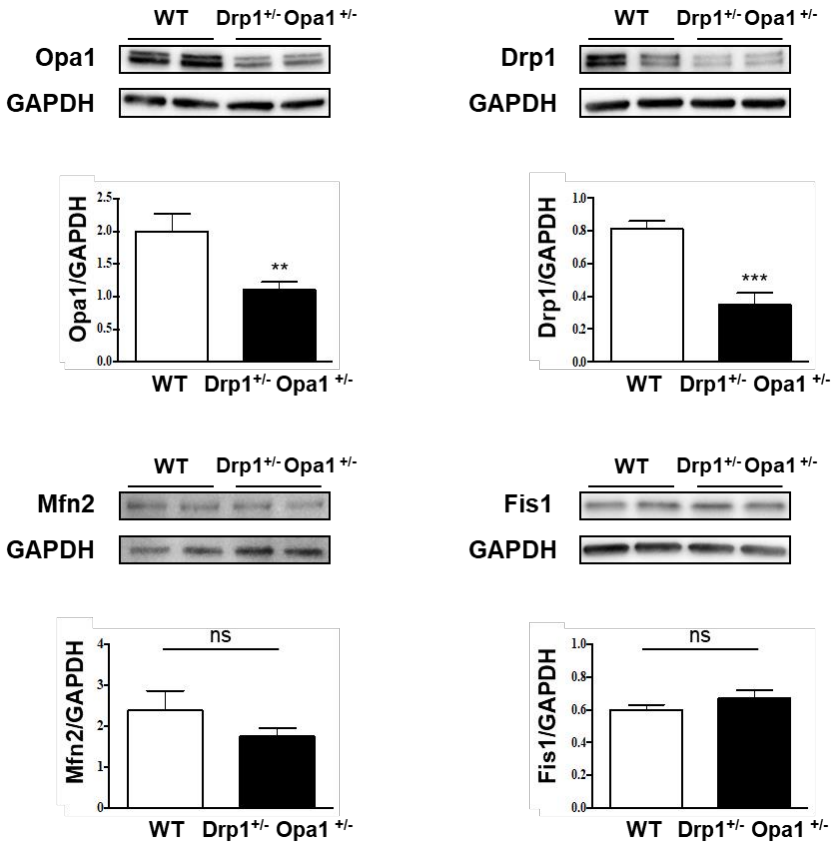

Figure 30: Mitochondrial dynamics protein expression. OPA1, MFN2, DRP1, and FIS1 expression assessed by means of western blotting (n=9-10/group). Immunoblots and histograms represented quantifications and GAPDH was used as a loading control. Values are expressed as mean ± SEM. ns= not significant, ** p=0.01, ***p<0.001.

We did not see any significant differences in protein expression of the mitochondrial respiratory chain complex and of Peroxisome proliferator-activated receptor gamma co-activator 1-alpha (PGC-1α) in 3-month old *Drp1*$^{+/-}$ *Opa1*$^{+/-}$ and their WT littermates (Fig. 31).

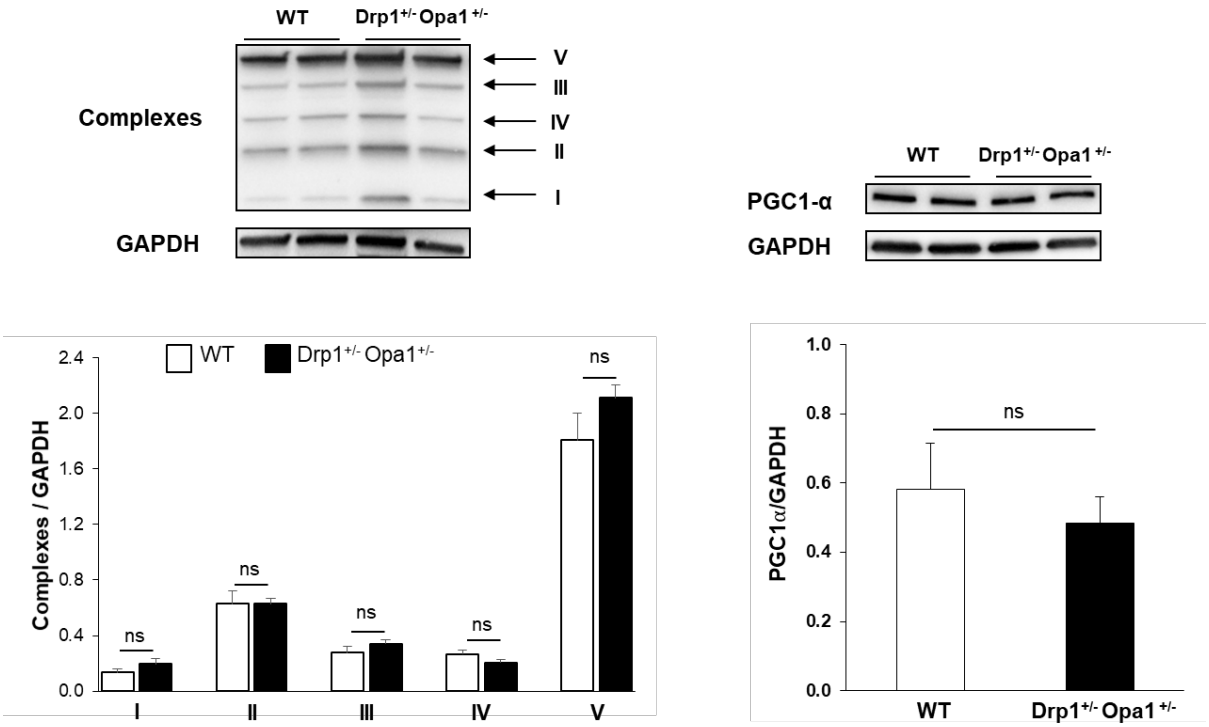

Figure 31: Mitochondrial respiratory chain complexes and PGC1α protein expression assessed by means of western blotting (n=9-10/group). Immunoblots and histograms represented quantifications and GAPDH was used as a loading control. Values are expressed as mean ± SEM. ns= not significant.

In the heart, we quantified levels of proteins implicated in mitophagy. More precisely, microtubule-associated proteins light chain 3B (LC3) I, II, sequestosome-1 or ubiquitin-binding protein p62, and Parkin (PARK2) protein levels in *Drp1*$^{+/-}$ *Opa1*$^{+/-}$ mice and WT. Whereas LC3-II/LC3-I was significantly lower in *Drp1*$^{+/-}$ *Opa1*$^{+/-}$ mice compared to WT mice (0.28±0.04 in *Drp1*$^{+/-}$ *Opa1*$^{+/-}$ mice vs. 0.39±0.03 in WT mice, p=0.03), LC3-I and LC3-II protein expression was not significantly different between the two groups. Similarly, p62 and PARK2 levels were not significantly different between *Drp1*$^{+/-}$ *Opa1*$^{+/-}$ mice and WT mice (Fig. 32).

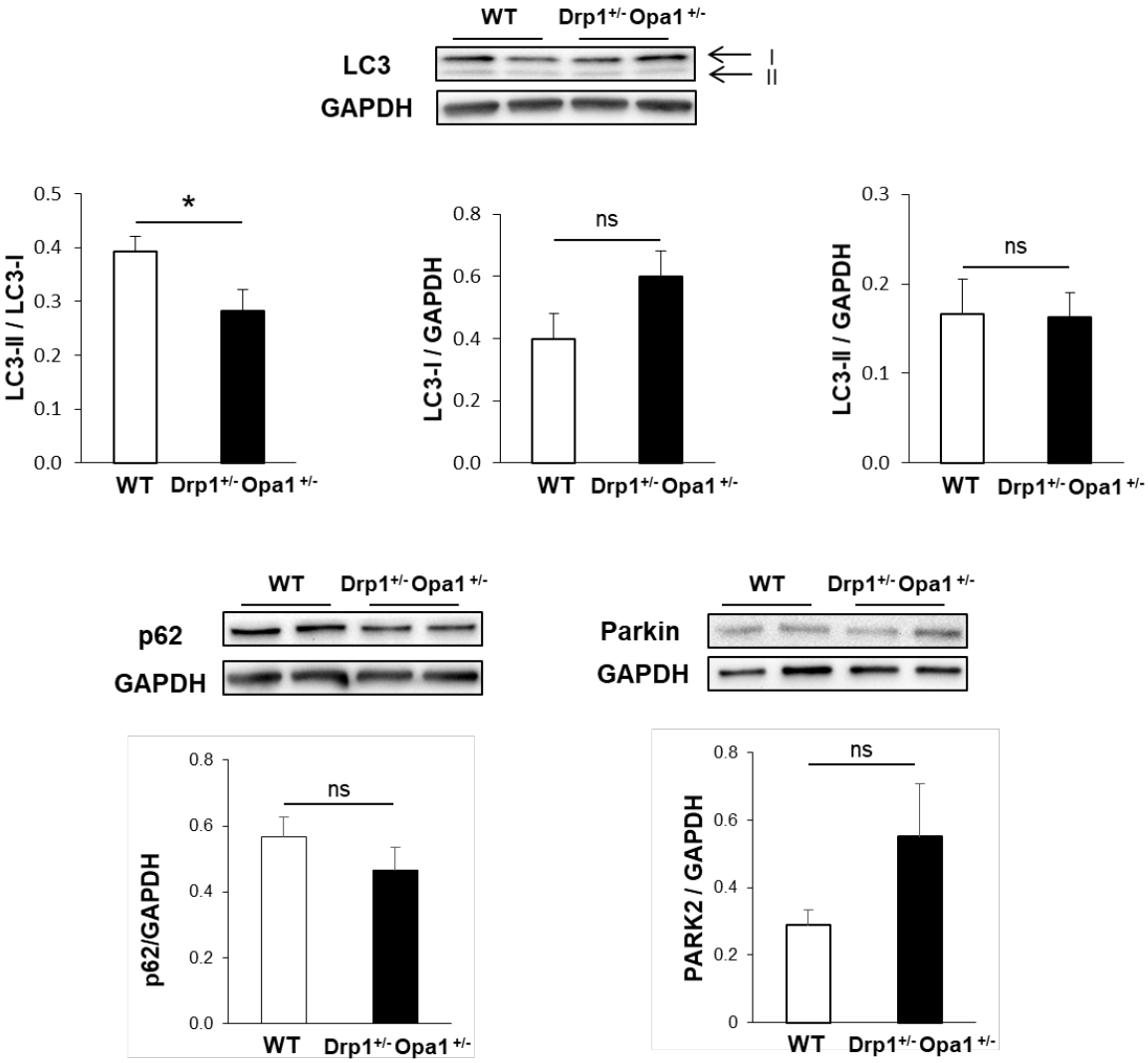

Figure 32: Representative immunoblot and quantification of autophagy proteins. Autophagy protein expression levels were assessed by means of western blot in quantitative analysis of LC3-I and LC3-II, p62 and PARK2 in *Drp1*$^{+/-}$ *Opa1*$^{+/-}$ and WT mice. The results are expressed as ratios of protein band densities to GAPDH or ratio of LC3-II/LC3-I (n=9-10 per group). Values are mean ± SEM. ns=not significant, *p<0.05.

To better understand the importance of both mitochondrial fusion and fission proteins in the heart, 3-month-old *Drp1*$^{+/-}$ *Opa1*$^{+/-}$ and WT mice were subjected to 30-min myocardial ischemia followed by 24-hour reperfusion (Fig. 33). AAR was evaluated using Evans Blue, afterwards myocardial I/R injuries were assessed using TTC staining. Both AAR/LV and the AN/AAR did not significantly differ between the two groups.

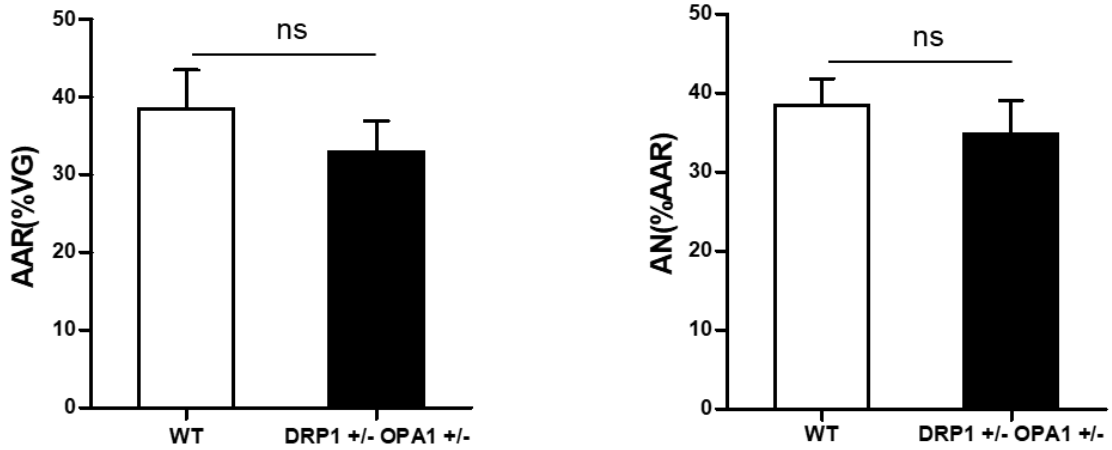

Figure 33: Histograms on the left showing quantification of area at risk (AAR) as a percentage of the total left ventricle (LV) and on the right area necrosis (AN) as a percentage of AAR (n=6-7/group). ns=not significant.

2.4. Discussion

Intrigue concerning the link between mitochondrial dynamics and myocardial I/R injuries has been raised in the past decade. Nevertheless, a lot of discrepancies have always existed concerning the role of mitochondrial dynamics proteins in these injuries.

Rewinding to 2006, excessive mitochondrial fragmentation was found in HL-1 cells after a simulated I/R (Brady, Hamacher-Brady, and Gottlieb 2006). Afterwards, Ong et al. established a link between DRP1, mitochondrial fission and H/R injuries (Ong et al. 2010). The authors used on one hand, a dominant negative construct of DRP1 to inhibit mitochondrial fission and on another hand a construct to overexpress MFN1, MFN2 in HL-1 cell model. In both cases, these constructs reduced the percentage of cell death and maintained the integrity of mitochondrial network after a simulated I/R. The same authors utilized an *in vivo* model of *Drp1* inhibition by injecting mdivi-1, and noticed a decrease in infarct size accompanied by an increase in mitochondrial elongation. Therefore, a conventional notion was widely recognized: mitochondrial fission is "harmful or pathological" and has to be inhibited, whereas mitochondrial fusion is "good or beneficial" and has to be upregulated or stimulated.

For a couple of years, results from different studies had the same outcome: inhibiting mitochondrial fission decreased injuries by either delaying mPTP opening (Ong et al. 2010), decreasing apoptosis (Din et al. 2013), or decreasing ROS production and increasing ATP production (Disatnik et al. 2013). Moreover, a recent work in our laboratory (Cf. Results, Study N◦1) showed a decrease in infarct size in a $Drp1^{+/-}$ deficient mouse model, engendered by a potential increase in mitophagy. However, Ikeda et al. described a mouse model with a cardiac specific homozygous deletion of *Drp1* ($Drp1^{-/-}$) inducible at 15 weeks post-natal. These mice were only viable 8 to 13 weeks after inducing genetic ablation, had cardiac hypertrophy, an aggravated infarct size, and showed a decrease in general and mitochondrial autophagy (Ikeda et al. 2015) . Regarding mitochondrial fusion proteins role in heart and in myocardial I/R injuries, studies conducted so far have been focused on genetic ablation of mitochondrial fusion proteins (Song et al. 2015; Piquereau et al. 2012; Le Page et al. 2016). Models showed cardiac hypertrophy with systolic dysfunction at baseline and exacerbated cardiac phenotype in stress conditions, however there is still a gap in studying myocardial I/R injuries while overexpressing mitochondrial fusion proteins in the heart.

Nonetheless, role of mitochondrial fission or fusion proteins separately as therapeutic targets is still not quite clear. To gain further insight into the relationship between mitochondrial dynamics proteins, heart function and myocardial I/R injuries we opted to work in a model where both mitochondrial fusion and fission were downregulated. Therefore, we crossed the two mice models on which we performed our previous studies ((Le Page et al. 2016); study N°1), the first one deficient for

DRP1, a mitochondrial fission protein, and the second one deficient for OPA1, a mitochondrial fusion protein. This generated a model deficient in both mitochondrial fission and fusion proteins. We sought to clarify the putative role of mitochondrial dynamics in heart health; is it the loss of mitochondrial fusion or fission that is responsible for the previously described phenotypes or is it the imbalance succeeding the loss? Would it be more detrimental to decrease both mechanisms or will double deficiency create a balance, enough to maintain normal cardiomyocyte cell functioning?

First of all, we started to characterize cardiac phenotype of these mice by assessing heart and left ventricle weight and function. Morphologically and functionally, hearts of *Drp1*$^{+/-}$ *Opa1*$^{+/-}$ were indistinguishable from those of WT littermates. Song et al. (Song et al. 2017) described a model similar to the one presented in this study (both mitochondrial fission and fusion proteins are abolished), a triple conditional cardiac knockout mouse model *Drp1*$^{-/-}$ *MFN1*$^{-/-}$ *MFN2*$^{-/-}$ (DRP1/MFN1/MFN2 TKO mice), where mice developed concentric cardiac hypertrophy and 50% of mice died 17 weeks after target gene ablation. Nevertheless, these data are an improvement compared to the lifespan of cKO *Drp1*$^{-/-}$ or DKO *Mfn1*$^{-/-}$ *Mfn2*-/- (Song et al. 2015). They suggested that observed mitochondrial adynamism mitigated but did not resolve cardiomyopathies provoked by interrupting either mitochondrial fusion or fission.

In our double deficient cardiomyocytes, large mitochondria was significantly more frequent compared to WT mice as if mitochondrial fusion is favored. Other mitochondrial dynamics proteins expression was not affected, meaning no compensatory mechanisms developed. Additionally, mitochondrial biogenesis was not altered since mitochondrial respiratory chain complexes and PGC1α (a protein implicated in mitochondrial biogenesis) protein expression was not affected by these deficiencies. In comparison, mitochondrial adynamism present in DRP1/MFN1/MFN2 TKO mice rendered mitochondria fragmented in cardiomyocytes with an absence of a filamentous interconnected network, an accumulation in the perinuclear region, and a modest respiratory uncoupling accompanied with an increase in mitochondrial mass. We did not evaluate mitochondrial respiratory parameters; nevertheless, the absence of changes in mitochondrial protein expression and of cardiac dysfunction did not give any evidence of mitochondrial dysfunction.

Afterwards, we evaluated expression levels of proteins implicated in mitophagy. The latter is an indispensable mitochondrial quality control pathway for identification and removal of individual organelles, which have become damaged or senescent. This process ensures the preservation of functional integrity of the cardiomyocytes mitochondrial pool (Cadete et al. 2019). Downregulation of either mitochondrial fusion or fission proteins have been shown to affect proper removal of mitochondria. In spite of that, contradictory results have been highlighted. For instance, Kageyama et al. and Song et al. (Song et al. 2015; Kageyama et al. 2014) showed an increase in mitophagy in cardiac specific conditional homozygous DRP1 knockout mice models, whilst Ikeda et al. and

Shirakabe et al. (Ikeda et al. 2015; Shirakabe et al. 2016) described a decrease in mitophagy flux in, respectively, a specific conditional homozygous DRP1 knockout mouse models and a cardiac specific heterozygous DRP1 knockout. It is noteworthy to mention that in all models presenting specific cardiac KO DRP1, viability reached its maximum of 13 weeks after inducing genetic ablation. Regarding MFN 1,2 and mitophagy, an ablation of these proteins in cardiac mycoytes has been shown to suppress mitophagy (Song et al. 2015; Chen and Dorn 2013). We evaluated mitophagy by quantifying LC3 levels. Even though, LC3-II/LC3-I ratio was significantly decreased in *Drp1*$^{+/-}$ *Opa1*$^{+/-}$, LC3-I and LC3-II protein expression individually was not statistically different between the two groups. Moreover, other mitophagy markers such as p62 and Parkin were comparable between the two groups suggesting that mitophagy was not affected by this genetic ablation. LC3-II/LC3-I ratio is usually used as an indicator of autophagy flux, however LC3-II is degraded after fusion of phagophores with lysosomes. Considering that LC3 immunoblotting is not the most apposite way to evaluate mitophagy or general autophagy, obtained results are to be considered carefully (Mizushima and Yoshimori 2007). Unchanged basal mitophagy rate is concordant with other obtained results considering that *Drp1*$^{+/-}$ *Opa1*$^{+/-}$ mice show a comparable cardiac phenotype to that of their WT littermates with no mitochondrial dysfunction observed at baseline. Referring to Song et al. DRP1/MFN1/MFN2 TKO mouse model, mitophagy was interrupted with an accumulation of morphologically and functionally abnormal mitochondria (Song et al. 2017).

Finally, when challenged, with a myocardial I/R, these mice showed an infarct size with an area at risk comparable to that of *Drp1*$^{+/+}$ *Opa1*$^{+/+}$ (WT). In previous work, we showed an increase in infarct size in *Opa1*$^{+/-}$ mice, and a decrease in these injuries in *Drp1*$^{+/-}$ mice. This suggests that balancing rather than normalizing fission/fusion could be more important. In addition to that, the absence of cardiac and mitochondrial dysfunction unlike in *Drp1*$^{+/-}$ and *Opa1*$^{+/-}$ mice; makes our result less surprising.

The constellation of our results herein are in line with findings of Song et al. 2017 (Song et al. 2017). It suggests that in our mouse model, mitochondrial dynamism deficiency was not an enough cause for a pathological cardiac phenotype. Additionally, and while considering our previous results (Study N°1; (Le Page et al. 2016)), we could suggest that an imbalance in mitochondrial dynamics has more consequences than simultaneously abrogating both mechanisms (mitochondrial hypo-dynamism or adynamism).

In this study, some limits are to be presented. We evaluated mitochondrial dynamics protein as well as mitophagy related protein expression at baseline and not after I/R. However, the absence of any myocardial dysfunction at baseline as well as the comparability of infarct size between double heterozygous and WT mice did not encourage us to explore these proteins expression in a I/R context. Moreover, in our model adaptive and compensatory mechanisms could be implemented since these

mice differ from other previously described models. Indeed, deficiency is not specifically cardiac tissue induced. It is present at embryogenesis levels and in whole body.

3. Conclusion

In summary, the role of the mitochondrial fusion and fission proteins in the adult heart at baseline and in terms of susceptibility to I/R myocardial injuries is quite complex. Our studies have confirmed furthermore the importance of mitochondrial dynamics protein in cardiomyocytes and their implication in myocardial I/R injuries. Our results led to two major conclusions:

- ✓ A mild deficiency in DRP1 seems to be cardioprotective, by a potential increase in defective mitochondria elimination, unlike documented exacerbated injuries seen in cardiac specific homozygous knockout mice models.
- ✓ Separate mitochondrial fusion or fission deficiency seems to have more consequences in cardiomyocytes than that of a combined fusion and fission deficiency. This implies that even if both mitochondrial fusion and fission proteins are downregulated, equipoise between these two mechanisms is of greater importance in cardiomyocytes than conserving the integrity of one mitochondrial dynamic mechanism (fusion or fission).

The use of genetic mouse models showed the functional inextricable link defined between mitochondrial dynamism, mitochondria size, mitochondrial function, and mitophagy. To conclude, interplay between mitochondrial fusion and fission is far greater than simply controlling mitochondria size and its manipulation is of potential therapeutic perspective.

Part 2:
Kynurenine pathway metabolites mediate cardioprotection

Study N°3: Kynurenic acid reduces myocardial ischemia/reperfusion injuries by activating antioxidant defense and mitophagy

Study N°4: Kynurenine mediates cardioprotection in acute myocardial infarction

1. Study N°3: Kynurenic acid reduces myocardial ischemia/reperfusion injuries by activating antioxidant defense and mitophagy

Manuscript in preparation

1.1. Scientific background

TRP is an essential amino acid in humans. It is either used for protein synthesis or catabolized via the serotonin or kynurenine pathway. The kynurenine pathway is the main route (95% of free TRP) of TRP degradation. IDO catalyze TRP oxidation to KYN. The latter can either be metabolized to KYNA or QA. KATs enzymes catalyze the transamination of KYN into KYNA. KYNA is a metabolite known for its neuroprotective abilities. It is an antagonist of NMDA receptors which are responsible for neuronal excitation signaling and implicated in cerebral I/R injuries. (Phillips et al. 2019).

Several studies reported a decrease of cerebral injuries after KYNA treatment in stroke model, bilateral carotid artery occlusion model…(Germano et al. 1987; Roucher et al. 1991). It was not until recently, that cardioprotective properties of KYNA were unraveled. It reduced injuries when injected 2-hr before and 2-hr after *in vivo* myocardial I/R in mice (Olenchock et al. 2016). Moreover, our previously mentioned results of KYN-increased concentrations with (Chao de la Barca et al. 2016) encouraged us furthermore to investigate the aforementioned cardioprotective properties to try to understand underlying mechanisms.

1.2. Article N°2

Kynurenic acid reduces myocardial ischemia/reperfusion injuries by activating antioxidant defense and mitophagy

Rima Kamel[a], MS; Delphine Baetz[c], PhD; Naïg Gueguen[a,d], PhD; Agnès Barbelivien[a]; Anne-Laure Guihot[a], BS; Louwana Allawa[a], MS; Jean Gallet[a], MD; Justine Beaumont[a], BS; Michel Ovize[c,e], MD, PhD; Daniel Henrion[a], PhD; Pascal Reynier[a,d], MD, PhD; Delphine Mirebeau-Prunier[a,d], MD, PhD; Sophie Tamareille[a*], PhD; Fabrice Prunier[a,b*], MD, PhD

[a]Laboratoire MITOVASC, CNRS UMR 6015 INSERM U1083, Université d'Angers, Angers, France
[b]Service de Cardiologie, CHU Angers, Angers, France
[c]Univ Lyon, CarMeN Laboratory, INSERM, Université Claude Bernard Lyon 1, 69500, Bron France
[d]Département de Biochimie et Génétique, CHU Angers, Angers, France
[e]Service d'Explorations Fonctionnelles Cardiovasculaires & CIC de Lyons, Hôpital Louis Pradel, Hospices Civils de Lyon, Lyon, France
*both authors contributed equally to this work as last co-authors

Corresponding author:
Prof. Fabrice Prunier
Laboratoire MITOVASC, Bâtiment IRIS 2, 3 rue Roger Amsler, 49100 Angers France
Tel: +33 (0)241 355 147, fax: +33 (0)241 354 004; email: FaPrunier@chu-angers.fr

Short title:
Kynurenic acid mediates cardioprotection

Keywords:
kynurenic acid, cardioprotection, mitophagy, oxidative stress

Highlights:

- Kynurenic acid mediates cardioprotection in a myocardial ischemia/reperfusion model
- FOXO3α phosphorylation is decreased after kynurenic acid treatment
- Mitophagy and antioxidant markers are implicated in observed cardioprotection

ABSTRACT

INTRODUCTION: Cardioprotective effect of Kynurenic acid (KYNA), a metabolite of the kynurenine pathway, has recently been reported. However, the mechanisms by which it may be protective are unknown. Hence, we sought to investigate its cardioprotective mechanisms in the context of myocardial ischemia/reperfusion.

METHODS: H9C2 cells hypoxia/reoxygenation (H/R) and rat *in vivo* myocardial ischemia/reperfusion models were used to test KYNA cardioprotective effect. H/R and H/R+KYNA groups were subjected to H/R and treated with vehicle or KYNA (1µM) respectively, at different times (pre=10 minutes before hypoxia, per=during hypoxia, post=during reoxygenation). MI and MI+KYNA groups underwent left coronary artery ligation and treated with vehicle (1M) or KYNA (300mg/Kg) respectively. Cell death was quantified by flow cytometry using propidium iodide and infarct size was quantified after TTC staining. Mitochondrial respiratory chain complexes activites were measured by spectrophotometry. Protein expression was evaluated by western blot and mRNA was quantified by RT-qPCR.

RESULTS: *In vitro*, KYNA treatment in pre, pre+per, pre+per+post groups significantly reduced H9C2 relative mortality by an average of 30% compared to vehicle group ($p=0.024$, $p=0.006$, $p=0.007$, respectively). Infarct size was significantly reduced in MI+KYNA group compared to MI group ($p=0.023$). KYNA treatment did not have any effect on the mitochondrial respiratory chain complex activity. GPR35, and SOD2 mRNA levels were increased in MI+KYNA group compared to MI group ($p=0.022$ and $p=0.049$ respectively for GPR35 and SOD2). A significant increase in PARK2 protein levels ($p=0.036$) marked a mitophagic stimulation. Additionally, ERK1/2, Akt and FOXO3α phosphorylation levels were significantly reduced after KYNA treatment ($p=0.005$, $p=0.047$ and $p<0.001$ respectively for ERK1/2, Akt, FOXO3α).

CONCLUSION: KYNA reduced ischemia/reperfusion injuries in both, *in vitro* and *in vivo* models. KYNA-mediated cardioprotection was associated with decreased ERK1/2 and Akt phosphorylation levels, which led to a decrease in FOXO3α phosphorylation, a mechanism that was associated with an increase in mitophagy and antioxidant defense mechanisms.

1. INTRODUCTION

Myocardial infarction remains one of the leading causes of mortality in developed countries (Montrief et al. 2019). Reperfusion is paramount to the salvage of ischemic myocardium. However final infarct size is due to two components: ischemic damages and reperfusion injuries. Whilst several pharmacological or ischemic conditioning strategies were capable of reducing myocardial reperfusion injuries in animal models and prove-of-concept clinical studies, (with limited number of patients) no effective cardioprotective strategy was translated to the clinical arena.

In previous works, we have shown a plasmatic kynurenine concentration increase in rats and humans after remote ischemic conditioning, suggesting a link between the kynurenine pathway and cardioprotection (Chao de la Barca et al. 2016; Kouassi Nzoughet et al. 2017). Moreover, rats receiving a kynurenine intraperitoneal injection 10 minutes before a myocardial ischemia/reperfusion exhibited a reduced infarct size compared to vehicle treated group. The kynurenine pathway is one of the main routes of tryptophan degradation, an essential amino acid. Approximatively, 95% of free tryptophan is oxidized into kynurenine, a rate limiting step controlled by Indolamine-2,3-Dioxygenase (IDO) or Tryptophan-2,3-Dioxygenase (TDO) in the liver. Afterwards, kynurenine is either transformed into kynurenic acid (KYNA) or into quinolinic acid, reactions catalyzed by kynurenine aminotransferase (KAT) and kynurenine 3-monooxygenase (KMO) respectively (Wang et al. 2015).

KYNA is a metabolite with pleiotropic effects (Wirthgen et al. 2017). In 2016, Olenchock *et al*. reported a cardioprotective effect of KYNA in an *ex vivo* and an *in vivo* myocardial ischemia/reperfusion mouse model (Olenchock et al. 2016). Altogether, these findings suggest a potential major role of kynurenine pathway in protecting the heart against ischemia/reperfusion injuries. However, mechanisms by which it is cardioprotective are largely unknown. KYNA has antioxidant properties (Lugo-Huitron et al. 2011; Perez-Gonzalez, Alvarez-Idaboy, and Galano 2015) and has been identified as a ligand of the recently de-orphanized G protein-coupled receptor 35 (GPR35) (Wirthgen et al. 2017). An emerging importance of GPR35 in cardiovascular diseases was recently documented (Ronkainen et al. 2014; Mackenzie et al. 2011). Like other G protein-coupled receptors, GPR35 has been shown to modulate signaling pathways which may be implicated in myocardial damage.

Mitophagy (mitochondrial autophagy), cell death, mitochondrial respiration, antioxidant defense being key targets of cardioprotective strategies (Yang and Hung 2009). In the present study, we sought to investigate the cardioprotective effect of KYNA and to elucidate potential implicated cardioprotective mechanisms in both *in vivo* rat myocardial infarction model and in vitro hypoxia/reoxygenation H9C2 cell model.

2. METHODS

2.1. *In vitro H9C2 hypoxia/reoxygenation*

H9C2-SV40 cells, an immortalized rat cardiomyoblasts cell line, were used for *in vitro* hypoxia/reoxygenation (Bochaton et al. 2015) in order to mimic myocardial ischemia/reperfusion. Cells were cultured in a standard cell culture media, Dulbecco's Modified Eagle Medium (DMEM) high glucose (4.5 g/L) with antibiotics (Penicillin and Streptomycin 10 mL/L) and 10% of Fetal Bovine Serum (FBS) (Dutscher, Brumath, France). Hypoxia was induced by washing away DMEM complete medium three times and by replacing it with a glucose and serum free isotonic solution (Tyrode's solution (mM)) (NaCl 130, KCl 5, Hepes 10, $MgCl_2$ 1, $CaCl_2$ 1.8, pH 7.4). Cells were placed in a hypoxia chamber flushed with a stream of pure nitrogen during 4 hours and 50 minutes at 37°C. Oxygen rate was kept at 0.5%. Reperfusion was mimicked by replacing the Tyrode's solution with complete medium in a standard incubator under normoxic conditions for 2 hours. Groups were defined as following (Fig. 1A):

- Control group: Cells did not undergo any intervention. Cells were kept in normoxic conditions and culture medium for 7 hours.
- H/R group: Cells underwent hypoxia/reoxygenation with DMSO (vehicle) treatment, 10 minutes before hypoxia and all through the procedure.
- H/R+KYNA group: Cells underwent hypoxia/reoxygenation with KYNA treatment (1µM) either 10 minutes before hypoxia (pre), or pre + during hypoxia (pre+per), or pre + per + during reoxygenation (pre+per+post).

2.2. *Cell death and mitochondrial membrane potential (ΔΨm) assessment*

At the end of reoxygenation (i.e 2 hours), cells were detached from the plates using Accutase (PAA Laboratories, Ontario, Canada). Cell death was quantified by flow cytometry (LSR-Fortessa X-20 BD Biosciences, New jersey, United states) using 1µg/mL Propidium Iodide (PI) (ex: 488 nm; em: 590 nm) (Sigma Aldrich, Missouri, United States). Cell death in H/R group was considered equal to 1, and other data was expressed as relative mortality compared to H/R. ΔΨm was quantified with 20mM of DilC1 (1,1',3,3,3',3'-Hexamethylindodicarbocyanine Iodide) (ex: 633 nm; em: 658 nm) (Enzo Life Sciences, Villeurbanne, France). Triplicate samples were prepared for each condition and a total of 10 000 events were acquired by FACS.

2.3. *Animal studies*

Male adult Wistar rats, aged 8 to 10 weeks and weighing 250 to 300g, were used in this study. They were kept in a temperature-controlled room (22°C±2°C) with an adequate 12 hours light-12 hours dark cycle. Food and water were available *ad libitum*. All experiments were conducted in agreement with the guidelines from EU Directive 2010/63/EU; French Decree no. 2013–118 of the European Parliament on the protection of animals used for scientific purposes. The protocol was

approved by the Ethics Committee in Animal Experimentation of Pays de la Loire and by the French Ministry of Higher Education and Research (APAFIS#8668-20 170 12417473589 v3).

Hearts were excised under deep anesthesia (60 mg/kg of sodium pentobarbital (Exagon®, Axience, France). Afterwards, in one set of experiments the hearts were excised for infarct size assessment and, in another set of experiments, freeze-clamped and stored at -80°C for RNA messenger expression analysis, Western blot (WB) analysis, and assessment of the mitochondrial respiratory chain complexes activity.

2.4. Myocardial ischemia/reperfusion rat model

Rats were anesthetized by means of intraperitoneal injection of 60 mg/kg of sodium pentobarbital (Exagon®, Axience, France), orotracheally intubated, and mechanically ventilated with room air by means of a small animal ventilator (SAR-830 A/P, CWE, United states). Body core temperature was maintained at 37 ± 0.5°C (HB101/2 RS; Bioseb, France). The pericardium was removed to expose the heart after a median sternotomy. Coronary occlusion was induced by realizing a left anterior descending coronary artery (LAD) ligature. Using a 7.0 monofilament suture (Premio 7.0, Peters Surgical, France) passed through a short length of tubing (PE50), a reversible snare was realized and clamped onto the epicardial surface directly above the coronary artery. The appearance of epicardial cyanosis and dyskinesis of the ischemic region confirmed ischemia. Following 40 minutes of occlusion, reperfusion was achieved by loosening the snare and confirmed by observing an epicardial hyperemic response. The depth of anesthesia was checked by toe pinch before and during surgery. An extra dose of 30 mg/kg pentobarbital was injected in case of positive nociceptive response. Rats were randomly assigned to one of the following groups (Fig. 1B):

- Sham group: animals undergoing all the surgical procedure except ligature of the coronary artery.

- MI group: animals undergoing myocardial ischemia/reperfusion and injected 10 minutes before ischemia with NaOH 1M (vehicle).

- MI+KYNA group: animals undergoing myocardial ischemia/reperfusion and injected 10 minutes before ischemia with 300mg/Kg KYNA (Sigma Aldrich, Missouri, United States). The dose was chosen based on previously published data (Germano et al. 1987; Leib et al. 1996).

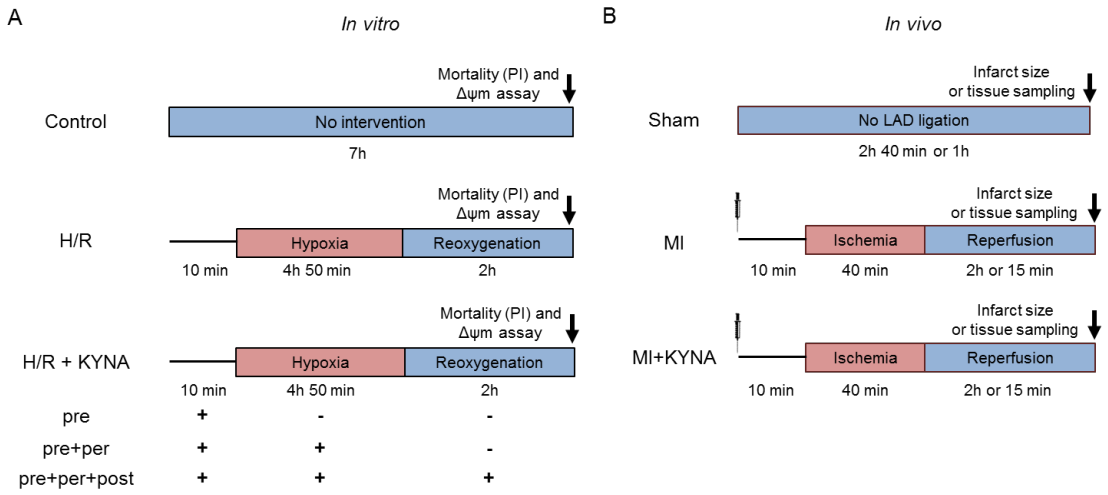

Fig. 1: *In vitro* and *in vivo* experimental design of protocols and groups. (A) *In vitro*: H9C2 control cells underwent no intervention, cells from the hypoxia/reoxygenation (H/R) groups were submitted to 4 hours 50 minutes of hypoxia followed by 2 hours of reoxygenation and were either treated with vehicle (DMSO) or with kynurenic acid (1µM) 10 minutes before hypoxia, or before and during hypoxia, or before, during and after hypoxia. Cell death quantification as well as mitochondrial membrane potential were performed 2 hours after reoxygenation. (B) *In vivo*: Sham animals underwent no injection and no left anterior descending coronary artery (LAD) ligation, MI group underwent 40 minutes of ischemia followed by 2 hours of reperfusion. 10 minutes before coronary artery occlusion vehicle (NaOH 1M) or kynurenic acid (300mg/Kg) was administrated intraperitoneally. Infarct size assessment using 2,3,5-triphenyltetrazolium chloride (TTC) staining after 2 hours of reperfusion, tissue sampling was performed after either 15 minutes or 2 hours of reperfusion.

2.5. Area-at-risk and infarct-size determination

Following 120 minutes of reperfusion, the hearts of the vehicle and the KYNA-treated groups were excised and the LAD was re-occluded using the monofilament suture kept in place. The area at risk (AAR) was outlined after a retrograde perfusion with Evans blue (1%). From the apex to the base, the heart was cut into five equal slices and then incubated with a 1% solution of 2.3.5-triphenyltetrazolium chloride (TTC, Sigma-Aldrich, Missouri, United states) in phosphate buffer at pH 7.4 and 37°C. TTC staining allows the distinction between infarcted myocardium in white and viable myocardium colored brick red. The slices were photographed. Infarct size was quantified using planimetry with Image J software (NIH, Maryland, United states). Area of necrosis (AN) was expressed as a percentage of the AAR (AN%AAR) and the AAR as a percentage of total left ventricular area (AAR%LV).

2.6. Real-time quantitative reverse transcription polymerase chain reaction (RT-qPCR)

We quantified the expression of genes encoding Catalase, GPR35 and Superoxide Dismutase 1, 2, 3 (SOD1, 2, 3) following 120 minutes of reperfusion. Genes encoding hypoxanthine phosphoribosyltransferase (hprt) and glucuronidase, beta (Gusb) were used as reference. Primer sequences are listed in Table 1.

Total RNA was extracted using RNeasy MiniKit (Qiagen, Germany) according to the manufacturer's instructions from approximately 30 µg of frozen left ventricular tissue samples from the ischemic zone of MI and MI+KYNA animals, or non-ischemic zone in sham. cDNA was synthesized using Quantitect Reverse Transcription kit (Qiagen, Allemagne) following the manufacturer's instructions. In a total volume of 20 µl reaction system (10 ng of cDNA), SYBR™ Select Master Mix (Applied biosystems, California, United states) was used to perform qPCR using a Lightcycler® 480 II thermocycler (Roche, Switzerland). Thermal cycling conditions were as following: 95°C for 3 min, followed by 40 cycles of 95°C for 15 s and 60 °C for 1 min. Results of target genes mRNA were normalized on the average of the Ct value of the reference genes mRNA and expressed as $2^{\Delta Ct}$ where ΔCt is the difference between Ct of reference genes and Ct of target gene.

Gene	NCBI Genbank	Forward sequence	Reverse sequence
Cat	*NM_012520.2*	5'-ttgccaaccacctgaaagat-3'	5'-agggtggacgtcagtgaaat-3'
Gpr35	*NM_001037359.1*	5'-ccaacttggccgtgtttatc-3'	5'-cctgcactgtcaggatcaaat-3'
Gusb	*NM_017015.2*	5'-ctctggtggccttacctgat-3'	5'-cagactcaggtgttgtcatcg-3'
Hprt	*NM_012583.2*	5'-gaccggttctgtcatgtcg-3'	5'-acctggttcatcatcactaatcac-3'
Sod1	*NM_017050.1*	5'-ggtccagcggatgaagag-3'	5'-ggacacattggccacacc-3'
Sod2	*NM_017051.2*	5'-attgccgcctgctctaatc-3'	5'-gatagtaagcgtgctcccaca-3'
Sod3	*NM_012880.1*	5'-cttgggagagcttgtcaggt-3'	5'-caccagtagcaggttgcaga-3'

Table 1: Forward and reverse primer sequences for target and reference genes.

2.7. Western blot (WB) analysis

Freeze-clamped ischemic (MI and MI+KYNA animals) and non-ischemic (sham) LV rat hearts were used following 15 minutes or 120 minutes of reperfusion for WB analysis. 40 µg of total proteins were separated by SDS-PAGE and transferred to a nitrocellulose or PVDF membrane. Membranes were incubated with antibodies diluted in TBS buffer containing 5% non-fat dried milk, against p-ERK1/2, ERK1/2, p-Akt, Akt, phosphorylated AMP-activated protein kinase (p-AMPKα), AMPKα, p-FOXO3α, FOXO3α (1/1000; Cell Signaling Technology, Massachusetts, Unites states), catalase (1/1000; Sigma-Aldrich, Missouri , Unites states), Total OXPHOS Rodent WB antibody Cocktail (1/250; Abcam, Cambridge, United Kingdom), Peroxisome proliferator-activated receptor

gamma co-activator 1alpha (PGC1α), Superoxide dismutase 2 (SOD2) (1/1000, abcam, Cambridge, United kingdom) SOD1 (1/500, Enzo Life Sciences, New York, United states), SOD3, Nucleoporin p62 (p62) (1/1000, Enzo Life Sciences, New York, United States), Parkin (PARK2) (1/1000, Abnova,Taïwan). GAPDH (1/10000; Sigma-Aldrich, Missouri, Unites States) and β-actin (1/1000; Sigma-Aldrich, Missouri, United States) were used as loading controls. Membranes were incubated with appropriate (rabbit or mouse) secondary antibodies (1/5000, Thermo Fisher Scientific, Massachusetts, United States) conjugated to horseradish peroxidase. The blots were developed using the enhanced chemi-luminescence method. The band densities were analyzed using Image Lab (BioRad, California, United States).

2.8. Mitochondrial respiratory chain complex enzymatic activity assessment

Activities of Lactate dehydrogenase (LDH), citrate synthase (CS) and the electron transport chain complexes (complexes I–IV) were spectrophotometrically measured at 37°C with a UV spectrophotometer (SAFAS, UVmc2, Monaco) in sham, MI and MI+KYNA left ventricle muscle homogenates after 2 hours of reperfusion. Homogenates were obtained after repeating two times the homogenization and centrifugation step (20 minutes at 650g) while discarding the pellet.

The activity of CS was measured in reaction medium consisting of 100 mM Tris·HCl pH 8.1, 150 µM 5,5′-dithio-bis(2-nitrobenzoic acid) (DTNB), 50 µM oxaloacetate, 30 µM acetyl-CoA, and 0,1% Triton X-100. After 2 minutes of incubation, the reaction was initiated by adding 10µL/mL of homogenate, and the change in optical density at 412 nm was recorded over 1 min.

NADH ubiquinone reductase (complex I) activity was assayed in KH_2PO_4 buffer pH 7.5, 3.75 mg/mL bovine serum albumin (BSA), 100 µM decylubiquinone, 10 µL/mL homogenate, with (to determine background rates, subsequently subtracted) or without 10 µM rotenone. After 2 minutes of incubation at 37°C, the reaction was initiated by adding 0.1 mM NADH. The activity was measured at 340 nm by monitoring the oxidation of NADH over 2 min.

The activity of succinate dehydrogenase (complex II) was measured after the reduction of 2,6-dichlorophenolindophenol (DCPIP) at 600 nm in a buffer containing 50 mM KH2PO4, 2,5 mg/mL BSA, 6.5 µM rotenone, 5 µmg/mL antimycin, 25 mM succinate, 1 mM KCN, and 100 µM DCPIP, pH 7.5. After 2 minutes of incubation at 37°C with 15 µL of homogenate, the reaction was initiated by the addition of 100 µM decylubiquinone, and the optical density was recorded for 2 min.

The activity of ubiquinone-cytochrome c reductase (complex III) was determined by monitoring the reduction of cytochrome c at 550 nm. Ten µL/mL of homogenate were incubated for 60 s in a reaction medium consisting of 100 mM KH2PO4 pH 7.5, 250 µM Ethylenediaminetetraacetic acid (EDTA), 1mg/mL BSA, 1mM KCN, 100 µM oxidized cytochrome c with or without 5µg/mL antimycin (non-enzymatic reduction of cytochrome c). The reaction was initiated by adding 100 µM decylubiquinol, and the optical density was measured over 40 seconds.

The specific activity of complex III was calculated by subtracting the activity of the non-enzymatic reaction from that of the total activity.

The activity of cytochrome-c oxidase (complex IV) was measured by monitoring the oxidation of reduced cytochrome c at 550 nm. An 80 μM solution of reduced cytochrome c (92–97% reduced using dithionite) in 55 mM KH2PO4, pH 7.0, was pre-incubated over 2 min. The reaction was initiated by adding 10 μL/mL of homogenate, and the change in optical density was measured over 40 seconds.

The activity of LDH was measured by monitoring the oxidation of NADH at 340 nm. The reaction was assayed in a buffer medium containing 95 mM KH2PO4 pH 7.1, 0.15% Triton 10X, 2.5 mM pyruvate, and 5 μL of homogenate. After 5 minutes incubation at 37°C, the reaction is initiated by addition of 100 μM NADH and measured over 30 to 60 seconds.

A control with beef heart mitochondria was executed in parallel with each set of samples to ensure proper running of experiment. The cellular protein content was determined using the BCA protein assay kit (Thermo scientific, Massachusetts, United States) with bovine serum albumin as standard. Specific complex activities were expressed as ratio of and normalized to citrate synthase activity.

2.9. Statistical analyses

Statistical analyses were performed using SPSS Statistics v.17.0 software (SPSS Inc, Chicago, IL, USA). Differences between two groups (for AAR%LV and AN%AAR) were evaluated using the Mann–Whitney U test. One-way ANOVA followed by a LSD *post-hoc* test was performed for multiple group comparisons. Data are reported as mean ± standard error of the mean (SEM). $p<0.05$ was considered significant.

3. RESULTS

3.1. *KYNA reduced in vitro cell death and prevented mitochondrial membrane potential decrease after hypoxia/reoxygenation*

To evaluate cytoprotective effects of KYNA *in vitro*, H9C2 cells were subjected to 4 hours 50 minutes of hypoxia followed by 2 hours of reoxygenation with either DMSO or KYNA treatments (Fig. 1A). As shown in figure 2, hypoxia/reoxygenation increased cell death compared to control (1.00 vs. 0.11±0.02; $p<0.001$). Relative mortality was significantly reduced in KYNA-treated groups compared to H/R group (0.69±0.10, 0.63±0.17, 0.64±0.19 for KYNA pre, KYNA pre+per, KYNA pre+per+post *vs*. 1.00 in H/R, $p=0.024$, $p=0.006$, and $p=0.007$ respectively). Hypoxia/reoxygenation led to a significant decrease in the number of cells with conserved mitochondrial membrane potential *(ΔΨm)* (46.8±7%) compared to control (91.5±7%, $p=0.003$). KYNA treatment was able to significantly increase number of cells with conserved *ΔΨm* (72.72±1.82%, 78.74±9.50%, 80.97±10.50%, $p=0.035$, $p=0.011$, $p=0.007$ *vs*. H/R; for KYNA pre, KYNA pre+per, KYNA pre+per+post respectively) (Fig. 2).

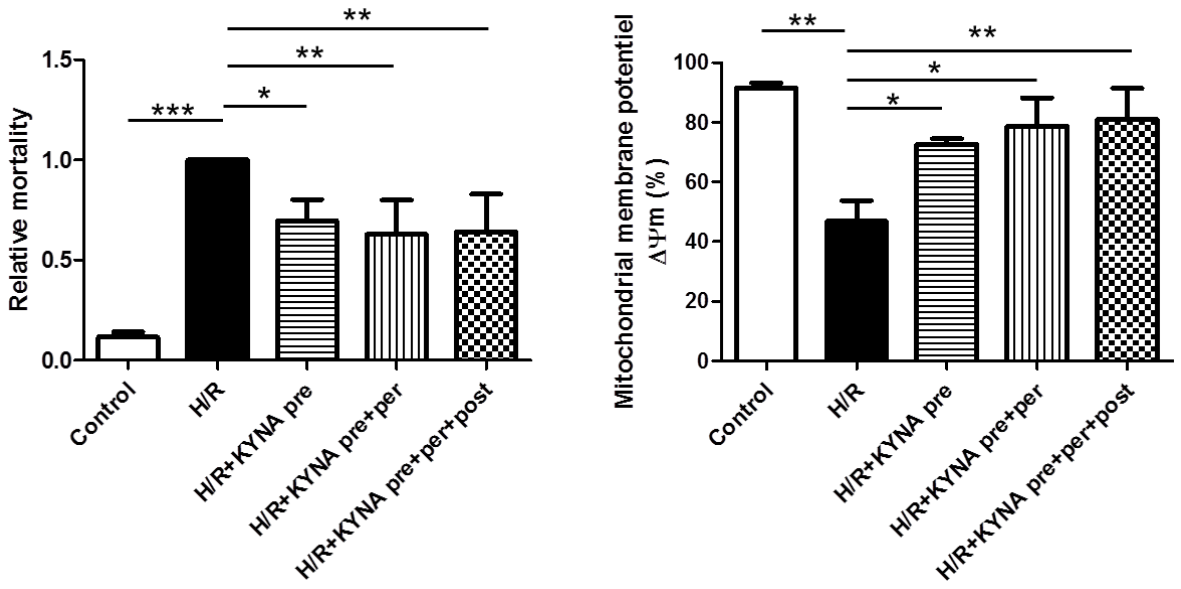

Fig. 2: Histograms showing (A) relative mortality and (B) percentage of cells with conserved mitochondrial membrane potential in control cells, that did not undergo hypoxia/reoxygenation (H/R), and cells that underwent hypoxia/reoxygenation either vehicle or KYNA (1μM)-treated. Treatment was performed either 10 minutes before hypoxia in DMEM medium (pre), or pre + during hypoxia (pre+per), or pre + per + during reoxygenation (pre+per+post) for KYNA, whereas vehicle (DMSO) treatment was performed at pre+per+post (n=3-9); Values are expressed as mean±SEM; * $p<0.05$.

3.2. KYNA reduced infarct size in vivo

In order to confirm results obtained *in vitro*, KYNA or NaOH was injected to male Wistar rats 10 minutes before a myocardial ischemia/reperfusion. Both MI and MI+KYNA groups were subjected to 40 minutes myocardial ischemia followed by 2 hours reperfusion (Fig. 1B). Infarct size was significantly lower in animals receiving KYNA as compared to those receiving vehicle only (AN%AAR = 53.3±3% in MI+KYNA *vs*. 62.2±2 % in MI, p=0.012), whereas AAR%LV was similar in the two groups (Fig. 3).

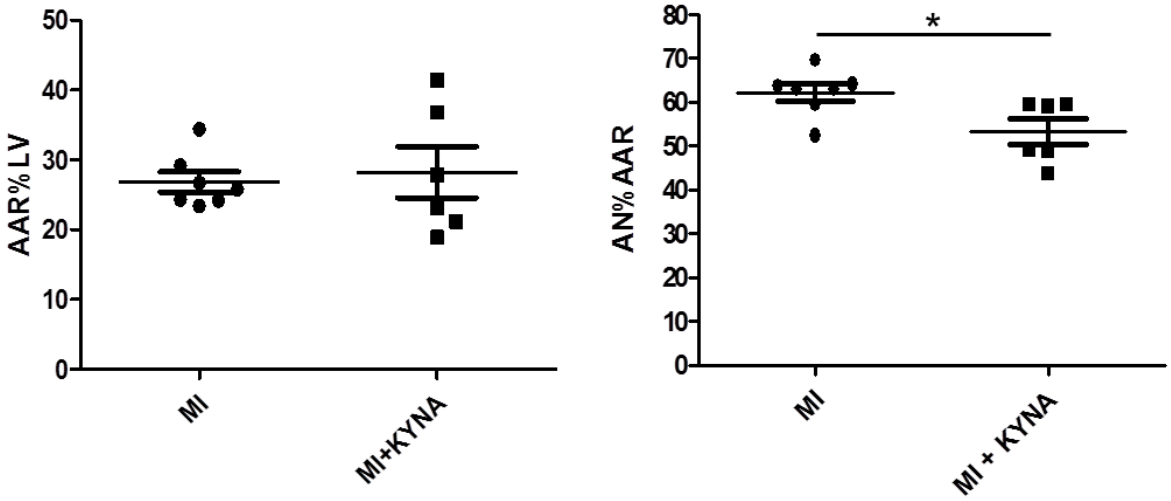

Fig. 3: Scatter dot plot showing area at risk (AAR) as a percentage of the total left ventricle (LV) and area of necrosis (AN) as a percentage of AAR after 2 hours of reperfusion (n=6-7); Values are expressed as mean±SEM; * p<0.05.

3.3. KYNA did not influence the mitochondrial respiratory chain complex activity

KYNA treatment did not influence mitochondrial respiratory chain complex protein expression. As shown in figure 4A, complex I and III proteins expression were increased, but did not reach statistical significance, in the MI group compared to sham, except for complex III (0.279±0.085 in MI *vs*. 0.076±0.023 in sham for complex I, p=0.08; 0.214±0.050 in MI *vs*. 0.144±0.017 in sham for complex III, p<0.001). PGC1-α protein expression, a transcription factor mediating mitochondrial biogenesis and oxidative phosphorylation, was not different in sham, MI and MI+KYNA groups (Fig. 4B). Afterwards, we evaluated activities of complex I, II, III and IV spectrophotometrically. We found a complex I deficiency (0.41±0.04 in MI *vs*. 0.53±0.03 in sham, p=0.052) and a complex III over-activation after ischemia (0.42±0.04 in MI *vs*. 0.29±0.03 in sham, p=0.04). Accordingly, complex ratio were significantly different between MI and sham group (0.92±0.06 in MI *vs*. 1.21±0.07 in sham for complex ratio I/II, p=0.01; 1.13±0.06 in MI *vs*. 0.55±0.04 in sham for complex

ratio III/I, p=0.039; 2.30±0.21 in MI *vs*. 1.25±0.16 in sham for complex ratio IV/I, p=0.01). However, KYNA treatment did not correct complex I deficiency or complex III over-activation (Fig. 4C).

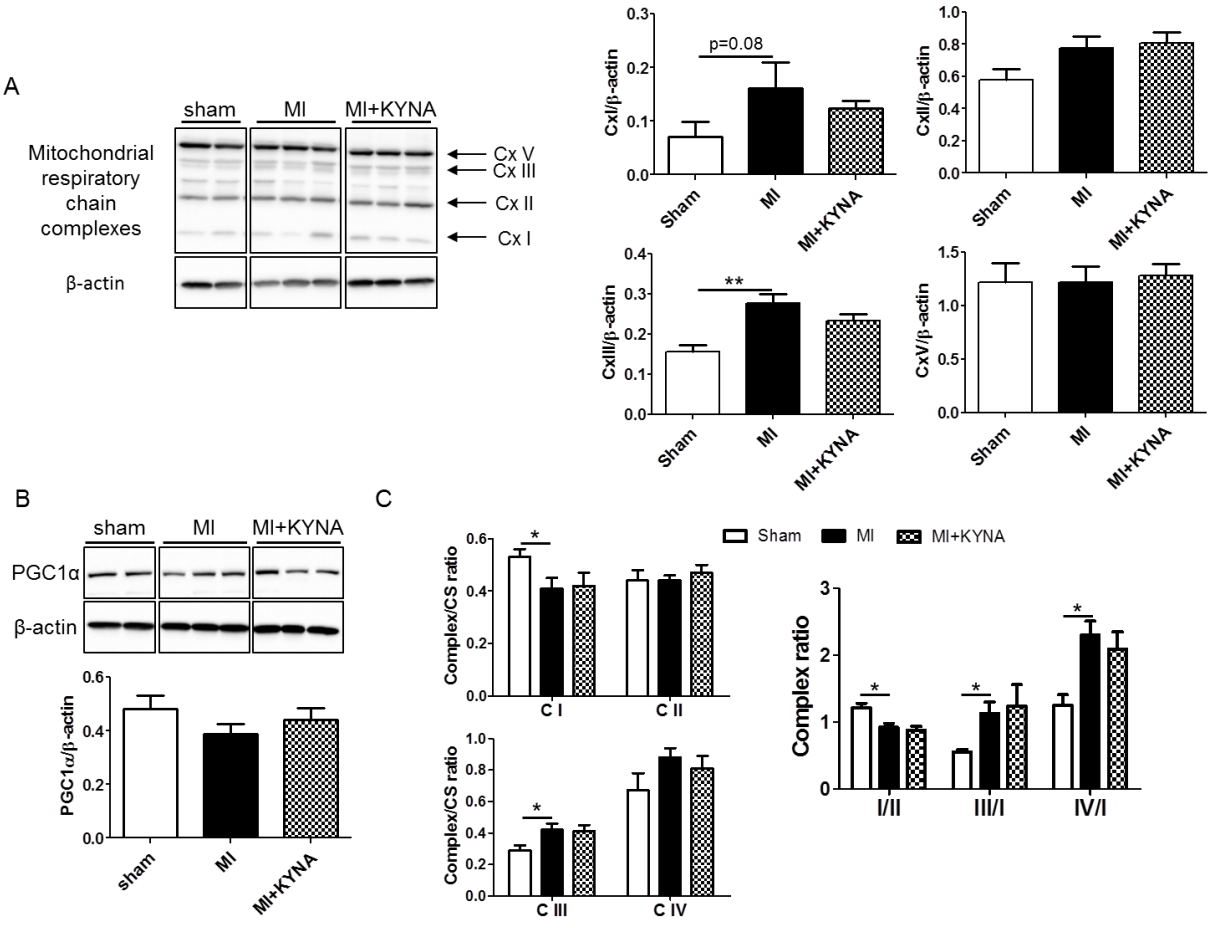

Fig. 4: Mitochondrial respiratory chain complex and PGC1α protein expression by means of western blot and mitochondrial respiratory chain complex activity by spectrophotometry. Representative immunoblots and histograms showing quantification of protein expression for (A) mitochondrial respiratory chain complex and (B) PGC1α in non-ischemic (sham), ischemic + vehicle (MI), and ischemic + kynurenic acid (MI+KYNA) left ventricle samples after 2 hours of reperfusion (n=5-10). β-actin was used as loading controls. (C) histograms showing complex over citrate synthase activity ratio (I/CS, II/CS, III/CS, IV/CS) or complex ratio activity (I/II, III/I, IV/I) in sham, MI, MI+KYNA left ventricle samples after 2 hours of reperfusion (n=5-10). Values are expressed as mean ± SEM; * p<0.05, *** p<0.001.

3.4. KYNA stimulated antioxidant defense after myocardial ischemia/reperfusion

KYNA has been reported having reactive oxygen species (ROS) scavenger properties. Thus, we evaluated mRNA as well as protein expression for SOD1, SOD2, SOD3, and catalase. SOD1 and catalase mRNA were significantly decreased after ischemia (28.50±1.81 in MI *vs*. 38.33±1.95 in sham for SOD1, p=0.004; 17.21±1.39 in MI *vs*. 26.08±1.24 in sham for catalase, p<0.001). SOD2 and

SOD3 mRNA were not changed after ischemia. KYNA treatment induced a significant increase in SOD2 mRNA expression (59.68±2.96 in MI+KYNA *vs*. 49.33±4.61 in MI, p=0.049) and an increase, although not significant, in SOD3 mRNA levels (2.64±0.18 in MI+KYNA *vs*. 2.24±0.15 in MI, p=0.08) (Fig. 5A). SOD1 and SOD2 protein levels were comparable among all groups. SOD3 protein levels were significantly higher in MI group (1.02±0.16) *vs*. sham group (0.44±0.02; p=0.005). Catalase protein levels were also significantly higher in MI group (0.42±0.03) *vs*. sham group (0.25±0.01; p=0.007). Finally, KYNA treatment showed a trend in increasing catalase protein levels compared to MI group (0.53±0.05 in MI+KYNA *vs*.0.42±0.03 in MI, p=0.055) (Fig. 5B).

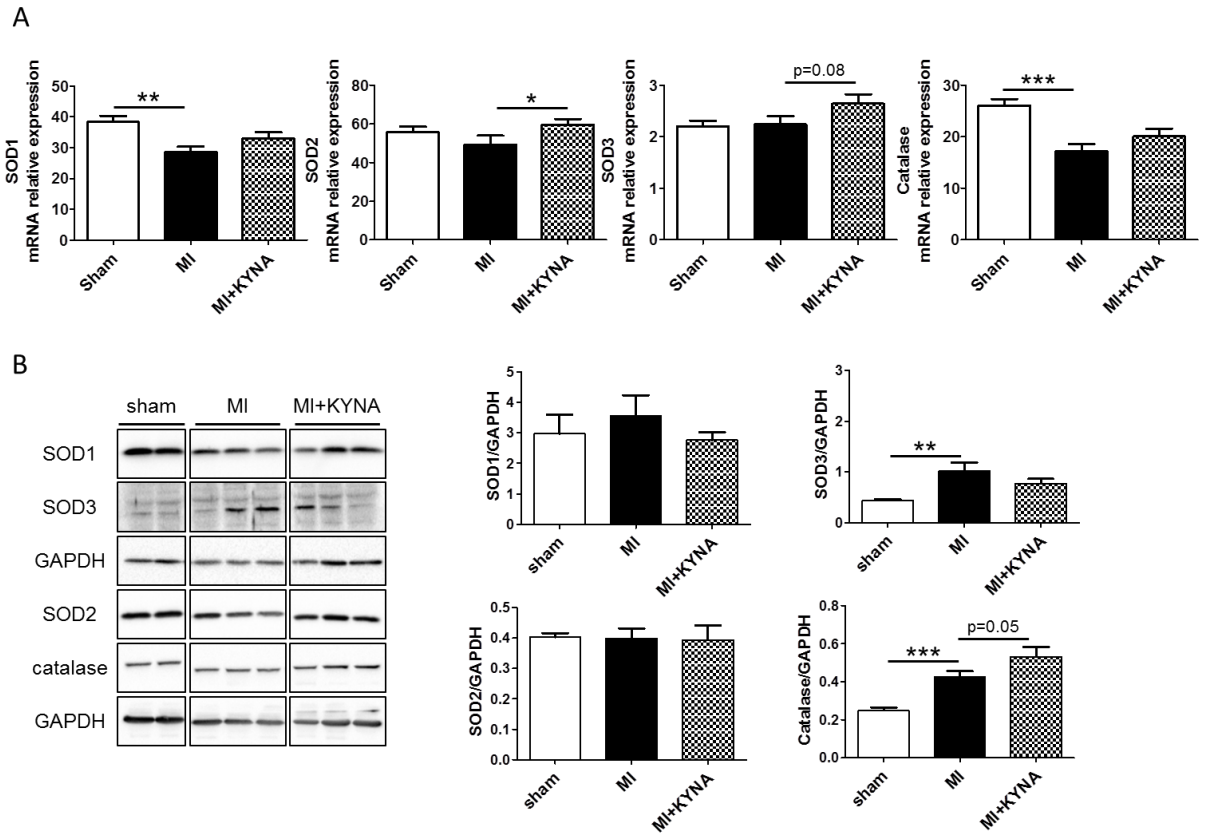

Fig. 5: Antioxidant markers mRNA and protein expression, respectively by means of RT-qPCR and western blot. (A) SOD1, 2, 3 and catalase mRNA expression in non-ischemic (sham), ischemic + vehicle (MI), and ischemic + kynurenic acid (MI+KYNA) left ventricle samples after 2 hours of reperfusion (n=6-11). (B) Representative immunoblots and histogram quantification of protein expression for SOD1, 2, 3 and catalase in sham, MI and MI + KYNA groups after 2 hours of reperfusion (n=6-9). GAPDH was used as loading control. Values are expressed as mean ± SEM. * p<0.05, ** p<0.01, *** p<0.001.

3.5. KYNA increased the mitophagy marker PARK2 after myocardial ischemia/reperfusion

We assessed whether KYNA was capable of stimulating mitophagy as a cardioprotective mechanism. P62 protein levels were significantly decreased after myocardial ischemia/reperfusion

compared to sham intervention (0.650±0.078 in MI *vs*. 0.399±0.041 in sham, p=0.005) with a trend to be even more reduced after KYNA treatment (0.268±0.050 in MI+KYNA *vs*. MI, p=0.094). In addition, PARK2 protein levels were significantly increased in MI group compared to sham group (0.157±0.012 in MI *vs*. 0.377±0.059 in sham, p=0.039). KYNA treatment significantly increased PARK2 protein levels compared to MI (0.590±0.095 in MI+KYNA, p=0.036) (Fig. 6).

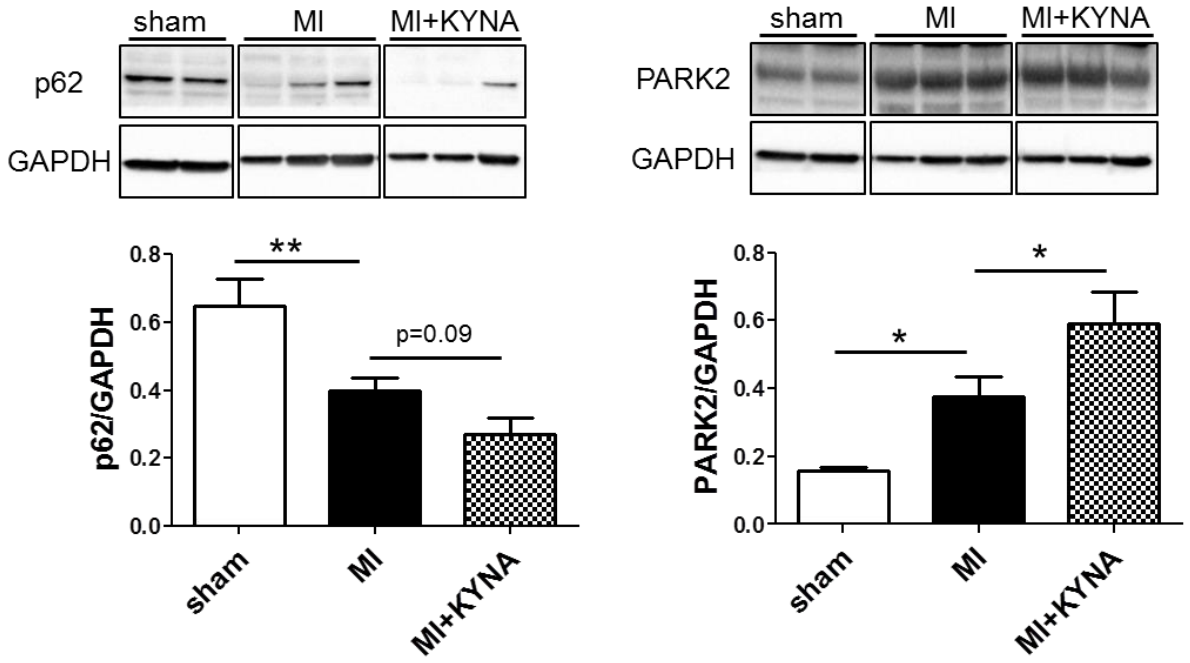

Fig. 6: Mitophagy protein markers expression using western blot. Representative immunoblots and histogram quantification of protein expression for p62 and PARK2 in non-ischemic (sham), ischemic + vehicle (MI), and ischemic + kynurenic acid (MI+KYNA) left ventricle samples after 2 hours of reperfusion (n=6-7). GAPDH was used as loading control. Values are expressed as mean ± SEM. * p<0.05, ** p<0.01.

3.6. KYNA increased GPR35 mRNA expression and reduced ERK1/2 and Akt phosphorylation levels after myocardial ischemia/reperfusion

KYNA is a known ligand of the G protein-coupled receptor GPR35. GPR35 mRNA expression was significantly increased in MI+KYNA group compared to MI group (0.0421±0.0082 in MI+KYNA *vs*. 0.0218±0.0037 in MI, p=0.022) (Fig. 7A). ERK1/2 and Akt kinases are known targets of G protein-coupled receptors; hence we evaluated the potential effect of GPR35 mRNA upregulation on their phosphorylation levels after 15 minutes of reperfusion. Myocardial ischemia/reperfusion induced an increase in ERK1/2 phosphorylation levels (1.61±0.36 in MI group *vs*. 0.07±0.04 in sham group, p<0.001). KYNA treatment induced a significant decrease in ERK1/2 phosphorylation (0.56±0.14 in MI+KYNA, p=0.005) as well as a significant decrease in Akt phosphorylation compared to MI group (0.67±0.06 in MI+KYNA *vs*. 0.92±0.10 in MI, p=0.047) (Fig. 7B).

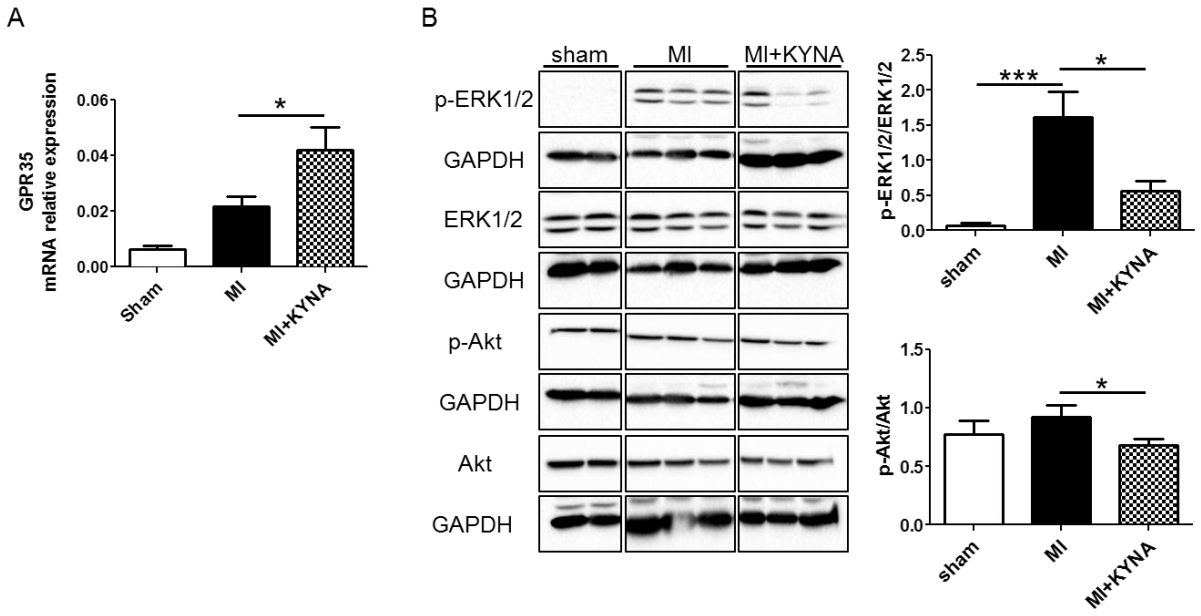

Fig. 7: GPR35 mRNA expression and protein expression levels for p-ERK1/2, ERK1/2, p-Akt, Akt respectively by means of RT-qPCR and WB. (A) GPR35 mRNA expression in sham, MI, and MI+KYNA left ventricle samples after 2 hours of reperfusion (n=6-11). (B) Representative immunoblots and histogram quantification of protein expression for p-ERK1/2, ERK1/2, p-Akt, Akt in sham, MI and MI + KYNA groups after 15 minutes of reperfusion (n=6-9). GAPDH was used as loading control. Data are expressed as mean ± SEM. * $p<0.05$, ** $p<0.01$, *** $p<0.001$.

3.7. KYNA inhibited FOXO3α phosphorylation

FOXO3α is a transcription factor known to regulate the expression of genes implicated in important cell functions (including oxidative stress, mitophagy…) and is regulated by AMPKα. Therefore we evaluated phosphorylation levels of both proteins. After 15 minutes of reperfusion, FOXO3α phosphorylation levels were significantly increased in MI group compared to sham group (6.22±1.61 vs. 1.68±0.51, $p=0.017$), whereas KYNA treatment significantly reduced FOXO3α phosphorylation levels (0.89±0.36, $p<0.001$ vs. MI). AMPKα phosphorylation levels were not significantly different among the groups.

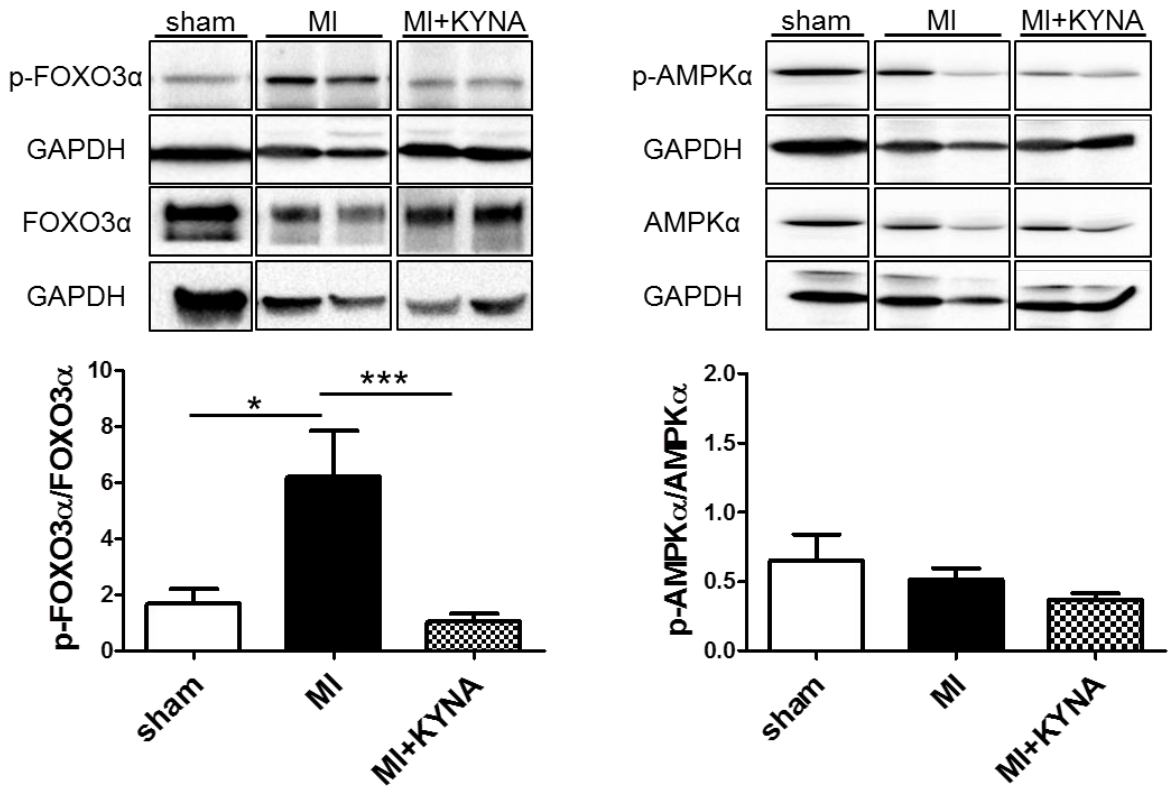

Fig. 8: Western blot analysis of AMPKα and FOXO3α phosphorylation. Representative immunoblots and histogram showing quantification of protein expression for AMPKα and FOXO3α in non-ischemic (sham), ischemic + vehicle (MI), and ischemic + kynurenic acid (MI+KYNA) left ventricle samples after 15 minutes of reperfusion (n=6-11). GAPDH was used as loading control. Values are expressed as mean ± SEM. * $p<0.05$, *** $p<0.001$.

4. DISCUSSION

Tryptophan is mainly catabolized through the kynurenine pathway. The first metabolite generated is kynurenine which in turn can be metabolized into KYNA. Previous studies demonstrated neuroprotective abilities of KYNA. In a neonatal rat cerebral ischemia/reperfusion model (left carotid artery ligation), KYNA was administrated at 300 mg/Kg 2 hours after cerebral hypoxia. This induced a reduction in brain lesions (Andine et al. 1988). In another model, a middle cerebral artery occlusion rat model, a pre-treatment with KYNA, also at 300 mg/Kg, reduced cerebral infarct size (Germano et al. 1987). Little is known regarding the ability of KYNA to protect the heart in the context of myocardial ischemia-reperfusion. We previously reported that increased plasmatic concentrations of kynurenine, the precursor of KYNA, were associated with the cardioprotection induced by remote ischemic conditioning (Chao de la Barca et al. 2016; Kouassi Nzoughet et al. 2017). Moreover, a protective role of KYNA was recently described in a mice model of myocardial ischemia/reperfusion injury (Olenchock et al. 2016). Olenchock et al. generated a mouse model with an alpha-ketoglutarate (αKG)-dependent dioxygenase's (*Egln1*) somatic gene ablation. EGLN1 senses oxygen and regulates the hypoxia-inducible factor (HIF) transcription factor, thus coordinating adaptive cellular response to hypoxia/ischemia (Kaelin and Ratcliffe 2008). These mice were protected against myocardial ischemia/reperfusion injuries *via* a KYNA increase. Authors reported that EGLN1 downregulation induced an accumulation of circulating α-ketoglutarate, which is the co-factor for KYNA production. KYNA, in its turn, was increased and mediated cardioprotection against myocardial ischemia/reperfusion injuries. They confirmed their findings by re-injecting KYNA to mice 2 hours before and 2 hours after a myocardial ischemia/reperfusion, and were capable of stimulating cardioprotection (Olenchock et al. 2016). However mechanisms and signaling pathways by which KYNA can mediate cardioprotection were unknown. In the present study, we showed that KYNA was capable of reducing ischemia/reperfusion injuries in both *in vitro* rat cardiomyoblast H9C2 hypoxia/reoxygenation cell model and *in vivo* myocardial infarction rat model. In addition, our results suggest that KYNA-induced cardioprotection may be associated with ERK1/2 and Akt phosphorylation inhibition, which leads to a decrease in FOXO3α degradation, hence increasing mitophagy and antioxidant defense mechanisms (Fig. 9).

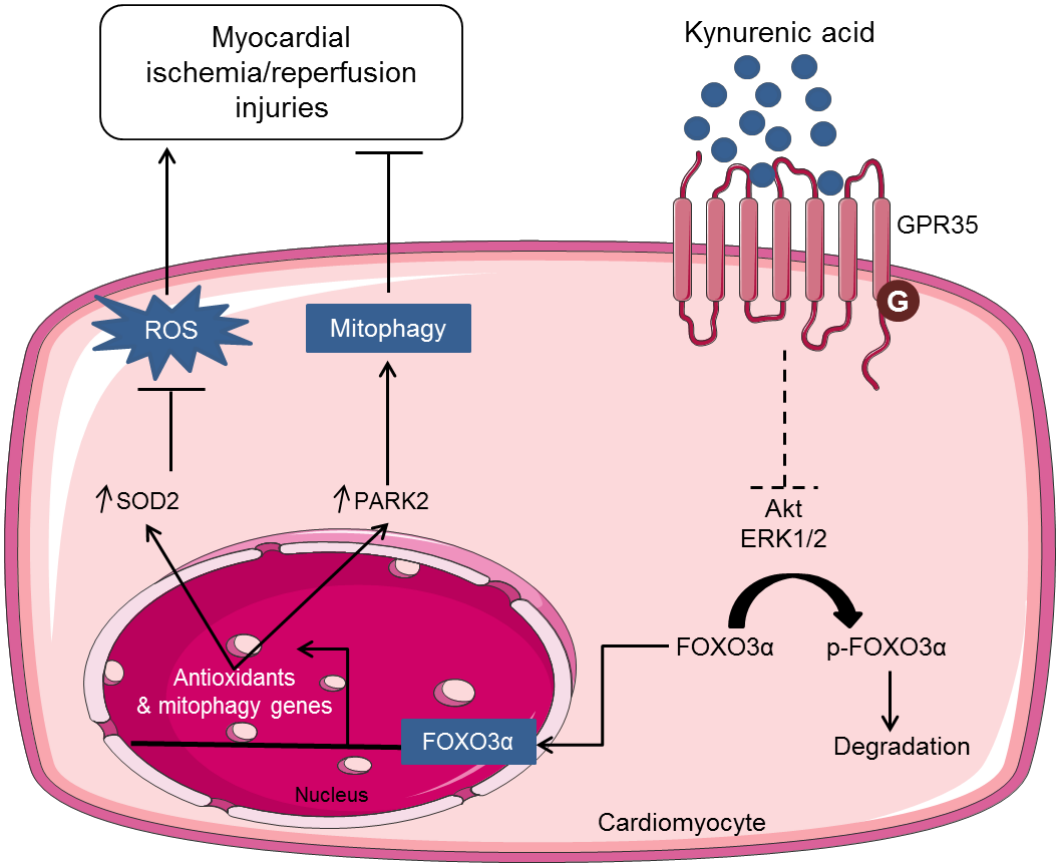

Fig. 9: Schematic representation summarizing proposed signaling pathways activated by KYNA to decrease myocardial ischemia/reperfusion injuries. KYNA inhibits ERK1/2 and Akt phosphorylation, kinases known to phosphorylate FOXO3α, thus promoting its degradation. Once, FOXO3α's inhibition is lifted, it can stimulate transcription of gene implicated in antioxidant defense and mitophagy. In turn, these proteins ensure a decrease in reactive oxygen species (ROS) and an adequate elimination of defective mitochondria respectively, which will allow myocardial ischemia/reperfusion injuries decrease. Moreover, KYNA up-regulates GPR35 expression. The latter's role in mediating ERK1/2 and Akt inhibition remains to be confirmed.

Ischemia/reperfusion injuries are associated with a dysfunction in oxidative phosphorylation (Lesnefsky et al. 1997). Indeed complex I and III's activity is modulated after ischemia (Rouslin 1983; Lesnefsky et al. 2001). These complexes are key sites generating ROS responsible for mitochondrial and eventual myocardial damage (Chen et al. 2003; Ambrosio et al. 1993) . A reversible blockage of complex I (e.g. by amobarbital) during ischemia largely avoided reperfusion injury (Chen et al. 2006; Chen et al. 2018). Cardioprotection is partly related to a lesser ROS damage, a better cytochrome c retention and a preservation of the outer membrane integrity (Chen et al. 2006). In a previous work, KYNA effect on mitochondrial respiration was assessed by oxygraphy (Baran et al. 2016; Baran et al. 2001; Baran et al. 2003). KYNA was capable of acting as an oxidative phosphorylation uncoupler thus decreasing mitochondrial respiration in mitochondria isolated from rat heart under basal conditions, i.e. without ischemia/reperfusion. Hence, we tested the hypothesis

that KYNA could decrease myocardial ischemia/reperfusion injuries by modulating mitochondrial function. In our model, KYNA did not influence mitochondrial respiratory chain complex I, II, III and IV protein expression or activities after ischemia/reperfusion, suggesting that KYNA-induced cardioprotection may not act through mitochondrial respiratory chain complexes modulation.

KYNA was identified as an endogenous ligand for GPR35, a G protein-coupled receptor, using inositol phosphate production and calcium mobilization assays (Wang et al. 2006). More importantly, KYNA was screened to show its effectiveness and selectiveness in activating approximately 40 other G protein-coupled receptors. KYNA did not activate other receptors, even GPR55, the closest homologue of GPR35, showing a certain specificity of KYNA towards GPR35. GPR35 was found positively regulated in the acute phase of myocardial infarction and in cultured cardiomyocytes hypoxia cell models (HL-1 and neonatal mouse cardiomyocytes) (Ronkainen et al. 2014). In 2014, Ronkainen et al. reported an increase in GPR35 mRNA after hypoxia that was concomitantly associated with an increase in HIF-1α mRNA expression (Ronkainen et al. 2014). Similarly with other G protein-coupled receptors, GPR35 has been suggested to modulate ERK1/2 and Akt phosphorylation levels (Oka et al. 2010; Deng, Hu, and Fang 2011). Indeed, using phospho-ERK1/2 immunoblotting, ligand activation of GPR35 was demonstrated (Oka et al. 2010; Deng, Hu, and Fang 2011). In these studies, 2-oleoyl lysophosphatidic acid and tyrphostin-51 were recognized as GPR35 agonists using this type of experiment. Use of pertussis toxin, which abolishes $G\alpha_{i/0}$ mediated response, confirmed ERK1/2 phosphorylation stimulation by GPR35 (Zhao et al. 2010). KYNA has been shown to either stimulate or inhibit ERK1/2 or Akt phosphorylation. In a work conducted on inguinal primary adipocytes, KYNA induced an increase of phosphorylation of ERK1/2. In contrast, KYNA decreased phosphorylation of Akt and ERK1/2 on colon adenocarcinoma HT-29 cells, (Walczak, Turski, and Rajtar 2014). Hence, the exact link between KYNA, GPR35 and ERK1/2, Akt is yet to be established. Furthermore, to the best of our knowledge, KYNA effect on cardiomyocytes has not been reported before the present study. In our *in vivo* model, KYNA-induced cardioprotection was associated with an upregulation of GPR35 mRNA, and an inhibition of ERK1/2 and Akt phosphorylation.

FOXO3α is a transcription factor known for its role in promoting transcription of genes implicated in mitophagy and antioxidant defense (Sundaresan et al. 2009; Yang and Hung 2009). FOXO3α's activity is regulated by multiple post-translational modifications. FOXO3α phosphorylation by ERK1/2 and Akt (Yang and Hung 2009) is a signal ensuring its degradation (Ronnebaum and Patterson 2010; Wang, Hu, and Liu 2017). Moreover, AMPKα activates FOXO3α translocation to the nucleus by inhibiting its Akt-induced phosphorylation (Yung et al. 2013). In our work the decrease in FOXO3α phosphorylation was associated with an ERK1/2 and Akt phosphorylation levels decrease. However, we did not highlight AMPK α activation at 15 min of

reperfusion. We found a SOD2 mRNA levels significant increase and a high trend of increase in catalase protein expression levels in the KYNA-treated group compared to vehicle-treated group. In a study by Wang et al. FOXO3α has been reportedly associated with increased antioxidant genes transcription, thus decreasing myocardial ischemia/reperfusion injuries (Wang et al. 2016). Furthermore, we found an increase in PARK2 levels suggesting an increase in mitophagy, associated with a decrease, although not significant, in p62 protein levels. Several studies showed the importance of FOXO3α in regulating Parkin-mediated mitophagy (Yu et al. 2017; Das et al. 2014; Mei et al. 2009). Indeed, Mei et al. demonstrated a direct interaction between FOXO3α and (PTEN)-induced putative kinase 1 (PINK1) promoter. PINK1 is an important factor in the Parkin-mediated mitochondrial autophagic pathway. Moreover, the importance of mitophagy has been highlighted in cardioprotection (Moyzis, Sadoshima, and Gustafsson 2015). For instance, Parkin-deficient mice presented larger infarct size compared to wild type, which was associated with a reduced mitophagy, and accumulation of defective mitochondria (Kubli et al. 2013). Moreover, Parkin loss in mice abolished cardioprotective effect of ischemic preconditioning (Huang et al. 2011). This proves that maintaining the integrity of mitophagy in cardiomyocytes is crucial.

5. LIMITS

Herein, our *in vitro* work demonstrated cytoprotective effects of KYNA in H9C2 cells, a widely used immortalized cardiomyoblast cell line. These cells present a phenotype different than that of adult cardiomyocytes. However, we confirmed KYNA-induced cardioprotection in an *in vivo* rat myocardial ischemia/reperfusion model and proposed possible mechanisms.

In order to decipher underlying mechanisms, we chose to work in a pre-treatment model with a high dose of KYNA. Hence, we will need further studies to translate our findings in the clinical arena.

6. CONCLUSION

KYNA reduced ischemia/reperfusion injuries in both *in vitro* and *in vivo* models. KYNA-mediated cardioprotection was associated with decreased ERK1/2 and Akt phosphorylation levels, which may have led to a decrease in FOXO3α phosphorylation, mechanism that was associated with an increased mitophagy and antioxidant defense mechanisms.

SOURCES OF FUNDING

This work was supported by a grant from Fédération Française de Cardiologie.

DISCLOSURE

None

ACKNOWLEDGMENTS

The authors would like to thank the University Hospital's Joint Animal Care Department (Service commun d'animalerie hospitalo-universitaire) and the PACEM (Plateforme d'Analyse Cellulaire et Moléculaire) platform.

REFERENCES

[1] T. Montrief, W.T. Davis, A. Koyfman, B. Long, Mechanical, inflammatory, and embolic complications of myocardial infarction: An emergency medicine review, Am J Emerg Med 37(6) (2019) 1175-1183 DOI: 10.1016/j.ajem.2019.04.003.

[2] J.M. Chao de la Barca, O. Bakhta, H. Kalakech, G. Simard, S. Tamareille, V. Catros, J. Callebert, C. Gadras, L. Tessier, P. Reynier, F. Prunier, D. Mirebeau-Prunier, Metabolic Signature of Remote Ischemic Preconditioning Involving a Cocktail of Amino Acids and Biogenic Amines, J Am Heart Assoc 5(9) (2016) DOI: 10.1161/JAHA.116.003891.

[3] J. Kouassi Nzoughet, C. Bocca, G. Simard, D. Prunier-Mirebeau, J.M. Chao de la Barca, D. Bonneau, V. Procaccio, F. Prunier, G. Lenaers, P. Reynier, A Nontargeted UHPLC-HRMS Metabolomics Pipeline for Metabolite Identification: Application to Cardiac Remote Ischemic Preconditioning, Anal Chem 89(3) (2017) 2138-2146 DOI: 10.1021/acs.analchem.6b04912.

[4] Q. Wang, D. Liu, P. Song, M.H. Zou, Tryptophan-kynurenine pathway is dysregulated in inflammation, and immune activation, Front Biosci (Landmark Ed) 20 (2015) 1116-43.

[5] E. Wirthgen, A. Hoeflich, A. Rebl, J. Gunther, Kynurenic Acid: The Janus-Faced Role of an Immunomodulatory Tryptophan Metabolite and Its Link to Pathological Conditions, Front Immunol 8 (2017) 1957 DOI: 10.3389/fimmu.2017.01957.

[6] B.A. Olenchock, J. Moslehi, A.H. Baik, S.M. Davidson, J. Williams, W.J. Gibson, A.A. Chakraborty, K.A. Pierce, C.M. Miller, E.A. Hanse, A. Kelekar, L.B. Sullivan, A.J. Wagers, C.B. Clish, M.G. Vander Heiden, W.G. Kaelin, Jr., EGLN1 Inhibition and Rerouting of alpha-Ketoglutarate Suffice for Remote Ischemic Protection, Cell 164(5) (2016) 884-95 DOI: 10.1016/j.cell.2016.02.006.

[7] R. Lugo-Huitron, T. Blanco-Ayala, P. Ugalde-Muniz, P. Carrillo-Mora, J. Pedraza-Chaverri, D. Silva-Adaya, P.D. Maldonado, I. Torres, E. Pinzon, E. Ortiz-Islas, T. Lopez, E. Garcia, B. Pineda, M. Torres-Ramos, A. Santamaria, V.P. La Cruz, On the antioxidant properties of kynurenic acid: free radical scavenging activity and inhibition of oxidative stress, Neurotoxicol Teratol 33(5) (2011) 538-47 DOI: 10.1016/j.ntt.2011.07.002.

[8] A. Perez-Gonzalez, J.R. Alvarez-Idaboy, A. Galano, Free-radical scavenging by tryptophan and its metabolites through electron transfer based processes, J Mol Model 21(8) (2015) 213 DOI: 10.1007/s00894-015-2758-2.

[9] V.P. Ronkainen, T. Tuomainen, J. Huusko, S. Laidinen, M. Malinen, J.J. Palvimo, S. Yla-Herttuala, O. Vuolteenaho, P. Tavi, Hypoxia-inducible factor 1-induced G protein-coupled receptor 35 expression is an early marker of progressive cardiac remodelling, Cardiovasc Res 101(1) (2014) 69-77 DOI: 10.1093/cvr/cvt226.

[10] A.E. Mackenzie, J.E. Lappin, D.L. Taylor, S.A. Nicklin, G. Milligan, GPR35 as a Novel Therapeutic Target, Front Endocrinol (Lausanne) 2 (2011) 68 DOI: 10.3389/fendo.2011.00068.

[11] J.Y. Yang, M.C. Hung, A new fork for clinical application: targeting forkhead transcription factors in cancer, Clin Cancer Res 15(3) (2009) 752-7 DOI: 10.1158/1078-0432.CCR-08-0124.

[12] T. Bochaton, C. Crola-Da-Silva, B. Pillot, C. Villedieu, L. Ferreras, M.R. Alam, H. Thibault, M. Strina, A. Gharib, M. Ovize, D. Baetz, Inhibition of myocardial reperfusion injury by ischemic postconditioning requires sirtuin 3-mediated deacetylation of cyclophilin D, J Mol Cell Cardiol 84 (2015) 61-9 DOI: 10.1016/j.yjmcc.2015.03.017.

[13] I.M. Germano, L.H. Pitts, B.S. Meldrum, H.M. Bartkowski, R.P. Simon, Kynurenate inhibition of cell excitation decreases stroke size and deficits, Ann Neurol 22(6) (1987) 730-4 DOI: 10.1002/ana.410220609.

[14] S.L. Leib, Y.S. Kim, D.M. Ferriero, M.G. Tauber, Neuroprotective effect of excitatory amino acid antagonist kynurenic acid in experimental bacterial meningitis, J Infect Dis 173(1) (1996) 166-71 DOI: 10.1093/infdis/173.1.166.

[15] P. Andine, A. Lehmann, K. Ellren, E. Wennberg, I. Kjellmer, T. Nielsen, H. Hagberg, The excitatory amino acid antagonist kynurenic acid administered after hypoxic-ischemia in neonatal rats offers neuroprotection, Neurosci Lett 90(1-2) (1988) 208-12.

[16] W.G. Kaelin, Jr., P.J. Ratcliffe, Oxygen sensing by metazoans: the central role of the HIF hydroxylase pathway, Mol Cell 30(4) (2008) 393-402 DOI: 10.1016/j.molcel.2008.04.009.

[17] E.J. Lesnefsky, B. Tandler, J. Ye, T.J. Slabe, J. Turkaly, C.L. Hoppel, Myocardial ischemia decreases oxidative phosphorylation through cytochrome oxidase in subsarcolemmal mitochondria, Am J Physiol 273(3 Pt 2) (1997) H1544-54 DOI: 10.1152/ajpheart.1997.273.3.H1544.

[18] W. Rouslin, Mitochondrial complexes I, II, III, IV, and V in myocardial ischemia and autolysis, Am J Physiol 244(6) (1983) H743-8 DOI: 10.1152/ajpheart.1983.244.6.H743.

[19] E.J. Lesnefsky, T.I. Gudz, C.T. Migita, M. Ikeda-Saito, M.O. Hassan, P.J. Turkaly, C.L. Hoppel, Ischemic injury to mitochondrial electron transport in the aging heart: damage to the iron-sulfur

protein subunit of electron transport complex III, Arch Biochem Biophys 385(1) (2001) 117-28 DOI: 10.1006/abbi.2000.2066.

[20] Q. Chen, E.J. Vazquez, S. Moghaddas, C.L. Hoppel, E.J. Lesnefsky, Production of reactive oxygen species by mitochondria: central role of complex III, J Biol Chem 278(38) (2003) 36027-31 DOI: 10.1074/jbc.M304854200.

[21] G. Ambrosio, J.L. Zweier, C. Duilio, P. Kuppusamy, G. Santoro, P.P. Elia, I. Tritto, P. Cirillo, M. Condorelli, M. Chiariello, et al., Evidence that mitochondrial respiration is a source of potentially toxic oxygen free radicals in intact rabbit hearts subjected to ischemia and reflow, J Biol Chem 268(25) (1993) 18532-41.

[22] Q. Chen, S. Moghaddas, C.L. Hoppel, E.J. Lesnefsky, Reversible blockade of electron transport during ischemia protects mitochondria and decreases myocardial injury following reperfusion, J Pharmacol Exp Ther 319(3) (2006) 1405-12 DOI: 10.1124/jpet.106.110262.

[23] Q. Chen, M. Younus, J. Thompson, Y. Hu, J.M. Hollander, E.J. Lesnefsky, Intermediary metabolism and fatty acid oxidation: novel targets of electron transport chain-driven injury during ischemia and reperfusion, Am J Physiol Heart Circ Physiol 314(4) (2018) H787-H795 DOI: 10.1152/ajpheart.00531.2017.

[24] H. Baran, K. Staniek, M. Bertignol-Sporr, M. Attam, C. Kronsteiner, B. Kepplinger, Effects of Various Kynurenine Metabolites on Respiratory Parameters of Rat Brain, Liver and Heart Mitochondria, Int J Tryptophan Res 9 (2016) 17-29 DOI: 10.4137/IJTR.S37973.

[25] H. Baran, K. Staniek, B. Kepplinger, L. Gille, K. Stolze, H. Nohl, Kynurenic acid influences the respiratory parameters of rat heart mitochondria, Pharmacology 62(2) (2001) 119-23 DOI: 10.1159/000056082.

[26] H. Baran, K. Staniek, B. Kepplinger, J. Stur, M. Draxler, H. Nohl, Kynurenines and the respiratory parameters on rat heart mitochondria, Life Sci 72(10) (2003) 1103-15.

[27] J. Wang, N. Simonavicius, X. Wu, G. Swaminath, J. Reagan, H. Tian, L. Ling, Kynurenic acid as a ligand for orphan G protein-coupled receptor GPR35, J Biol Chem 281(31) (2006) 22021-8 DOI: 10.1074/jbc.M603503200.

[28] S. Oka, R. Ota, M. Shima, A. Yamashita, T. Sugiura, GPR35 is a novel lysophosphatidic acid receptor, Biochem Biophys Res Commun 395(2) (2010) 232-7 DOI: 10.1016/j.bbrc.2010.03.169.

[29] H. Deng, H. Hu, Y. Fang, Tyrphostin analogs are GPR35 agonists, FEBS Lett 585(12) (2011) 1957-62 DOI: 10.1016/j.febslet.2011.05.026.

[30] P. Zhao, H. Sharir, A. Kapur, A. Cowan, E.B. Geller, M.W. Adler, H.H. Seltzman, P.H. Reggio, S. Heynen-Genel, M. Sauer, T.D. Chung, Y. Bai, W. Chen, M.G. Caron, L.S. Barak, M.E. Abood, Targeting of the orphan receptor GPR35 by pamoic acid: a potent activator of extracellular signal-regulated kinase and beta-arrestin2 with antinociceptive activity, Mol Pharmacol 78(4) (2010) 560-8 DOI: 10.1124/mol.110.066746.

[31] K. Walczak, W.A. Turski, G. Rajtar, Kynurenic acid inhibits colon cancer proliferation in vitro: effects on signaling pathways, Amino Acids 46(10) (2014) 2393-401 DOI: 10.1007/s00726-014-1790-3.

[32] N.R. Sundaresan, M. Gupta, G. Kim, S.B. Rajamohan, A. Isbatan, M.P. Gupta, Sirt3 blocks the cardiac hypertrophic response by augmenting Foxo3a-dependent antioxidant defense mechanisms in mice, J Clin Invest 119(9) (2009) 2758-71 DOI: 10.1172/JCI39162.

[33] S.M. Ronnebaum, C. Patterson, The FoxO family in cardiac function and dysfunction, Annu Rev Physiol 72 (2010) 81-94 DOI: 10.1146/annurev-physiol-021909-135931.

[34] X. Wang, S. Hu, L. Liu, Phosphorylation and acetylation modifications of FOXO3a: Independently or synergistically?, Oncol Lett 13(5) (2017) 2867-2872 DOI: 10.3892/ol.2017.5851.

[35] M.M. Yung, D.W. Chan, V.W. Liu, K.M. Yao, H.Y. Ngan, Activation of AMPK inhibits cervical cancer cell growth through AKT/FOXO3a/FOXM1 signaling cascade, BMC Cancer 13 (2013) 327 DOI: 10.1186/1471-2407-13-327.

[36] X.X. Wang, X.L. Wang, M.M. Tong, L. Gan, H. Chen, S.S. Wu, J.X. Chen, R.L. Li, Y. Wu, H.Y. Zhang, Y. Zhu, Y.X. Li, J.H. He, M. Wang, W. Jiang, SIRT6 protects cardiomyocytes against ischemia/reperfusion injury by augmenting FoxO3alpha-dependent antioxidant defense mechanisms, Basic Res Cardiol 111(2) (2016) 13 DOI: 10.1007/s00395-016-0531-z.

[37] W. Yu, B. Gao, N. Li, J. Wang, C. Qiu, G. Zhang, M. Liu, R. Zhang, C. Li, G. Ji, Y. Zhang, Sirt3 deficiency exacerbates diabetic cardiac dysfunction: Role of Foxo3A-Parkin-mediated mitophagy, Biochim Biophys Acta Mol Basis Dis 1863(8) (2017) 1973-1983 DOI: 10.1016/j.bbadis.2016.10.021.

[38] S. Das, G. Mitrovsky, H.R. Vasanthi, D.K. Das, Antiaging properties of a grape-derived antioxidant are regulated by mitochondrial balance of fusion and fission leading to mitophagy triggered by a signaling network of Sirt1-Sirt3-Foxo3-PINK1-PARKIN, Oxid Med Cell Longev 2014 (2014) 345105 DOI: 10.1155/2014/345105.

[39] Y. Mei, Y. Zhang, K. Yamamoto, W. Xie, T.W. Mak, H. You, FOXO3a-dependent regulation of Pink1 (Park6) mediates survival signaling in response to cytokine deprivation, Proc Natl Acad Sci U S A 106(13) (2009) 5153-8 DOI: 10.1073/pnas.0901104106.

[40] A.G. Moyzis, J. Sadoshima, A.B. Gustafsson, Mending a broken heart: the role of mitophagy in cardioprotection, Am J Physiol Heart Circ Physiol 308(3) (2015) H183-92 DOI: 10.1152/ajpheart.00708.2014.

[41] D.A. Kubli, X. Zhang, Y. Lee, R.A. Hanna, M.N. Quinsay, C.K. Nguyen, R. Jimenez, S. Petrosyan, A.N. Murphy, A.B. Gustafsson, Parkin protein deficiency exacerbates cardiac injury and reduces survival following myocardial infarction, J Biol Chem 288(2) (2013) 915-26 DOI: 10.1074/jbc.M112.411363.

[42] C. Huang, A.M. Andres, E.P. Ratliff, G. Hernandez, P. Lee, R.A. Gottlieb, Preconditioning involves selective mitophagy mediated by Parkin and p62/SQSTM1, PLoS One 6(6) (2011) e20975 DOI: 10.1371/journal.pone.0020975.

1.3. Supplementary results

We assessed cell death and mitochondrial membrane potential (ΔΨm) after subjecting H9C2 cells to 4h50 min of hypoxia followed by 2 hours of reoxygenation *in vitro*. Cells were subjected to either vehicle (MI) or KYNA treatment (MI+KYNA) at a concentration different than that reported in the previous manuscript (10µM). Mortality in H/R group was considered equal to 1, and other data was expressed as relative mortality compared to H/R. KYNA treatment was performed as following: added to medium either 10 min before hypoxia (pre), or added before and during hypoxia (pre+per), or added before, during and after hypoxia (pre+per+post). Relative mortality was significantly reduced in KYNA-treated pre, pre+per and pre+per+post groups compared to H/R group (0.67±0.07, 0.63±0.07, 0.65±0.06, for KYNA pre, pre+per and pre+per+post vs H/R group; p=0.011, p=0.005, p=0.007 respectively). However, although KYNA treatment induced an increase in ΔΨm, it was not significant in comparison to H/R group (59.8±8.8%, 65.5±7.1%, 64.3±7.0%, for KYNA pre, pre+per and pre+per+post vs H/R group, p=0.179, p=0.057, p=0.074 respectively) (Fig. 47).

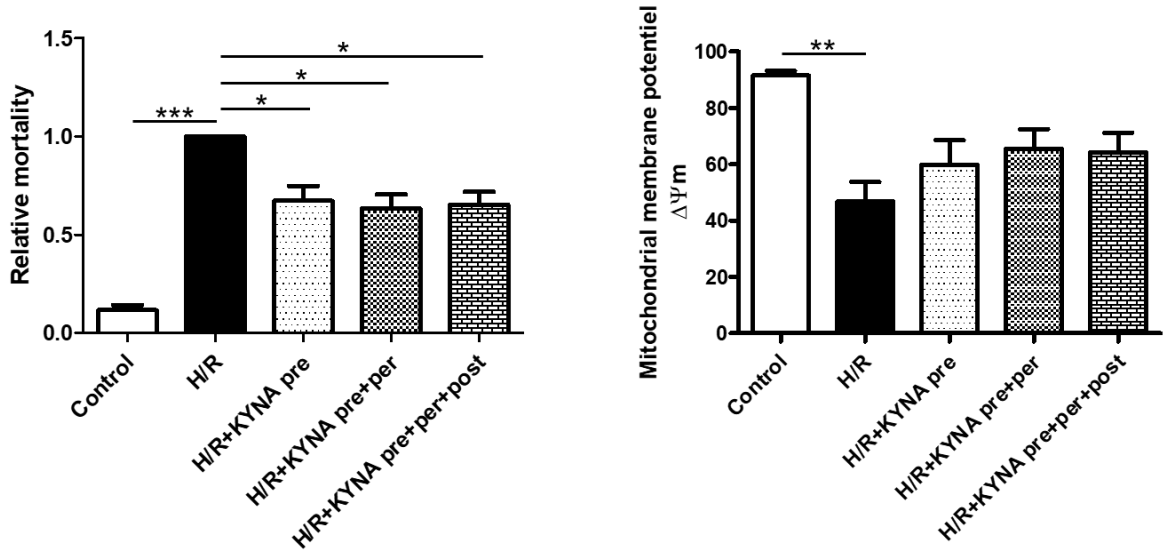

Figure 34: Histograms showing (A) relative mortality and (B) percentage of cells with conserved mitochondrial membrane potential of control cells, that did not undergo hypoxia/reoxygenation (H/R), and cells that underwent H/R either vehicle (DMSO) or KYNA-treated (10µM). Treatment was performed either 10 min before hypoxia in DMEM medium (pre), or pre + during hypoxia (per), or pre + per + during reoxygenation (post) (n=3-9); Values are expressed as mean±SEM; * p<0.05, ***p<0.001.

Since Akt and ERK1//2 are also implicated in survival pathway signaling, we assessed STAT3 and GSK3β phosphorylation levels. MI increased p-GSK3β/GSK3β and p-STAT3/STAT3 levels in MI (1.14±0.11, 1.37±0.14 for p-GSK3β and p-STAT3 respectively) compared to sham (0.72±0.19, 0.074±0.02; p=0.05, p<0.001 for p-GSK3β and p-STAT3 respectively). However KYNA treatment did not have any significant influence on these levels compared to MI (Fig. 48).

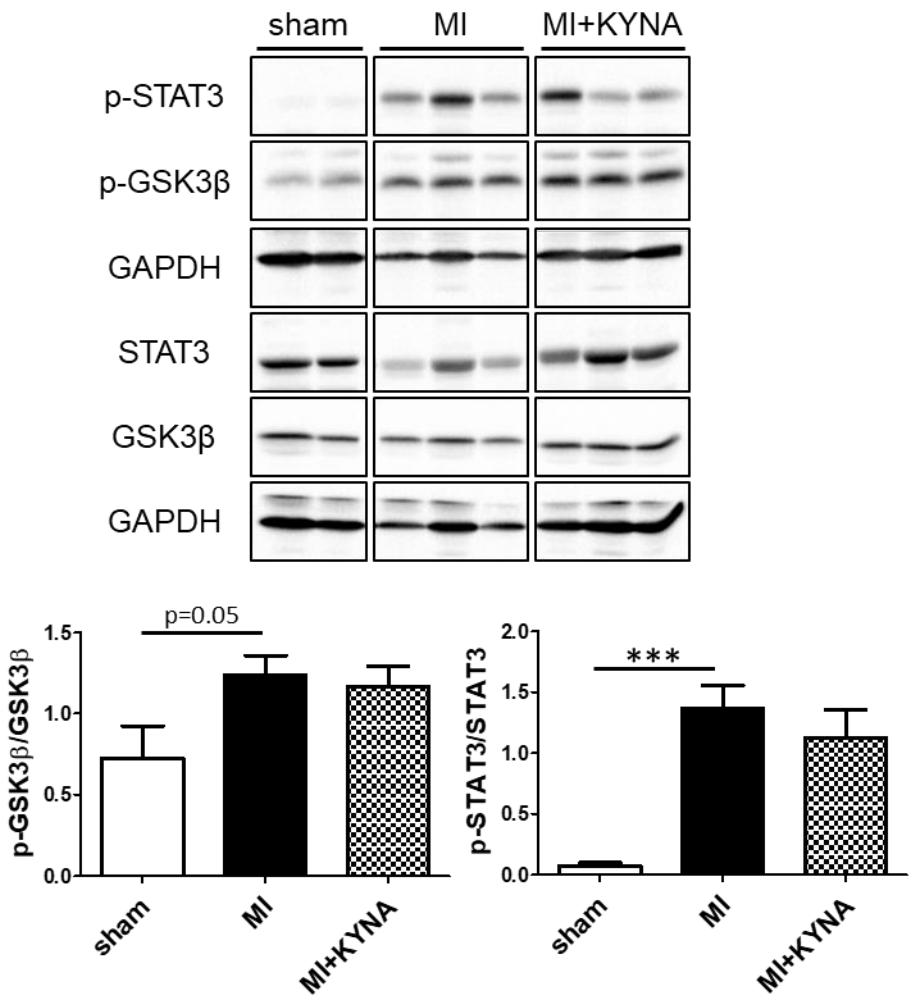

Figure 35: Representative immunoblots and histograms quantification of protein expression for p-GSK3β, GSK3β, p-STAT3 and STAT3 in non-ischemic (sham), ischemic + vehicle (MI), and ischemic + KYNA (MI+KYNA) left ventricle samples after 15 min of reperfusion (n=6-11). GAPDH was used as loading control. Values are expressed as mean ± SEM. *** $p<0.001$.

2. Study N°4: Kynurenine mediates cardioprotection in acute myocardial infarction

Work in progress

2.1. Scientific background

Reperfusion remains the sole treatment of MI. However, after revealing the existence of myocardial reperfusion injuries, cardioprotective strategies became one of the most discussed topics in cardiovascular research. In a canine model, remote ischemic conditioning (RIC) decreased myocardial I/R injuries (Przyklenk et al. 1993). Yet, mechanisms and molecules implicated in this cardioprotective strategy remain unclear.

A study conducted by Shimizu et al. showed that hydrophobic metabolites with low molecular weight are plasmatic factors involved in RIC-mediated cardioprotection (Shimizu et al. 2009). To better understand the nature of these factors, we performed a metabolic study in our laboratory. Plasma was sampled from rats undergoing or not 4 cycles of I/R (clamping/de-clamping) of the right upper femoral artery. Plasma was also sampled from human before and after 3 cycles of 5-minute inflation / 5-minute deflation of an automated upper-arm cuff inflator. We applied a targeted quantitative metabolomic approach combined to mass spectrometry to analyze the rat and human plasma samples. Our study showed an increase of a couple metabolites of which KYN. We hypothesized that KYN, a metabolite with a low molecular weight and hydrophobic characteristics, was potentially implicated in cardioprotection conferred by RIC. Therefore, KYN was injected to rats 10 minutes before a myocardial I/R. Compared to vehicle-treated animals, infarct size in KYN-treated group was reduced (Chao de la Barca et al. 2016). Nevertheless, mechanisms and signaling pathway implicated in KYN-mediated cardioprotection are unknown. Hence, the purpose of our study was to understand mechanisms underlying KYN-mediated cardioprotection.

2.2. Materials and methods

2.2.1. *In vitro* H9C2 hypoxia/reoxygenation

In vitro H9C2 H/R was performed as previously described in study N°3. Groups were defined as following (Fig. 34A):

-Control: This group did not undergo any intervention. Cells were kept in normoxic conditions and culture medium for 7h.

-H/R: This group underwent H/R with vehicle (DMSO) treatment, 10 minutes before hypoxia (pre), during hypoxia (per) and during reoxygenation (post) (pre+per+post).

-H/R+KYN: This group underwent H/R with KYN treatment (0.1 or 1µM) either pre, pre+per or pre+per+post.

Mortality in vehicle group was considered equal to 1, and other data was expressed as relative mortality compared to vehicle.

2.2.2. Animal studies

Male adult Wistar rats, aged 8 to 10 weeks and weighing 250 to 300 g, were used in this study. They were kept in a temperature-controlled room (22°C ± 2°C) with an adequate 12 light-12h dark cycle. Food and water were available ad libitum. All experiments were conducted in agreement with the guidelines from EU Directive 2010/63/EU; French Decree no. 2013–118 of the European Parliament on the protection of animals used for scientific purposes. The protocol was approved by the Ethics Committee in animal experimentation of Pays de la Loire and by the French Ministry of Higher Education and Research (APAFIS#8668-20 170 12417473589 v3). Hearts were excised under deep anesthesia (60 mg/kg of sodium pentobarbital (Exagon®, Axience, India). Afterwards, in one set of experiments the hearts were excised for infarct size assessment and, in another set of experiments, freeze clamped and stored at -80◦C for RNA messenger expression analysis, Western blot (WB) analysis, and assessment of the mitochondrial respiratory chain complexes activity.

2.2.3. Myocardial ischemia/reperfusion rat model

Experimental procedure, Area-at-risk and infarct-size determination was performed as previously described in study N°3. Rats were randomly assigned to one of the following groups (Fig. 34B):

- Sham group: animals undergoing all the surgical procedure except ligature of the coronary artery.
- MI group: animals undergoing myocardial I/R and injected 10 min before ischemia with NaOH 1M (vehicle).
- MI+KYN group: animals undergoing myocardial I/R and injected 10 min before ischemia with 150mg/Kg KYN.

2.2.4. Acetylated protein profile

Freeze-clamped ischemic LV rat hearts were used from all groups (sham, MI and MI+KYN) following 15 min reperfusion for WB analysis on whole cell lysate of acetylated protein profile. 100µg of total proteins were separated by SDS-PAGE and transferred to a PVDF membrane. After, 3h saturation in Odyssey buffer PBS 1X, membranes were incubated with antibody (Anti-acetyl Lysine antibody: 1/250, Abcam) also diluted in Odyssey buffer (Li-Cor®) diluted in PBS 1X. Membranes were incubated with rabbit secondary antibody (1/5000, Thermo Fisher Scientific). Blots were developed using the enhanced chemi-luminescence method. The band densities were analyzed using Image Lab (BioRad).

2.2.5. Statistics

Statistical analyses were performed using SPSS Statistics v.17.0 software (SPSS Inc.). Differences between two groups (for AAR%LV and AN%AAR) were evaluated using the Mann–Whitney U test, when normal distribution condition was not fulfilled. One-way ANOVA followed by a LSD post-hoc test was performed for multiple group comparisons, after normal distribution verification. Data are reported as mean ± standard error of the mean (SEM). $p<0.05$ was considered significant.

Cell death and mitochondrial membrane potential (ΔΨm) assessment, Quantitative real-time polymerase chain reaction (qPCR), Western Blot and mitochondrial respiratory chain complex enzymatic activity assessment were performed as previously described in study N°3.

2.3. Results

It is worth to note that Sham and MI groups are the same in Study N°3 and 4. Work was performed on both metabolites (KYN and KYNA) simultaneously. However, data is represented separately.

We assessed KYN cytoprotective and cardioprotective effect in an *in vitro* H9C2 cell model and in an *in vivo* male rat model as described in Fig. 34A and Fig. 34B respectively.

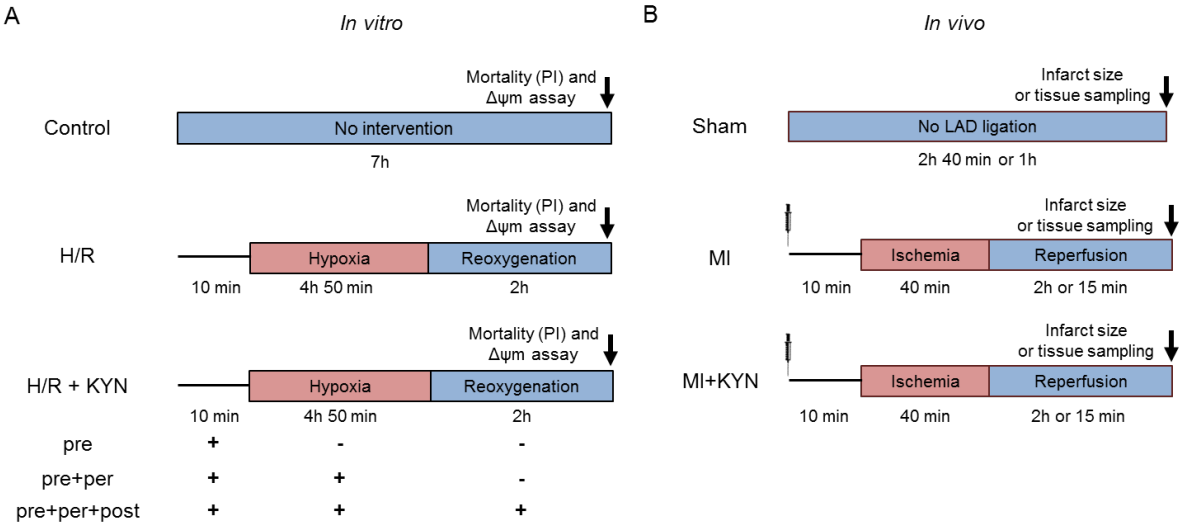

Figure 36: Schematic representation of *in vivo* and *in vitro* experiments and groups. (A) *In vitro*: H9C2 control cells underwent no intervention, cells from the hypoxia/reoygenation (H/R) groups were submitted to 4h 50 min of hypoxia followed by 2 hours of reoxygenation and were either treated with vehicle (DMSO) or with KYN (0.1 or 1 µM) 10 min before hypoxia (pre), or before and during hypoxia (pre+per), or before, during and after hypoxia (pre+per+post). Cell death quantification (n=3-8) as well as mitochondrial membrane potential (n=3-9) were performed 2 hours after reoxygenation. (B) *In vivo*: Sham animals underwent no injection and no left anterior descending coronary artery (LAD) ligation, MI group underwent 40 min of ischemia followed by 2 hours of reperfusion. 10 min before coronary artery occlusion vehicle NaOH (1M) or KYN (150mg/Kg) was administrated intraperitoneally. Infarct size assessment using 2,3,5-triphenyltetrazolium chloride (TTC) staining after 2 hours of reperfusion, tissue sampling was performed after either 15 min or 2 hours of reperfusion.

We assessed cell death and mitochondrial membrane potential after subjecting H9C2 cells to 4h50 min of hypoxia followed by 2 hours of reoxygenation *in vitro*. Cells were subjected to either vehicle (H/R) or KYN treatment (H/R+KYN). Relative mortality was significantly reduced in KYN-treated pre+per and pre+per+post groups at 0.1µM and 1µM compared to H/R group (0.47±0.09, 0.47±0.14, 0.69±0.09, 0.71±0.10 for KYN pre+per 0.1 µM, KYN pre+per+post 0.1µM, KYN pre+per 1µM, KYN pre+per+post 1µM *vs*. H/R group, $p<0.001$, $p<0.001$, $p=0.008$, $p=0.015$ respectively). Accordingly, KYN treatment restored the percentage of cells with a conserved mitochondrial membrane potential *(ΔΨm)* after H/R (74.4±5.7% in KYN pre+per 0.1 µM, 74.3±8.9% in KYN pre+per+post 0.1µM, 56.7±6.5% in KYN pre+per 1µM, 60±6.5% in KYN pre+per+post 1µM *vs*. 43±3.5% in H/R; $p=0.002$, $p=0.002$, $p=0.058$, $p=0.024$) (Fig. 35).

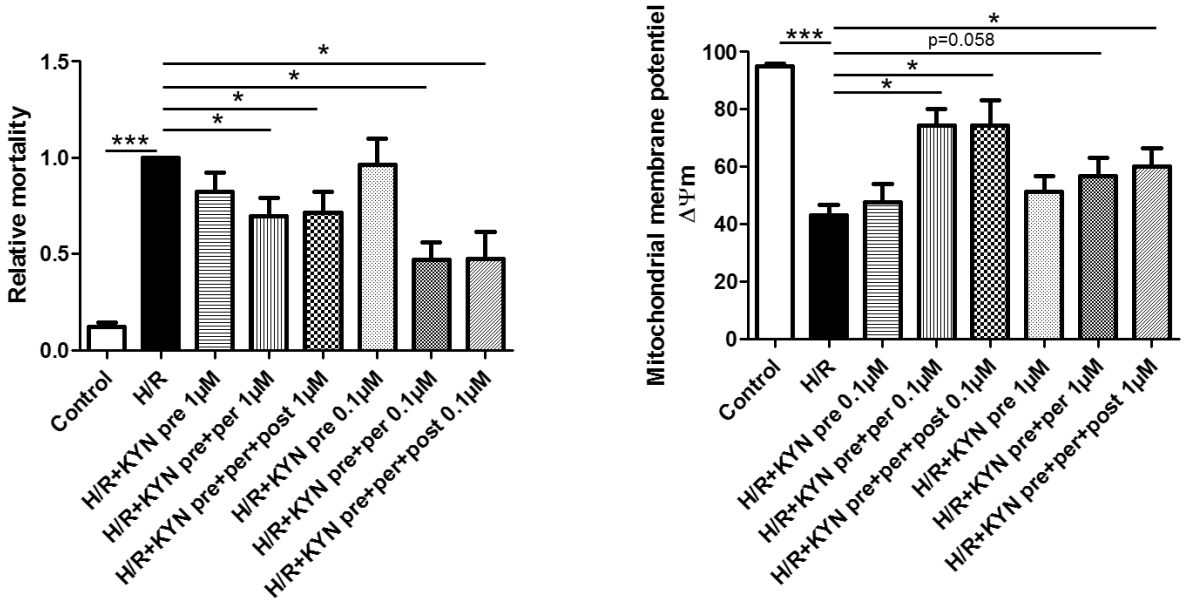

Figure 37: Histograms showing (A) relative mortality and (B) percentage of cells with conserved mitochondrial membrane potential of control (CT) cells, that did not undergo hypoxia/reoxygenation (H/R), and cells that underwent H/R either vehicle (DMSO) or KYN (0.1 or 1µM)-treated. Treatment was performed either 10 min before hypoxia in DMEM medium (pre), or pre + during hypoxia (per), or pre + per + during reoxygenation (post) (n=3-9); Values are expressed as mean±SEM; * p<0.05, ***p<0.001.

In vivo, KYN was injected to male Wistar rats 10 minutes before a myocardial I/R. Both vehicle (MI) and KYN-treated groups were subjected to 40-min myocardial ischemia followed by 2 hours reperfusion. TTC staining after I/R in KYN-treated rats showed a significantly reduced infarct size compared to vehicle-treated animals (52.5±4% *vs*. 37.2±4%, respectively; p=0.039), whereas AAR/LV was comparable between the two groups (Fig. 36).

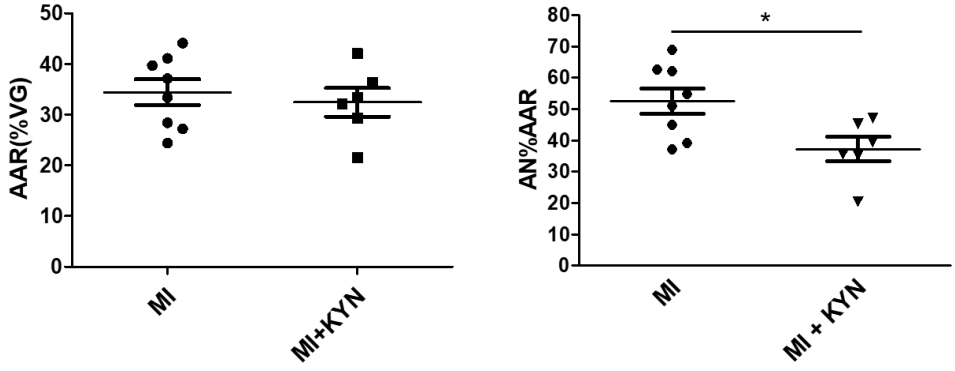

Figure 38: Histograms showing area at risk (AAR) as a percentage of the total left ventricle (LV) and area of necrosis (AN) as a percentage of AAR in left ventricle samples after 2 hours of reperfusion (n=6-8/group); Values are expressed as mean±SEM; * p<0.05.

Acetylated protein profile was realized on whole cell fraction after 15 minutes of reperfusion, and was comparable between the groups. Silent information regulator 1 (SIRT1) protein expression, an NAD-dependent deacetylase, was quantified after 2 hours of reperfusion and was not significantly different between sham, MI, MI+KYN groups (Fig. 37).

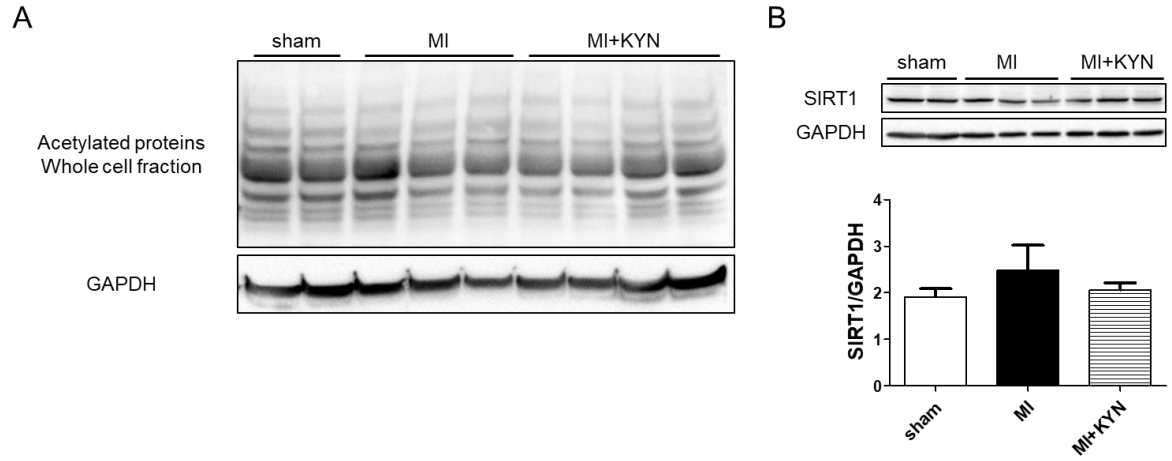

Figure 39: Representative immunoblots of (A) acetylated protein profile after 15 min of reperfusion (B) with histograms showing quantification of Silent information regulator 1 (SIRT1) protein expression after 2 hours of reperfusion in non-ischemic (sham), ischemic + vehicle (MI), and ischemic + KYN (MI+KYN) left ventricle samples (n=6-11). GAPDH was used as loading control. Values are expressed as mean±SEM.

We quantified protein expression and activity of complex I, II, III and IV in sham, MI and MI+KYN left ventricle samples after 2 hours of reperfusion respectively by western blot and spectrophotometry. Complex I, II, and III protein expression in the MI group were increased compared to sham. However, this increase was only significant for complex III (0.214±0.050 in MI *vs*. 0.144±0.017 in sham, $p<0.001$). KYN treatment significantly reduced the MI associated increase of complex III protein expression (0.202±0.02 in MI+KYN, $p=0.03$) (Fig 38A). We additionally quantified PGC1-α, a transcription factor implicated in mitochondrial biogenesis and oxidative phosphorylation, protein expression. The latter was comparable between sham, MI and MI+KYN groups (Fig. 38B). Although MI induced a complex I deficiency and a complex III over-activation, KYN treatment was not capable of restoring complex activity (Fig. 38C).

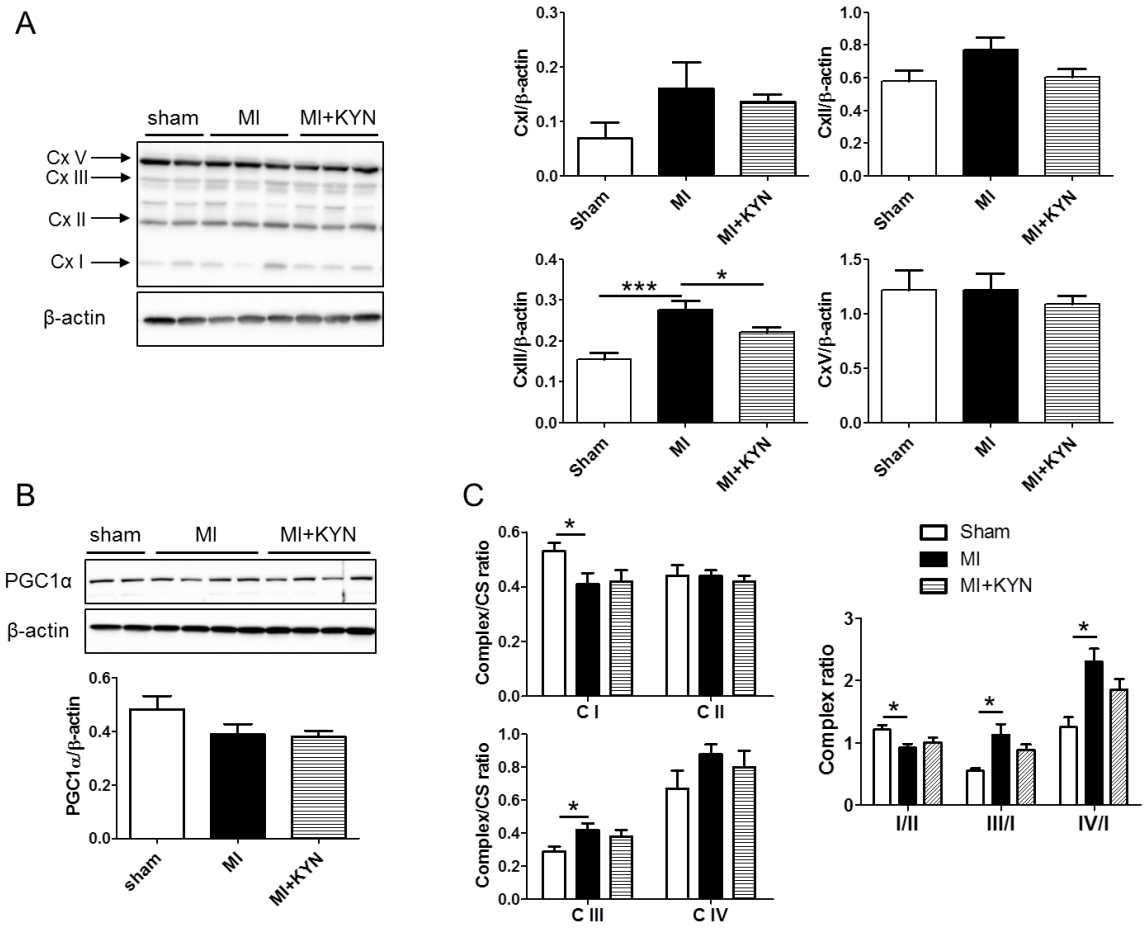

Figure 40: Representative immunoblots and histograms showing quantification of protein expression for (A) mitochondrial respiratory chain complex and (B) PGC1α in non-ischemic (sham), ischemic + vehicle (MI), and ischemic + KYN (MI+KYN) left ventricle samples after 2 hours of reperfusion (n=5-10). β-actin was used as loading control. (C) Histograms showing quantification of complex over citrate synthase activity ratio (I/CS, II/CS, III/CS, IV/CS) or complex ratio activity (I/II, III/I, IV/I) assessed by means of spectrophotometry in sham, MI, MI+KYNA left ventricle samples after 2 hours of reperfusion (n=5-11). Values are expressed as mean±SEM; * $p<0.05$, *** $p<0.001$.

A significant increase in GPR35 mRNA was observed after MI (0.022±0.0037 in MI group *vs*. 0.0065±0.0012 in sham, p=0.01). KYN treatment increased GPR35 gene expression compared to MI, however it was not significant (0.029±0.0044 in MI+KYN group *vs*. 0.022±0.0037 in MI group, p=0.19) (Fig. 39A). We also assessed phosphorylation levels of ERK1/2 and Akt kinases, possible targets of GPR35, after 15 min of reperfusion. MI induced an increase in ERK1/2 phosphorylation levels (1.61±0.36 in MI group *vs*. 0.07±0.04 in sham group, p=0.001). However, KYN treatment induced a significant decrease in ERK1/2 phosphorylation (0.58±0.18 in MI+KYN group *vs*. 1.61±0.36 in MI, p=0.008) as well as a decrease, but not significant, in Akt phosphorylation (0.68±0.08 in MI+KYNA group *vs*. 0.92±0.10 in MI, p=0.07) (Fig. 39B).

Akt and ERK1//2 are implicated in survival pathway signaling. Therefore, we assessed STAT3 and GSK3β phosphorylation levels, downstream kinases of SAFE and RISK survival

pathways respectively. MI significantly increased p-GSK3β/GSK3β and p-STAT3/STAT3 levels in MI (1.14±0.11, 1.37±0.14 for p-GSK3β and p-STAT3 respectively) compared to sham (0.72±0.19, 0.074±0.02; p=0.037, p<0.001 for p-GSK3β and p-STAT3 respectively). However KYN treatment did not have any influence on these levels compared to MI (Fig. 39C).

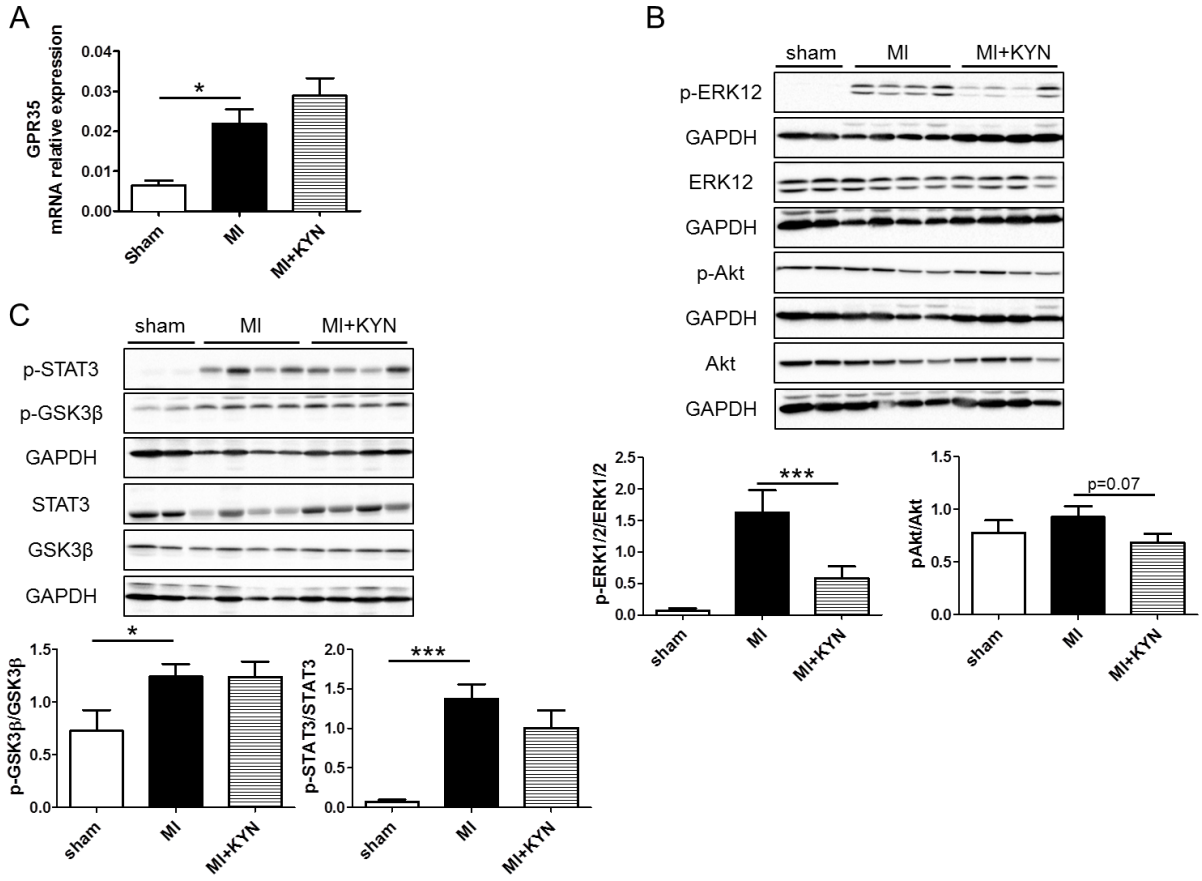

Figure 41: GPR35 mRNA expression and protein expression of p-ERK1/2, ERK1/2, p-Akt, Akt, p-GSK3β, GSK3β, p-STAT3 and STAT3, respectively by means of quantitative polymerase chain reaction and western blot. (A) GPR35 mRNA expression in sham, (MI), and KYN (MI+KYN) left ventricle samples after 2 hours of reperfusion (n=6-11). (B) Representative immunoblots and histogram quantification of protein expression for p-ERK1/2, ERK1/2, p-Akt, Akt, p-GSK3β, GSK3β, p-STAT3 and STAT3 in sham, MI and MI + KYN groups after 15 min of reperfusion (n=6-11). GAPDH was used as loading control. Data are expressed as mean±SEM. * p<0.05, *** p<0.001.

After 15 min of reperfusion, AMPKα phosphorylation levels were not significantly different among the groups. FOXO3α phosphorylation levels were significantly increased in MI group compared to sham group (6.22±1.61 *vs*. 1.68±0.51, p=0.044), whereas KYN treatment reduced, but not significantly FOXO3α phosphorylation levels (3.18±1.15 in MI+KYN, p=0.1) (Fig. 40).

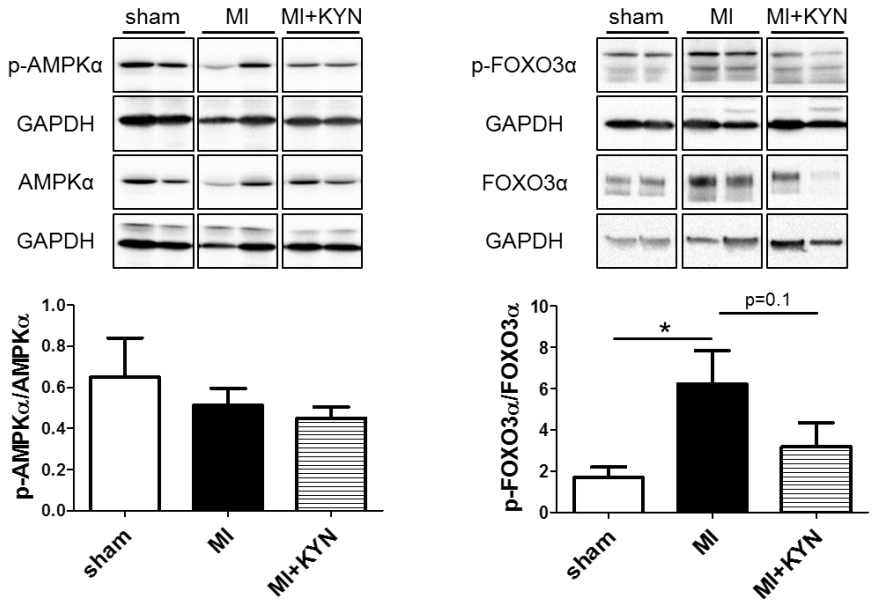

Figure 42: Representative immunoblots and histograms quantification of protein expression for p-AMPKα, AMPKα, p-FOXO3α and FOXO3α in non-ischemic (sham), ischemic + vehicle (MI), and ischemic + KYN (MI+KYN) left ventricle samples after 15 min of reperfusion (n=6-11). GAPDH was used as loading control. Values are expressed as mean±SEM. * p<0.05.

We quantified p62, PARK2, LC3b-II protein levels; the first two proteins are markers of mitochondrial autophagy, whereas the last protein is a marker of general autophagy. p62 was significantly decreased after myocardial I/R compared to sham (0.65±0.07 *vs*. 0.40±0.04, p=0.005) and even more reduced with KYN treatment (0.17±0.04) compared to MI (p=0.007). PARK2 protein levels were increased in MI group compared to sham group (0.157±0.012 *vs*. 0.377±0.059, p=0.09), but no significant difference was observed between MI and MI+KYN groups. LC3b-II protein levels were not significantly different between groups. (Fig. 41).

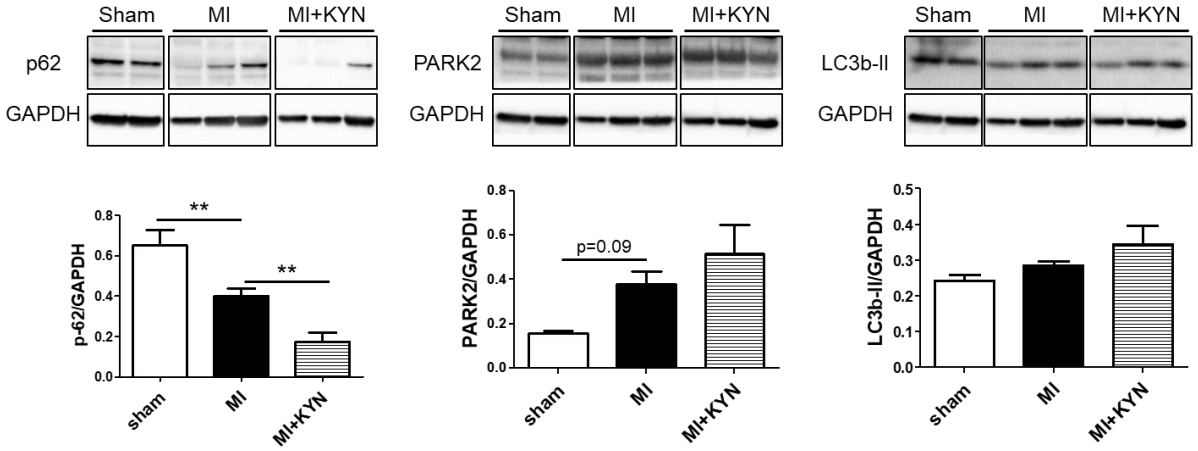

Figure 43: Representative immunoblots and histogram quantification of protein expression for p62, PARK2 and LC3b-II in non-ischemic (sham), ischemic + vehicle (MI), and ischemic + KYN (MI+KYN) left ventricle samples after 2 hours of reperfusion (n=6-7). GAPDH was used as loading control. Values are expressed as mean±SEM. ** p<0.01.

We evaluated mRNA expression of SOD1, SOD2, SOD3, and catalase in sham, MI and MI+KYN groups after 2 hours of reperfusion. SOD1 and catalase mRNA levels were significantly reduced after ischemia (28.50±1.81 in MI for SOD1 *vs*. 38.33±1.95 in sham, p=0.001; 17.21±1.39 in MI for catalase *vs*. 26.08±1.24 in sham, p<0.001). SOD2 and SOD3 mRNA were not changed after ischemia. KYN treatment induced a significant increase in SOD1 mRNA expression (33.28±1.32 in MI+KYN group *vs*. 28.5±1.81 in MI, p=0.04). There was also a tendency for an increase in SOD2 mRNA levels in MI+KYN group compared to MI (54.01±2.15 in MI+KYN group *vs*. 49.33±4.61 in MI, p=0.07) (Fig. 42).

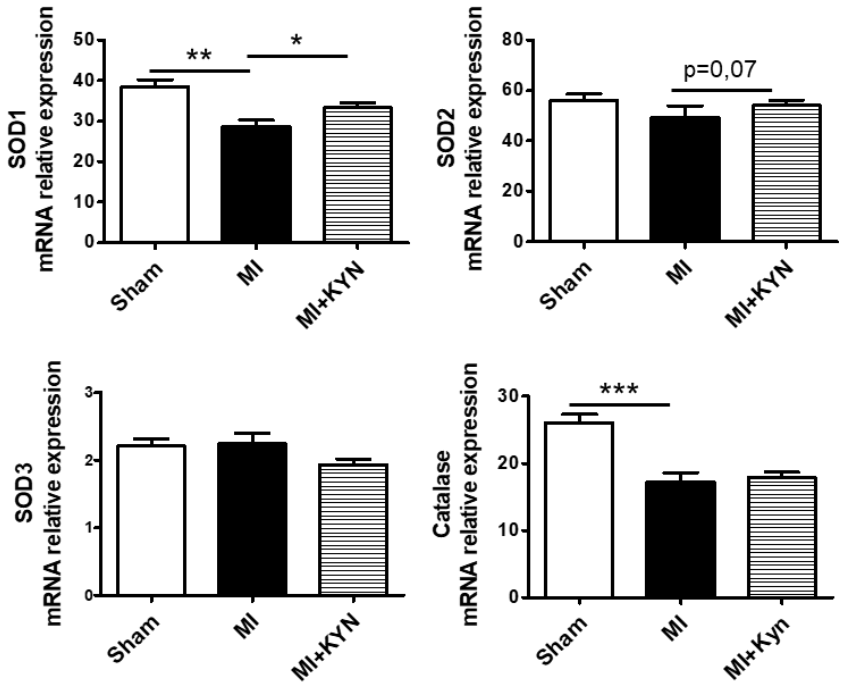

Figure 44: Anti-oxidant markers gene expression, by means of RT-qPCR. SOD1, 2, 3 and catalase mRNA expression in non-ischemic (sham), ischemic + vehicle (MI), and ischemic + KYN (MI+KYN) left ventricle samples after 2 hours of reperfusion (n=6-11). Values are expressed as mean±SEM. * p<0.05, ** p<0.01, *** p<0.001.

SOD1 protein levels were significantly reduced in MI+KYN group (2.15±0.21) compared to MI group (3.56±0.67) (p=0.042). SOD2 protein levels were comparable amongst all groups. SOD3 protein levels increased after ischemia (1.02±0.16 in MI group *vs*. 0.44±0.02 in sham group; p=0.005). Catalase protein levels were also significantly higher in MI group (0.42±0.03) vs sham group (0.25±0.01) (p=0.022). KYN treatment had a tendency in increasing catalase protein levels compared to MI group (p=0.094) (Fig. 43).

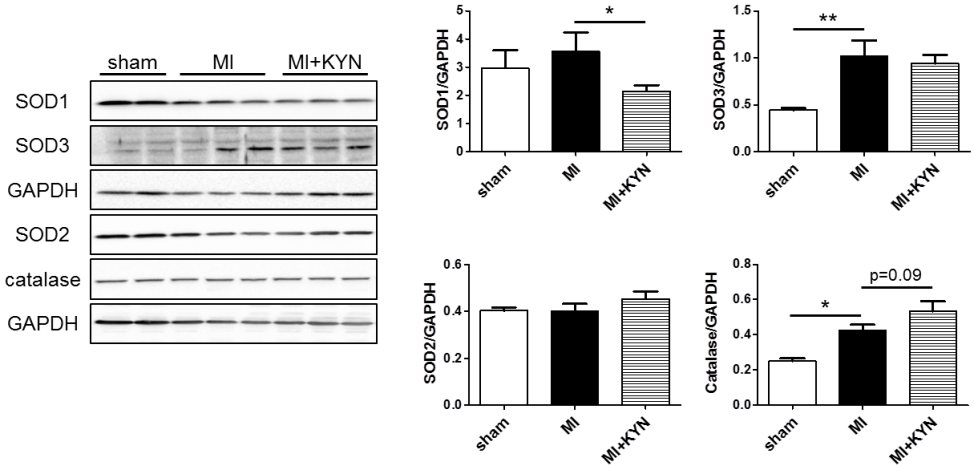

Figure 45: Representative immunoblots and histogram quantification of SOD1, 2, 3 and catalase protein expression in non-ischemic (sham), ischemic + vehicle (MI), and ischemic + KYN (MI+KYN) left ventricle samples after 2 hours of reperfusion (n=6-11). GAPDH was used as loading control. Values are expressed as mean±SEM. * $p<0.05$, ** $p<0.01$.

2.4. Discussion

KYN is a metabolite of TRP catabolism. Once TRP is ingested, it is oxidized into KYN, which itself is metabolized into two different pathways. KYN is either transformed into KYNA by KAT enzymes or into QA, a reaction catalyzed by KMO enzyme (Chen and Guillemin 2009). These two molecules (KYNA and QA) have long been studied due to their neuromodulator properties. KYNA is an antagonist of NMDA receptors, whereas QA is a neuro-excitotoxin, acting as a NMDA receptor agonist. Equilibrium between these two catabolic routes is crucial in maintaining proper neurotransmission in the brain (Stone and Darlington 2013). Studies were conducted in order to inhibit QA formation and to promote KYNA formation. For instance, in a focal cerebral ischemia model produced by electrocoagulation of the distal middle cerebral artery in mice, KYN reduced brain infarction; and in a bilateral carotid occlusion model, KYN-treatment reduced neuronal cell lost. This was accredited to an elevation in a neuroprotective molecule KYNA (Gigler et al. 2007). In the heart, kynurenine pathway remains poorly studied. Our previously published data showed that KYN was increased after RIC, and that KYN pre-treatment was capable of reducing infarct size in a myocardial I/R rat model (Chao de la Barca et al. 2016).

Herein, KYN treatment reduced cell death and prevented mitochondrial membrane potential decrease in an *in vitro* H9C2 hypoxia/reoxygenation cell model. Additionally, in an *in vivo* rat myocardial I/R model, TTC staining proved a reduced infarct size when rats were treated with a KYN injection peritoneally before a myocardial I/R. This is in line with our previously published data, however mechanisms underlying this cardioprotection remains to be cleared. More precisely, is it KYN by **itself** or its transformation into **KYNA** or **QA** or a **mixture** of both of them that is responsible for cardioprotection?

QA is a precursor of the *de novo* NAD^+ synthesis. The latter is known to be a crucial co-factor in numerous cellular reactions. It is notably an important co-factor for sirtuins which are desacetylase proteins. Their cardioprotective role was demonstrated in many studies (D'Onofrio, Servillo, and Balestrieri 2018). Indeed, mice overexpressing SIRT1 were endogenously protected against I/R injuries with a possible implication of endothelial nitric oxide synthase phosphorylation, NF-κB, and stimulation of autophagy (Nadtochiy et al. 2011). The importance of kynurenine pathway NAD^+ synthesis has been denoted in a study where NAD^+ levels were measured in the presence of different concentrations of different metabolites on human neuronal cells. Depending on the metabolite and its concentration, NAD^+ either increased or decreased due to cell toxicity (Braidy et al. 2009). Therefore we studied the profile of protein acetylation in whole cell. However, no specific acetylation pattern was found when comparing sham, MI and MI+KYN. Moreover, SIRT1 proteins expression was modified neither by myocardial infarction nor by KYN-treatment. However, we did not assess SIRT1 activity which could have been increased without the increase in protein expression level. Moreover,

remote ischemic conditioning decreased protein acetylation levels in liver, an effect abrogated with IDO inhibitor, 1-Methyl-D-tryptophan (Cf. Annexes 2). This leads to think that maybe KYN-mediated cardioprotection involves another organ: the liver.

Furthermore, we investigated other potential signaling pathways. Firstly, we assessed the mitochondrial respiratory chain complex activity, since mitochondrial dysfunction is a major factor leading to cardiomyocyte apoptosis (Gao et al. 2015). Evidence by Baran et al. on many occurrences, showed that kynurenine pathway metabolites can influence cardiac mitochondrial respiratory parameters assessed by oxygraphy at baseline. More precisely, KYNA was shown as a phosphorylation uncoupler (Baran et al. 2003; Baran et al. 2001; Baran et al. 2016). Using spectrophotometry, we assessed complex I-IV activity after myocardial I/R. As expected, ischemia caused a complex I and III dysfunction. However, KYN-treatment did not improve myocardial I/R-induced complex activity dysfunction. The controversy with literature can be due to many reasons. The most important one is that our study is conducted after I/R whereas other studies were conducted at baseline. Moreover, we cannot extrapolate the biodisponibility of KYN to cells in order to compare concentrations used *in vivo* (our study) and *in vitro* (Baran et al. 2003; Baran et al. 2001; Baran et al. 2016).

A work conducted in parallel in our lab (Study N°3), revealed a link between KYNA, ERK1/2, Akt and FOXO3α with a possible GPR35 implication. Since KYNA is a byproduct of KYN metabolism, we wanted to see if KYN is capable of stimulating the same pathways.

KYNA is a ligand of GPR35 (Wang et al. 2006), a G-coupled protein, capable of regulating phosphorylation of ERK1/2 and Akt (Zhao et al. 2010). Therefore, we evaluated gene expression of GPR35. GPR35 mRNA was significantly increased after ischemia, in line with literature (Ronkainen et al. 2014). And, Although, KYN-treatment increased GPR35 mRNA expression, this did not reach statistical significance. It has been reported that ERK1/2 and Akt phosphorylation levels, in cell models, can either be increased or decreased after KYNA treatment (Walczak, Turski, and Rajtar 2014; Agudelo et al. 2018), however the exact link with GPR35 is not well deciphered. Herein and similarly to findings with KYNA, ERK1/2 phosphorylation levels were significantly decreased with KYN-treatment. And, even though Akt phosphorylation levels were reduced, it was not significant. It is worth to note that phosphorylation levels of GSK3β and STAT3, proteins associated to ERK1/2 and Akt survival pathways (Tamareille et al. 2011), were not influenced by KYN treatment (MI+KYN) compared to MI.

ERK1/2 and Akt are kinases known to regulate FOXO3α, a transcription factor present in the cytoplasm. Its phosphorylation by ERK1/2 or Akt promotes its degradation (Yang and Hung 2009). AMPKα is a known activator of FOXO3α by inhibiting its phosphorylation (Yung et al. 2013).

AMPKα phosphorylation levels, assessed by western blot, were modulated neither by ischemia nor by KYN-treatment. Moreover, FOXO3α phosphorylation levels were significantly increased after ischemia, and reduced after KYN-treatment; however, again, this reduction did not reach statistical significance. Modulation of GPR35, ERK1/2, Akt, and FOXO3α by KYN was similar to that of KYNA-treatment, but with a lesser impact, hence an inferior statistical significance. The lesser impact can be due to either an inferior concentration of KYN (150mg/Kg) compared to KYNA (300mg/Kg) or that QA route is favored over KYNA route in KYN metabolism.

Mitophagy and anti-oxidative stress defense activation can play a role in cardioprotection (Moyzis, Sadoshima, and Gustafsson 2015; Gonzalez-Montero et al. 2018). Moreover, FOXO3α is a transcription factor that regulates expression of genes coding for proteins implicated in mitophagy (Yu et al. 2017; Mei et al. 2009) and anti-oxidant defense (Wang et al. 2016). Even though FOXO3α phosphorylation levels were not significantly reduced by KYN-treatment, we still evaluated gene expression levels implicated in mitophagy and oxidative stress defense.

We evaluated p62 levels, a protein degraded by general and mitochondrial autophagy. P62 levels were decreased by ischemia and even more decreased by KYN-treatment, meaning that mitophagy is further stimulated with KYN-treatment. However, PARK2 levels, protein implicated in mitophagy, and LC3b-II levels, protein implicated in autophagy, were not modified by KYN treatment. LC3b-II is degraded by autophagy and thus, depending on the timeline at which autophagy is evaluated, LC3b-II could be not detected. Therefore, western blot analysis of LC3b-II is to be interpreted carefully. PARK2 levels usually reflect Parkin-dependent mitophagy. An absence of PARK2 increase could mean that general autophagy and not mitochondrial autophagy is stimulated.

Afterwards, we evaluated mRNA and protein expression of SOD1, 2, 3 and Catalase. SOD1 mRNA expression was significantly higher, whereas protein expression was significantly decreased. This discrepancy could be due to rapid protein consumption or a brief half-life, following oxidative stress. The latter result with a SOD2 mRNA and catalase protein expression trend in increase, leads us to say that at 2 hours of reperfusion, anti-oxidant defense are activated.

It seems that KYN—mediated cardioprotection could be due in part to its metabolization into KYNA, activation of mitophagy or anti-oxidant stress. However, even if proteins acetylation profile did not differ with KYN-treatment, kynurenine pathway is still a main route of *de novo* NAD^+ synthesis. In a myocardial I/R mice model, increasing NAD^+ levels, after ischemia, with nicotinamide mononucleotide, reduced injuries (Yamamoto et al. 2014). Therefore further exploring of NAD^+ dependent signaling pathways is to be performed. Moreover, KYN is a ligand of the AhR receptor. The latter has been shown to participate in myocardial I/R injuries by regulating mitochondrial

apoptosis (Wang and Xu 2019). Thus, studying AhR target genes such as cytochrome P450 could be interesting.

3. Conclusion

The kynurenine pathway has long been studied for its importance in neurodegenerative diseases (Tan, Yu, and Tan 2012). KYNA and QA are both metabolites with great neuromodulator properties. It is not until recently that scientists began to take interest in the role of the kynurenine pathway in the heart. Our findings (Chao de la Barca et al. 2016) linking remote ischemic conditioning, a cardioprotective strategy, and KYN encouraged us to investigate even more the role of kynurenine pathway metabolites in cardioprotection and underlying mechanisms. Our main findings are:

KYN and KYNA were both capable of conferring cytoprotection and cardioprotection respectively in *in vitro* and *in vivo* models.

KYNA cardioprotective mechanisms seem to implicate an inhibition of ERK1/2 and Akt, an activation of FOXO3α which in turn stimulates anti-oxidant defense and the elimination of defective mitochondria by mitophagy. However, GPR35 implication needs to be confirmed.

KYN cardioprotective mechanisms remain to be clarified. It is not quite understood if it is KYN can mediate cardioprotection by itself or if it is its metabolization into KYNA or QA, precursor of NAD^+ that mediate cardioprotection.

GENERAL discussion

Reperfusion injury is the paradoxical tissue response exhibited after crucial re-establishment of blood flow in the ischemic myocardium. Etiology of myocardial I/R injury has been well characterized. However, knowledge of underlying mechanisms of myocardial damage has yet to be successfully translated into strategies for cardioprotection in the clinical arena (Nichols et al. 2014). Mitochondria are one of the key players in I//R injuries. It is axiomatic that mitochondria are crucial for proper cardiomyocytes contractility and heart function; being at the intersection of uncountable catabolic and anabolic cellular reactions and the main source of ATP, a function even more important in this blood pump. Despite these mitochondria's dual benefit of consuming ROS and generating ATP, during stress conditions, herein MI, mitochondria have two adverse consequences, which are ROS accumulation and decline in ATP (Dorn 2015b).

Mitochondrial function is tightly associated and regulated by mitochondrial structure. Unlike previously considered theories, mitochondria are dynamic organelles, constantly changing their structure in response to outer stimuli. These changes are called mitochondrial dynamics: mitochondrial fusion and mitochondrial fission (Tilokani et al. 2018).

Mitochondrial dynamics proteins have been shown indispensable in cardiomyocytes development and survival (Zhang et al. 2017; Sharp et al. 2014; Wai et al. 2015). Nonetheless, numerous discrepancies exist concerning the role of mitochondrial fusion and fission proteins in myocardial I/R injuries. Until recently, it has been sought that excessive fusion is beneficial and that excessive fission is detrimental to the cell; hence, many authors inhibited fission to preserve mitochondrial morphology after stress (Ong et al. 2010). Nevertheless, other authors (Ikeda et al. 2015) showed completely opposite results, where cardiac specific homozygous deletion of DRP1 was detrimental to the heart, and a cardiac specific heterozygous deletion of DRP1 exacerbated I/R injuries due to a deregulated mitophagy, process by which dysfunctional mitochondria are eliminated.

We had already studied a mouse model deficient in mitochondrial fusion protein OPA1, where myocardial I/R injuries were worsened compared to their WT littermates (Le Page et al. 2016). In another study (Cf. Results, Study N°1), we showed a decrease in infarct size in a mouse model deficient in the mitochondrial fission protein DRP1. *Drp1*$^{+/-}$ mice did not show any sign of myocardial dysfunction, meaning that DRP1 protein was maintained at a level high enough to ensure the integrity of the mitochondrial network. Even though mitochondria seemed enlarged, this however did not affect cardiomyocytes function. However, when challenged these mice showed a certain resistance to myocardial I/R injuries compared to their WT littermates. This means that, in these mice, cardiomyocytes were conditioned to better face stressful conditions, possibly by an enhanced mitophagy. In another study, using a mice model heterozygously deficient for both OPA1 and DRP1, we showed that inhibiting either mitochondrial fusion or fission by itself had more impact on cardiomyocytes than inhibiting both mechanisms simultaneously (Cf. Results, Study N°2). In yeast,

simultaneous absence of fission and fusion proteins restores a normal mitochondrial morphology similar to wild type despite the presence of mitochondrial dysfunctions, in contrast to a model where only one mechanism is shut down (Bernhardt et al. 2015). Recently, a triple homozygous knockout mice model for DRP1, MFN1, and MFN2, further proved that mitochondrial adynamism in the heart, although is detrimental, but is of a lesser impact than separate mitochondrial fusion or fission downregulation (Song et al. 2017).

It has been described, with some controversial data, that mitochondrial dynamics is important to ensure proper flow of mitophagy. For example, Song et al. (Song et al. 2015) showed that Parkin-dependent mitophagy is increased after DRP1 downregulation, whereas Ikeda et al. showed an accumulation of damaged mitochondria after suppressed mitophagy in a DRP1 cardiac specific deficient mouse model (Ikeda et al. 2015). In fact, Parkin ubiquinates DRP1 for degradation (Wang et al. 2011). In line with these findings, Kageyama et al. demonstrated in a *Parkin*$^{-/-}$ mice model that DRP1 levels are increased (Kageyama et al. 2014). In a normal, not genetically-modified, mouse heart Parkin mRNA and protein expression are present at very low levels but are upregulated after cardiac myocyte-specific deletion of DRP1. Albeit, observations marked a mitochondrial fragmentation after downregulation of mitochondrial fusion proteins like MFN1,2 (Song et al. 2015), mitophagic flux was decreased, (Song et al. 2015; Song et al. 2017). PINK1 can phosphorylate MFN2 and thus promotes Parkin translocation to mitochondria (Chen and Dorn 2013). Ablation of PINK1 in mice induces early left ventricular dysfunction and cardiac hypertrophy (Billia et al. 2011). An apparent inextricably link exists between Parkin, DRP1, MFN1,2 and mitophagy, which can explain all of these controversial findings. Regardless, what is certain is the importance of mitochondrial dynamics protein in ensuring mitochondria quality control, and proper elimination of damaged and dysfunctional organelles.

Conditioning is defined in the dictionary as following: ‘a way to accustom, to behave in a certain way or to accept certain circumstances’. Ischemic conditioning, more precisely, remote ischemic conditioning, has long been considered as a cardioprotective strategy in animal models, and had the advantage of being easily applied and translated into clinical studies (Lim and Hausenloy 2012), albeit its effectiveness is yet to be proved. The heart is conditioned to better face challenging situations by submitting it to less stressful conditions which permits the myocardium to activate certain endogenous protective signaling pathways after MI.

In a recently published study (Chao de la Barca et al. 2016), we documented an increase in KYN plasmatic concentrations associated with RIC. KYN is the first product of TRP metabolism, and can later be metabolized into KYNA or QA (Wang et al. 2012). Kynurenine pathway has attracted scientist’s attention, for neuromodulator properties of KYNA and QA. The same pathway leads to the formation of two metabolites with opposite consequences. KYNA is an antagonist (Perkins, Collins, and Stone 1982; Schwarcz et al. 2012; Vecsei et al. 2013), unlike QA, which is an agonist and an activator of NMDA receptors (Perkins et al. 1981; Stone et al. 1981). NMDA receptors modulation of

activity is implicated in many neurodegenerative diseases and in cerebral I/R injuries (Fujigaki, Yamamoto, and Saito 2017; Majlath, Toldi, and Vecsei 2014; Majlath, Tajti, and Vecsei 2013). NMDA is responsible for excitatory neuronal transmission (Klockgether 1987). When exceeding physiological activation this leads to aggravated I/R injuries. In a global cerebral I/R canine model induced by cardiac arrest, NMDA receptor binding was increased (Wei et al. 1997). In another study, brain damage caused by a middle cerebral artery occlusion, was mediated by a NMDA receptor's activation (Luo et al. 2018). Precisely, calcium influx driven by NMDA receptors was shown to increase adverse effect of myocardial I/R in rat hearts *ex vivo* (Liu et al. 2017). Therefore, modulation of the kynurenine pathway enzyme activity has been a therapeutic target (Phillips et al. 2019). KMO inhibitors were described and used to decrease cerebral I/R injuries by decreasing QA production and rerouting kynurenine pathway to KYNA synthesis (Cozzi, Carpenedo, and Moroni 1999).

In contrast to the extensive knowledge of kynurenine pathway involvement in neurodegenerative diseases and implication in cerebral I/R injuries, implication of this metabolic route in myocardial I/R injuries has not been studied until recently. In a study that opted to understand mechanisms implicated in remote ischemic conditioning, authors demonstrated the implication of the alpha-ketoglutarate dependent dioxygenase (*Egln1*), a protein that senses oxygen and regulates the hypoxia-inducible factor (HIF) in cardioprotection using an *Egln1*$^{-/-}$ mice model (Olenchock et al. 2016). Cardioprotection was described being mediated by KYNA which production was increased after alpha-ketoglutarate accumulation. However, mechanisms explaining KYNA-mediated cardioprotection were not studied.

In our work, KYNA-mediated cardioprotection was a consequence of an enhanced mitophagy and an increase in anti-oxidant defense system. Although, KYN-mediated cardioprotection, possibly implicates other processes and actors that we have yet to explore, both mitophagy and anti-oxidant defense mechanism were stimulated.

The half-life of mitochondria has been accounted to range from a few days to weeks (Menzies and Gold 1971). A proper elimination of defective mitochondria is critical for cardiac homeostasis (Kubli et al. 2013; Kubli, Quinsay, and Gustafsson 2013; Hoshino et al. 2013). As shown by our results and by other studies (Matsui et al. 2007; Hamacher-Brady, Brady, and Gottlieb 2006; Moyzis, Sadoshima, and Gustafsson 2015), autophagy and mitophagy, are increased in myocardium after stress conditions, a response activated by the cell in means of protection. Additionally, Parkin-deficient mice have increased mortality, due to accumulation of dysfunctional mitochondria after MI (Kubli et al. 2013). In addition, in an *ex vivo* myocardial I/R mouse model, PINK1-deficient hearts had an increased susceptibility to injuries (Lee et al. 2011).

When mitochondria are excessively solicited, uncontrollably, ROS molecules are produced. This oxidative stress is a major contributor to I/R injuries (Sun et al. 2018). In a canine myocardial I/R

model, SOD, an anti-oxidant molecule, with an extended half-life was responsible for myocardial salvage (Chi et al. 1989). Another study demonstrated that using a selective SOD mimetic in rat myocardial I/R decreased infarct size, neutrophil infiltration in the myocardium, lipid peroxidation, and post-reperfusion calcium overload (Masini et al. 2002). Moreover, an increase in SOD2, and catalase mRNA and protein expression, as well as an increase in their activities, has been associated with cardioprotection in myocardial I/R (Wang et al. 2016).

In both parts of this thesis (mitochondrial dynamics and kynurenine pathway) the importance of mitochondria and mitophagy has emerged. FOXO3α is an important transcription factor in regulating parkin-mediated mitophagy (Mei et al. 2009; Das et al. 2014; Yu et al. 2017). In a study, normal and stressed (phenylephrine treated) cardiomyocytes, as well as a rat model of heart failure with preserved ejection fraction, were used to study the importance of FOXO3α regulating *Bnip3* gene expression in a cardiac stress model: heart failure. FOXO3α/BNIP3 signaling was capable of regulating mitochondrial morphology and function. An increase in autophagy, stimulation of mitochondrial fission and inhibition of mitochondrial fusion protein OPA1 were observed with FOXO3α-dependent BNIP3 upregulation. However, and controversially to what we describe in our work, FOXO3α's upregulation of BNIP3 in heart failure is maladaptive and leads to decreased mitochondrial membrane potential, mitochondrial fragmentation, excessive mitophagy, and apoptosis (Chaanine et al. 2016). This emphasizes the importance of a fine regulation of mitochondrial function and morphology and how mitophagy can ensure mitochondrial network integrity. Therefore, it is possible that KYN and KYNA-mediated cardioprotection can influence mitochondrial dynamics. Considering general and mitochondrial autophagy's increase in KYN-mediated and KYNA-mediated cardioprotection, and mitochondrial dynamics importance in ensuring autophagy/mitophagy processes, exploring mitochondrial dynamics protein levels, and mitochondrial morphology after KYN and KYNA-treatment could be interesting.

Conclusion and perspectives

This work was conducted to 1) understand mitochondrial dynamics proteins implication in myocardial I/R injuries; and 2) to study underlying mechanisms of kynurenine pathway metabolites-induced cardioprotection.

Firstly, our results highlighted the importance of mitochondrial dynamics in myocardial I/R injuries, and the indispensability of maintaining mitochondrial network's integrity that is tightly correlated to its mitochondrial function. We showed that a partial fission inhibition could potentially be beneficial to myocardial I/R injuries. However, further elaborated studies on mitophagy are required to better understand DRP1's role in adequate mitochondrial removal and its implication in observed cardioprotection. Indeed, studying expression of other proteins implicated in mitophagy like Beclin and PINK could be interesting. Moreover, Chloroquine, an inhibitor of lysosome fusion (Mauthe et al. 2018), could be used to study mitophagy flux. Additionally, we showed that abrogating mitochondrial dynamism by partially inhibiting fusion and fission proteins, did not have an influence on cardiac morphology and function. These data mark, on one hand, the importance of keeping a well-balanced fusion-fission processes and on another hand, the existence of adaptive mechanisms in these studied mice which were necessary for their survival.

Secondly, we confirmed the cytoprotective effect of KYN and KYNA in both a rat myocardial infarction model and an *in vitro* H9C2 H/R cell model. We also explored and deciphered some actors that could play a role in kynurenine pathway metabolites-induced cardioprotection like FOXO3α, a transcription factor that regulates the expression of genes involved in mitophagy and anti-oxidant defense system. GPR35's role in KYNA-induced cardioprotection remains to be confirmed. GPR35 KO mice could be used to validate our hypothesis. Likewise, mechanisms underlying KYN-mediated cardioprotection should be further explored. Utilization of kynurenine pathway inhibitors, KMO inhibitors and KATs inhibitors could give a better apprehension of cardioprotective mechanisms. Finally, even if our work still needs to be completed, our results are the first to give insights on signaling pathways implicated in kynurenine pathway metabolites-induced cardioprotection. As mentioned beforehand, it could be interesting to explore KYN and KYNA-treatment's effect on mitochondrial dynamics proteins, since MFN2 and DRP1 are both crucial proteins in mitophagy.

To conclude, regulating mitophagy, a mechanism responsible for appropriate removal of defective mitochondria, seems crucial in improving myocardial I/R injuries. Indeed, our work proves furthermore that mitochondria and mitochondrial dynamics proteins are potential therapeutic targets in treating myocardial I/R injuries.

Annexes

1. Increase in Cardiac Ischemia-Reperfusion Injuries in Opa1$^{+/-}$ mouse model

PLOS ONE

RESEARCH ARTICLE

Increase in Cardiac Ischemia-Reperfusion Injuries in Opa1$^{+/-}$ Mouse Model

Sophie Le Page[1,2,3☯‡], Marjorie Niro[1,2,3☯‡], Jérémy Fauconnier[4], Laura Cellier[1,2], Sophie Tamareille[1,2], Abdallah Gharib[5], Arnaud Chevrollier[1,6], Laurent Loufrani[1,6], Céline Grenier[1,6], Rima Kamel[1,2], Emmanuelle Sarzi[7], Alain Lacampagne[4], Michel Ovize[5], Daniel Henrion[1,6], Pascal Reynier[1,6], Guy Lenaers[1,6], Delphine Mirebeau-Prunier[1,6‡], Fabrice Prunier[1,2,3‡*]

1 Institut MITOVASC, Université Angers, CHU Angers, Angers, France, **2** Laboratoire Cardioprotection Remodelage et Thrombose, Angers, France, **3** Service de Cardiologie, CHU Angers, Angers, France, **4** INSERM U1046, Université Montpellier I et II, Montpellier, France, **5** INSERM UMR 1060, CarMeN, Lyon, France, **6** INSERM UMR_S1083, CNRS UMR_C6214, BNMI, Angers, France, **7** Institut des Neurosciences de Montpellier, INSERM U1051, Université Montpellier I et II, Montpellier, France

☯ These authors contributed equally to this work.
‡ SLP and MN are first co-authors of this work. DMP and FP also contributed equally to this work as last co-authors.
* FaPrunier@chu-angers.fr

Citation: Le Page S, Niro M, Fauconnier J, Cellier L, Tamareille S, Gharib A, et al. (2016) Increase in Cardiac Ischemia-Reperfusion Injuries in Opa1$^{+/-}$ Mouse Model. PLoS ONE 11(10): e0164066. doi:10.1371/journal.pone.0164066

Editor: Luc Bertrand, Université catholique de Louvain, BELGIUM

Received: June 22, 2016

Accepted: September 19, 2016

Published: October 10, 2016

Data Availability Statement: All relevant data are within the paper.

Funding: SLP received funding from the French Ministry of Education and Research and MN from the Fédération Française de Cardiologie. JF and AL were supported by the Fondation de France and Fondation pour la Recherche Médicale. This work was carried out in the context of the PREMMI (Pôle de Recherche et d'Enseignement en Médecine Mitochondriale) project, supported by the University of Angers, the University Hospital of Angers, the French region Pays de la Loire and Angers Loire Métropole.

Abstract

Background

Recent data suggests the involvement of mitochondrial dynamics in cardiac ischemia/reperfusion (I/R) injuries. Whilst excessive mitochondrial fission has been described as detrimental, the role of fusion proteins in this context remains uncertain.

Objectives

To investigate whether Opa1 (protein involved in mitochondrial inner-membrane fusion) deficiency affects I/R injuries.

Methods and Results

We examined mice exhibiting *Opa1*^{delTTAG} mutations (Opa1$^{+/-}$), showing 70% Opa1 protein expression in the myocardium as compared to their wild-type (WT) littermates. Cardiac left-ventricular systolic function assessed by means of echocardiography was observed to be similar in 3-month-old WT and Opa1$^{+/-}$ mice. After subjection to I/R, infarct size was significantly greater in Opa1$^{+/-}$ than in WTs both *in vivo* (43.2±4.1% *vs*. 28.4 ±3.5%, respectively; p<0.01) and *ex vivo* (71.1±3.2% *vs*. 59.6±8.5%, respectively; p<0.05). No difference was observed in the expression of other main fission/fusion protein, oxidative phosphorylation, apoptotic markers, or mitochondrial permeability transition pore (mPTP) function. Analysis of calcium transients in isolated ventricular cardiomyocytes demonstrated a lower sarcoplasmic reticulum Ca^{2+} uptake, whereas cytosolic Ca^{2+} removal from the Na^{+}/Ca^{2+} exchanger (NCX) was increased, whilst SERCA2a, phospholamban, and NCX protein expression levels were unaffected in Opa1$^{+/-}$

Competing Interests: The authors have declared that no competing interests exist.

compared to WT mice. Simultaneous whole-cell patch-clamp recordings of mitochondrial Ca^{2+} movements and ventricular action potential (AP) showed impairment of dynamic mitochondrial Ca^{2+} uptake and a marked increase in the AP late repolarization phase in conjunction with greater occurrence of arrhythmia in Opa1$^{+/-}$ mice.

Conclusion

Opa1 deficiency was associated with increased sensitivity to I/R, imbalance in dynamic mitochondrial Ca^{2+} uptake, and subsequent increase in NCX activity.

Background

Mitochondria are double-membrane organelles that are essential to the life of eukaryotic cells, due to their special role at the crossroads of the survival and apoptotic pathways, and constitute the primary hosts of ATP production. This is particularly true in relation to the heart, which requires high rates of energy conversion, with mitochondria occupying around 30% of total cardiomyocyte volume [1].

Far removed from the traditional concept of static organelles, mitochondria have been revealed to be highly dynamic structures, altering their inner and outer membranes by means of fission and fusion mechanisms through the action of proteins located on inner and outer membranes [2]. The fission process, leading to mitochondrial fragmentation, is mediated by the cytosolic dynamin-related protein 1 (Drp1) and outer-membrane human fission factor 1 (Fis1). On the contrary, mitochondrial fusion is mediated by the action of outer-membrane mitofusins (Mfn 1 & 2) and inner-membrane optic atrophy factor 1 (Opa1). In line with others, our research team found that *OPA1* mutations were typically responsible for dominant optic atrophy (DOA, MIM#165500), an inherited disease affecting retinal ganglion cells while altering optic nerve integrity [3,4], in addition to a large spectrum of neurological syndromes [5].

Recent studies suggest involvement of mitochondrial dynamics in cardiovascular diseases, particularly in ischemia/reperfusion (I/R) injury, and infer potential protection means through modulation of fusion and fission protein expression [1]. Excessive fission has thus been associated with I/R injury and cell apoptosis [6]. Whilst some works suggest that inhibition of excessive mitochondrial fission through Fis1 and Drp1 modulation may be cardioprotective [7–9], the effects induced by modulation of the fusion proteins Mfn-2 and Opa1 were subject to contention. In fact, a fusion deficit induced through Mfn-2 deficiency had been unexpectedly linked to improved death protection and recovery after coronary artery ligation in an *in vivo* murine model [10]. Moreover, initial experiments conducted in Opa1-deficient models reported inconsistent results [11–13]. It is important to note that cardiomyocytes from Opa1--deficient mice models were more sensitive to simulated I/R [12], but it remains unknown whether this deficiency is of significance *in vivo* in the context of I/R.

The objective of this study was thus to investigate whether Opa1 deficiency would influence cardiac I/R injury *in vivo*. In order to respond to this question, we studied heterozygous mice carrying the most recurrent Opa1^{delTTAG} mutation, found in patients with dominant optic atrophy [14].

Methods

Opa1^{delTTAG} mice and breeding

As previously described, our group generated a knock-in *Opa1* mouse model carrying the recurrent Opa1^{delTTAG} mutation [15]. Briefly, C57Bl6/J mice were genetically modified to obtain the Opa1^{delTTAG} heterozygous mutation (Opa1$^{+/-}$) that is observed in 30% of patients affected by dominant optic atrophy [15]. Homozygous Opa1$^{-/-}$ is lethal in the early stages of fetal development. Male Opa1$^{+/-}$ mice and their counterpart wild-type (WT) controls exhibiting Opa1$^{+/+}$ were fed and hydrated without any restrictions. They were held in the animal facility of the UMR INSERM 1083-CNRS 6214 in Angers, France. All experiments were performed in compliance with the European Union and French guiding principles on the protection of animals used for scientific purposes (EU Directive 2010/63/EU; French Decree no. 2013–118). The protocol was approved by the local ethics committee (Comité d'Ethique en Expérimentation Animale des Pays de la Loire) and by the national committee (MENESR, 2015101511544187/APAFIS 3723).

Echocardiography

Anesthetized mice (ketamine 60mg/Kg, intraperitoneal) underwent transthoracic echocardiography (TTE) as previously described [16]. Left-ventricular end-diastolic diameter (LVEDD), fractional shortening (FS), and heart rate were determined using 2D M-mode echocardiography. At the time of sacrifice, heart weight was measured and correlated to body weight (HW/BW).

Blood pressure assessment

Blood pressure was measured by means of tail-cuff plethysmography (Visitech BP2000 System) in awake mice. For each mouse, the mean systolic blood pressure was averaged from 15 measurements recorded for 15 minutes every day for five consecutive days.

Cardiomyocytes isolation and calcium transients

The mice's hearts were subjected to enzymatic digestion (Liberase TH, Roche®) as previously described [17,18]. Immediately after excision and cannulation, hearts were retrogradely perfused at 37°C in a free-calcium perfusion buffer containing 5.5mM glucose, 113mM NaCl, 4.7mM KCl, 0.6mM KH_2PO_4, 0.6mM Na_2HPO_4, 1.2mM $MgSO_4$, 12mM $NaHCO_3$, 10mM $KHCO_3$, 10mM HEPES, and 30mM taurine; pH = 7.4. The hearts were then perfused with the same buffer containing 0.1mg/mL Liberase TH (Roche®, France) for 5 to 10 minutes in order to achieve complete digestion. The left ventricles were then mechanically dissociated in the same solution, enzyme-free and containing 10mM of butanedione monoxime (BDM) (10% SVF), in order to stop enzymatic activity. Cells were transferred to a BDM-free buffer (5% SVF), and calcium concentration was progressively raised to a final concentration of 1mM.

Isolated cardiomyocytes were loaded with fluo-4 AM (4μM for 20 min, Molecular Probes, Eugene, Oregon, USA) and then placed on the stage of an inverted confocal microscope (LSM510 Meta Zeiss, Carl Zeiss, Jena, Germany) equipped with a 63x water-immersion objective (NA: 1.2). Cells were field-stimulated at 1Hz in a tyrode solution containing: 135mM NaCl, 4mM KCl, 1.8mM $CaCl_2$, 1mM $MgCl_2$, and 2mM HEPES (NaOH-adjusted pH of 7.4). Triggered calcium transients were recorded in line-scan mode (1.5ms/line, 3,000 lines/cell) along the longitudinal axis of the cell. Fluo-4 was excited at 488nm, and emitted light was collected using a 505nm-long pass filter. The laser intensity employed (<10% of maximum) had no noticeable detrimental effect on the fluorescent signal or on cell function over the course of the experiment.

Analysis was performed using the software ImageJ (NIH, Bethesda, Maryland, USA). In order to enable comparison between cells, the change in fluorescence (ΔF) was divided by the fluorescence detected immediately prior to the 1Hz stimulation pulse ($F0$). For assessment of sarcoplasmic reticulum (SR) Ca^{2+} content, cardiomyocytes were paced 1-2min at 1Hz to reach steady-state Ca^{2+} transients and SR Ca^{2+} load. Stimulation was subsequently stopped, and caffeine (10mM) applied to empty the SR.

The course of field-stimulated Ca^{2+} transients and caffeine-induced SR Ca^{2+} release was assessed by analyzing the maximum amplitude and time constant (τ) of the exponential part of the late decay phase. The time-to-peak normalized to the peak amplitude was also determined for stimulated Ca^{2+} transients.

Mitochondrial calcium measurement and ventricular action potential

Mitochondrial Ca^{2+} movements and ventricular action potential (AP) were simultaneously recorded by means of a whole-cell patch-clamp technique, as previously described [18,19]. Briefly, after loading with Rhod-2 AM (5μM for 40 min at 37°C, TEFLabs, Austin, Texas, USA), the left-ventricular cardiomyocytes were placed on the stage of an inverted confocal microscope (LSM510 Meta Zeiss, 63x objective, NA: 1.2) and superfused with a standard tyrode solution containing 135mM NaCl, 4mM KCl, 1.8mM $CaCl_2$, 1mM $MgCl_2$, 2mM HEPES, and 10mM glucose at an NaOH-adjusted pH of 7.4. Subsequently, isolated cardiomyocytes were whole-cell-patch-clamped using an Axopatch 200B (Molecular Devices, Sunnyvale, California, USA), and patch pipettes (2-3MΩ) were filled with an internal solution containing 130mM KCl, 25mM HEPES, 3mM MgATP, 0.4mM NaGTP, 5mM NaCl, and 0.5mM EGTA at a KOH-adjusted pH of 7.2. Such an approach allows the dialysis of cytosolic rhod-2 [18,19]. APs were elicited using a current clamp by means of 0.2ms current injections of suprathreshold intensity and stimulated routinely at 1Hz as previously described [20]. Shifts in dye fluorescence were recorded in line-scan mode (1.54ms/line) along the short axis of the cell. As regards fluo-4 signals, confocal images were analyzed using the software ImageJ, and the change in fluorescence (ΔF) was divided by the fluorescence detected immediately prior to the 1Hz stimulation pulse ($F0$). APs were recorded and analyzed using the software program Pclamp 10 (Axon Instruments). AP durations were measured at 20%, 30%, 50%, 90%, and 95% of the repolarization phase.

Mitochondrial morphology and function

Electron microscopy. Hearts from 3-month old mice were fixed by a retrogradely perfusion with 2% glutaraldehyde in cacodylate buffer (100mM sodium cacodylate and 2 mM $MgCl_2$; pH 7.3). Then, left-ventricular papillary muscles were isolated and post-fixed as previously described [21]. Ultra-thin longitudinal sections were cut, and examined using an electron microscope. 20,000x-magnified images were used in the software ImageJ in order to assess the number and area of mitochondria. A mean of 20 fields were analyzed per mouse.

Mitochondrial respiration. Oxidative phosphorylation was determined as previously described [22]. The hearts were excised, and mitochondria isolated. Complex activity was assessed using 350μg of mitochondrial proteins. Complex I was determined by adding 5mM Glutamate/Malate/Puryvate (GMP), complex II by adding rotenone in conjunction with succinate, and complex IV by adding antimycine with PMDP ascorbate.

Mitochondrial permeability transition pore experiments. Mitochondrial permeability transition pore (mPTP) opening was assessed as previously described [23]. Calcium retention capacity (CRC) measurement using 250μg of mitochondrial proteins was performed at baseline and after the adjunction of cyclosporine A (1μM) in Opa1$^{+/-}$ and WT mice.

I/R experiments

Ex vivo I/R. Opa1$^{+/-}$ and WT mice were anesthetized by means of an intraperitoneal injection of sodium pentobarbital (100mg/kg, Ceva Santé Animal®, Libourne, France). Heparin (1,000 IU/kg, Heparine Choay®) was also administered to prevent intracoronary clot formation. The heart was rapidly excised and immediately immersed in ice-cold modified Krebs-Henseleit buffer containing: 118.5mmol/l NaCl; 4.7mmol/l KCl; 25mmol/l $NaHCO_3$; 1.2mmol/l $MgSO_4$; 1.2mmol/l KH_2PO_4; 1.8mmol/l $CaCl_2$; and 11mmol/l glucose (pH 7.4). The heart was mounted on a Langendorff-perfusion apparatus (ADInstruments, Dunedin, New Zealand) and retrogradely perfused through the aorta with non-recirculating buffer saturated with 95% O_2 and 5% CO_2 at 37°C. The heart was maintained in a thermostatic chamber at 37°C. Perfusion was maintained at a constant pressure of 80mmHg. After a 20-minute stabilization period, the hearts were subjected to 30 minutes of global ischemia and 2 hours of reperfusion.

In vivo I/R. Opa1$^{+/-}$ and WT mice were anesthetized by means of intraperitoneal sodium pentobarbital injections (90mg/kg; Ceva Santé Animale) prior to endotracheal intubation and mechanical ventilation using MiniVent 845® (Hugo-Sachs Elektronik—Harvard Apparatus GmbH, March, Germany). The mice received an injection of heparin (1,000 IU/kg, Heparine Choay®, Sanofi, Gentilly, France) prior to thoracotomy. Temperatures were monitored during the procedure and strictly maintained at 36.5° to 38°C. The thorax was opened via a left lateral thoracotomy, and the pericardium removed. Coronary ligation was performed on the left coronary artery using a monofilament (PROLENE 7.0®, Ethicon, LLC, Cincinnati, Ohio, USA), placed in a polyethylene tube to create a reversible snare, as previously described [24]. Ischemia was induced by clamping the tube and confirmed through observations of dyskinesia and cyanosis of the myocardial region below the suture. It was maintained for 45 minutes, followed by 120 minutes of reperfusion by loosening the snare.

Infarct size assessment. For *in vivo* experiments, coronary ligation was repeated at the end of the reperfusion period, and 400μl of Evans Blue (Sigma®) were injected through the left-ventricular apex, coloring the perfused (non-ischemic) myocardium blue. The area-at-risk (AAR) was then identified as the non-blue myocardium area and expressed as a percentage of left-ventricular area (LV). After heart extraction, the left ventricle was cut into six to seven slices before staining it with 2,3,5-triphenyltetrazolium chloride (TTC). The slices were subsequently submerged in 4% paraformaldehyde for 10 minutes, thereby delimiting the viable myocardium in red and area of necrosis (AN) in white. Quantification (planimetry) was performed using the software ImageJ 1.47. Infarct size was expressed as a percentage of the AAR (AN/AAR).

For isolated perfused hearts, infarct size was calculated after TTC staining and expressed as a percentage of the LV (AN/LV).

Analysis of apoptosis

TUNEL staining was carried out on thin slices of heart tissue from AAR fixed in 4% paraformaldehyde, using the DeadEnd™ Fluorimetric TUNEL System (Promega®, Fitchburg, Wisconsin, USA), whilst adhering to manufacturers' instructions. Propidium iodide (red) and fluorescein (green) were used to color total and apoptotic nuclei, respectively. Slides were observed using a confocal fluorescence microscope. Caspase-3 activity was determined using the Caspase 3 Colorimetric Assay Kit (Abcam® plc, Cambridge, UK), thereby adhering to manufacturer's instructions. Absorbance of ρ-nitroaniline was determined via spectrophotometry at 405nm and employed as an indirect indicator of the amount of substrate cleaved by caspase-3.

Western blot analysis

Mitochondrial fission (Drp1, Fis1) and fusion protein (Opa1, Mfn2) expression was assessed at basal condition and after the *in vivo* I/R procedure by western blot analysis as previously described [25]. 40 μg of total proteins was separated by SDS-PAGE and transferred to a nitrocellulose or PVDF membrane. Primary antibody incubation was extended at night at 4°C for Opa1 (BD Transduction Laboratories®; 1/1000), Mfn2 (Sigma-Aldrich®; 1/2000), Fis1 (Santa Cruz®; 1/500), Drp1 (BD Transduction Laboratories®; 1/1000), Bax (Cell Signalling®; 1/1000), SERCA2a, NCX (Abcam; 1/1000), PLB, p-PLBser16 (Badrilla, 1/500, 1/2500) and Bcl-2 (BD Transduction Laboratories®; 1/1000). Membranes were incubated with appropriate secondary antibody conjugated to horseradish peroxidase (Santa Cruz Biotechnology). GAPDH expression was used as a loading control. The blots were developed using the enhanced chemiluminescence method. Semi-quantification of band intensity was performed using the software ImageJ.

Statistical analysis

Statistical analyses were performed using the software SPSS Version 15.0 for Windows (SPSS Inc., Chicago, Illinois, USA). Results were expressed as mean±standard error of the mean (SEM). After testing linear variable distribution, group differences were assessed using ANOVA, followed by Student's *t*-test. A non-parametric Mann-Whitney test was employed when appropriate. A p-value <0.05 was considered statistically significant.

Results

Cardiac structure and function in Opa1$^{+/-}$ mice

We characterized cardiac function by means of echocardiography in 3- and 6-month-old Opa1$^{+/-}$ and WT mice. At 3 months of age, BW, HW, were not significantly different between Opa1$^{+/-}$ (n = 11) and WT (n = 6) mice, as well as left-ventricular size and function (n = 9 per group) (Fig 1A–1D). At 6 months of age, Opa1$^{+/-}$ mice exhibited an alteration of left-ventricular systolic function (FS = 45±1% in Opa1$^{+/-}$ *vs*. 59±1% in WT [n = 10 per group], $p<0.01$), associated with significant dilation of the left ventricle (LVEDD = 3.35±0.13mm in Opa1$^{+/-}$ *vs*. 2.97±0.1mm in WT group, $p<0.05$). As at 3 months, no statistical difference in BW and indexed HW was observed between Opa1$^{+/-}$ and WT groups at 6 months. It is important to note that heart rates recorded at the time of echocardiography did not differ significantly between the groups at the same age (542±17bpm in WT and 548±20bpm in Opa1$^{+/-}$ at 3 months, and 580±15bpm in WT and 545±20bpm in Opa1$^{+/-}$ at 6 months). Systolic blood pressure likewise displayed no significant difference between groups at 3 months (120±2mmHg in WT and 118±1mmHg in Opa1$^{+/-}$) and 6 months (120±1mmHg in WT and 122±2mmHg in Opa1$^{+/-}$; n = 12/group).

Given that we previously reported aberrant structural conformation of myofibrils with large punctuated mitochondria and sarcomere disorganization, with large zones of autophagic and mitophagic materials in 5-month-old Opa1$^{+/-}$ [15], we performed electron microscopy analysis in 3-month-old mice (n = 6/group). No difference was observed in structural conformation, nor the number and area of mitochondria between WT and Opa1$^{+/-}$ mice (Fig 1E and 1F).

Response of Opa1$^{+/-}$ mice to I/R

In order to investigate whether a decreased expression of the fusion protein Opa1 affects I/R sensitivity, the following experiments were performed on 3-month-old mice exhibiting preserved cardiac morphological and functional parameters.

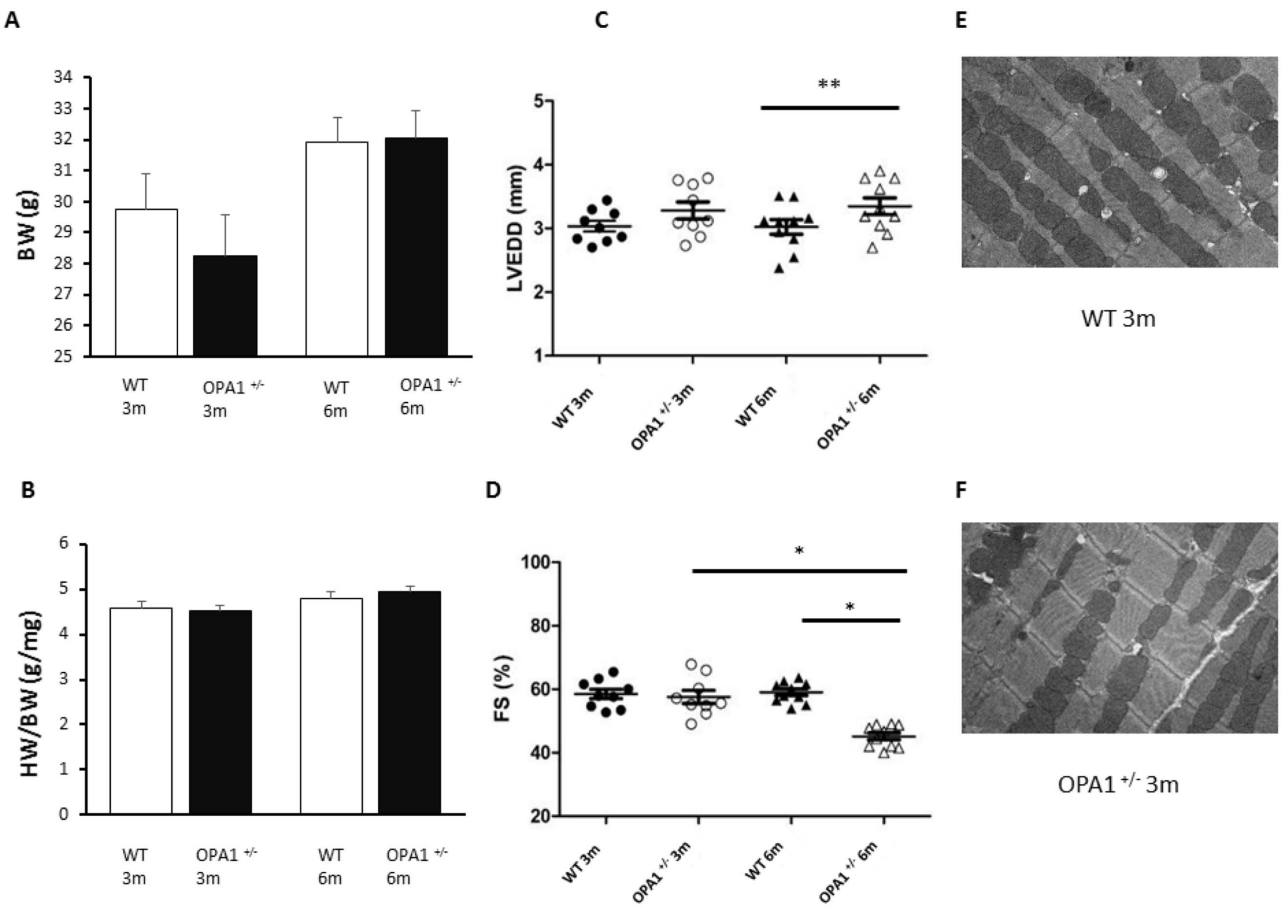

Fig 1. Cardiac morphology and function. BW (**A**) and HW/BW ratio (**B**) in 3- and 6-month-old Opa1$^{+/-}$ (n = 11 and 12 respectively) and WT (n = 6 and 15 respectively) mice. **C, D**: Echocardiography parameters in 3- and 6-month-old mice,(n = 9/group at 3 months and 10/group at 6 months) whereby **C** represents left-ventricular end-diastolic diameter (LVEDD), and **D** depicts fractional shortening (FS). **E, F**: Examples of electron microscopy images at 12,000x magnification in 3-month-old WT (**E**) and Opa$^{+/-}$ (**F**) mice. Values are mean ± SEM. * *p<0.05* and ** *p<0.01*. Non-parametric Mann-Whitney test (HW/BW) and t-test (BW, LVEDD and FS) according to distribution.

doi:10.1371/journal.pone.0164066.g001

First, hearts from 11 WT and 12 Opa1$^{+/-}$ mice were subjected to 30 minutes of *ex vivo* global ischemia and 2 hours of reperfusion. As shown in Fig 2A–2C, infarct size was significantly greater in the Opa1$^{+/-}$ group as compared to the WT group (AN/LV = 71.1±3.2% *vs*. 59.6 ±8.5%, respectively; $p<0.05$). Similarly, Opa1$^{+/-}$ mice displayed significantly greater infarct size than the control group when subjected *in vivo* to coronary artery ligation for 45 min, followed by 2 hours of reperfusion (AN/AAR = 43.2±4.1% in OPA1$^{+/-}$ *vs*. 28.4±3.5% in WT, n = 8/group, $p<0.01$), whilst AAR/LV did not differ between groups (Fig 2D–2F). Thus, decreased Opa1 expression increased susceptibility to myocardial I/R.

Evaluation of mitochondrial physiology

To gain insight into the cellular mechanisms responsible for I/R susceptibility, we assessed mitochondrial parameters. First, we assessed whether decreased Opa1 expression affects the amounts of the other proteins involved in mitochondrial dynamics. Myocardial expression of Opa1, Mfn2 fusion and Drp1, Fis1 fission proteins were assessed in 3-month-old mice. Opa1 expression was significantly lower in Opa1$^{+/-}$ mice ($p<0.01$), whilst expression of Drp1, Fis1, and Mfn2 was similar between the WT (n = 6) and Opa1$^{+/-}$ (n = 6) groups (Fig 3). Similar

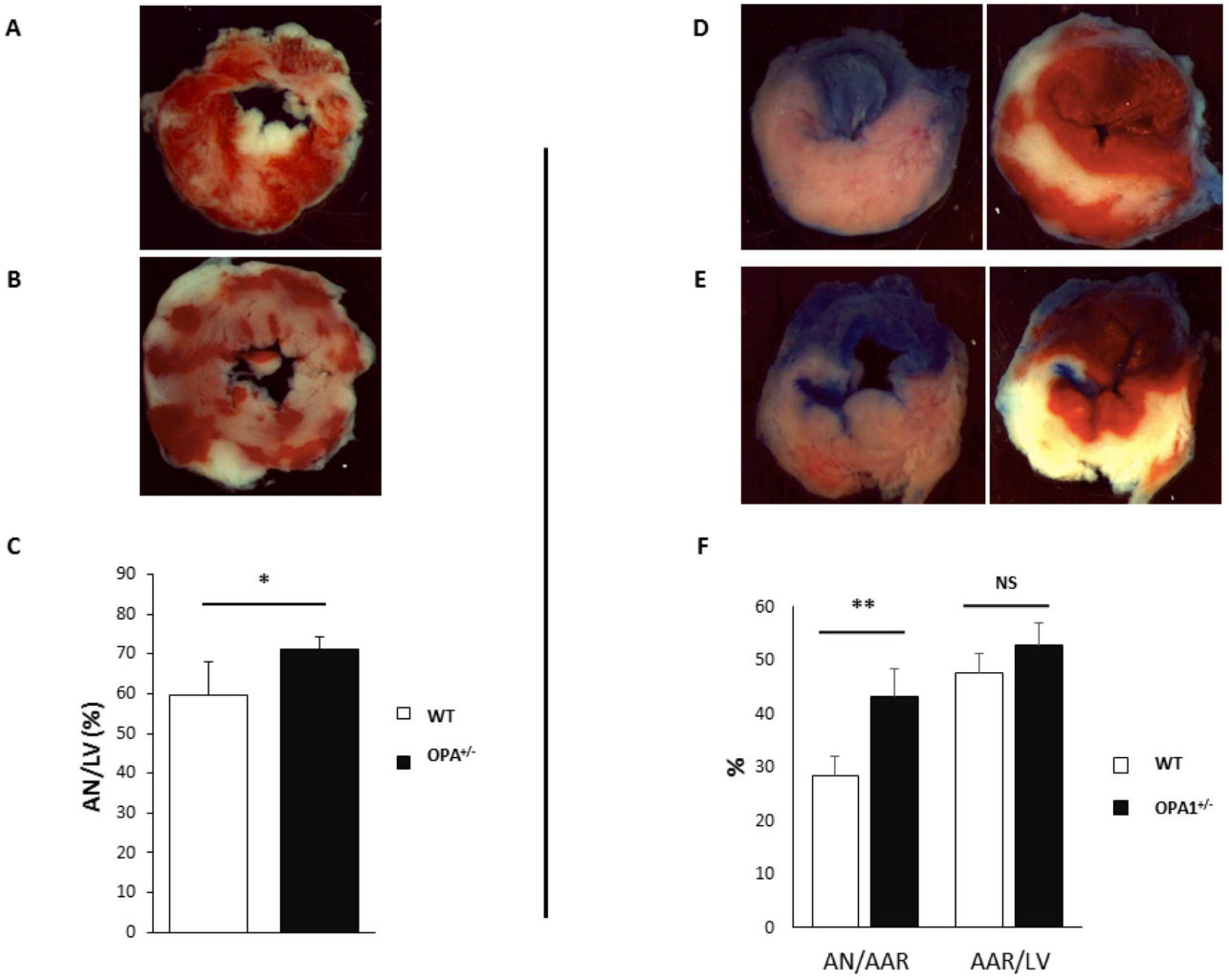

Fig 2. Infarct size. A, B: Examples of left-ventricular sections with TTC staining after 30 minutes of ischemia and 2 hours of reperfusion *ex vivo* in WT (**A**) and Opa1$^{+/-}$ (**B**) mice, and histograms showing AN as a percentage of total LV in WT (n = 11) and OPA1$^{+/-}$ (n = 12) mice (**C**). **D, E**: Examples of left-ventricular sections with TTC-staining after 45 minutes of ischemia and 2 hours of reperfusion *in vivo* in WT (**D**) and OPA1$^{+/-}$ (**E**) mice. On the left side, images before TTC staining showing Evans blue coloration of the perfused myocardium and AAR as the non-blue area. On the right side, images after TTC staining showing AN in white. **F**: Histograms showing AN as a percentage of AAR and AAR as a percentage of total LV area in Opa1$^{+/-}$ and WT mice (n = 8/group). Values are mean ± SEM. * *p<0.05 and* ** *p<0.01*. Non-parametric Mann-Whitney test (AN/AAR) and t-test (AAR/LV).

doi:10.1371/journal.pone.0164066.g002

results were obtained after 45 minutes of ischemia and 2 hours of reperfusion. We further characterized mitochondrial respiration in Opa1$^{+/-}$ and WT mice, by assessing the respirations of complex I, II and IV in baseline conditions and state 3 / state 4 respiration ratio, without evidencing significant difference (n = 6/group). After 45 minutes of ischemia and 2 hours of reperfusion, oxidative phosphorylation was clearly reduced in both groups, with no significant difference between Opa1$^{+/-}$ and WT mice (Fig 4). In addition, we evaluated the parameters related to apoptosis, and found that the expression of the pro-apoptotic Bax after I/R was significantly higher in the *Opa1*$^{+/-}$ group (n = 4) compared to the WT group (n = 6) ($p<0.05$) (Fig 5A–5D), although Bcl-2 expression and Bax/Bcl-2 ratio were not different between groups. Moreover, the number of apoptotic TUNEL-positive nuclei did not differ between Opa1$^{+/-}$ and WT groups (respectively 11.5±3.5%, n = 8 *vs*. 9.1±2.7%, n = 7; p = 0.56) nor the caspase-3 activity (n = 7/group; p = 0.21).

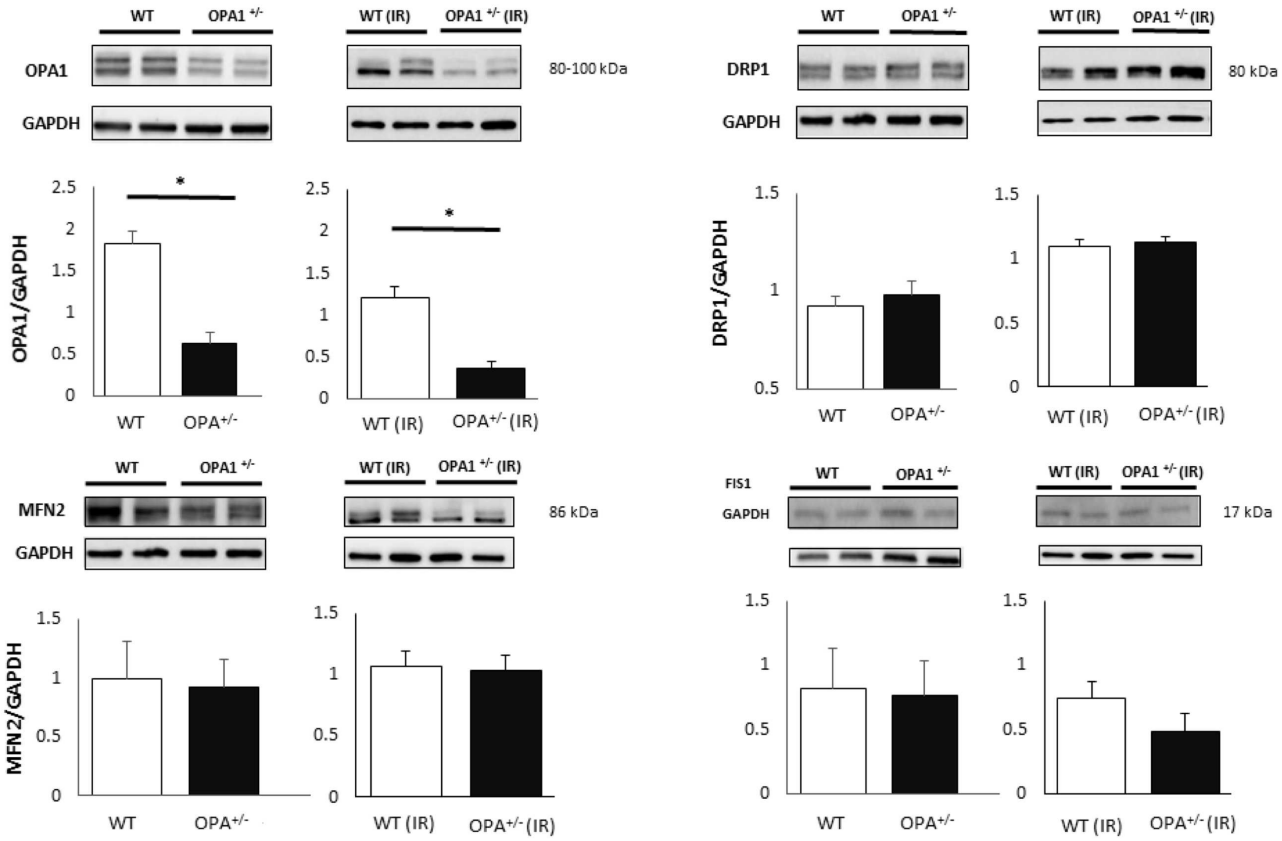

Fig 3. Baseline and post-I/R fission and fusion protein expression. Opa1, Mfn2, Drp1, and Fis1 expression assessed by means of western blotting at baseline (n = 6/group) and after I/R (n = 3-6/group). GAPDH was used as a loading control. Values are mean ± SEM. * p<0.01.

doi:10.1371/journal.pone.0164066.g003

mPTP function

Finally, we assessed the opening of the mPTP. Under baseline conditions, calcium retention capacity was not significantly different in the Opa1$^{+/-}$ group than in the WT group (Fig 5E). Administration of cyclosporine A, a selective mPTP inhibitor, significantly increased calcium retention, but to similar degrees in both groups. After 45 minutes of ischemia and 2 hours of reperfusion, Opa1$^{+/-}$ mice displayed similar calcium retention capacities to WT mice. Moreover, there was no significant difference in baseline and post-I/R calcium retention capacity. When compared to baseline, the post-I/R effect of cyclosporine A adjunction was reduced.

Calcium transients

We subsequently compared calcium transients in isolated cardiomyocytes stimulated at 1Hz. In Opa1$^{+/-}$ left-ventricular cells, the amplitude of calcium transients was significantly lower and exhibited a slower decay time constant compared to WT cardiomyocytes (Fig 6A–6C). This indicates that SR calcium uptake is affected in Opa1$^{+/-}$ cells. Similarly, the extend of caffeine-induced SR calcium release was comparable in WT and Opa1$^{+/-}$ myocytes. That said, the decay time constant, which depends primarily upon sarcolemmal Na^+/Ca^{2+} exchanger (NCX) activity, proved to be much faster in Opa1$^{+/-}$ myocytes (Fig 6D–6F). Overall, these results suggest that, in Opa1$^{+/-}$, SR Ca^{2+} uptake was decreased, whereas cytosolic Ca^{2+} removal due to NCX increased. It is important to note that myocardial expressions of SERCA2a, total and

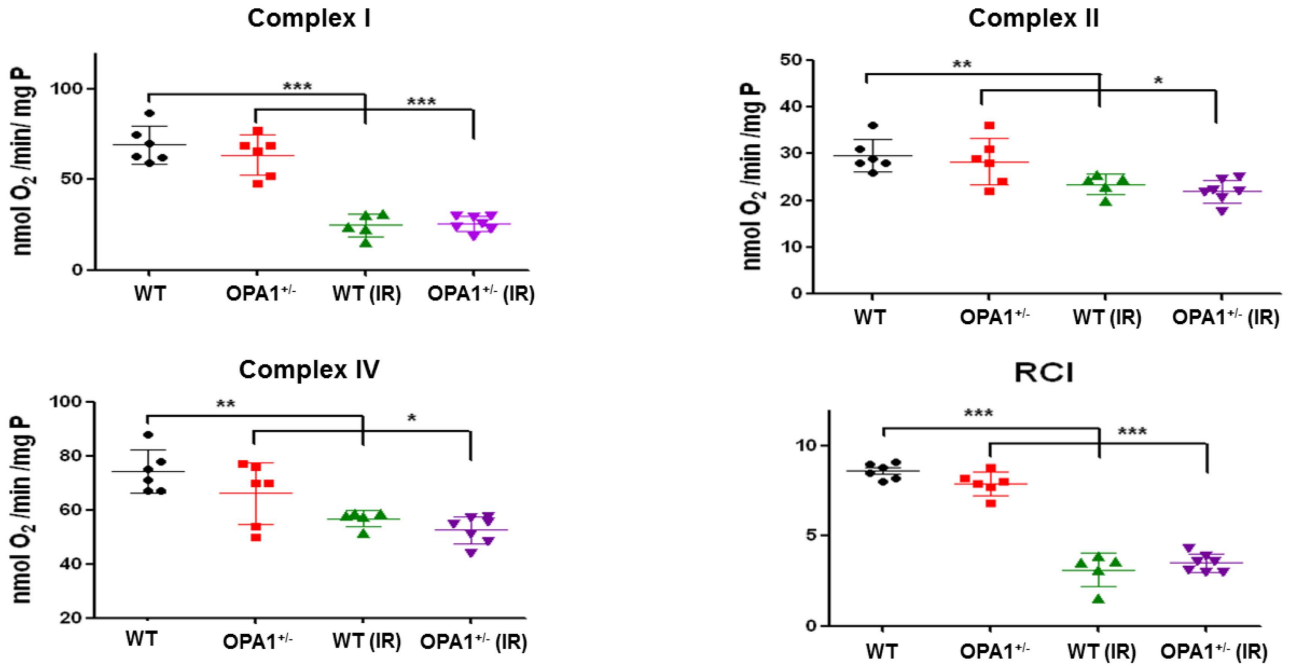

Fig 4. Baseline and post-I/R oxidative phosphorylation. Complex I, II, and IV oxygen consumption were measured in WT and Opa1$^{+/-}$ mouse hearts at baseline and after I/R (n = 6/group). The I/R protocol consisted of 45 minutes of ischemia and 2 hours of reperfusion. The ratio [state 3 rate]: [state 4 rate] is represented by means of the respiratory control index (RCI) in both groups at baseline and after I/R. Values are mean ± SEM. *p<0.05, **p<0.01, ***p<0.001.

doi:10.1371/journal.pone.0164066.g004

phosphorylated phospholamban, and NCX proteins were not significantly different between WT (n = 6) and Opa1$^{+/-}$ (n = 4) groups in 3-month-old mice.

We subsequently determined whether mitochondrial Ca^{2+} movements and AP durations were affected in Opa1$^{+/-}$ ventricular cardiomyocytes. To this end, we simultaneously recorded rhod-2 signals and AP using a whole-cell patch-clamp technique. As shown in Fig 7, and in accordance with increased Ca^{2+} extrusion through NCX, AP durations in Opa1$^{+/-}$ cardiomyocytes were significantly increased during the late phase of repolarization. Furthermore, 50% of Opa1$^{+/-}$ cardiomyocytes were triggered soon after depolarization (6/12 cells), whereas no such arrhythmia was observed in WT cardiomyocytes (Fig 7). On the other hand, mitochondrial Ca^{2+} uptake during steady-state AP was lower and exhibited a slower rate of increase. The mitochondrial Ca^{2+} decay time constant was not significantly affected in Opa1$^{+/-}$ cardiomyocytes compared to the WT group (Fig 8). Altogether, these results indicate that in Opa1$^{+/-}$ cardiomyocytes, mitochondrial Ca^{2+} uptake is impaired, whereas the late repolarization phase of APs is markedly increased with an enhanced arrhythmia triggering.

Discussion

The susceptibility of the myocardium to develop I/R injury is highly related to the mitochondrial functions [26]. Indeed, during ischemia, cardiac mitochondria are subjected to hypoxia, calcium overload, low pH, and ATP depletion. Reperfusion abruptly subjects mitochondria to a rapid pH recovery, oxidative stress, restoration of mitochondrial membrane potential, and calcium overload, all of which inducing mPTP opening [27]. mPTP opening at reperfusion onset is a primary trigger of cardiomyocyte death [28]. Of note, modulation of mitochondrial dynamics may affect susceptibility to I/R injury by preventing mitochondrial dysfunction and

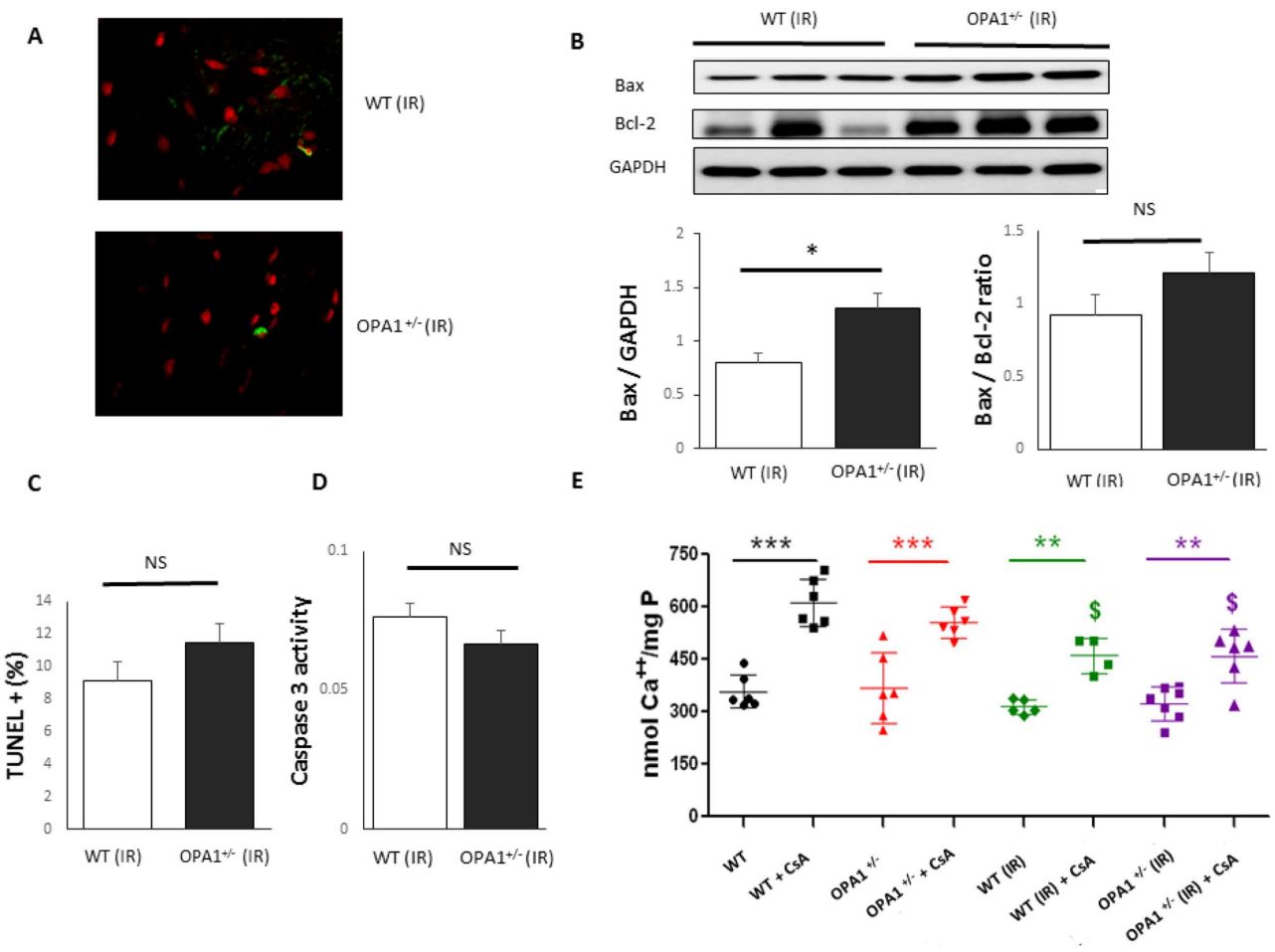

Fig 5. Apoptosis assessment and sensitivity to mPTP. A: Examples of TUNEL images of left-ventricular sections in confocal microscopy (70x magnification) after I/R. Cell nuclei are stained in red (propidium iodide, wavelength = 620 nm). TUNEL-positive nuclei appear in green (fluorescein, wavelength = 460 nm). **B**: Bax and Bcl-2 protein expressions (n = 4-6/group). **C**: Percentage of TUNEL-positive nuclei compared to total nuclei (n = 8 in Opa1$^{+/-}$ and 7 in WT). **D**: Caspase 3 activity amongst Opa1$^{+/-}$ (n = 7) and WT (n = 7) groups. **E**: mPTP opening sensitivity at baseline and after I/R (n = 6/group). Required calcium overload for mPTP opening in WT and Opa1$^{+/-}$ groups at baseline, after I/R, with or without use of cyclosporine analog (CsA). The I/R protocol included 45 minutes of ischemia and 2 hours of reperfusion. Values are mean ± SEM. *p<0.05, **p<0.01, ***p<0.001. $^{\$}p$< 0.05 compared to the same group at baseline + CsA. Non-parametric Mann-Whitney test (TUNEL and Bax/Bcl2 ratio) and t-test (Bax expression and caspase 3 activity).

doi:10.1371/journal.pone.0164066.g005

mPTP inhibition [6]. Whilst excessive fission has been associated with I/R injury and cell death, it was unclear whether loss of the fusion protein Opa1 likewise contributes to the occurrence of I/R injury *in vivo*. Our study demonstrated that Opa1 deficiency is associated with increased sensitivity to I/R in mice exhibiting the Opa1^{delTTAG} mutation, both *ex vivo* and *in vivo*.

Several studies have reported mitochondrial fragmentation in cardiac cells subjected to simulated I/R [6,11,29], a phenomenon associated with a reduction in Opa1 protein expression [11]. However, most of these studies were performed *in vitro*. Ong et al. have shown that suppression of fission and stimulation of fusion by Drp1 downregulation, expression of dominant-negative Drp1, treatment with mdivi-1, or overexpression of Mfn1 or Mfn2 in HL-1 cardiac cell, prevented mPTP opening and reduced cell death after I/R [6].

In order to investigate *in vivo* the role of Opa1 deficiency in cardiac I/R injury, we studied our previously generated knock-in OPA1 mouse model [15]. This model carrying the recurrent

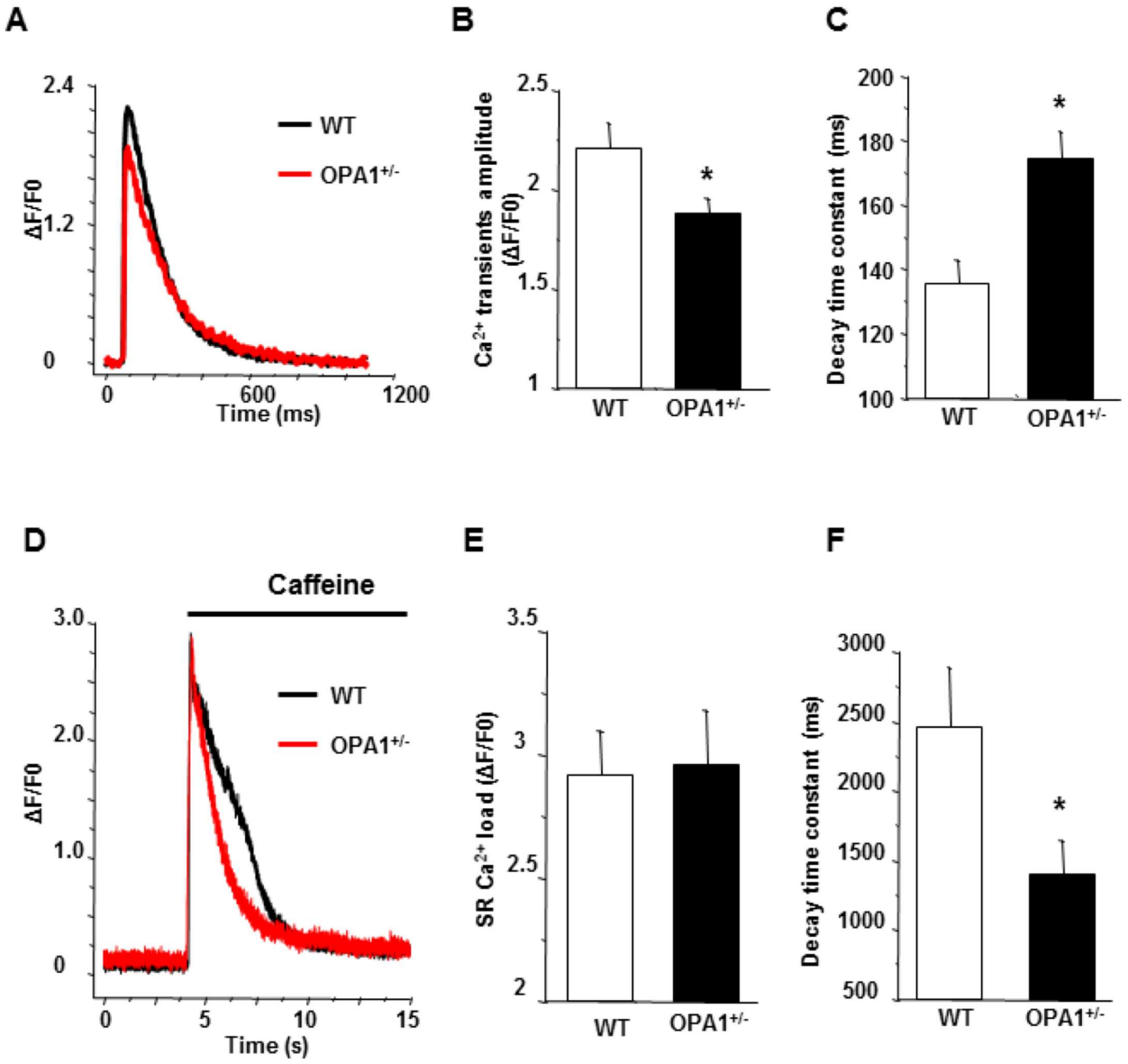

Fig 6. Calcium transients and SR calcium load in Opa1$^{+/-}$ isolated left-ventricular cardiomyocytes. A: Typical calcium transients recorded under field stimulation at 1Hz in WT (black) and Opa1$^{+/-}$ (red) isolated left-ventricular cardiomyocytes using fluo-4 calcium dye. **B**: Mean values of peak calcium transients (WT, n = 32 cells and 4 animals, *vs.* Opa1$^{+/-}$, n = 43 cells and 5 animals; *p<0.05). **C**: Mean values of decay time constant of steady-state Ca^{2+} transients (WT, n = 32 cells and 4 animals, *vs.* Opa1$^{+/-}$, n = 43 cells and 5 animals; *p<0.05). **D**: Typical example of a caffeine-induced SR Ca^{2+} release in WT (black) and Opa1$^{+/-}$ (red) left-ventricular cardiomyocytes using fluo-4 calcium dye. **E**: Mean values of maximum amplitude of caffeine-induced SR Ca^{2+} release, indicative of SR Ca^{2+} load (WT, n = 7 cells and 4 animals, *vs.* Opa1$^{+/-}$, n = 11 cells and 5 animals; p>0.05). **F**: Mean values of decay time constant of caffeine-induced SR Ca^{2+} release, indicative of cytosolic Ca^{2+} extrusion (WT, n = 7 cells and 4 animals, *vs.* Opa1$^{+/-}$, n = 11 cells and 5 animals; *p<0.05). Statistical test was t-test.

doi:10.1371/journal.pone.0164066.g006

Opa1^{delTTAG} heterozygous mutation affected one third of patients exhibiting dominant optic atrophy. The mouse displayed a multi-systemic poly-degenerative phenotype and presented a combination of visual failure, deafness, encephalomyopathy, peripheral neuropathy, ataxia, and cardiomyopathy [15]. Whilst cardiac muscles from these mice displayed aberrant structural conformation of myofibrils with large punctuated mitochondria but normal cristae

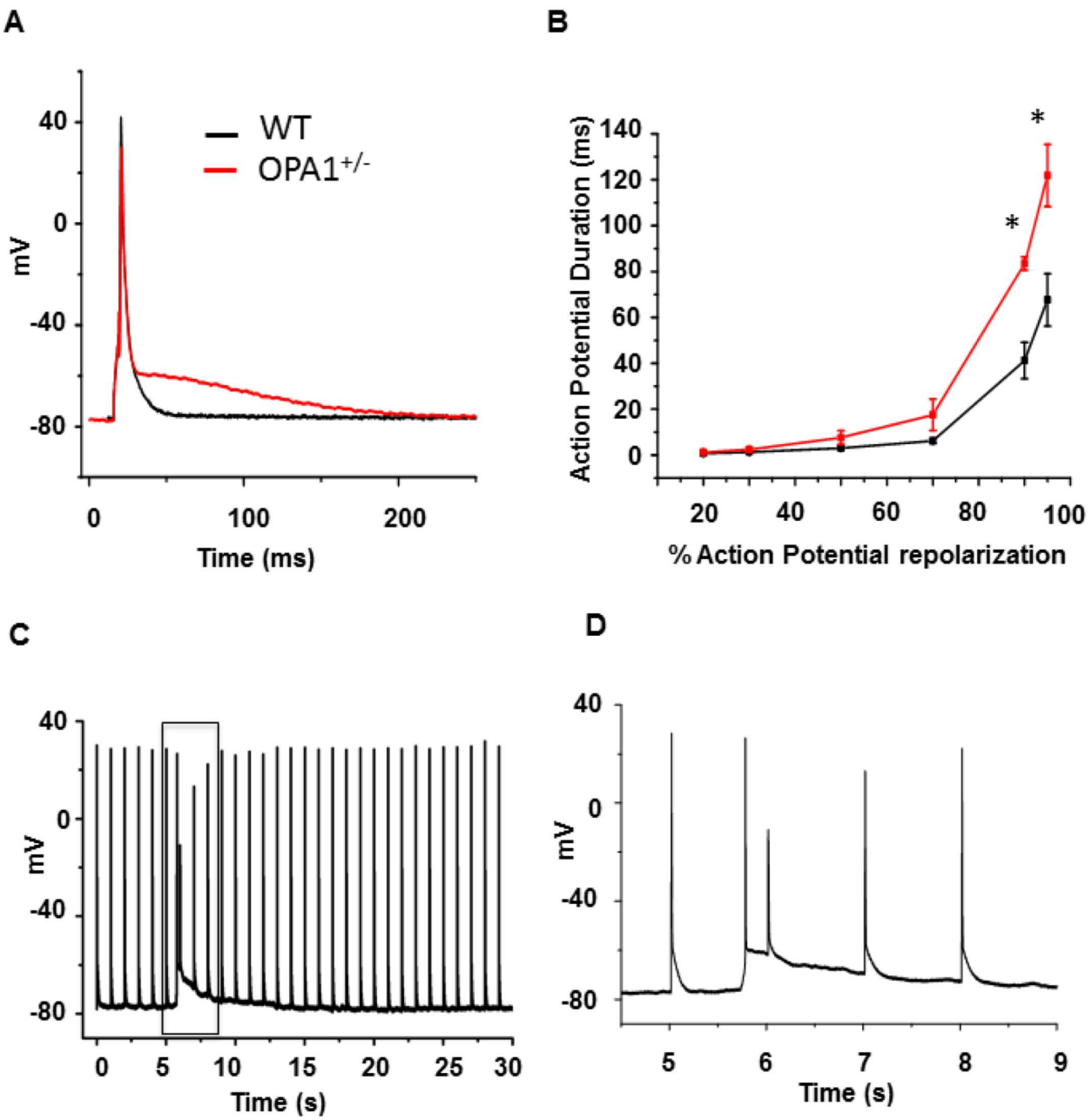

Fig 7. Opa1$^{+/-}$ left-ventricular cardiomyocyte AP. A: Typical AP recorded using whole-cell patch-clamp technique with current clamp at 1Hz in WT (black) and Opa1$^{+/-}$ (red) isolated left-ventricular cardiomyocytes. **B**: Mean values of AP duration at different percentages of AP repolarization (WT: n = 12 cells and 3 animals *vs.* Opa1$^{+/-}$: n = 12 cells and 4 animals; *p<0.05). **C**, **D**: Frame **C** displays 30 seconds of continuous AP recording at a pacing rate of 1Hz early after depolarization, whilst frame **D** shows a magnified view of the early post-depolarization period. Note that 6/12 Opa1$^{+/-}$ cells present such arrhythmic events, whereas WT myocytes underwent no early subsequent depolarization. Statistical test was t-test.

doi:10.1371/journal.pone.0164066.g007

organization and sarcomer disorganization, with large zones of autophagic and mitophagic materials at 5 months [15], we observed no difference with the WT littermates at 3 months of age, indicating age-related onset of cardiomyopathy.

In line with the age-related development of cardiac muscular dysfunction and mitochondrial structure abnormalities in this mouse model, we observed normal cardiac function at 3

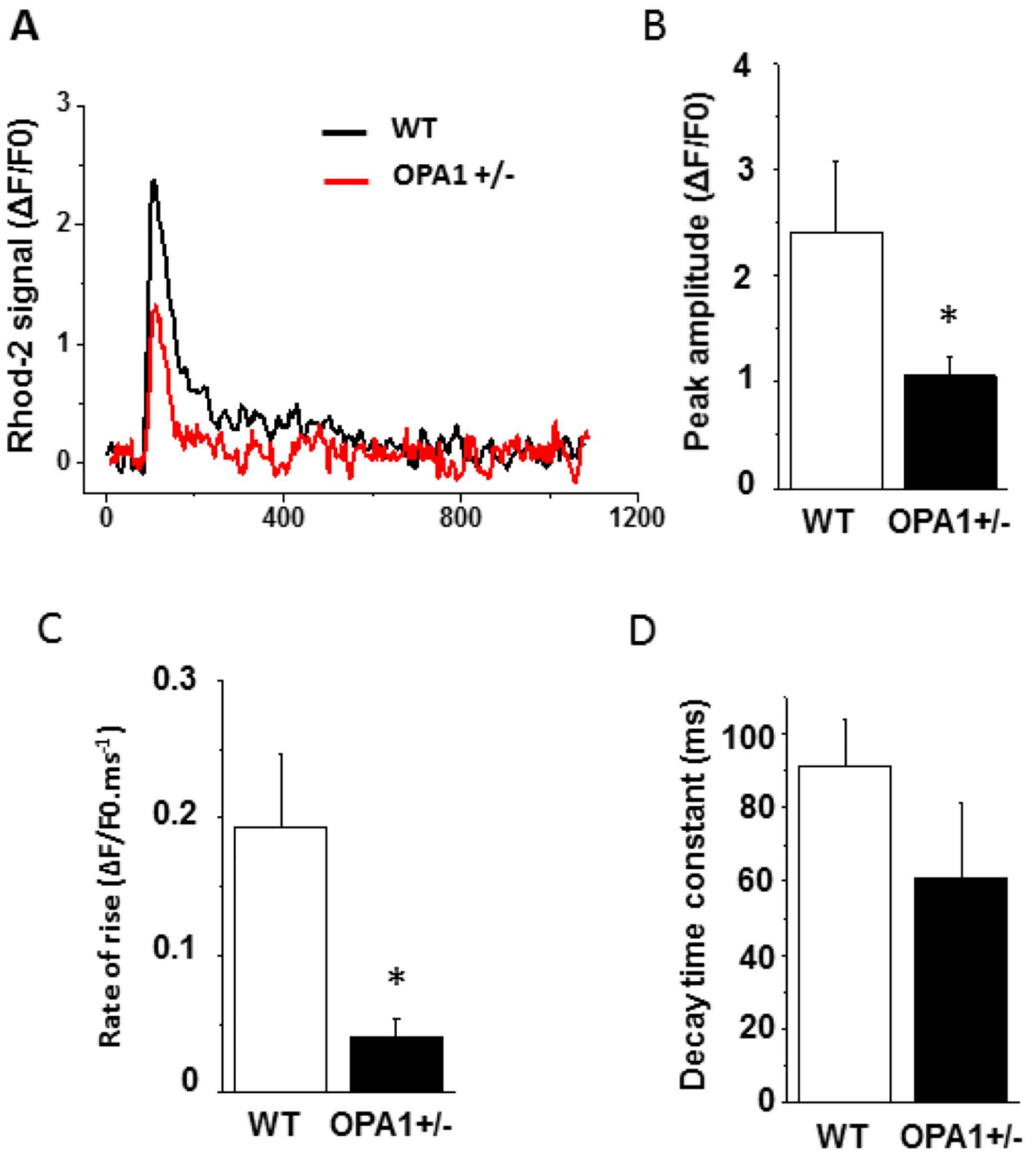

Fig 8. Dynamic mitochondrial Ca^{2+} movements during APs recorded using Rhod-2 in conjunction with a whole-cell patch-clamp technique. A: Typical rhod-2 signal during a steady-state AP recorded at 1Hz in WT (black) and Opa1$^{+/-}$ (red) isolated left-ventricular cardiomyocytes. **B**: Mean values of peak rhod-2 signal. **C**: Rate of rise. **D**: Decay time constant in WT (n = 12 cells and 3 animals) and Opa1$^{+/-}$ cells (n = 12 cells and 4 animals; *p<0.05). Statistical test was t-test.

doi:10.1371/journal.pone.0164066.g008

months and moderate alteration of left-ventricular systolic function at 6 months. In another knock-in Opa1 model, Chen *et al*. reported similar, late-onset, cardiac dysfunction, associated with no significant cardiac functional or gross structural abnormalities at 3 months, but impaired systolic function at 12 months [12]. In our Knowledge, cardiac involvement in patients carrying OPA1 mutation has only been recently reported for the first time in two sisters harboring a homozygous OPA1 mutation leading to lethal encephalopathy and

hypertrophic cardiomyopathy [30]. As we wished to explore the role of Opa1 deficiency prior to the occurrence of cardiac functional impairment, we opted to subject the mice to I/R at 3 months. At this age, Opa1 expression had decreased by 70% in the heart and, importantly, none of the other major fusion/fission proteins (Drp1, Fis1, and Mfn2) were affected.

Similarly to the data observed *in vitro* in other Opa1-deficient models, we recorded greater infarct size in Opa1-deficient mice subjected to I/R *in vivo*. Although acute I/R injury has been linked to mPTP opening at reperfusion onset following a period of ischemia [27], we observed no increased sensitivity to mPTP in Opa1-deficient mice either at baseline or after I/R. Furthermore, mitochondrial respiration was also not impaired in Opa1-deficient mice at baseline, and oxidative phosphorylation was lower both in OPA1-deficient mice and controls after I/R.

Calcium flux constitutes one of the major cellular factors in myocardial I/R injury [31,32]. As stated, Opa1$^{+/-}$ ventricular cardiomyocytes displayed a reduced calcium transient amplitude with a slower decay time constant, whereas the rate of calcium transient increase remained unaffected compared to WT cardiomyocytes [12]. Furthermore, our data suggests enhanced cytosolic Ca^{2+} removal by means of the NCX, characterized by a faster decline of the caffeine-induced Ca^{2+} transients and a drastic increase in the late repolarization phase of the Aps [33,34]. Increased NCX activity is associated with greater occurrence of arrhythmias, such as delayed after depolarization (DADs) and/or early after depolarization (EADs) [35]. The involvement of NCX in DADs is well-established and is related to increased NCX-dependent Ca^{2+} extrusion during diastole, which generates an inward current and the resting membrane potential depolarization, whereas the NCX contribution to EADs genesis is more complex. Increased Ca^{2+} extrusion during the AP repolarization phase slows down AP repolarization, favoring l-type Ca2+ current reactivation and triggering of EADs [36]. Enhanced NCX activity and increased AP were not associated with an increased expression of NCX in Opa1$^{+/-}$ or a shift in SR Ca^{2+} load and SERCA2a^{2+}/PLB, but with a decrease in beat-to-beat mitochondrial Ca^{2+} uptake. Decreased dynamic mitochondrial Ca^{2+} uptake may thus destabilize Ca^{2+} flux equilibrium between SR Ca^{2+} uptake, NCX Ca^{2+} removal, and mitochondria in controlling cytosolic Ca^{2+} homeostasis during Aps [37]. Whilst no definitive explanation prevails as to why Opa1 deficiency is associated with increased susceptibility to cardiac I/R injury, it may be postulated that an imbalance in Ca^{2+} fluxes and the subsequent increase in NCX activity may contribute to the observed reperfusion injury. Indeed, increased NCX Ca^{2+} extrusion may raise steady-state intracellular Na^+ levels during normoxia, which, during ischemia, may combine with the intracellular Na^+ rise mediated by Na^+/K^+ ATPase inhibition and acidosis. Increased ischemic Na^+ levels would thus raise Ca^{2+} influx via NCX reverse mode, thereby increasing cytosolic Ca^{2+} overload during ischemia and subsequent reperfusion injuries [35].

On the other hand, Varanita T *et al*. recently reported genetically mild Opa1 overexpression to be associated with reduced occurrence of cardiac injury in Langendorff-perfused hearts subjected to I/R [38]. It is worth noting that protection from I/R injury was not limited to the heart, as infarct size was likewise smaller in brains subjected to I/R. The commonly accepted conclusion is that fused mitochondria are more tolerant to ischemia and better adapt to factors causing mPTP opening at reperfusion onset. That said, a recent report has been the subject of contention regarding this concept. In a cardiac-specific Drp1 heterozygous knockout mouse, Ikeda *et al*. reported cardiac mitochondrial elongation associated with increased susceptibility to I/R [39]. Drp1 downregulation induced accumulation of damaged mitochondria and impaired mitochondrial autophagy. This data underscores that mitochondrial dynamics is an active process requiring a tight equilibrium between fusion and fission in order to maintain efficient cardiac cell functions, especially in critical situations such as I/R.

Limits

We employed a knock-in *Opa1* mouse model carrying the recurrent Opa^{delTTAG} mutation in order to assess the role of mitochondrial dynamics in the development of I/R injury *in vivo* as well as *ex vivo*. As a consequence of this chronic Opa1 deficiency, several unsuspected compensation mechanisms may have occurred in addition to the increase in NCX activity.

Moreover, we observed no significant increase in apoptosis in Opa1-deficient mice as an underlying cause for their higher infarct size. Due to the dynamic nature of apoptosis, it could be postulated that we overlooked such an increase by assessing apoptosis at single point in time. It is worth noting that Chen *et al*. likewise did not find any marker of increased apoptosis activity in their OPA1-deficient model using TUNEL, histological, Bak1, bcl2, bcl2/1, Bnip3, bk, and bax analysis [12]. Finally, calcium regulation was investigated in normoxic cardiomyocytes. It would be of interest to obtain similar information after hypoxia/reoxygenation.

Conclusion

Opa1 deficiency was associated with an increased sensitivity to I/R in mice with the Opa1^{delTTAG} mutation, both *ex vivo* and *in vivo*. The mechanism seems to be related to an imbalance in dynamic mitochondrial Ca^{2+} uptake and the subsequent increase in NCX activity.

Acknowledgments

The authors would like to thank the "*Service commun d'animalerie hospitalo-universitair e*", the university hospital's Joint Animal Care Department, and the "Service commun d'imagerie et d'analyses microscopiques", the Joint Imaging Department of the University of Angers. Furthermore, we are grateful to Renée Ventura-Clapier for her advice concerning cardiac mitochondrial imaging.

Author Contributions

Conceptualization: DMP FP.

Data curation: SLP.

Formal analysis: SLP MN JF LC ST AG DMP FP.

Funding acquisition: GL FP.

Investigation: SLP MN JF LC ST AG.

Methodology: JF AG DMP FP.

Project administration: FP.

Resources: PR GL FP.

Supervision: DMP FP.

Validation: SLP MN JF LC ST AG AC LL CG RK ES AL MO DH PR GL DMP FP.

Visualization: AC LL CG RK ES AL MO DH PR GL.

Writing – original draft: SLP MN JF FP.

Writing – review & editing: JF LC ST PR GL DMP FP.

References

1. Hall AR, Burke N, Dongworth RK, Hausenloy DJ. Mitochondrial fusion and fission proteins: novel therapeutic targets for combating cardiovascular disease. Br J Pharmacol 2014; 171:1890–1906. doi: 10.1111/bph.12516 PMID: 24328763
2. Youle RJ, van der Bliek AM. Mitochondrial fission, fusion, and stress. Science 2012; 337:1062–1065. doi: 10.1126/science.1219855 PMID: 22936770
3. Alexander C, Votruba M, Pesch UE, Thiselton DL, Mayer S, Moore A et al. OPA1, encoding a dynamin-related GTPase, is mutated in autosomal dominant optic atrophy linked to chromosome 3q28. Nat Genet 2000; 26:211–215. doi: 10.1038/79944 PMID: 11017080
4. Delettre C, Lenaers G, Griffoin JM, Gigarel N, Lorenzo C, Belenguer P et al. Nuclear gene OPA1, encoding a mitochondrial dynamin-related protein, is mutated in dominant optic atrophy. Nat Genet 2000; 26:207–210. doi: 10.1038/79936 PMID: 11017079
5. Chao de la Barca JM, Prunier-Mirebeau D, Amati-Bonneau P, Ferre M, Sarzi E, Bris C, et al. OPA1-related disorders: Diversity of clinical expression, modes of inheritance and pathophysiology. Neurobiol Dis 2016; 90:20–26. doi: 10.1016/j.nbd.2015.08.015 PMID: 26311407
6. Ong SB, Subrayan S, Lim SY, Yellon DM, Davidson SM, Hausenloy DJ. Inhibiting mitochondrial fission protects the heart against ischemia/reperfusion injury. Circulation 2010; 121:2012–2022. doi: 10.1161/CIRCULATIONAHA.109.906610 PMID: 20421521
7. Disatnik MH, Ferreira JC, Campos JC, Gomes KS, Dourado PM, Qi X et al. Acute inhibition of excessive mitochondrial fission after myocardial infarction prevents long-term cardiac dysfunction. J Am Heart Assoc 2013; 2:e000461. doi: 10.1161/JAHA.113.000461 PMID: 24103571
8. Sharp WW, Fang YH, Han M, Zhang HJ, Hong Z, Banathy A et al. Dynamin-related protein 1 (Drp1)-mediated diastolic dysfunction in myocardial ischemia-reperfusion injury: therapeutic benefits of Drp1 inhibition to reduce mitochondrial fission. Faseb j 2014; 28:316–326. doi: 10.1096/fj.12-226225 PMID: 24076965
9. Zepeda R, Kuzmicic J, Parra V, Troncoso R, Pennanen C, Riquelme JA et al. Drp1 loss-of-function reduces cardiomyocyte oxygen dependence protecting the heart from ischemia-reperfusion injury. J Cardiovasc Pharmacol 2014; 63:477–487. doi: 10.1097/FJC.0000000000000071 PMID: 24477044
10. Papanicolaou KN, Khairallah RJ, Ngoh GA, Chikando A, Luptak I, O'Shea KM et al. Mitofusin-2 maintains mitochondrial structure and contributes to stress-induced permeability transition in cardiac myocytes. Mol Cell Biol 2011; 31:1309–1328. doi: 10.1128/MCB.00911-10 PMID: 21245373
11. Chen L, Gong Q, Stice JP, Knowlton AA. Mitochondrial OPA1, apoptosis, and heart failure. Cardiovasc Res 2009; 84:91–99. doi: 10.1093/cvr/cvp181 PMID: 19493956
12. Chen L, Liu T, Tran A, Lu X, Tomilov AA, Davies V et al. OPA1 mutation and late-onset cardiomyopathy: mitochondrial dysfunction and mtDNA instability. J Am Heart Assoc 2012; 1:e003012. doi: 10.1161/JAHA.112.003012 PMID: 23316298
13. Piquereau J, Caffin F, Novotova M, Prola A, Garnier A, Mateo P et al. Down-regulation of OPA1 alters mouse mitochondrial morphology, PTP function, and cardiac adaptation to pressure overload. Cardiovasc Res 2012; 94:408–417. doi: 10.1093/cvr/cvs117 PMID: 22406748
14. Ferre M, Caignard A, Milea D, Leruez S, Cassereau J, Chevrollier A et al. Improved locus-specific database for OPA1 mutations allows inclusion of advanced clinical data. Hum Mutat 2015; 36:20–25. doi: 10.1002/humu.22703 PMID: 25243597
15. Sarzi E, Angebault C, Seveno M, Gueguen N, Chaix B, Bielicki G et al. The human OPA1delTTAG mutation induces premature age-related systemic neurodegeneration in mouse. Brain 2012; 135:3599–3613. doi: 10.1093/brain/aws303 PMID: 23250881
16. Prunier F, Gaertner R, Louedec L, Michel JB, Mercadier JJ, Escoubet B. Doppler echocardiographic estimation of left ventricular end-diastolic pressure after MI in rats. Am J Physiol Heart Circ Physiol 2002; 283:H346–352. doi: 10.1152/ajpheart.01050.2001 PMID: 12063308
17. Fauconnier J, Lanner JT, Zhang SJ, Tavi P, Bruton JD, Katz A et al. Insulin and inositol 1,4,5-trisphosphate trigger abnormal cytosolic Ca2+ transients and reveal mitochondrial Ca2+ handling defects in cardiomyocytes of ob/ob mice. Diabetes 2005; 54:2375–2381. doi: 10.2337/diabetes.54.8.2375 PMID: 16046304
18. Paillard M, Tubbs E, Thiebaut PA, Gomez L, Fauconnier J, Da Silva CC et al. Depressing mitochondria-reticulum interactions protects cardiomyocytes from lethal hypoxia-reoxygenation injury. Circulation 2013; 128:1555–1565. doi: 10.1161/CIRCULATIONAHA.113.001225 PMID: 23983249
19. Dague E, Genet G, Lachaize V, Guilbeau-Frugier C, Fauconnier J, Mias C et al. Atomic force and electron microscopic-based study of sarcolemmal surface of living cardiomyocytes unveils unexpected

mitochondrial shift in heart failure. J Mol Cell Cardiol 2014; 74:162–172. doi: 10.1016/j.yjmcc.2014.05.006 PMID: 24839910

20. Fauconnier J, Bedut S, Le Guennec JY, Babuty D, Richard S. Ca2+ current-mediated regulation of action potential by pacing rate in rat ventricular myocytes. Cardiovasc Res 2003; 57:670–680. doi: 10.1016/S0008-6363(02)00731-9 PMID: 12618229
21. Wilding JR, Joubert F, de Araujo C, Fortin D, Novotova M, Veksler V et al. Altered energy transfer from mitochondria to sarcoplasmic reticulum after cytoarchitectural perturbations in mice hearts. J Physiol 2006; 575:191–200. doi: 10.1113/jphysiol.2006.114116 PMID: 16740607
22. Teixeira G, Chiari P, Fauconnier J, Abrial M, Couture-Lepetit E, Harisseh R et al. Involvement of Cyclophilin D and Calcium in Isoflurane-induced Preconditioning. Anesthesiology 2015; 123:1374–1384. doi: 10.1097/ALN.0000000000000876 PMID: 26460965
23. Gharib A, De Paulis D, Li B, Augeul L, Couture-Lepetit E, Gomez L et al. Opposite and tissue-specific effects of coenzyme Q2 on mPTP opening and ROS production between heart and liver mitochondria: role of complex I. J Mol Cell Cardiol 2012; 52:1091–1095. doi: 10.1016/j.yjmcc.2012.02.005 PMID: 22387164
24. Kalakech H, Tamareille S, Pons S, Godin-Ribuot D, Carmeliet P, Furber A et al Role of hypoxia inducible factor-1alpha in remote limb ischemic preconditioning. J Mol Cell Cardiol 2013; 65:98–104. doi: 10.1016/j.yjmcc.2013.10.001 PMID: 24140799
25. Tamareille S, Mateus V, Ghaboura N, Jeanneteau J, Croue A, Henrion D et al. RISK and SAFE signaling pathway interactions in remote limb ischemic perconditioning in combination with local ischemic postconditioning. Basic Res Cardiol 2011; 106:1329–1339. doi: 10.1007/s00395-011-0210-z PMID: 21833651
26. Heusch G. Molecular basis of cardioprotection: signal transduction in ischemic pre-, post-, and remote conditioning. Circ Res 2015; 116:674–699. doi: 10.1161/CIRCRESAHA.116.305348 PMID: 25677517
27. Gomez L, Li B, Mewton N, Sanchez I, Piot C, Elbaz M et al. Inhibition of mitochondrial permeability transition pore opening: translation to patients. Cardiovasc Res 2009; 83:226–233. doi: 10.1093/cvr/cvp063 PMID: 19221132
28. Heusch G, Boengler K, Schulz R. Inhibition of mitochondrial permeability transition pore opening: the Holy Grail of cardioprotection. Basic Res Cardiol 2010; 105:151–154. doi: 10.1007/s00395-009-0080-9 PMID: 20066536
29. Brady NR, Hamacher-Brady A, Gottlieb RA. Proapoptotic BCL-2 family members and mitochondrial dysfunction during ischemia/reperfusion injury, a study employing cardiac HL-1 cells and GFP biosensors. Biochim Biophys Acta 2006; 1757:667–678. doi: 10.1016/j.bbabio.2006.04.011 PMID: 16730326
30. Spiegel R, Saada A, Flannery PJ, Burte F, Soiferman D, Khayat M et al. Fatal infantile mitochondrial encephalomyopathy, hypertrophic cardiomyopathy and optic atrophy associated with a homozygous OPA1 mutation. J Med Genet 2016; 53:127–131. doi: 10.1136/jmedgenet-2015-103361 PMID: 26561570
31. Fauconnier J, Roberge S, Saint N, Lacampagne A. Type 2 ryanodine receptor: a novel therapeutic target in myocardial ischemia/reperfusion. Pharmacol Ther 2013; 138:323–332. doi: 10.1016/j.pharmthera.2013.01.015 PMID: 23384595
32. Prunier F, Kawase Y, Gianni D, Scapin C, Danik SB, Ellinor PT et al. Prevention of ventricular arrhythmias with sarcoplasmic reticulum Ca2+ ATPase pump overexpression in a porcine model of ischemia reperfusion. Circulation 2008; 118:614–624. doi: 10.1161/CIRCULATIONAHA.108.770883 PMID: 18645052
33. Bogeholz N, Pauls P, Bauer BK, Schulte JS, Dechering DG, Frommeyer G et al. Suppression of Early and Late Afterdepolarizations by Heterozygous Knockout of the Na+/Ca2+ Exchanger in a Murine Model. Circ Arrhythm Electrophysiol 2015; 8:1210–1218. doi: 10.1161/CIRCEP.115.002927 PMID: 26338832
34. Yao A, Su Z, Nonaka A, Zubair I, Lu L, Philipson KD et al. Effects of overexpression of the Na+-Ca2+ exchanger on [Ca2+]i transients in murine ventricular myocytes. Circ Res 1998; 82:657–665. doi: 10.1161/01.RES.82.6.657 PMID: 9546374
35. Pott C, Eckardt L, Goldhaber JI. Triple threat: the Na+/Ca2+ exchanger in the pathophysiology of cardiac arrhythmia, ischemia and heart failure. Curr Drug Targets 2011; 12:737–747. doi: 10.2174/138945011795378559 PMID: 21291388
36. Qu Z, Xie LH, Olcese R, Karagueuzian HS, Chen PS, Garfinkel A et al. Early afterdepolarizations in cardiac myocytes: beyond reduced repolarization reserve. Cardiovasc Res 2013; 99:6–15. doi: 10.1093/cvr/cvt104 PMID: 23619423
37. Bers DM. Calcium fluxes involved in control of cardiac myocyte contraction. Circ Res 2000; 87:275–281. doi: 10.1161/01.RES.87.4.275 PMID: 10948060

38. Varanita T, Soriano ME, Romanello V, Zaglia T, Quintana-Cabrera R, Semenzato M et al. The OPA1-dependent mitochondrial cristae remodeling pathway controls atrophic, apoptotic, and ischemic tissue damage. Cell Metab 2015; 21:834–844. doi: 10.1016/j.cmet.2015.05.007 PMID: 26039448

39. Ikeda Y, Shirakabe A, Maejima Y, Zhai P, Sciarretta S, Toli J et al. Endogenous Drp1 mediates mitochondrial autophagy and protects the heart against energy stress. Circ Res 2015; 116:264–278. doi: 10.1161/CIRCRESAHA.116.303356 PMID: 25332205

2. Tryptophane-Kynurenine pathway in the remote ischemic conditioning mechanism

Basic Research in Cardiology

Tryptophane-kynurenine pathway in the remote ischemic conditioning mechanism

--Manuscript Draft--

Manuscript Number:	BRIC-D-19-00062
Full Title:	Tryptophane-kynurenine pathway in the remote ischemic conditioning mechanism
Article Type:	Original Contribution
Keywords:	remote ischemia reperfusion; myocardial infarction; kynurenine; tryptophan; NAD+
Corresponding Author:	Delphine PRUNIER, MDPHD UMR CNRS 6015 INSERM1083 ANGERS, FRANCE
Corresponding Author Secondary Information:	
Corresponding Author's Institution:	UMR CNRS 6015 INSERM1083
Corresponding Author's Secondary Institution:	
First Author:	Oussama Bakhta
First Author Secondary Information:	
Order of Authors:	Oussama Bakhta
	Adrien Pascaud
	Xavier Dieu
	Justine Beaumont
	Judith Kouassi Nzoughet
	Rima Kamel
	Mikaël Croyal
	Sophie Tamareille
	Gilles Simard
	Juan Manuel Chao de la Barca
	Pascal Reynier
	Fabrice Prunier
	Delphine PRUNIER, MDPHD
Order of Authors Secondary Information:	
Funding Information:	Centre Hospitalier Universitaire d'Angers (FR) (AOI2017) — Not applicable
Abstract:	The actual protective mechanisms underlying cardioprotection with remote ischemic conditioning (RIC) remain unclear. Recent data suggest that RIC induces kynurenine (KYN) and kynurenic acid (KYNA) synthesis, two metabolites derived from tryptophan (TRP), yet a causal relation between TRP pathway and RIC remains to be established. We sought to study the impact of RIC on the levels of TRP and its main metabolites within tissues, and to assess whether blocking kynurenine (KYN) synthesis from TRP would inhibit RIC-induced cardioprotection. In rats exposed to 40-minute coronary occlusion and 2-hour reperfusion, infarct size was significantly smaller in RIC-treated animals (35.7 ± 3.0% vs. 46.5 ± 2.2%, p=0.01). This protection was lost in rats that received 1-methyl-tryptophan (1-MT) pretreatment, an inhibitor of KYN synthesis from TRP. Levels of TRP and 9 compounds spanning its

	metabolism through the serotonin and KYN pathways were measured by reversed-phase liquid-chromatography-tandem mass spectrometry (LC-MS/MS) in the liver, heart, and limb skeletal muscle, either exposed or not to RIC. In the liver, RIC induced a significant increase in xanthurenic acid and nicotinic acid, along with a trend towards TRP and nicotinamide level increases. Likewise, RIC increased NAD-dependent deacetylase sirtuin activity in the liver. Pretreatment with 1-MT suppressed the RIC-induced increases in NAD-dependent deacetylase sirtuin activity. Altogether, these findings indicate that RIC mechanism is dependent on TRP-KYN pathway activation.

To: Gerd Heusch, Editor-in-Chief; Basic Research in Cardiology

Dear Gerd,

I am writing to you to request your consideration of our manuscript entitled **"Tryptophane-kynurenine pathway in the remote ischemic conditioning mechanism**" for publication in Cardiovascular Research.

First described 25 years ago, remote ischemic conditioning (RIC) remains the most promising conditioning approach in acute myocardial infarction (MI). In a recent study, RIC improved cardiac mortality and hospitalization for heart failure in 500 patients with reperfused MI.

While the actual protective mechanisms underlying RIC remain largely unclear, a well-accepted theory holds that both a neural pathway to the remote organ and humoral factors do seem to be involved. Based on intensive research to identify protective humoral factors, it is largely admitted that potential candidates must be small, hydrophobic, lyophilizable, and thermolabile. In this respect, several metabolites prove to be good candidates. We and others have identified kynurenine (KYN) and kynurenic acid (KYNA), two metabolites derived from tryptophan (TRP), as potentially mediators involved in RIC mechanism. However, a causal relation between TRP pathway modulation and RIC remained to be established. Hence, we sought to investigate the RIC's impact on TRP and its main metabolite levels in liver, heart, and blood, and to assess whether a blocking KYN synthesis from TRP would inhibit the RIC-induced cardioprotection.

Using a rat model, we observed that RIC increased several hepatic TRP-derived metabolite levels, along with NAD-dependent deacetylase sirtuin activity in the liver. In addition, the RIC-induced cardioprotective effect was abolished by 1-MT pretreatment that inhibited KYN synthetisis from TRP. Interestingly, 1-MT pretreatment likewise suppressed the increase in NAD-dependent deacetylase sirtuin activity induced by RIC. **Altogether, these findings indicate for the first time that RIC mechanism is dependent on TRP-KYN pathway activation.**

We would like to state that the manuscript, or part of it, has neither been published nor is currently under consideration for publication by any other journal. All authors have read and approved the manuscript, and they have no conflicts of interest to disclose.

Yours sincerely,
Fabrice Prunier, MD, PhD

Tryptophane-kynurenine pathway in the remote ischemic conditioning mechanism

Oussama Bakhta[1]; Adrien Pascaud[1]; Xavier Dieu[1]; Justine Beaumont[1]; Judith Kouassi Nzoughet[1]; Rima Kamel[1]; Mikaël Croyal[2,3]; Sophie Tamareille[1]; Gilles Simard[1]; Juan Manuel Chao de la Barca[1]; Pascal Reynier[1]; Fabrice Prunier[1] and Delphine Mirebeau-Prunier[1]

1 Institut Mitovasc, UMR CNRS 6015 – INSERM U1083, CHU d'Angers, Université d'Angers, France

2 CRNHO, West Human Nutrition Research Center, Nantes, France

3 INRA, UMR 1280 PhAN, Nantes, France.

OB and AP contributed equally to this work as first co-authors.

FP and DM-P contributed equally to this work as last co-authors.

Correspondence to Delphine Mirebeau-Prunier,

Biochimie, CHU d'Angers, 4 rue Larrey 49933 ANGERS Cedex 09, France

Telephone : +33 241 35 62 37

E-mail: deprunier@chu-angers.fr

ORCID 0000-0003-0223-1753

Abstract:

The actual protective mechanisms underlying cardioprotection with remote ischemic conditioning (RIC) remain unclear. Recent data suggest that RIC induces kynurenine (KYN) and kynurenic acid (KYNA) synthesis, two metabolites derived from tryptophan (TRP), yet a causal relation between TRP pathway and RIC remains to be established. We sought to study the impact of RIC on the levels of TRP and its main metabolites within tissues, and to assess whether blocking kynurenine (KYN) synthesis from TRP would inhibit RIC-induced cardioprotection.

In rats exposed to 40-minute coronary occlusion and 2-hour reperfusion, infarct size was significantly smaller in RIC-treated animals (35.7 ± 3.0% *vs*. 46.5 ± 2.2%, p=0.01). This protection was lost in rats that received 1-methyl-tryptophan (1-MT) pretreatment, an inhibitor of KYN synthesis from TRP. Levels of TRP and 9 compounds spanning its metabolism through the serotonin and KYN pathways were measured by reversed-phase liquid-chromatography-tandem mass spectrometry (LC-MS/MS) in the liver, heart, and limb skeletal muscle, either exposed or not to RIC. In the liver, RIC induced a significant increase in xanthurenic acid and nicotinic acid, along with a trend towards TRP and nicotinamide level increases. Likewise, RIC increased NAD-dependent deacetylase sirtuin activity in the liver. Pretreatment with 1-MT suppressed the RIC-induced increases in NAD-dependent deacetylase sirtuin activity. Altogether, these findings indicate that RIC mechanism is dependent on TRP-KYN pathway activation.

Key Words: remote ischemia reperfusion; myocardial infarction; kynurenine; tryptophan; NAD+

INTRODUCTION

Mortality from acute myocardial infarction (MI) has declined due to the increasing number of patients undergoing primary percutaneous coronary intervention, along with the progress made in medical therapy. However, MI remains one of the leading causes of death worldwide. Whilst prompt reperfusion of jeopardized myocardium proves to be the most effective way of limiting infarct size, which is a major determinant of cardiac remodeling and heart failure, reperfusion itself causes lethal myocardial ischemia-reperfusion injury [23]. Several conditioning strategies towards reducing infarct size have been trialed, with none so far transferred to the clinical setting [13]. First described 25 years ago by Przyklenk et al., remote ischemic conditioning (RIC) that consists of applying transient ischemia-reperfusion episodes to a tissue remote from the ischemic myocardium remains the most promising conditioning approach in acute MI [11, 22]. Adjunct cardioprotection by RIC using transient limb ischemia as a stimulus in acute MI patients has been revealed in numerous clinical trials since its first report by Botker et al. in 2010 [5, 10]. More importantly, Gaspar et al. demonstrated that RIC improved clinical outcomes via beneficial effects on cardiac mortality and hospitalization for heart failure in 516 patients with reperfused MI [9].

While the actual protective mechanisms underlying RIC remain largely unclear, a well-accepted theory holds that both a neural pathway to the remote organ and humoral factors do seem to be involved [12, 17, 21]. Based on intensive research to identify protective humoral factors, it is largely admitted that potential candidates must be small, hydrophobic, lyophilizable, and thermolabile [13]. In this respect, several metabolites prove to be good candidates. We [7, 18] and others [19] have identified kynurenine (KYN) and kynurenic acid (KYNA), two metabolites derived from tryptophan (TRP), as potentially mediators involved in RIC mechanism. However, a causal relation between TRP pathway modulation and RIC

remained to be established. Hence, we sought to investigate the RIC's impact on TRP and its main metabolite levels in liver, heart, and blood, and to assess whether a blocking KYN synthesis from TRP would inhibit the RIC-induced cardioprotection.

MATERIAL AND METHODS

Study groups and experimental animal models

Experimental procedures with animals were performed in accordance with the guidelines provided by Directive 2010/63/EU of the European Parliament on the protection of animals used for scientific purposes. This point were approved by the regional ethics committee "Comité d'Ethique en Experimentation Animale des Pays de la Loire" and by the French Ministry of Higher Education and Research (APAFIS # 316, July 23, 2015).
Ischemia reperfusion injury and RIC were performed as previously described [14]. The rats were anesthetized by an intraperitoneal injection of sodium pentobarbital (60 mg/Kg i.p., Ceva Santé Animale, France). Male Wistar rats, 8- to 10-week-old, were divided into four groups (**Fig.1A**). In the first group (MI), rats were subjected to 40 min of myocardial ischemia followed by 2 hours of reperfusion without any further intervention. In the second group, (MI+RIC) rats were subjected to RIC maneuver, consisting of a sequence of four cycles of 5 min of limb ischemia and 5 min of limb reperfusion before 40 min of myocardial ischemia followed by 2 hours of reperfusion. Finally, in the third (MI+1-MT) and fourth group (MI+RIC+1MT), 1-methyl-tryptophan (1-MT, 5mg/L, Sigma-Aldrich Co®, *Missouri, USA*) [19] was added to the drinking water 72 hours prior to MI or RIC+MI procedures, respectively. Of note, 1-MT is an inhibitor of dioxygenase blocking KYN synthesis from TRP [6].

At the end of the 2h-reperfusion period, the rat were euthanized by heart excision. Area at risk (AAR) and area of necrosis (AN) were measured, as previously described [14]. AAR was obtained as a percentage of the entire left ventricle (LV) area; the infarct size was calculated as a percentage of AAR (AN/AAR).

To measure the levels of TRP and its main metabolites within the liver, heart, and limb skeletal muscle exposed to intermittent ischemia, additional rat groups were subjected to RIC with or without 1-MT pretreatment, as described above (**Fig. 1B**). In a control group, the upper right femoral artery was exposed, though not clamped, in order to induce a sham procedure of RIC. Liver, left cardiac ventricle, and then limb skeletal muscle exposed to RIC were collected immediately after ending the RIC conditioning procedure or after a similar duration in the control group, then stored at -80°C until analysis.

Quantification of TRP and its mains metabolites

TRP and its metabolites were assayed in tissue samples by reversed-phase liquid-chromatography-tandem mass spectrometry (LC-MS/MS), as previously described [15]. Briefly, standard solutions were generated by pooling and diluting stock solutions of compounds in an aqueous mixture containing 2.7mM EDTA and 1% formic acid. Tissue samples (50mg) were then homogenized in 200µL of the aqueous mixture containing 2.7mM EDTA and 1% formic acid. Proteins were precipitated by adding 500µL of acetonitrile containing exogenous internal standards to homogenates (50µL) and standard solutions (50µL). After centrifugation (15 000g, 15 min), supernatants were evaporated to dryness under a nitrogen stream. Dried samples were then dissolved in 100µL of the aqueous mixture containing 2.7mM EDTA and 1% formic acid, with 10µL injected into the analytical system. LC-MS/MS analyses were performed on a Xevo® TQD mass spectrometer with an electrospray interface and Acquity H-Class® UPLC™ device (Waters Corporation, Milford, MA, USA). Data acquisition and analyses were performed using MassLynx® and

TargetLynx® software, respectively (Version 4.1, Waters Corporation), as previously described [15].

Quantification of α-ceto-glutarate

The protocol of sample preparation from tissues (muscle, liver, and heart) for extracting metabolites was described elsewhere (Application note 1004-1, Biocrates, http://www.biocrates.com/images/stories/pdf/biocrates_appl.note_1004-1.pdf; in the public domain). In brief, tissue samples (50mg) were homogenized using a Precellys homogenizer (Bertin Technologies, Montigny-le-Bretonneux, France) at +4°C. Then, 10µL of 2-ketoglutaric acid-d6 (10 µg/ml) internal standard were subsequently added to the Precellys tube. Following centrifugation, the supernatant was filtered through 0.22µm spin-filter and evaporated to dryness in a miVac duo concentrator (Genevac Ltd, Ipswich, United Kingdom). The dry extract was reconstituted with 200µL of a 2% aqueous MeOH solution prior to UHPLC–HRMS analysis. Quantification of α-ketoglutaric acid (AKG) was performed on a Dionex Ultimate 3000 UHPLC system (Dionex Sunnyvale, USA) coupled to a Thermo Scientific Q Exactive™ HRMS (Thermo Fisher Scientific, Bremen, Germany), in line with the conditions we recently reported [18].

NAD and NADH quantification

NAD (nicotinamide adenine dinucleotide) and NADH concentrations were measured using the NAD/NADH assay kit (ab65348 Abcam, Cambridge, United Kingdom) with 20mg of liver tissue that was harvested, grinded, homogenized, and filtered under a 10-kDa column (ab933349, Abcam, Cambridge, United Kingdom) according to the manufacturer's instructions.

Protein acetylation analysis

Mitochondria were isolated from rat liver tissue. Briefly, approximately 300mg of liver tissue were harvested, grinded, and homogenized in an extraction buffer containing: saccharose (100mM), KCl (50mM), Tris/HCl (50mM), EGTA (5mM), and BSA (1mg/mL). A cocktail of protease (complete™ Protease Inhibitor Cocktail, Merck) and histone deacetylase inhibitors (nicotinamide 10mM and trichostatin A 1μM) was added. Next, 100μg of mitochondrial protein was separated using SDS-PAGE for the protein acetylation assessment (anti-acetyl lysine primary antibody, Abcam ab80178, Cambridge, United Kingdom). VDAC 1 (Abcam, Cambridge, United Kingdom) was used as a loading control.

Statistics

Statistical analyses were performed using SPSS Version 17.0 (SPSS Inc, Chicago, USA). All values were expressed as mean±standard error of the mean (SEM). One-way analysis of variance (ANOVA) was conducted in order to assess the differences between groups, followed by *post-hoc* Fisher's least significant difference (LSD)-corrected multiple comparison test. When the normal distribution between two variables could not be reasonably assessed, the nonparametric Mann-Whitney test was employed for comparing means for tryptophan metabolite measurements. The significance level was set at $p<0.05$.

RESULTS

RIC reduced infarct size via TRP-KYN pathway

Using a rat MI model, we performed myocardial coronary occlusion and reperfusion preceded either by RIC (MI+RIC group) or not (MI group) (**Fig 2**). The 1-MT pretreatment was

administrated in order to prevent KYN synthesis from TRP (MI+1-MT group and MI+RIC+1-MT group).

While AAR did not significantly differ among the four groups, infarct size was significantly smaller in the MI+RIC group (AN/AAR = 35.7 ± 3.0%), as compared with the MI group (AN/AAR = 46.5 ± 2.2%, p=0.01). This RIC-induced cardioprotection was abolished in animals pretreated with 1-MT (AN/AAR = 46.2 ± 5.0% in MI+RIC+1-MT group vs. MI+RIC group, p=0.04). On the opposite, 1-MT pretreatment did not affect infarct size in rats that were not exposed to RIC (AN/AAR = 45.5 ± 4.0% in MI+1-MT group, p=0.83 vs. MI group).

RIC altered TRP-derived metabolite levels in tissues

Skeletal muscle, liver, and heart samples from RIC and control groups were analyzed using LC-MS/MS for the simultaneous quantification of TRP and 9 compounds spanning its metabolism through the serotonin and kynurenine pathways (KYN, KYNA, xanthurenic acid, anthranilic acid, quinolinic acid, NAD, nicotinamide, and nicotinic acid). The metabolite concentrations in the RIC and control groups have been reported in Table 1. Concerning these metabolites, we have observed a decrease in xanthurenic acid in the heart, along with a decrease in KYN, KYNA, and quinolinic acid in the skeletal muscle exposed to RIC. In the liver, RIC induced a significant increase in xanthurenic acid and nicotinic acid, along with a trend towards TRP and nicotinamide level increases.

Levels of α-ceto-glutarate were not affected by RIC

The quantification of α-keto-glutarate, a co-substrate of KYN transaminase, did not differ between RIC and control groups in skeletal muscle (18.2 ± 5.2nmol/g of tissue vs.13.4 ± 2.9nmol/g of tissue, respectively; p = 0.10), liver (7.0 ± 2.5nmol/g of tissue vs. 5.8 ±

1.4nmol/g of tissue, respectively; p = 0.36), and heart samples (13.8 ± 5.0 nmol/g of tissue vs. 16.0 ± 9.1nmol/g of tissue, respectively; p = 0.60).

RIC altered NAD activity in the liver

Given that TRP-KYN pathway leads to nicotinamide and NAD synthesis, RIC induced a trend towards an increased NAD/NADH ratio in the liver (2.85 ± 1.03 in the RIC group vs. 1.68 ± 0.50 in the control group, p = 0.03) (**Fig 3A**). Furthermore, pretreatment with 1-MT blocked the NAD/NADH increase in RIC+1-MT group (2.04 ± 0.53, p=0.49 versus control group).

Deacetylase sirtuin proteins are known to employ NAD as co-substrate, and we observed lower lysine mitochondrial protein acetylation levels in the RIC group versus control group (**Fig 3B**). This effect was abolished by a 1-MT pretreatment in the RIC+1-MT group, likely indicating RIC-induced lysine protein desacetylation to be dependent of the TRP-KYN pathway.

DISCUSSION

While the protective mechanisms underlying RIC remain largely unclear, involvement of TRP-derived metabolites in the RIC mechanism has recently been suggested by two independent research groups [7, 18, 19]. Nevertheless, the causal relation between TRP pathway modulation and RIC has not yet been established. Using a rat model, we observed that RIC increased several hepatic TRP-derived metabolite levels, along with NAD-dependent deacetylase sirtuin activity in the liver. In addition, the RIC-induced cardioprotective effect was abolished by 1-MT pretreatment that inhibited KYN synthetisis from TRP. Interestingly, 1-MT pretreatment likewise suppressed the increase in NAD-dependent deacetylase sirtuin activity induced by RIC. Altogether, these findings indicate that RIC mechanism is dependent on TRP-KYN pathway activation.

Using a metabolomic approach in rats, we previously reported RIC to be associated with a plasmatic increase in KYN concentrations, a metabolite derived from TRP [7]. The RIC-induced KYN increase was further confirmed using the same rat samples, as well as via another experiment set using different metabolomics techniques [18]. Interestingly, a significant increase in KYN and decrease in TRP concentrations were likewise found after RIC in human plasma [7]. KYN was also shown to be cardioprotective when injected prior to coronary occlusion-reperfusion in rats [7]. However, the protective doses proved to be much higher than those assessed in response to RIC, raising doubts about KYN's causal involvement. By the same time, in a rat model mimicking chronic skeletal muscle hypoxia via oxygen sensor loss, Olenchock et al. reported increased circulating α-keto-glutarate levels, which in turn stimulated the KYNA production in the liver, being necessary and sufficient to mediate cardioprotection in the coronary occlusion-reperfusion setting [19]. Even if this particular study did not assess the RIC effect on KYNA production in the liver, these two distinct studies suggested that RIC might act throughTRP pathway modulation in the liver.

KYN is synthetised from TRP via a limiting stage control by TDO in the liver or IDO in other tissues. Under normal conditions, TDO metabolizes 95% TRP within the liver, being the main determinant of distributing hepatic TRP and KYN to the other tissues. In the liver, KYN is subsequently converted into KYNA, xanthurenic acid, and picolinic acid, leading to NAD synthesis.

In the plasma, 90-95% of TRP are bound to albumin, with only free TRP immediately available to the tissues. Following RIC, plasmatic TRP concentration was decreased in plasma [7], whereas we report here a TRP increase in the liver observed 15 min post-RIC. The mechanism's rapidity is likely compatible with increased free TRP uptake by the liver following TDO activation. Free and total TRP blood levels were shown to decrease by 30% following TDO induction [2]. One may suggests that the TRP increases we observed, in the liver, 15 min after RIC stimulus were related to increased TDO activity by allosteric regulation that does not require protein synthesis [3]. As the liver is the most relevant determinant of KYN distribution to other tissues, TDO activation is likely compatible with the plasmatic KYN increases observed after RIC.

Free TRP proves to be labile, with the equilibration between free and bound TRP rapidly influenced by nutritional, hormonal, and pharmacological agents [1]. The non-esterified fatty acids (NEFA) are physiological molecules able to displace albumin-bound TRP [8]. Hence, increases in NEFA induced by RIC may quickly modify the equilibration between free and albumin-bound TRP [20]. Along this line, NEFA level increases have been described in the myocardial ischemia setting [20]. Increases in free TRP uptake by the liver, along with

changes in the balance between free and albumin-bound TRP secondary to increases in NEFA or other unidentified substances, may all account for the modified TRP pathway in liver.

All the enzymes required to convert KYN into KYNA, xanthurenic acid, picolinic acid, and NAD are available in the liver. We found that in the liver, RIC increased nicotinamide and nicotinic acid levels and a trend towards TRP and nicotinamide, which are precursors of NAD. NAD is the coactivator of sirtuins, which are NAD-dependent deacetylase proteins involved in metabolism regulation [16]. Sirtuins are activated in the event of energy deficits and reduced carbohydrate energy sources, which allows for cellular adaptations designed to improve metabolic efficiency to occur. Following RIC, we have observed an increased NAD/NADH ratio within the liver associated with a decrease in lysine mitochondrial protein acetylation levels, indicating an increased sirtuin activity. All these effects were lost following 1-MT, indicating RIC to be effective by increasing sirtuin activity secondary to TRP-KYN activation in the liver. Interestingly, intravenous NAD administration was found to be cardioprotective in a rat myocardial infarction model [24]. Moreover, local ischemic postconditioning was shown to prevent lethal reperfusion injury through increased SIRT3 activity [4].

Limitations

While our data strongly suggest that RIC mechanism requires TRP-KYN pathway activation, there is no definitive answer yet as to how this pathway is being activated in the liver by a RIC stimulus applied to the limb. Yet, in a mice model of skeletal muscle inactivation of oxygen sensor EGLN1, authors reported that increased levels of α-keto-glutarate stimulated hepatic KYNA production, which in turn exerted cardioprotective effects [19]. Of note is that

the stimulus used in this study differed from the classic RIC stimulus consisting of repeated ischemia-reperfusion sequences applied to the limb.

Furthermore, it is still unknown how TRP-KYN pathway modulation observed in the liver may protect the heart or other organs exposed to ischemia-reperfusion. Even if the liver proves to be the main source of TRP and KYN metabolites, one cannot exclude that RIC modulates TRP-KYN in the heart at a different timing than that we have studied here.

Conclusion

RIC increased several hepatic TRP-derived metabolite levels, as well as NAD-dependent deacetylase sirtuin activity in the liver. Inhibition of KYN synthesis from TRP suppressed the increase in NAD-dependent deacetylase sirtuin activity induced by RIC, and at the same time abolished the RIC-induced cardioprotective effect, indicating that RIC mechanism is dependent on TRP-KYN pathway activation.

Acknowledgments

The authors would like to thank the "*Service commun d'animalerie hospitalo-universitaire*", the university hospital's Joint Animal Care Department, for taking care of the animals.

Funding. Grant from Angers University Hospital..

Conflict of Interest: none declared

REFERENCES

1. Badawy AA (2010) Plasma free tryptophan revisited: what you need to know and do before measuring it. J Psychopharmacol 24:809-815 doi:10.1177/0269881108098965
2. Badawy AA (2017) Tryptophan availability for kynurenine pathway metabolism across the life span: Control mechanisms and focus on aging, exercise, diet and nutritional supplements. Neuropharmacology 112:248-263 doi:10.1016/j.neuropharm.2015.11.015
3. Badawy AA, Evans M (1975) Regulation of rat liver tryptophan pyrrolase by its cofactor haem: Experiments with haematin and 5-aminolaevulinate and comparison with the substrate and hormonal mechanisms. Biochem J 150:511-520
4. Bochaton T, Crola-Da-Silva C, Pillot B, Villedieu C, Ferreras L, Alam MR, Thibault H, Strina M, Gharib A, Ovize M, Baetz D (2015) Inhibition of myocardial reperfusion injury by ischemic postconditioning requires sirtuin 3-mediated deacetylation of cyclophilin D. J Mol Cell Cardiol 84:61-69 doi:10.1016/j.yjmcc.2015.03.017
5. Botker HE, Kharbanda R, Schmidt MR, Bottcher M, Kaltoft AK, Terkelsen CJ, Munk K, Andersen NH, Hansen TM, Trautner S, Lassen JF, Christiansen EH, Krusell LR, Kristensen SD, Thuesen L, Nielsen SS, Rehling M, Sorensen HT, Redington AN, Nielsen TT (2010) Remote ischaemic conditioning before hospital admission, as a complement to angioplasty, and effect on myocardial salvage in patients with acute

myocardial infarction: a randomised trial. Lancet 375:727-734 doi:10.1016/S0140-6736(09)62001-8

6. Cady SG, Sono M (1991) 1-Methyl-DL-tryptophan, beta-(3-benzofuranyl)-DL-alanine (the oxygen analog of tryptophan), and beta-[3-benzo(b)thienyl]-DL-alanine (the sulfur analog of tryptophan) are competitive inhibitors for indoleamine 2,3-dioxygenase. Arch Biochem Biophys 291:326-333
7. Chao de la Barca JM, Bakhta O, Kalakech H, Simard G, Tamareille S, Catros V, Callebert J, Gadras C, Tessier L, Reynier P, Prunier F, Mirebeau-Prunier D (2016) Metabolic Signature of Remote Ischemic Preconditioning Involving a Cocktail of Amino Acids and Biogenic Amines. J Am Heart Assoc 5 doi:10.1161/JAHA.116.003891
8. Curzon G, Friedel J, Knott PJ (1973) The effect of fatty acids on the binding of tryptophan to plasma protein. Nature 242:198-200
9. Gaspar A, Lourenco AP, Pereira MA, Azevedo P, Roncon-Albuquerque R, Jr., Marques J, Leite-Moreira AF (2018) Randomized controlled trial of remote ischaemic conditioning in ST-elevation myocardial infarction as adjuvant to primary angioplasty (RIC-STEMI). Basic Res Cardiol 113:14 doi:10.1007/s00395-018-0672-3
10. Heusch G (2018) 25 years of remote ischemic conditioning: from laboratory curiosity to clinical outcome. Basic Res Cardiol 113:15 doi:10.1007/s00395-018-0673-2
11. Heusch G (2017) Critical Issues for the Translation of Cardioprotection. Circ Res 120:1477-1486 doi:10.1161/CIRCRESAHA.117.310820
12. Heusch G (2015) Molecular basis of cardioprotection: signal transduction in ischemic pre-, post-, and remote conditioning. Circ Res 116:674-699 doi:10.1161/CIRCRESAHA.116.305348

13. Heusch G, Gersh BJ (2017) The pathophysiology of acute myocardial infarction and strategies of protection beyond reperfusion: a continual challenge. Eur Heart J 38:774-784 doi:10.1093/eurheartj/ehw224

14. Hibert P, Prunier-Mirebeau D, Beseme O, Chwastyniak M, Tamareille S, Lamon D, Furber A, Pinet F, Prunier F (2013) Apolipoprotein a-I is a potential mediator of remote ischemic preconditioning. PLoS One 8:e77211 doi:10.1371/journal.pone.0077211

15. Honorio de Melo Martimiano P, de Sa Braga Oliveira A, Ferchaud-Roucher V, Croyal M, Aguesse A, Grit I, Ouguerram K, Lopes de Souza S, Kaeffer B, Bolanos-Jimenez F (2017) Maternal protein restriction during gestation and lactation in the rat results in increased brain levels of kynurenine and kynurenic acid in their adult offspring. J Neurochem 140:68-81 doi:10.1111/jnc.13874

16. Katsyuba E, Auwerx J (2017) Modulating NAD(+) metabolism, from bench to bedside. EMBO J 36:2670-2683 doi:10.15252/embj.201797135

17. Kleinbongard P, Skyschally A, Heusch G (2017) Cardioprotection by remote ischemic conditioning and its signal transduction. Pflugers Arch 469:159-181 doi:10.1007/s00424-016-1922-6

18. Kouassi Nzoughet J, Bocca C, Simard G, Prunier-Mirebeau D, Chao de la Barca JM, Bonneau D, Procaccio V, Prunier F, Lenaers G, Reynier P (2017) A Nontargeted UHPLC-HRMS Metabolomics Pipeline for Metabolite Identification: Application to Cardiac Remote Ischemic Preconditioning. Anal Chem 89:2138-2146 doi:10.1021/acs.analchem.6b04912

19. Olenchock BA, Moslehi J, Baik AH, Davidson SM, Williams J, Gibson WJ, Chakraborty AA, Pierce KA, Miller CM, Hanse EA, Kelekar A, Sullivan LB, Wagers AJ, Clish CB, Vander Heiden MG, Kaelin WG, Jr. (2016) EGLN1 Inhibition and

Rerouting of alpha-Ketoglutarate Suffice for Remote Ischemic Protection. Cell 164:884-895 doi:10.1016/j.cell.2016.02.006

20. Oliver MF (2015) Fatty acids and the risk of death during acute myocardial ischaemia. Clin Sci (Lond) 128:349-355 doi:10.1042/CS20140404

21. Pickard JM, Botker HE, Crimi G, Davidson B, Davidson SM, Dutka D, Ferdinandy P, Ganske R, Garcia-Dorado D, Giricz Z, Gourine AV, Heusch G, Kharbanda R, Kleinbongard P, MacAllister R, McIntyre C, Meybohm P, Prunier F, Redington A, Robertson NJ, Suleiman MS, Vanezis A, Walsh S, Yellon DM, Hausenloy DJ (2015) Remote ischemic conditioning: from experimental observation to clinical application: report from the 8th Biennial Hatter Cardiovascular Institute Workshop. Basic Res Cardiol 110:453 doi:10.1007/s00395-014-0453-6

22. Przyklenk K, Bauer B, Ovize M, Kloner RA, Whittaker P (1993) Regional ischemic 'preconditioning' protects remote virgin myocardium from subsequent sustained coronary occlusion. Circulation 87:893-899

23. Yellon DM, Hausenloy DJ (2007) Myocardial reperfusion injury. N Engl J Med 357:1121-1135 doi:10.1056/NEJMra071667

24. Zhang Y, Wang B, Fu X, Guan S, Han W, Zhang J, Gan Q, Fang W, Ying W, Qu X (2016) Exogenous NAD(+) administration significantly protects against myocardial ischemia/reperfusion injury in rat model. Am J Transl Res 8:3342-3350

Figure legends

Figure 1. Experimental protocol in a rat model. **A** Effect RIC and/or 1MT on I/R injury. Each group underwent 40 minutes of myocardial ischemia (MI) followed by 120 minutes of reperfusion. **B** Effect on TRP pathway of RIC or RIC and 1MT, muscle, heart, and liver. The RIC procedure consisted in four cycles of 5 minutes limb-ischemia followed by four cycles of 5 minutes of reperfusion prior to MI. The 1MT was given per os, during the 72 hours prior to the procedure

Figure 2. Effect of RIC and 1MT on infarct size. Infarct size corresponds to the area of necrosis (AN) as a percentage of area at risk (AAR) *p<0,05

Figure 3. Study of NAD/NADH ratio in the liver (A) and representative immunoblot of liver mitochondrial protein acetylation and VDAC 1, (B) in control, RIC or RIC+1MT.*P <0 .05

Figure 1

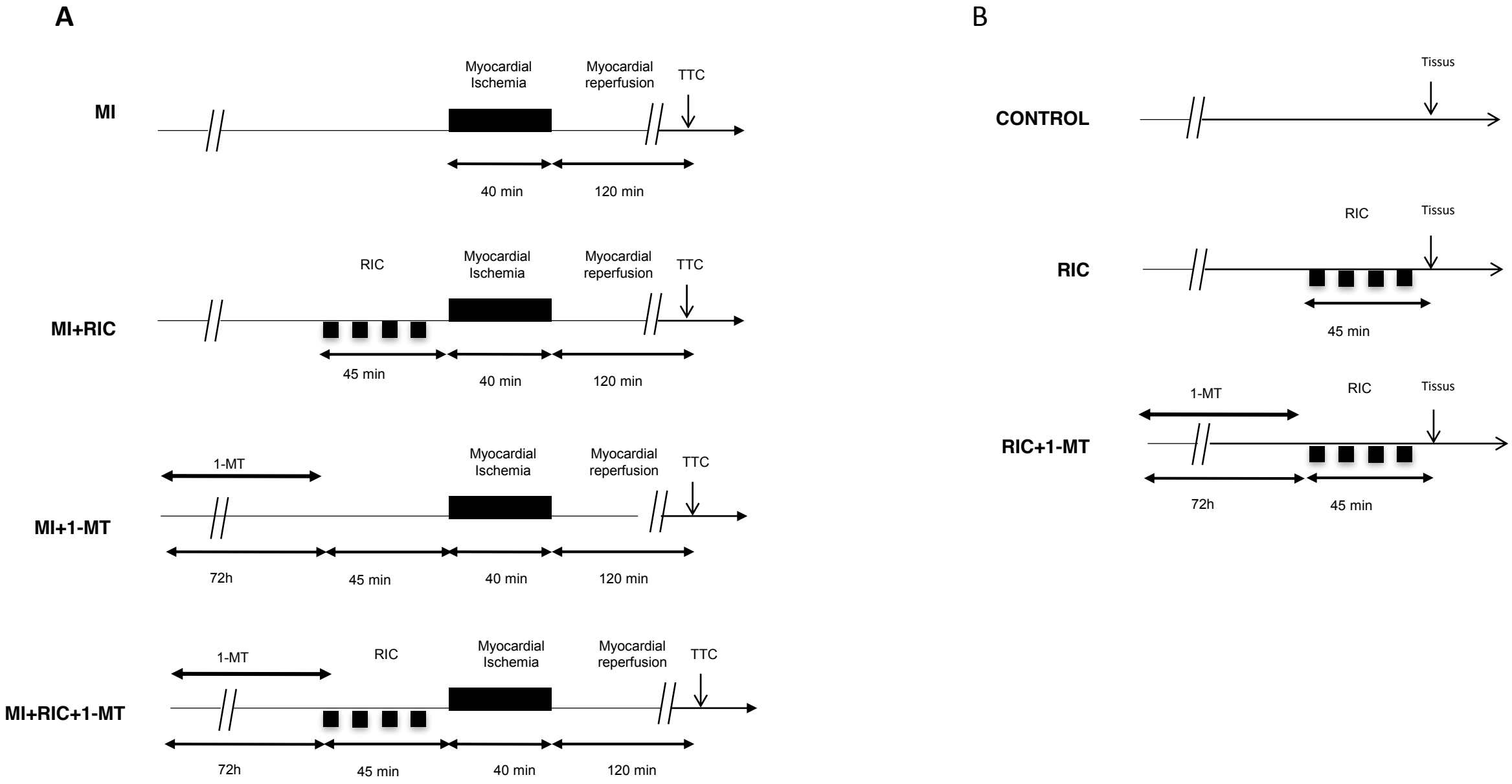
A
MI
Myocardial Ischemia
Myocardial reperfusion
TTC
40 min
120 min
MI+RIC
RIC
45 min
MI+1-MT
1-MT
72h
MI+RIC+1-MT
B
CONTROL
Tissus
RIC
RIC+1-MT

Figure 2

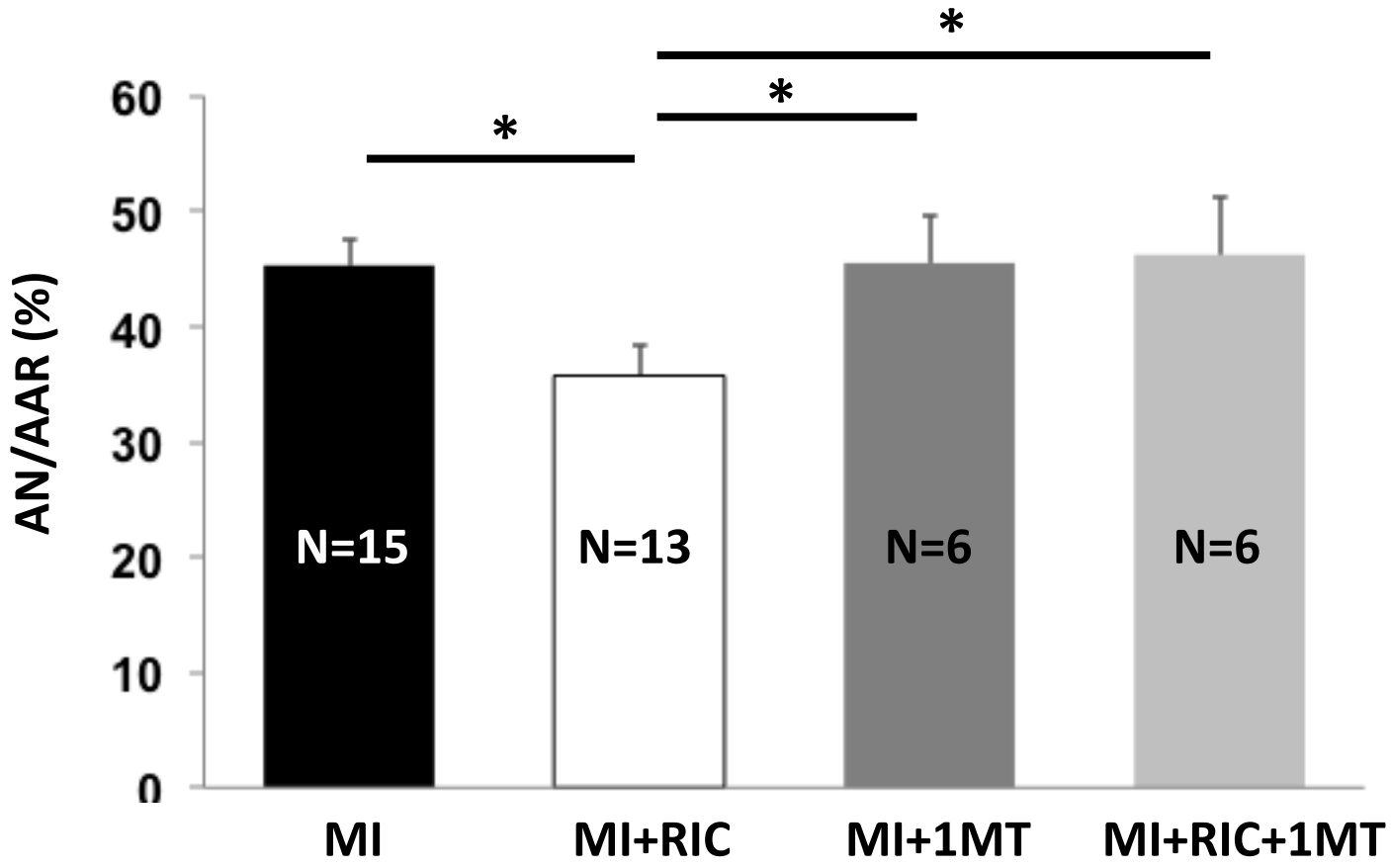

Figure 3

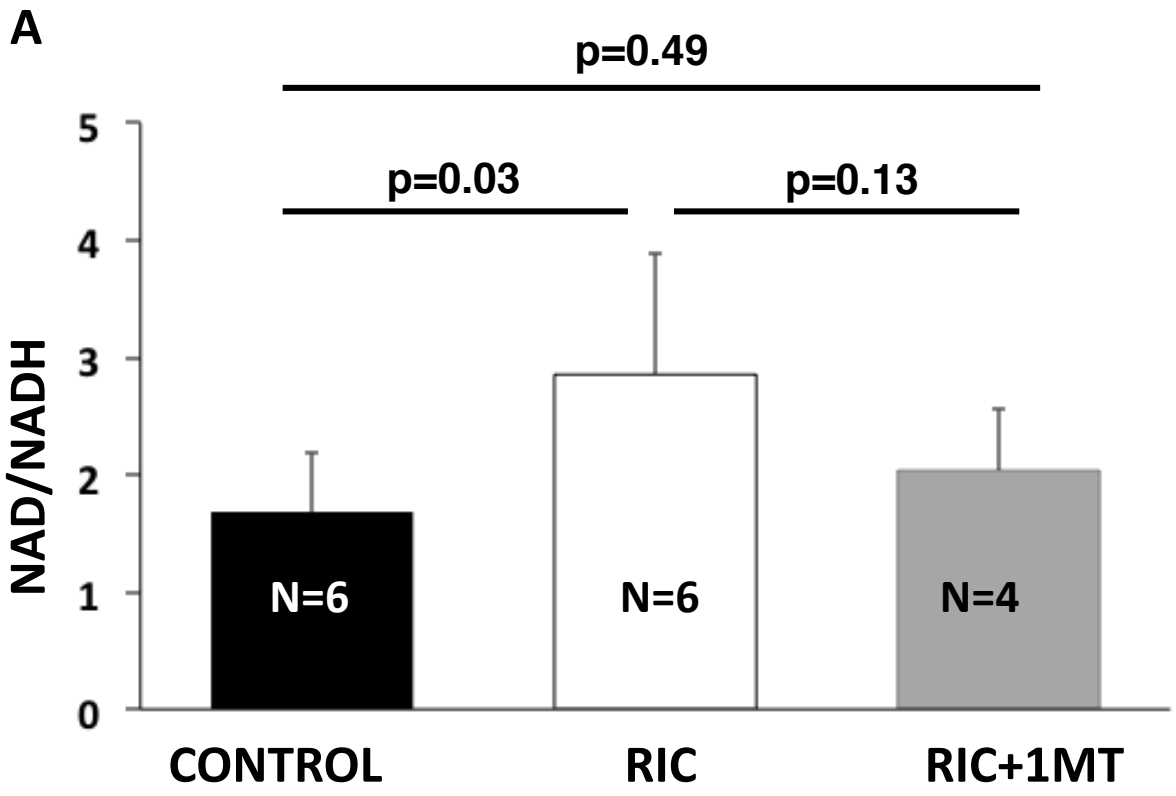
A
p=0.49
p=0.03
p=0.13
NAD/NADH
5
4
3
2
1
0
N=6
N=6
N=4
CONTROL
RIC
RIC+1MT

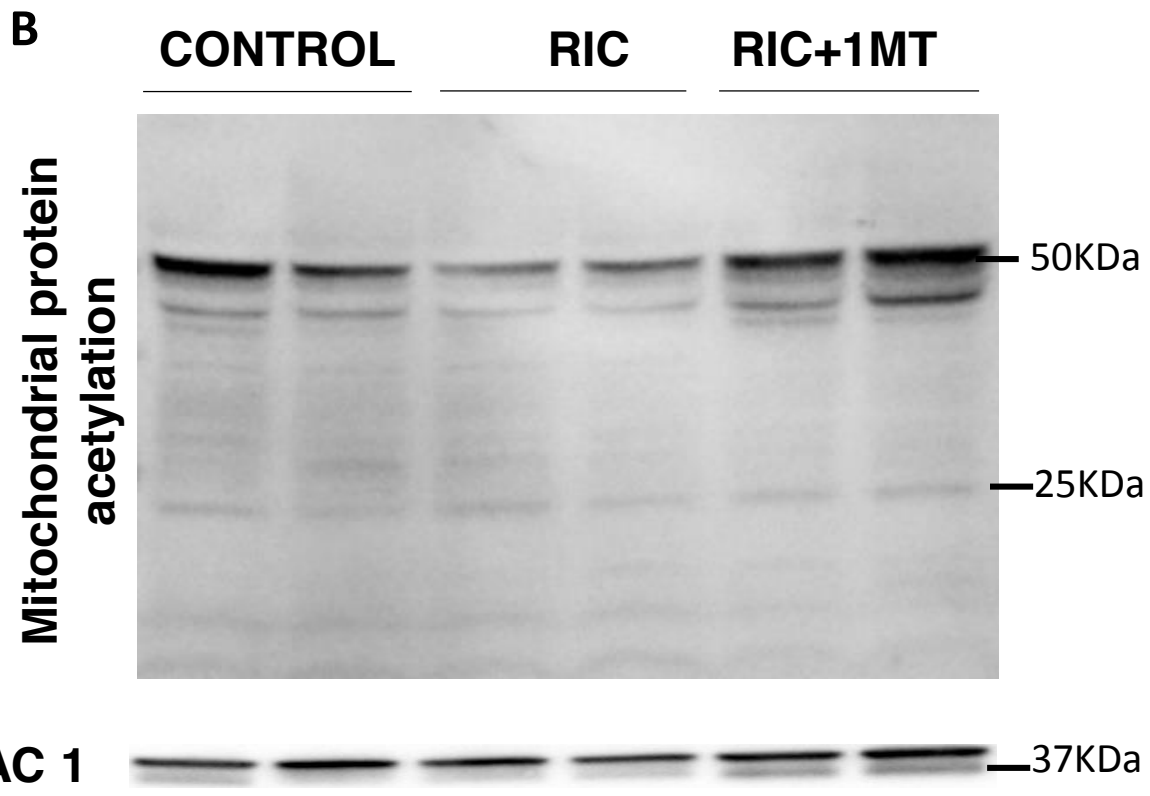
B
CONTROL
RIC
RIC+1MT
Mitochondrial protein acetylation
50KDa
25KDa
VDAC 1
37KDa

Table 1

	Muscle			Liver			Heart		
	RIC	Control	p	RIC	Control	p	RIC	Control	p
Tryptophan	0.301±0.021	0.362±0.033	0.142	2.928±0.138	2.332±0.189	0.035	0.455±0.015	0.494±0.021	0.180
Serotonin	0.023±0.004	0.022±0.004	0.950	ND	ND	ND	ND	ND	ND
Kynurenine	0.036±0.003	0.051±0.005	0.035	0.037±0.002	0.037±0.004	0.277	0.041±0.003	0.047±0.003	0.110
Kynurenic acid	$7\ 10^{e-4}\pm10^{e-4}$	$10\ 10^{e-4}\pm10^{e-4}$	0.046	$12\ 10^{e-4}\pm8\ 10^{e-4}$	$11\ 10^{e-4}\pm10^{e-4}$	0.225	ND	ND	ND
Xanthurenic acid	$12\ 10^{e-4}\pm10^{e-4}$	$14\ 10^{e-4}\pm10^{e-4}$	0.482	0.012±0.001	0.009±0.001	0.048	$14\ 10^{e-4}\pm10^{e-4}$	$19\ 10^{e-4}\pm10^{e-4}$	0.006
Anthranilic acid	ND	ND	ND	$43\ 10^{e-4}\pm4\ 10^{e-4}$	$36\ 10^{e-4}\pm3\ 10^{e-4}$	0.142	ND	ND	ND
Quinolinic acid	0.062±0.006	0.078±0.006	0.048	1.261±0.098	1.363±0.135	0.749	0.098±0.006	0.085±0.005	0.180
NAD	0.015±0.002	0.016±0.003	0.949	0.020±0.002	0.025±0.006	0.655	0.013±0.001	0.015±0.001	0.482
Nicotinamide	1.395±0.208	1.441±0.294	0.749	3.589±0.252	2.969±0.237	0.085	3.108±0.207	3.157±0.178	0.848
Nicotinic acid	0.018±0.003	0.020±0.004	0.949	0.062±0.003	0.050±0.004	0.035	0.024±0.002	0.030±0.004	0.338

Table 1: Effect of ischemic remote conditioning on tryptophan pathway in tissues of rats. Rats were subjected to remote ischemic conditioning by using a vascular clamp placed on the upper right femoral artery in order to induce 4 cycles of 5-min limb ischemia interspersed by 5-min limb reperfusion. RIC group was compared to control group where the upper right femoral artery was exposed but not clamped. Data are expressed by mean±SEM. N=5-7 for each group

References

Abdallah, Y., A. Gkatzoflia, D. Gligorievski, S. Kasseckert, G. Euler, K. D. Schluter, M. Schafer, H. M. Piper, and C. Schafer. 2006. 'Insulin protects cardiomyocytes against reoxygenation-induced hypercontracture by a survival pathway targeting SR Ca2+ storage', *Cardiovasc Res*, 70: 346-53.

Abdallah, Y., S. A. Kasseckert, W. Iraqi, M. Said, T. Shahzad, A. Erdogan, C. Neuhof, D. Gunduz, K. D. Schluter, H. Tillmanns, H. M. Piper, H. P. Reusch, and Y. Ladilov. 2011. 'Interplay between Ca2+ cycling and mitochondrial permeability transition pores promotes reperfusion-induced injury of cardiac myocytes', *J Cell Mol Med*, 15: 2478-85.

Adaniya, S. M., O. Uchi J, M. W. Cypress, Y. Kusakari, and B. S. Jhun. 2019. 'Posttranslational modifications of mitochondrial fission and fusion proteins in cardiac physiology and pathophysiology', *Am J Physiol Cell Physiol*, 316: C583-C604.

Agudelo, L. Z., T. Femenia, F. Orhan, M. Porsmyr-Palmertz, M. Goiny, V. Martinez-Redondo, J. C. Correia, M. Izadi, M. Bhat, I. Schuppe-Koistinen, A. T. Pettersson, D. M. S. Ferreira, A. Krook, R. Barres, J. R. Zierath, S. Erhardt, M. Lindskog, and J. L. Ruas. 2014. 'Skeletal muscle PGC-1alpha1 modulates kynurenine metabolism and mediates resilience to stress-induced depression', *Cell*, 159: 33-45.

Agudelo, L. Z., D. M. S. Ferreira, I. Cervenka, G. Bryzgalova, S. Dadvar, P. R. Jannig, A. T. Pettersson-Klein, T. Lakshmikanth, E. G. Sustarsic, M. Porsmyr-Palmertz, J. C. Correia, M. Izadi, V. Martinez-Redondo, P. M. Ueland, O. Midttun, Z. Gerhart-Hines, P. Brodin, T. Pereira, P. O. Berggren, and J. L. Ruas. 2018. 'Kynurenic Acid and Gpr35 Regulate Adipose Tissue Energy Homeostasis and Inflammation', *Cell Metab*, 27: 378-92 e5.

Alavi, M. V., S. Bette, S. Schimpf, F. Schuettauf, U. Schraermeyer, H. F. Wehrl, L. Ruttiger, S. C. Beck, F. Tonagel, B. J. Pichler, M. Knipper, T. Peters, J. Laufs, and B. Wissinger. 2007. 'A splice site mutation in the murine Opa1 gene features pathology of autosomal dominant optic atrophy', *Brain*, 130: 1029-42.

Ambrosio, G., J. L. Zweier, C. Duilio, P. Kuppusamy, G. Santoro, P. P. Elia, I. Tritto, P. Cirillo, M. Condorelli, M. Chiariello, and et al. 1993. 'Evidence that mitochondrial respiration is a source of potentially toxic oxygen free radicals in intact rabbit hearts subjected to ischemia and reflow', *J Biol Chem*, 268: 18532-41.

Anderson, G., and M. Maes. 2017. 'Interactions of Tryptophan and Its Catabolites With Melatonin and the Alpha 7 Nicotinic Receptor in Central Nervous System and Psychiatric Disorders: Role of the Aryl Hydrocarbon Receptor and Direct Mitochondria Regulation', *Int J Tryptophan Res*, 10: 1178646917691738.

Andine, P., A. Lehmann, K. Ellren, E. Wennberg, I. Kjellmer, T. Nielsen, and H. Hagberg. 1988. 'The excitatory amino acid antagonist kynurenic acid administered after hypoxic-ischemia in neonatal rats offers neuroprotection', *Neurosci Lett*, 90: 208-12.

Anzell, A. R., R. Maizy, K. Przyklenk, and T. H. Sanderson. 2018. 'Mitochondrial Quality Control and Disease: Insights into Ischemia-Reperfusion Injury', *Mol Neurobiol*, 55: 2547-64.

Asp, L., A. S. Johansson, A. Mann, B. Owe-Larsson, E. M. Urbanska, T. Kocki, M. Kegel, G. Engberg, G. B. Lundkvist, and H. Karlsson. 2011. 'Effects of pro-inflammatory cytokines on expression of kynurenine pathway enzymes in human dermal fibroblasts', *J Inflamm (Lond)*, 8: 25.

Avkiran, M., and M. S. Marber. 2002. 'Na(+)/H(+) exchange inhibitors for cardioprotective therapy: progress, problems and prospects', *J Am Coll Cardiol*, 39: 747-53.

Badawy, A. A. 2017. 'Kynurenine Pathway of Tryptophan Metabolism: Regulatory and Functional Aspects', *Int J Tryptophan Res*, 10: 1178646917691938.

Baglole, C. J., S. B. Maggirwar, T. A. Gasiewicz, T. H. Thatcher, R. P. Phipps, and P. J. Sime. 2008. 'The aryl hydrocarbon receptor attenuates tobacco smoke-induced cyclooxygenase-2 and prostaglandin production in lung fibroblasts through regulation of the NF-kappaB family member RelB', *J Biol Chem*, 283: 28944-57.

Balamurugan, A., M. Phillips, J. P. Selig, H. Felix, and K. Ryan. 2018. 'Association Between System Factors and Acute Myocardial Infarction Mortality', *South Med J*, 111: 556-64.

Baran, H., G. Amann, B. Lubec, and G. Lubec. 1997. 'Kynurenic acid and kynurenine aminotransferase in heart', *Pediatr Res*, 41: 404-10.

Baran, H., K. Staniek, M. Bertignol-Sporr, M. Attam, C. Kronsteiner, and B. Kepplinger. 2016. 'Effects of Various Kynurenine Metabolites on Respiratory Parameters of Rat Brain, Liver and Heart Mitochondria', *Int J Tryptophan Res*, 9: 17-29.

Baran, H., K. Staniek, B. Kepplinger, L. Gille, K. Stolze, and H. Nohl. 2001. 'Kynurenic acid influences the respiratory parameters of rat heart mitochondria', *Pharmacology*, 62: 119-23.

Baran, H., K. Staniek, B. Kepplinger, J. Stur, M. Draxler, and H. Nohl. 2003. 'Kynurenines and the respiratory parameters on rat heart mitochondria', *Life Sci*, 72: 1103-15.

Belenguer, P., and L. Pellegrini. 2013. 'The dynamin GTPase OPA1: more than mitochondria?', *Biochim Biophys Acta*, 1833: 176-83.

Bellance, N., P. Lestienne, and R. Rossignol. 2009. 'Mitochondria: from bioenergetics to the metabolic regulation of carcinogenesis', *Front Biosci (Landmark Ed)*, 14: 4015-34.

Benhabbouche, S., C. Crola da Silva, M. Abrial, and R. Ferrera. 2011. '[The basis of ischemia-reperfusion and myocardial protection]', *Ann Fr Anesth Reanim*, 30 Suppl 1: S2-16.

Bernhardt, D., M. Muller, A. S. Reichert, and H. D. Osiewacz. 2015. 'Simultaneous impairment of mitochondrial fission and fusion reduces mitophagy and shortens replicative lifespan', *Sci Rep*, 5: 7885.

Billia, F., L. Hauck, F. Konecny, V. Rao, J. Shen, and T. W. Mak. 2011. 'PTEN-inducible kinase 1 (PINK1)/Park6 is indispensable for normal heart function', *Proc Natl Acad Sci U S A*, 108: 9572-7.

Bochaton, T., C. Crola-Da-Silva, B. Pillot, C. Villedieu, L. Ferreras, M. R. Alam, H. Thibault, M. Strina, A. Gharib, M. Ovize, and D. Baetz. 2015. 'Inhibition of myocardial reperfusion injury by ischemic postconditioning requires sirtuin 3-mediated deacetylation of cyclophilin D', *J Mol Cell Cardiol*, 84: 61-9.

Boengler, K., E. Ungefug, G. Heusch, and R. Schulz. 2013. 'The STAT3 inhibitor stattic impairs cardiomyocyte mitochondrial function through increased reactive oxygen species formation', *Curr Pharm Des*, 19: 6890-5.

Bordelon, Y. M., M. F. Chesselet, D. Nelson, F. Welsh, and M. Erecinska. 1997. 'Energetic dysfunction in quinolinic acid-lesioned rat striatum', *J Neurochem*, 69: 1629-39.

Brady, N. R., A. Hamacher-Brady, and R. A. Gottlieb. 2006. 'Proapoptotic BCL-2 family members and mitochondrial dysfunction during ischemia/reperfusion injury, a study employing cardiac HL-1 cells and GFP biosensors', *Biochim Biophys Acta*, 1757: 667-78.

Braidy, N., R. Grant, B. J. Brew, S. Adams, T. Jayasena, and G. J. Guillemin. 2009. 'Effects of Kynurenine Pathway Metabolites on Intracellular NAD Synthesis and Cell Death in Human Primary Astrocytes and Neurons', *Int J Tryptophan Res*, 2: 61-9.

Braidy, N., G. J. Guillemin, and R. Grant. 2011. 'Effects of Kynurenine Pathway Inhibition on NAD Metabolism and Cell Viability in Human Primary Astrocytes and Neurons', *Int J Tryptophan Res*, 4: 29-37.

Braschi, E., R. Zunino, and H. M. McBride. 2009. 'MAPL is a new mitochondrial SUMO E3 ligase that regulates mitochondrial fission', *EMBO Rep*, 10: 748-54.

Braunwald, E., and R. A. Kloner. 1982. 'The stunned myocardium: prolonged, postischemic ventricular dysfunction', *Circulation*, 66: 1146-9.

Briston, T., M. Roberts, S. Lewis, B. Powney, M. Staddon J, G. Szabadkai, and M. R. Duchen. 2017. 'Mitochondrial permeability transition pore: sensitivity to opening and mechanistic dependence on substrate availability', *Sci Rep*, 7: 10492.

Bubenik, G. A., and S. J. Konturek. 2011. 'Melatonin and aging: prospects for human treatment', *J Physiol Pharmacol*, 62: 13-9.

Bugger, H., C. N. Witt, and C. Bode. 2016. 'Mitochondrial sirtuins in the heart', *Heart Fail Rev*, 21: 519-28.

Cadete, V. J. J., G. Vasam, K. J. Menzies, and Y. Burelle. 2019. 'Mitochondrial quality control in the cardiac system: An integrative view', *Biochim Biophys Acta Mol Basis Dis*, 1865: 782-96.

Carlstedt-Duke, J. M. 1979. 'Tissue distribution of the receptor for 2,3,7,8-tetrachlorodibenzo-p-dioxin in the rat', *Cancer Res*, 39: 3172-6.

Cassidy-Stone, A., J. E. Chipuk, E. Ingerman, C. Song, C. Yoo, T. Kuwana, M. J. Kurth, J. T. Shaw, J. E. Hinshaw, D. R. Green, and J. Nunnari. 2008. 'Chemical inhibition of the mitochondrial division dynamin reveals its role in Bax/Bak-dependent mitochondrial outer membrane permeabilization', *Dev Cell*, 14: 193-204.

Cereghetti, G. M., A. Stangherlin, O. Martins de Brito, C. R. Chang, C. Blackstone, P. Bernardi, and L. Scorrano. 2008. 'Dephosphorylation by calcineurin regulates translocation of Drp1 to mitochondria', *Proc Natl Acad Sci U S A*, 105: 15803-8.

Cervenka, I., L. Z. Agudelo, and J. L. Ruas. 2017. 'Kynurenines: Tryptophan's metabolites in exercise, inflammation, and mental health', *Science*, 357.

Chaanine, A. H., E. Kohlbrenner, S. I. Gamb, A. J. Guenzel, K. Klaus, A. U. Fayyaz, K. S. Nair, R. J. Hajjar, and M. M. Redfield. 2016. 'FOXO3a regulates BNIP3 and modulates mitochondrial calcium, dynamics, and function in cardiac stress', *Am J Physiol Heart Circ Physiol*, 311: H1540-H59.

Chang, C. R., and C. Blackstone. 2007a. 'Cyclic AMP-dependent protein kinase phosphorylation of Drp1 regulates its GTPase activity and mitochondrial morphology', *J Biol Chem*, 282: 21583-7.

———. 2007b. 'Drp1 phosphorylation and mitochondrial regulation', *EMBO Rep*, 8: 1088-9; author reply 89-90.

Chao de la Barca, J. M., O. Bakhta, H. Kalakech, G. Simard, S. Tamareille, V. Catros, J. Callebert, C. Gadras, L. Tessier, P. Reynier, F. Prunier, and D. Mirebeau-Prunier. 2016. 'Metabolic Signature of Remote Ischemic Preconditioning Involving a Cocktail of Amino Acids and Biogenic Amines', *J Am Heart Assoc*, 5.

Chao de la Barca, J. M., G. Simard, E. Sarzi, T. Chaumette, G. Rousseau, S. Chupin, C. Gadras, L. Tessier, M. Ferre, A. Chevrollier, V. Desquiret-Dumas, N. Gueguen, S. Leruez, C. Verny, D. Milea, D. Bonneau, P. Amati-Bonneau, V. Procaccio, C. Hamel, G. Lenaers, P. Reynier, and D. Prunier-Mirebeau. 2017. 'Targeted Metabolomics Reveals Early Dominant Optic Atrophy Signature in Optic Nerves of Opa1delTTAG/+ Mice', *Invest Ophthalmol Vis Sci*, 58: 812-20.

Chen, L., Q. Gong, J. P. Stice, and A. A. Knowlton. 2009. 'Mitochondrial OPA1, apoptosis, and heart failure', *Cardiovasc Res*, 84: 91-9.

Chen, L., and A. A. Knowlton. 2011. 'Mitochondrial dynamics in heart failure', *Congest Heart Fail*, 17: 257-61.

Chen, L., T. Liu, A. Tran, X. Lu, A. A. Tomilov, V. Davies, G. Cortopassi, N. Chiamvimonvat, D. M. Bers, M. Votruba, and A. A. Knowlton. 2012. 'OPA1 mutation and late-onset cardiomyopathy: mitochondrial dysfunction and mtDNA instability', *J Am Heart Assoc*, 1: e003012.

Chen, Q., S. Moghaddas, C. L. Hoppel, and E. J. Lesnefsky. 2006. 'Reversible blockade of electron transport during ischemia protects mitochondria and decreases myocardial injury following reperfusion', *J Pharmacol Exp Ther*, 319: 1405-12.

Chen, Q., E. J. Vazquez, S. Moghaddas, C. L. Hoppel, and E. J. Lesnefsky. 2003. 'Production of reactive oxygen species by mitochondria: central role of complex III', *J Biol Chem*, 278: 36027-31.

Chen, Q., M. Younus, J. Thompson, Y. Hu, J. M. Hollander, and E. J. Lesnefsky. 2018. 'Intermediary metabolism and fatty acid oxidation: novel targets of electron transport chain-driven injury during ischemia and reperfusion', *Am J Physiol Heart Circ Physiol*, 314: H787-H95.

Chen, Y., and G. W. Dorn, 2nd. 2013. 'PINK1-phosphorylated mitofusin 2 is a Parkin receptor for culling damaged mitochondria', *Science*, 340: 471-5.

Chen, Y., and G. J. Guillemin. 2009. 'Kynurenine pathway metabolites in humans: disease and healthy States', *Int J Tryptophan Res*, 2: 1-19.

Chi, L. G., Y. Tamura, P. T. Hoff, M. Macha, K. P. Gallagher, M. A. Schork, and B. R. Lucchesi. 1989. 'Effect of superoxide dismutase on myocardial infarct size in the canine heart after 6 hours of regional ischemia and reperfusion: a demonstration of myocardial salvage', *Circ Res*, 64: 665-75.

Cho, B., S. Y. Choi, H. M. Cho, H. J. Kim, and W. Sun. 2013. 'Physiological and pathological significance of dynamin-related protein 1 (drp1)-dependent mitochondrial fission in the nervous system', *Exp Neurobiol*, 22: 149-57.

Cho, D. H., T. Nakamura, J. Fang, P. Cieplak, A. Godzik, Z. Gu, and S. A. Lipton. 2009. 'S-nitrosylation of Drp1 mediates beta-amyloid-related mitochondrial fission and neuronal injury', *Science*, 324: 102-5.

Civelli, O., R. K. Reinscheid, Y. Zhang, Z. Wang, R. Fredriksson, and H. B. Schioth. 2013. 'G protein-coupled receptor deorphanizations', *Annu Rev Pharmacol Toxicol*, 53: 127-46.

Cozzi, A., R. Carpenedo, and F. Moroni. 1999. 'Kynurenine hydroxylase inhibitors reduce ischemic brain damage: studies with (m-nitrobenzoyl)-alanine (mNBA) and 3,4-dimethoxy-[-N-4-(nitrophenyl)thiazol-2yl]-benzenesulfonamide (Ro 61-8048) in models of focal or global brain ischemia', *J Cereb Blood Flow Metab*, 19: 771-7.

Cuffy, M. C., A. M. Silverio, L. Qin, Y. Wang, R. Eid, G. Brandacher, F. G. Lakkis, D. Fuchs, J. S. Pober, and G. Tellides. 2007. 'Induction of indoleamine 2,3-dioxygenase in vascular smooth muscle cells by interferon-gamma contributes to medial immunoprivilege', *J Immunol*, 179: 5246-54.

D'Onofrio, N., L. Servillo, and M. L. Balestrieri. 2018. 'SIRT1 and SIRT6 Signaling Pathways in Cardiovascular Disease Protection', *Antioxid Redox Signal*, 28: 711-32.

Das, S., G. Mitrovsky, H. R. Vasanthi, and D. K. Das. 2014. 'Antiaging properties of a grape-derived antioxidant are regulated by mitochondrial balance of fusion and fission leading to mitophagy triggered by a signaling network of Sirt1-Sirt3-Foxo3-PINK1-PARKIN', *Oxid Med Cell Longev*, 2014: 345105.

Davidson, S. M., P. Ferdinandy, I. Andreadou, H. E. Botker, G. Heusch, B. Ibanez, M. Ovize, R. Schulz, D. M. Yellon, D. J. Hausenloy, D. Garcia-Dorado, and Cardioprotection Cost Action. 2019. 'Multitarget Strategies to Reduce Myocardial Ischemia/Reperfusion Injury: JACC Review Topic of the Week', *J Am Coll Cardiol*, 73: 89-99.

Davidson, S. M., D. Hausenloy, M. R. Duchen, and D. M. Yellon. 2006. 'Signalling via the reperfusion injury signalling kinase (RISK) pathway links closure of the mitochondrial permeability transition pore to cardioprotection', *Int J Biochem Cell Biol*, 38: 414-9.

Delettre, C., J. M. Griffoin, J. Kaplan, H. Dollfus, B. Lorenz, L. Faivre, G. Lenaers, P. Belenguer, and C. P. Hamel. 2001. 'Mutation spectrum and splicing variants in the OPA1 gene', *Hum Genet*, 109: 584-91.

Delettre, C., G. Lenaers, J. M. Griffoin, N. Gigarel, C. Lorenzo, P. Belenguer, L. Pelloquin, J. Grosgeorge, C. Turc-Carel, E. Perret, C. Astarie-Dequeker, L. Lasquellec, B. Arnaud, B. Ducommun, J. Kaplan, and C. P. Hamel. 2000. 'Nuclear gene OPA1, encoding a mitochondrial dynamin-related protein, is mutated in dominant optic atrophy', *Nat Genet*, 26: 207-10.

Deng, H., H. Hu, and Y. Fang. 2011. 'Tyrphostin analogs are GPR35 agonists', *FEBS Lett*, 585: 1957-62.

Dieterich, S., U. Bieligk, K. Beulich, G. Hasenfuss, and J. Prestle. 2000. 'Gene expression of antioxidative enzymes in the human heart: increased expression of catalase in the end-stage failing heart', *Circulation*, 101: 33-9.

Dikov, D., and A. S. Reichert. 2011. 'How to split up: lessons from mitochondria', *EMBO J*, 30: 2751-3.

Din, S., M. Mason, M. Volkers, B. Johnson, C. T. Cottage, Z. Wang, A. Y. Joyo, P. Quijada, P. Erhardt, N. S. Magnuson, M. H. Konstandin, and M. A. Sussman. 2013. 'Pim-1 preserves mitochondrial morphology by inhibiting dynamin-related protein 1 translocation', *Proc Natl Acad Sci U S A*, 110: 5969-74.

DiNatale, B. C., I. A. Murray, J. C. Schroeder, C. A. Flaveny, T. S. Lahoti, E. M. Laurenzana, C. J. Omiecinski, and G. H. Perdew. 2010. 'Kynurenic acid is a potent endogenous aryl hydrocarbon

receptor ligand that synergistically induces interleukin-6 in the presence of inflammatory signaling', *Toxicol Sci*, 115: 89-97.

Disatnik, M. H., J. C. Ferreira, J. C. Campos, K. S. Gomes, P. M. Dourado, X. Qi, and D. Mochly-Rosen. 2013. 'Acute inhibition of excessive mitochondrial fission after myocardial infarction prevents long-term cardiac dysfunction', *J Am Heart Assoc*, 2: e000461.

Divorty, N., G. Milligan, D. Graham, and S. A. Nicklin. 2018. 'The Orphan Receptor GPR35 Contributes to Angiotensin II-Induced Hypertension and Cardiac Dysfunction in Mice', *Am J Hypertens*, 31: 1049-58.

Dong, Y., V. V. R. Undyala, and K. Przyklenk. 2016. 'Inhibition of mitochondrial fission as a molecular target for cardioprotection: critical importance of the timing of treatment', *Basic Res Cardiol*, 111: 59.

Dorn, G. W., 2nd. 2015a. 'Gone fission...: diverse consequences of cardiac Drp1 deficiency', *Circ Res*, 116: 225-8.

———. 2015b. 'Mitochondrial dynamism and heart disease: changing shape and shaping change', *EMBO Mol Med*, 7: 865-77.

———. 2019. 'Evolving Concepts of Mitochondrial Dynamics', *Annu Rev Physiol*, 81: 1-17.

Doroudgar, S., and C. C. Glembotski. 2013. 'New concepts of endoplasmic reticulum function in the heart: programmed to conserve', *J Mol Cell Cardiol*, 55: 85-91.

Downey, J. M. 1990. 'Free radicals and their involvement during long-term myocardial ischemia and reperfusion', *Annu Rev Physiol*, 52: 487-504.

Drsata, J. 2003. 'Tryptophan metabolism via transamination. In vitro aminotransferase assay using dinitrophenylhydrazine method', *Adv Exp Med Biol*, 527: 511-7.

Flaherty, J. T., B. Pitt, J. W. Gruber, R. R. Heuser, D. A. Rothbaum, L. R. Burwell, B. S. George, D. J. Kereiakes, D. Deitchman, N. Gustafson, and et al. 1994. 'Recombinant human superoxide dismutase (h-SOD) fails to improve recovery of ventricular function in patients undergoing coronary angioplasty for acute myocardial infarction', *Circulation*, 89: 1982-91.

Fouquet, G., T. Coman, O. Hermine, and F. Cote. 2019. 'Serotonin, hematopoiesis and stem cells', *Pharmacol Res*, 140: 67-74.

Frye, R. A. 2000. 'Phylogenetic classification of prokaryotic and eukaryotic Sir2-like proteins', *Biochem Biophys Res Commun*, 273: 793-8.

Fujigaki, H., Y. Yamamoto, and K. Saito. 2017. 'L-Tryptophan-kynurenine pathway enzymes are therapeutic target for neuropsychiatric diseases: Focus on cell type differences', *Neuropharmacology*, 112: 264-74.

Fukui, S., R. Schwarcz, S. I. Rapoport, Y. Takada, and Q. R. Smith. 1991. 'Blood-brain barrier transport of kynurenines: implications for brain synthesis and metabolism', *J Neurochem*, 56: 2007-17.

Galluzzi, L., M. C. Maiuri, I. Vitale, H. Zischka, M. Castedo, L. Zitvogel, and G. Kroemer. 2007. 'Cell death modalities: classification and pathophysiological implications', *Cell Death Differ*, 14: 1237-43.

Galluzzi, L., I. Vitale, S. A. Aaronson, J. M. Abrams, D. Adam, P. Agostinis, E. S. Alnemri, L. Altucci, I. Amelio, D. W. Andrews, M. Annicchiarico-Petruzzelli, A. V. Antonov, E. Arama, E. H. Baehrecke, N. A. Barlev, N. G. Bazan, F. Bernassola, M. J. M. Bertrand, K. Bianchi, M. V. Blagosklonny, K. Blomgren, C. Borner, P. Boya, C. Brenner, M. Campanella, E. Candi, D. Carmona-Gutierrez, F. Cecconi, F. K. Chan, N. S. Chandel, E. H. Cheng, J. E. Chipuk, J. A. Cidlowski, A. Ciechanover, G. M. Cohen, M. Conrad, J. R. Cubillos-Ruiz, P. E. Czabotar, V. D'Angiolella, T. M. Dawson, V. L. Dawson, V. De Laurenzi, R. De Maria, K. M. Debatin, R. J. DeBerardinis, M. Deshmukh, N. Di Daniele, F. Di Virgilio, V. M. Dixit, S. J. Dixon, C. S. Duckett, B. D. Dynlacht, W. S. El-Deiry, J. W. Elrod, G. M. Fimia, S. Fulda, A. J. Garcia-Saez, A. D. Garg, C. Garrido, E. Gavathiotis, P. Golstein, E. Gottlieb, D. R. Green, L. A. Greene, H. Gronemeyer, A. Gross, G. Hajnoczky, J. M. Hardwick, I. S. Harris, M. O. Hengartner, C. Hetz, H. Ichijo, M. Jaattela, B. Joseph, P. J. Jost, P. P. Juin, W. J. Kaiser, M. Karin, T. Kaufmann, O. Kepp, A. Kimchi, R. N. Kitsis, D. J. Klionsky, R. A. Knight, S. Kumar, S. W. Lee, J. J. Lemasters, B. Levine, A. Linkermann, S. A. Lipton, R. A. Lockshin, C. Lopez-Otin, S. W. Lowe, T. Luedde, E. Lugli, M. MacFarlane, F. Madeo, M. Malewicz, W. Malorni, G. Manic, J. C. Marine, S. J. Martin, J. C. Martinou, J. P. Medema, P. Mehlen, P. Meier, S. Melino, E. A. Miao, J. D. Molkentin, U. M. Moll, C. Munoz-Pinedo, S. Nagata, G. Nunez, A. Oberst, M. Oren, M. Overholtzer, M. Pagano, T. Panaretakis, M. Pasparakis, J. M. Penninger, D. M. Pereira, S. Pervaiz, M. E. Peter, M. Piacentini, P. Pinton, J. H. M. Prehn, H. Puthalakath, G. A. Rabinovich, M. Rehm, R. Rizzuto, C. M. P. Rodrigues, D. C. Rubinsztein, T. Rudel, K. M. Ryan, E. Sayan, L. Scorrano, F. Shao, Y. Shi, J. Silke, H. U. Simon, A. Sistigu, B. R. Stockwell, A. Strasser, G. Szabadkai, S. W. G. Tait, D. Tang, N. Tavernarakis, A. Thorburn, Y. Tsujimoto, B. Turk, T. Vanden Berghe, P. Vandenabeele, M. G. Vander Heiden, A. Villunger, H. W. Virgin, K. H. Vousden, D. Vucic, E. F. Wagner, H. Walczak, D. Wallach, Y. Wang, J. A. Wells, W. Wood, J. Yuan, Z. Zakeri, B. Zhivotovsky, L. Zitvogel, G. Melino, and G. Kroemer. 2018. 'Molecular mechanisms of cell death: recommendations of the Nomenclature Committee on Cell Death 2018', *Cell Death Differ*, 25: 486-541.

Gao, D., L. Zhang, R. Dhillon, T. T. Hong, R. M. Shaw, and J. Zhu. 2013. 'Dynasore protects mitochondria and improves cardiac lusitropy in Langendorff perfused mouse heart', *PLoS One*, 8: e60967.

Gao, S., H. Li, X. J. Feng, M. Li, Z. P. Liu, Y. Cai, J. Lu, X. Y. Huang, J. J. Wang, Q. Li, S. R. Chen, J. T. Ye, and P. Q. Liu. 2015. 'alpha-Enolase plays a catalytically independent role in doxorubicin-induced cardiomyocyte apoptosis and mitochondrial dysfunction', *J Mol Cell Cardiol*, 79: 92-103.

Gao, X., X. Xu, J. Pang, C. Zhang, J. M. Ding, X. Peng, Y. Liu, and J. M. Cao. 2007. 'NMDA receptor activation induces mitochondrial dysfunction, oxidative stress and apoptosis in cultured neonatal rat cardiomyocytes', *Physiol Res*, 56: 559-69.

Germano, I. M., L. H. Pitts, B. S. Meldrum, H. M. Bartkowski, and R. P. Simon. 1987. 'Kynurenate inhibition of cell excitation decreases stroke size and deficits', *Ann Neurol*, 22: 730-4.

Gho, B. C., R. G. Schoemaker, M. A. van den Doel, D. J. Duncker, and P. D. Verdouw. 1996. 'Myocardial protection by brief ischemia in noncardiac tissue', *Circulation*, 94: 2193-200.

Gigler, G., G. Szenasi, A. Simo, G. Levay, L. G. Harsing, Jr., K. Sas, L. Vecsei, and J. Toldi. 2007. 'Neuroprotective effect of L-kynurenine sulfate administered before focal cerebral ischemia in mice and global cerebral ischemia in gerbils', *Eur J Pharmacol*, 564: 116-22.

Gobaille, S., V. Kemmel, D. Brumaru, C. Dugave, D. Aunis, and M. Maitre. 2008. 'Xanthurenic acid distribution, transport, accumulation and release in the rat brain', *J Neurochem*, 105: 982-93.

Goda, K., M. Hisaoka, and T. Ueda. 1987. 'Photoinduced electron transfer reaction from N-formyl-L-kynurenine and L-kynurenine to cytochrome C', *Biochem Int*, 15: 635-43.

Gonzalez-Montero, J., R. Brito, A. I. Gajardo, and R. Rodrigo. 2018. 'Myocardial reperfusion injury and oxidative stress: Therapeutic opportunities', *World J Cardiol*, 10: 74-86.

Goody, M. F., and C. A. Henry. 2018. 'A need for NAD+ in muscle development, homeostasis, and aging', *Skelet Muscle*, 8: 9.

Grall, S., D. Prunier-Mirebeau, S. Tamareille, V. Mateus, D. Lamon, A. Furber, and F. Prunier. 2013. 'Endoplasmic reticulum stress pathway involvement in local and remote myocardial ischemic conditioning', *Shock*, 39: 433-9.

Guillemin, G. J. 2012. 'Quinolinic acid, the inescapable neurotoxin', *FEBS J*, 279: 1356-65.

Guo, C., K. L. Hildick, J. Luo, L. Dearden, K. A. Wilkinson, and J. M. Henley. 2013. 'SENP3-mediated deSUMOylation of dynamin-related protein 1 promotes cell death following ischaemia', *EMBO J*, 32: 1514-28.

Guo, J., D. J. Williams, H. L. Puhl, 3rd, and S. R. Ikeda. 2008. 'Inhibition of N-type calcium channels by activation of GPR35, an orphan receptor, heterologously expressed in rat sympathetic neurons', *J Pharmacol Exp Ther*, 324: 342-51.

Gupta, S. L., J. M. Carlin, P. Pyati, W. Dai, E. R. Pfefferkorn, and M. J. Murphy, Jr. 1994. 'Antiparasitic and antiproliferative effects of indoleamine 2,3-dioxygenase enzyme expression in human fibroblasts', *Infect Immun*, 62: 2277-84.

Hadebe, N., M. Cour, and S. Lecour. 2018. 'The SAFE pathway for cardioprotection: is this a promising target?', *Basic Res Cardiol*, 113: 9.

Hales, K. G. 2004. 'The machinery of mitochondrial fusion, division, and distribution, and emerging connections to apoptosis', *Mitochondrion*, 4: 285-308.

Hall, A. R., N. Burke, R. K. Dongworth, and D. J. Hausenloy. 2014. 'Mitochondrial fusion and fission proteins: novel therapeutic targets for combating cardiovascular disease', *Br J Pharmacol*, 171: 1890-906.

Hamacher-Brady, A., N. R. Brady, and R. A. Gottlieb. 2006. 'Enhancing macroautophagy protects against ischemia/reperfusion injury in cardiac myocytes', *J Biol Chem*, 281: 29776-87.

Han, Q., T. Cai, D. A. Tagle, and J. Li. 2010. 'Thermal stability, pH dependence and inhibition of four murine kynurenine aminotransferases', *BMC Biochem*, 11: 19.

Han, Z., J. Cao, D. Song, L. Tian, K. Chen, Y. Wang, L. Gao, Z. Yin, Y. Fan, and C. Wang. 2014. 'Autophagy is involved in the cardioprotection effect of remote limb ischemic postconditioning on myocardial ischemia/reperfusion injury in normal mice, but not diabetic mice', *PLoS One*, 9: e86838.

Hansen, K. B., F. Yi, R. E. Perszyk, H. Furukawa, L. P. Wollmuth, A. J. Gibb, and S. F. Traynelis. 2018. 'Structure, function, and allosteric modulation of NMDA receptors', *J Gen Physiol*, 150: 1081-105.

Harder, Z., R. Zunino, and H. McBride. 2004. 'Sumo1 conjugates mitochondrial substrates and participates in mitochondrial fission', *Curr Biol*, 14: 340-5.

Harris, C. A., A. F. Miranda, J. J. Tanguay, R. J. Boegman, R. J. Beninger, and K. Jhamandas. 1998. 'Modulation of striatal quinolinate neurotoxicity by elevation of endogenous brain kynurenic acid', *Br J Pharmacol*, 124: 391-9.

Haun, F., T. Nakamura, and S. A. Lipton. 2013. 'Dysfunctional Mitochondrial Dynamics in the Pathophysiology of Neurodegenerative Diseases', *J Cell Death*, 6: 27-35.

Hausenloy, D. J., and D. M. Yellon. 2013. 'Myocardial ischemia-reperfusion injury: a neglected therapeutic target', *J Clin Invest*, 123: 92-100.

———. 2016. 'Ischaemic conditioning and reperfusion injury', *Nat Rev Cardiol*, 13: 193-209.

Hearse, D. J., and A. Tosaki. 1987. 'Free radicals and reperfusion-induced arrhythmias: protection by spin trap agent PBN in the rat heart', *Circ Res*, 60: 375-83.

Heusch, G. 2015. 'Molecular basis of cardioprotection: signal transduction in ischemic pre-, post-, and remote conditioning', *Circ Res*, 116: 674-99.

Heusch, G., H. E. Botker, K. Przyklenk, A. Redington, and D. Yellon. 2015. 'Remote ischemic conditioning', *J Am Coll Cardiol*, 65: 177-95.

Heusch, G., P. Kleinbongard, D. Bose, B. Levkau, M. Haude, R. Schulz, and R. Erbel. 2009. 'Coronary microembolization: from bedside to bench and back to bedside', *Circulation*, 120: 1822-36.

Heymans, S., E. Hirsch, S. D. Anker, P. Aukrust, J. L. Balligand, J. W. Cohen-Tervaert, H. Drexler, G. Filippatos, S. B. Felix, L. Gullestad, D. Hilfiker-Kleiner, S. Janssens, R. Latini, G. Neubauer, W. J. Paulus, B. Pieske, P. Ponikowski, B. Schroen, H. P. Schultheiss, C. Tschope, M. Van Bilsen, F. Zannad, J. McMurray, and A. M. Shah. 2009. 'Inflammation as a therapeutic target in heart failure? A scientific statement from the Translational Research Committee of the Heart Failure Association of the European Society of Cardiology', *Eur J Heart Fail*, 11: 119-29.

Hoppins, S., and J. Nunnari. 2009. 'The molecular mechanism of mitochondrial fusion', *Biochim Biophys Acta*, 1793: 20-6.

Hoshino, A., Y. Mita, Y. Okawa, M. Ariyoshi, E. Iwai-Kanai, T. Ueyama, K. Ikeda, T. Ogata, and S. Matoba. 2013. 'Cytosolic p53 inhibits Parkin-mediated mitophagy and promotes mitochondrial dysfunction in the mouse heart', *Nat Commun*, 4: 2308.

Huang, C., A. M. Andres, E. P. Ratliff, G. Hernandez, P. Lee, and R. A. Gottlieb. 2011. 'Preconditioning involves selective mitophagy mediated by Parkin and p62/SQSTM1', *PLoS One*, 6: e20975.

Ibanez, B., G. Heusch, M. Ovize, and F. Van de Werf. 2015. 'Evolving therapies for myocardial ischemia/reperfusion injury', *J Am Coll Cardiol*, 65: 1454-71.

Ibanez, B., C. Macaya, V. Sanchez-Brunete, G. Pizarro, L. Fernandez-Friera, A. Mateos, A. Fernandez-Ortiz, J. M. Garcia-Ruiz, A. Garcia-Alvarez, A. Iniguez, J. Jimenez-Borreguero, P. Lopez-Romero, R. Fernandez-Jimenez, J. Goicolea, B. Ruiz-Mateos, T. Bastante, M. Arias, J. A. Iglesias-Vazquez, M. D. Rodriguez, N. Escalera, C. Acebal, J. A. Cabrera, J. Valenciano, A. Perez de Prado, M. J. Fernandez-Campos, I. Casado, J. C. Garcia-Rubira, J. Garcia-Prieto, D. Sanz-Rosa, C. Cuellas, R. Hernandez-Antolin, A. Albarran, F. Fernandez-Vazquez, J. M. de la Torre-Hernandez, S. Pocock, G. Sanz, and V. Fuster. 2013. 'Effect of early metoprolol on infarct size in ST-segment-elevation myocardial infarction patients undergoing primary percutaneous coronary intervention: the Effect of Metoprolol in Cardioprotection During an Acute Myocardial Infarction (METOCARD-CNIC) trial', *Circulation*, 128: 1495-503.

Ighodaro, O. M., and O. A. Akinloye. 2018. 'First line defence antioxidants-superoxide dismutase (SOD), catalase (CAT) and glutathione peroxidase (GPX): Their fundamental role in the entire antioxidant defence grid', *Alexandria Journal of Medicine*, 54: 287-93.

Iguchi, M., Y. Kujuro, K. Okatsu, F. Koyano, H. Kosako, M. Kimura, N. Suzuki, S. Uchiyama, K. Tanaka, and N. Matsuda. 2013. 'Parkin-catalyzed ubiquitin-ester transfer is triggered by PINK1-dependent phosphorylation', *J Biol Chem*, 288: 22019-32.

Ikeda, Y., A. Shirakabe, Y. Maejima, P. Zhai, S. Sciarretta, J. Toli, M. Nomura, K. Mihara, K. Egashira, M. Ohishi, M. Abdellatif, and J. Sadoshima. 2015. 'Endogenous Drp1 mediates mitochondrial autophagy and protects the heart against energy stress', *Circ Res*, 116: 264-78.

Ishihara, N., M. Nomura, A. Jofuku, H. Kato, S. O. Suzuki, K. Masuda, H. Otera, Y. Nakanishi, I. Nonaka, Y. Goto, N. Taguchi, H. Morinaga, M. Maeda, R. Takayanagi, S. Yokota, and K. Mihara. 2009. 'Mitochondrial fission factor Drp1 is essential for embryonic development and synapse formation in mice', *Nat Cell Biol*, 11: 958-66.

Ito, H. 2006. 'No-reflow phenomenon and prognosis in patients with acute myocardial infarction', *Nat Clin Pract Cardiovasc Med*, 3: 499-506.

Jenkins, T. A., J. C. Nguyen, K. E. Polglaze, and P. P. Bertrand. 2016. 'Influence of Tryptophan and Serotonin on Mood and Cognition with a Possible Role of the Gut-Brain Axis', *Nutrients*, 8.

Jennings, R. B., H. M. Sommers, G. A. Smyth, H. A. Flack, and H. Linn. 1960. 'Myocardial necrosis induced by temporary occlusion of a coronary artery in the dog', *Arch Pathol*, 70: 68-78.

Jeremy M Berg, John L Tymoczko, and Lubert Stryer. 2002. *Biochemistry* (W. H. Freeman: New York).

Ji, L., X. Zhang, W. Liu, Q. Huang, W. Yang, F. Fu, H. Ma, H. Su, H. Wang, J. Wang, H. Zhang, and F. Gao. 2013. 'AMPK-regulated and Akt-dependent enhancement of glucose uptake is essential in ischemic preconditioning-alleviated reperfusion injury', *PLoS One*, 8: e69910.

Juhaszova, M., D. B. Zorov, S. H. Kim, S. Pepe, Q. Fu, K. W. Fishbein, B. D. Ziman, S. Wang, K. Ytrehus, C. L. Antos, E. N. Olson, and S. J. Sollott. 2004. 'Glycogen synthase kinase-3beta mediates convergence of protection signaling to inhibit the mitochondrial permeability transition pore', *J Clin Invest*, 113: 1535-49.

Kaelin, W. G., Jr., and P. J. Ratcliffe. 2008. 'Oxygen sensing by metazoans: the central role of the HIF hydroxylase pathway', *Mol Cell*, 30: 393-402.

Kageyama, Y., M. Hoshijima, K. Seo, D. Bedja, P. Sysa-Shah, S. A. Andrabi, W. Chen, A. Hoke, V. L. Dawson, T. M. Dawson, K. Gabrielson, D. A. Kass, M. Iijima, and H. Sesaki. 2014. 'Parkin-independent mitophagy requires Drp1 and maintains the integrity of mammalian heart and brain', *EMBO J*, 33: 2798-813.

Kalakech, H., P. Hibert, D. Prunier-Mirebeau, S. Tamareille, F. Letournel, L. Macchi, F. Pinet, A. Furber, and F. Prunier. 2014. 'RISK and SAFE signaling pathway involvement in apolipoprotein A-I-induced cardioprotection', *PLoS One*, 9: e107950.

Kane, J. J., M. L. Murphy, J. K. Bissett, N. deSoyza, J. E. Doherty, and K. D. Straub. 1975. 'Mitochondrial function, oxygen extraction, epicardial S-T segment changes and tritiated digoxin distribution after reperfusion of ischemic myocardium', *Am J Cardiol*, 36: 218-24.

Kessler, M., T. Terramani, G. Lynch, and M. Baudry. 1989. 'A glycine site associated with N-methyl-D-aspartic acid receptors: characterization and identification of a new class of antagonists', *J Neurochem*, 52: 1319-28.

Kharbanda, R. K., U. M. Mortensen, P. A. White, S. B. Kristiansen, M. R. Schmidt, J. A. Hoschtitzky, M. Vogel, K. Sorensen, A. N. Redington, and R. MacAllister. 2002. 'Transient limb ischemia induces remote ischemic preconditioning in vivo', *Circulation*, 106: 2881-3.

Klockgether, T. 1987. 'Excitatory amino acid receptor-mediated transmission of somatosensory evoked potentials in the rat thalamus', *J Physiol*, 394: 445-61.

Konstantinidis, K., R. S. Whelan, and R. N. Kitsis. 2012. 'Mechanisms of cell death in heart disease', *Arterioscler Thromb Vasc Biol*, 32: 1552-62.

Kouassi Nzoughet, J., C. Bocca, G. Simard, D. Prunier-Mirebeau, J. M. Chao de la Barca, D. Bonneau, V. Procaccio, F. Prunier, G. Lenaers, and P. Reynier. 2017. 'A Nontargeted UHPLC-HRMS Metabolomics Pipeline for Metabolite Identification: Application to Cardiac Remote Ischemic Preconditioning', *Anal Chem*, 89: 2138-46.

Kroemer, G., B. Dallaporta, and M. Resche-Rigon. 1998. 'The mitochondrial death/life regulator in apoptosis and necrosis', *Annu Rev Physiol*, 60: 619-42.

Krug, A., Rochemont Du Mesnil de, and G. Korb. 1966. 'Blood supply of the myocardium after temporary coronary occlusion', *Circ Res*, 19: 57-62.

Kubli, D. A., and A. B. Gustafsson. 2012. 'Mitochondria and mitophagy: the yin and yang of cell death control', *Circ Res*, 111: 1208-21.

Kubli, D. A., M. N. Quinsay, and A. B. Gustafsson. 2013. 'Parkin deficiency results in accumulation of abnormal mitochondria in aging myocytes', *Commun Integr Biol*, 6: e24511.

Kubli, D. A., X. Zhang, Y. Lee, R. A. Hanna, M. N. Quinsay, C. K. Nguyen, R. Jimenez, S. Petrosyan, A. N. Murphy, and A. B. Gustafsson. 2013. 'Parkin protein deficiency exacerbates cardiac injury and reduces survival following myocardial infarction', *J Biol Chem*, 288: 915-26.

Lakhan, S. E., M. Caro, and N. Hadzimichalis. 2013. 'NMDA Receptor Activity in Neuropsychiatric Disorders', *Front Psychiatry*, 4: 52.

Larigot, L., L. Juricek, J. Dairou, and X. Coumoul. 2018. 'AhR signaling pathways and regulatory functions', *Biochim Open*, 7: 1-9.

Laskey, W. K., S. Yoon, N. Calzada, and M. J. Ricciardi. 2008. 'Concordant improvements in coronary flow reserve and ST-segment resolution during percutaneous coronary intervention for acute myocardial infarction: a benefit of postconditioning', *Catheter Cardiovasc Interv*, 72: 212-20.

Le Floc'h, N., W. Otten, and E. Merlot. 2011. 'Tryptophan metabolism, from nutrition to potential therapeutic applications', *Amino Acids*, 41: 1195-205.

Le Page, S., M. Niro, J. Fauconnier, L. Cellier, S. Tamareille, A. Gharib, A. Chevrollier, L. Loufrani, C. Grenier, R. Kamel, E. Sarzi, A. Lacampagne, M. Ovize, D. Henrion, P. Reynier, G. Lenaers, D. Mirebeau-Prunier, and F. Prunier. 2016. 'Increase in Cardiac Ischemia-Reperfusion Injuries in Opa1+/- Mouse Model', *PLoS One*, 11: e0164066.

Lecour, S., R. M. Smith, B. Woodward, L. H. Opie, L. Rochette, and M. N. Sack. 2002. 'Identification of a novel role for sphingolipid signaling in TNF alpha and ischemic preconditioning mediated cardioprotection', *J Mol Cell Cardiol*, 34: 509-18.

Lee, Y., H. Y. Lee, R. A. Hanna, and A. B. Gustafsson. 2011. 'Mitochondrial autophagy by Bnip3 involves Drp1-mediated mitochondrial fission and recruitment of Parkin in cardiac myocytes', *Am J Physiol Heart Circ Physiol*, 301: H1924-31.

Leib, S. L., Y. S. Kim, D. M. Ferriero, and M. G. Tauber. 1996. 'Neuroprotective effect of excitatory amino acid antagonist kynurenic acid in experimental bacterial meningitis', *J Infect Dis*, 173: 166-71.

Leipnitz, G., C. Schumacher, K. Scussiato, K. B. Dalcin, C. M. Wannmacher, A. T. Wyse, C. S. Dutra-Filho, M. Wajner, and A. Latini. 2005. 'Quinolinic acid reduces the antioxidant defenses in cerebral cortex of young rats', *Int J Dev Neurosci*, 23: 695-701.

Lesnefsky, E. J., T. I. Gudz, C. T. Migita, M. Ikeda-Saito, M. O. Hassan, P. J. Turkaly, and C. L. Hoppel. 2001. 'Ischemic injury to mitochondrial electron transport in the aging heart: damage to the iron-sulfur protein subunit of electron transport complex III', *Arch Biochem Biophys*, 385: 117-28.

Lesnefsky, E. J., B. Tandler, J. Ye, T. J. Slabe, J. Turkaly, and C. L. Hoppel. 1997. 'Myocardial ischemia decreases oxidative phosphorylation through cytochrome oxidase in subsarcolemmal mitochondria', *Am J Physiol*, 273: H1544-54.

Leung, J. C., B. R. Travis, J. W. Verlander, S. K. Sandhu, S. G. Yang, A. H. Zea, I. D. Weiner, and D. M. Silverstein. 2002. 'Expression and developmental regulation of the NMDA receptor subunits in the kidney and cardiovascular system', *Am J Physiol Regul Integr Comp Physiol*, 283: R964-71.

Li, Y., T. Liu, S. Liao, Y. Li, Y. Lan, A. Wang, Y. Wang, and B. He. 2015. 'A mini-review on Sirtuin activity assays', *Biochem Biophys Res Commun*, 467: 459-66.

Liesa, M., M. Palacin, and A. Zorzano. 2009. 'Mitochondrial dynamics in mammalian health and disease', *Physiol Rev*, 89: 799-845.

Lim, S. Y., and D. J. Hausenloy. 2012. 'Remote ischemic conditioning: from bench to bedside', *Front Physiol*, 3: 27.

Lim, W. Y., C. M. Messow, and C. Berry. 2012. 'Cyclosporin variably and inconsistently reduces infarct size in experimental models of reperfused myocardial infarction: a systematic review and meta-analysis', *Br J Pharmacol*, 165: 2034-43.

Liu, T., R. Yu, S. B. Jin, L. Han, U. Lendahl, J. Zhao, and M. Nister. 2013. 'The mitochondrial elongation factors MIEF1 and MIEF2 exert partially distinct functions in mitochondrial dynamics', *Exp Cell Res*, 319: 2893-904.

Liu, Z. Y., S. Hu, Q. W. Zhong, C. N. Tian, H. M. Ma, and J. J. Yu. 2017. 'N-Methyl-D-Aspartate Receptor-Driven Calcium Influx Potentiates the Adverse Effects of Myocardial Ischemia-Reperfusion Injury Ex Vivo', *J Cardiovasc Pharmacol*, 70: 329-38.

Low, F. N. 1956. 'Mitochondrial structure', *J Biophys Biochem Cytol*, 2: 337-40.

Lugo-Huitron, R., T. Blanco-Ayala, P. Ugalde-Muniz, P. Carrillo-Mora, J. Pedraza-Chaverri, D. Silva-Adaya, P. D. Maldonado, I. Torres, E. Pinzon, E. Ortiz-Islas, T. Lopez, E. Garcia, B. Pineda, M. Torres-Ramos, A. Santamaria, and V. P. La Cruz. 2011. 'On the antioxidant properties of

kynurenic acid: free radical scavenging activity and inhibition of oxidative stress', *Neurotoxicol Teratol*, 33: 538-47.

Luo, Y., H. Ma, J. J. Zhou, L. Li, S. R. Chen, J. Zhang, L. Chen, and H. L. Pan. 2018. 'Focal Cerebral Ischemia and Reperfusion Induce Brain Injury Through alpha2delta-1-Bound NMDA Receptors', *Stroke*, 49: 2464-72.

Ma, X. J., X. H. Zhang, C. M. Li, and M. Luo. 2006. 'Effect of postconditioning on coronary blood flow velocity and endothelial function in patients with acute myocardial infarction', *Scand Cardiovasc J*, 40: 327-33.

Mackenzie, A. E., J. E. Lappin, D. L. Taylor, S. A. Nicklin, and G. Milligan. 2011. 'GPR35 as a Novel Therapeutic Target', *Front Endocrinol (Lausanne)*, 2: 68.

Majlath, Z., J. Tajti, and L. Vecsei. 2013. 'Kynurenines and other novel therapeutic strategies in the treatment of dementia', *Ther Adv Neurol Disord*, 6: 386-97.

Majlath, Z., J. Toldi, and L. Vecsei. 2014. 'The potential role of kynurenines in Alzheimer's disease: pathomechanism and therapeutic possibilities by influencing the glutamate receptors', *J Neural Transm (Vienna)*, 121: 881-9.

Makino, A., J. Suarez, T. Gawlowski, W. Han, H. Wang, B. T. Scott, and W. H. Dillmann. 2011. 'Regulation of mitochondrial morphology and function by O-GlcNAcylation in neonatal cardiac myocytes', *Am J Physiol Regul Integr Comp Physiol*, 300: R1296-302.

Maroko, P. R., P. Libby, W. R. Ginks, C. M. Bloor, W. E. Shell, B. E. Sobel, and J. Ross, Jr. 1972. 'Coronary artery reperfusion. I. Early effects on local myocardial function and the extent of myocardial necrosis', *J Clin Invest*, 51: 2710-6.

Marsboom, G., P. T. Toth, J. J. Ryan, Z. Hong, X. Wu, Y. H. Fang, T. Thenappan, L. Piao, H. J. Zhang, J. Pogoriler, Y. Chen, E. Morrow, E. K. Weir, J. Rehman, and S. L. Archer. 2012. 'Dynamin-related protein 1-mediated mitochondrial mitotic fission permits hyperproliferation of vascular smooth muscle cells and offers a novel therapeutic target in pulmonary hypertension', *Circ Res*, 110: 1484-97.

Masini, E., S. Cuzzocrea, E. Mazzon, C. Marzocca, P. F. Mannaioni, and D. Salvemini. 2002. 'Protective effects of M40403, a selective superoxide dismutase mimetic, in myocardial ischaemia and reperfusion injury in vivo', *Br J Pharmacol*, 136: 905-17.

Matsuda, S., Y. Kitagishi, and M. Kobayashi. 2013. 'Function and characteristics of PINK1 in mitochondria', *Oxid Med Cell Longev*, 2013: 601587.

Matsui, Y., H. Takagi, X. Qu, M. Abdellatif, H. Sakoda, T. Asano, B. Levine, and J. Sadoshima. 2007. 'Distinct roles of autophagy in the heart during ischemia and reperfusion: roles of AMP-activated protein kinase and Beclin 1 in mediating autophagy', *Circ Res*, 100: 914-22.

Matsushima, S., and J. Sadoshima. 2015. 'The role of sirtuins in cardiac disease', *Am J Physiol Heart Circ Physiol*, 309: H1375-89.

Mauthe, M., I. Orhon, C. Rocchi, X. Zhou, M. Luhr, K. J. Hijlkema, R. P. Coppes, N. Engedal, M. Mari, and F. Reggiori. 2018. 'Chloroquine inhibits autophagic flux by decreasing autophagosome-lysosome fusion', *Autophagy*, 14: 1435-55.

McClanahan, T.B. & Nao, Brian & Wolke, L.J. & Martin, B.J. & Mertz, T.E. & Gallagher, K.P. 1993. 'Brief renal occlusion and reperfusion reduces myocardial infarct size in rabbits.', *FASEB J*.

Mei, Y., Y. Zhang, K. Yamamoto, W. Xie, T. W. Mak, and H. You. 2009. 'FOXO3a-dependent regulation of Pink1 (Park6) mediates survival signaling in response to cytokine deprivation', *Proc Natl Acad Sci U S A*, 106: 5153-8.

Menzies, R. A., and P. H. Gold. 1971. 'The turnover of mitochondria in a variety of tissues of young adult and aged rats', *J Biol Chem*, 246: 2425-9.

Merkwirth, C., and T. Langer. 2008. 'Mitofusin 2 builds a bridge between ER and mitochondria', *Cell*, 135: 1165-7.

Min, K. D., M. Asakura, Y. Liao, K. Nakamaru, H. Okazaki, T. Takahashi, K. Fujimoto, S. Ito, A. Takahashi, H. Asanuma, S. Yamazaki, T. Minamino, S. Sanada, O. Seguchi, A. Nakano, Y. Ando, T. Otsuka, H. Furukawa, T. Isomura, S. Takashima, N. Mochizuki, and M. Kitakaze. 2010. 'Identification of genes related to heart failure using global gene expression profiling of human failing myocardium', *Biochem Biophys Res Commun*, 393: 55-60.

Mizushima, N., and T. Yoshimori. 2007. 'How to interpret LC3 immunoblotting', *Autophagy*, 3: 542-5.

Monassier, L., E. Ayme-Dietrich, G. Aubertin-Kirch, and A. Pathak. 2016. 'Targeting myocardial reperfusion injuries with cyclosporine in the CIRCUS Trial - pharmacological reasons for failure', *Fundam Clin Pharmacol*, 30: 191-3.

Montrief, T., W. T. Davis, A. Koyfman, and B. Long. 2019. 'Mechanical, inflammatory, and embolic complications of myocardial infarction: An emergency medicine review', *Am J Emerg Med*, 37: 1175-83.

Moyzis, A. G., J. Sadoshima, and A. B. Gustafsson. 2015. 'Mending a broken heart: the role of mitophagy in cardioprotection', *Am J Physiol Heart Circ Physiol*, 308: H183-92.

Murphy, J. G., J. D. Marsh, and T. W. Smith. 1987. 'The role of calcium in ischemic myocardial injury', *Circulation*, 75: V15-24.

Murry, C. E., R. B. Jennings, and K. A. Reimer. 1986. 'Preconditioning with ischemia: a delay of lethal cell injury in ischemic myocardium', *Circulation*, 74: 1124-36.

Nadtochiy, S. M., H. Yao, M. W. McBurney, W. Gu, L. Guarente, I. Rahman, and P. S. Brookes. 2011. 'SIRT1-mediated acute cardioprotection', *Am J Physiol Heart Circ Physiol*, 301: H1506-12.

Nakamura, N., Y. Kimura, M. Tokuda, S. Honda, and S. Hirose. 2006. 'MARCH-V is a novel mitofusin 2- and Drp1-binding protein able to change mitochondrial morphology', *EMBO Rep*, 7: 1019-22.

Nath, M. C., and N. V. Shastri. 1970. 'Effect of acetoacetate on the activities of certain liver enzymes taking part in the tryptophan to nicotinic acid pathway in rats', *Enzymologia*, 38: 3-8.

Ndoye, A., and A. T. Weeraratna. 2016. 'Autophagy- An emerging target for melanoma therapy', *F1000Res*, 5.

Neubauer, S. 2007. 'The failing heart--an engine out of fuel', *N Engl J Med*, 356: 1140-51.

Nichols, M., N. Townsend, P. Scarborough, and M. Rayner. 2014. 'Cardiovascular disease in Europe 2014: epidemiological update', *Eur Heart J*, 35: 2950-9.

Niinisalo, P., A. Raitala, M. Pertovaara, S. S. Oja, T. Lehtimaki, M. Kahonen, A. Reunanen, A. Jula, L. Moilanen, Y. A. Kesaniemi, M. S. Nieminen, and M. Hurme. 2008. 'Indoleamine 2,3-dioxygenase activity associates with cardiovascular risk factors: the Health 2000 study', *Scand J Clin Lab Invest*, 68: 767-70.

Nishino, Y., T. Miura, T. Miki, J. Sakamoto, Y. Nakamura, Y. Ikeda, H. Kobayashi, and K. Shimamoto. 2004. 'Ischemic preconditioning activates AMPK in a PKC-dependent manner and induces GLUT4 up-regulation in the late phase of cardioprotection', *Cardiovasc Res*, 61: 610-9.

Noakes, R. 2015. 'The aryl hydrocarbon receptor: a review of its role in the physiology and pathology of the integument and its relationship to the tryptophan metabolism', *Int J Tryptophan Res*, 8: 7-18.

O'Dowd, B. F., T. Nguyen, A. Marchese, R. Cheng, K. R. Lynch, H. H. Heng, L. F. Kolakowski, Jr., and S. R. George. 1998. 'Discovery of three novel G-protein-coupled receptor genes', *Genomics*, 47: 310-3.

Oka, S., R. Ota, M. Shima, A. Yamashita, and T. Sugiura. 2010. 'GPR35 is a novel lysophosphatidic acid receptor', *Biochem Biophys Res Commun*, 395: 232-7.

Olenchock, B. A., J. Moslehi, A. H. Baik, S. M. Davidson, J. Williams, W. J. Gibson, A. A. Chakraborty, K. A. Pierce, C. M. Miller, E. A. Hanse, A. Kelekar, L. B. Sullivan, A. J. Wagers, C. B. Clish, M. G. Vander Heiden, and W. G. Kaelin, Jr. 2016. 'EGLN1 Inhibition and Rerouting of alpha-Ketoglutarate Suffice for Remote Ischemic Protection', *Cell*, 164: 884-95.

Ong, S. B., A. R. Hall, and D. J. Hausenloy. 2013. 'Mitochondrial dynamics in cardiovascular health and disease', *Antioxid Redox Signal*, 19: 400-14.

Ong, S. B., S. B. Kalkhoran, H. A. Cabrera-Fuentes, and D. J. Hausenloy. 2015. 'Mitochondrial fusion and fission proteins as novel therapeutic targets for treating cardiovascular disease', *Eur J Pharmacol*, 763: 104-14.

Ong, S. B., S. B. Kalkhoran, S. Hernandez-Resendiz, P. Samangouei, S. G. Ong, and D. J. Hausenloy. 2017. 'Mitochondrial-Shaping Proteins in Cardiac Health and Disease - the Long and the Short of It!', *Cardiovasc Drugs Ther*, 31: 87-107.

Ong, S. B., S. Subrayan, S. Y. Lim, D. M. Yellon, S. M. Davidson, and D. J. Hausenloy. 2010. 'Inhibiting mitochondrial fission protects the heart against ischemia/reperfusion injury', *Circulation*, 121: 2012-22.

Otera, H., C. Wang, M. M. Cleland, K. Setoguchi, S. Yokota, R. J. Youle, and K. Mihara. 2010. 'Mff is an essential factor for mitochondrial recruitment of Drp1 during mitochondrial fission in mammalian cells', *J Cell Biol*, 191: 1141-58.

Ovize, M., G. F. Baxter, F. Di Lisa, P. Ferdinandy, D. Garcia-Dorado, D. J. Hausenloy, G. Heusch, J. Vinten-Johansen, D. M. Yellon, R. Schulz, and Cardiology Working Group of Cellular Biology of Heart of European Society of. 2010. 'Postconditioning and protection from reperfusion injury: where do we stand? Position paper from the Working Group of Cellular Biology of the Heart of the European Society of Cardiology', *Cardiovasc Res*, 87: 406-23.

Palmer, C. S., L. D. Osellame, D. Laine, O. S. Koutsopoulos, A. E. Frazier, and M. T. Ryan. 2011. 'MiD49 and MiD51, new components of the mitochondrial fission machinery', *EMBO Rep*, 12: 565-73.

Papanicolaou, K. N., R. J. Khairallah, G. A. Ngoh, A. Chikando, I. Luptak, K. M. O'Shea, D. D. Riley, J. J. Lugus, W. S. Colucci, W. J. Lederer, W. C. Stanley, and K. Walsh. 2011. 'Mitofusin-2 maintains mitochondrial structure and contributes to stress-induced permeability transition in cardiac myocytes', *Mol Cell Biol*, 31: 1309-28.

Papanicolaou, K. N., G. A. Ngoh, E. R. Dabkowski, K. A. O'Connell, R. F. Ribeiro, Jr., W. C. Stanley, and K. Walsh. 2012. 'Cardiomyocyte deletion of mitofusin-1 leads to mitochondrial fragmentation and improves tolerance to ROS-induced mitochondrial dysfunction and cell death', *Am J Physiol Heart Circ Physiol*, 302: H167-79.

Pedersen, E. R., G. F. Svingen, H. Schartum-Hansen, P. M. Ueland, M. Ebbing, J. E. Nordrehaug, J. Igland, R. Seifert, R. M. Nilsen, and O. Nygard. 2013. 'Urinary excretion of kynurenine and tryptophan, cardiovascular events, and mortality after elective coronary angiography', *Eur Heart J*, 34: 2689-96.

Perez-Gonzalez, A., J. R. Alvarez-Idaboy, and A. Galano. 2015. 'Free-radical scavenging by tryptophan and its metabolites through electron transfer based processes', *J Mol Model*, 21: 213.

Perkins, M. N., J. F. Collins, and T. W. Stone. 1982. 'Isomers of 2-amino-7-phosphonoheptanoic acid as antagonists of neuronal excitants', *Neurosci Lett*, 32: 65-8.

Perkins, M. N., T. W. Stone, J. F. Collins, and K. Curry. 1981. 'Phosphonate analogues of carboxylic acids as aminoacid antagonists on rat cortical neurones', *Neurosci Lett*, 23: 333-6.

Phillips, R. S., E. C. Iradukunda, T. Hughes, and J. P. Bowen. 2019. 'Modulation of Enzyme Activity in the Kynurenine Pathway by Kynurenine Monooxygenase Inhibition', *Front Mol Biosci*, 6: 3.

Pillai, V. B., N. R. Sundaresan, G. Kim, M. Gupta, S. B. Rajamohan, J. B. Pillai, S. Samant, P. V. Ravindra, A. Isbatan, and M. P. Gupta. 2010. 'Exogenous NAD blocks cardiac hypertrophic response via activation of the SIRT3-LKB1-AMP-activated kinase pathway', *J Biol Chem*, 285: 3133-44.

Piper, H. M., D. Garcia-Dorado, and M. Ovize. 1998. 'A fresh look at reperfusion injury', *Cardiovasc Res*, 38: 291-300.

Piquereau, J., F. Caffin, M. Novotova, C. Lemaire, V. Veksler, A. Garnier, R. Ventura-Clapier, and F. Joubert. 2013. 'Mitochondrial dynamics in the adult cardiomyocytes: which roles for a highly specialized cell?', *Front Physiol*, 4: 102.

Piquereau, J., F. Caffin, M. Novotova, A. Prola, A. Garnier, P. Mateo, D. Fortin, H. Huynh le, V. Nicolas, M. V. Alavi, C. Brenner, R. Ventura-Clapier, V. Veksler, and F. Joubert. 2012. 'Down-regulation of OPA1 alters mouse mitochondrial morphology, PTP function, and cardiac adaptation to pressure overload', *Cardiovasc Res*, 94: 408-17.

Prunier, F., R. Gaertner, L. Louedec, J. B. Michel, J. J. Mercadier, and B. Escoubet. 2002. 'Doppler echocardiographic estimation of left ventricular end-diastolic pressure after MI in rats', *Am J Physiol Heart Circ Physiol*, 283: H346-52.

Przyklenk, K., B. Bauer, M. Ovize, R. A. Kloner, and P. Whittaker. 1993. 'Regional ischemic 'preconditioning' protects remote virgin myocardium from subsequent sustained coronary occlusion', *Circulation*, 87: 893-9.

Reimer, K. A., J. E. Lowe, M. M. Rasmussen, and R. B. Jennings. 1977. 'The wavefront phenomenon of ischemic cell death. 1. Myocardial infarct size vs duration of coronary occlusion in dogs', *Circulation*, 56: 786-94.

Ristagno, G., M. Fries, L. Brunelli, F. Fumagalli, R. Bagnati, I. Russo, L. Staszewsky, S. Masson, G. Li Volti, A. Zappala, M. Derwall, A. Brucken, R. Pastorelli, and R. Latini. 2013. 'Early kynurenine pathway activation following cardiac arrest in rats, pigs, and humans', *Resuscitation*, 84: 1604-10.

Rodriguez-Martinez, E., A. Camacho, P. D. Maldonado, J. Pedraza-Chaverri, D. Santamaria, S. Galvan-Arzate, and A. Santamaria. 2000. 'Effect of quinolinic acid on endogenous antioxidants in rat corpus striatum', *Brain Res*, 858: 436-9.

Rodriguez, E., M. Mendez-Armenta, J. Villeda-Hernandez, S. Galvan-Arzate, R. Barroso-Moguel, F. Rodriguez, C. Rios, and A. Santamaria. 1999. 'Dapsone prevents morphological lesions and lipid peroxidation induced by quinolinic acid in rat corpus striatum', *Toxicology*, 139: 111-8.

Ronkainen, V. P., T. Tuomainen, J. Huusko, S. Laidinen, M. Malinen, J. J. Palvimo, S. Yla-Herttuala, O. Vuolteenaho, and P. Tavi. 2014. 'Hypoxia-inducible factor 1-induced G protein-coupled receptor 35 expression is an early marker of progressive cardiac remodelling', *Cardiovasc Res*, 101: 69-77.

Ronnebaum, S. M., and C. Patterson. 2010. 'The FoxO family in cardiac function and dysfunction', *Annu Rev Physiol*, 72: 81-94.

Rossi, F., R. Miggiano, D. M. Ferraris, and M. Rizzi. 2019. 'The Synthesis of Kynurenic Acid in Mammals: An Updated Kynurenine Aminotransferase Structural KATalogue', *Front Mol Biosci*, 6: 7.

Roucher, P., P. Meric, J. L. Correze, J. Mispelter, B. Tiffon, J. M. Lhoste, and J. Seylaz. 1991. 'Metabolic effects of kynurenate during reversible forebrain ischemia studied by in vivo 31P-nuclear magnetic resonance spectroscopy', *Brain Res*, 550: 54-60.

Rouslin, W. 1983. 'Mitochondrial complexes I, II, III, IV, and V in myocardial ischemia and autolysis', *Am J Physiol*, 244: H743-8.

Rozsa, E., H. Robotka, L. Vecsei, and J. Toldi. 2008. 'The Janus-face kynurenic acid', *J Neural Transm (Vienna)*, 115: 1087-91.

Saks, V. A., V. I. Veksler, A. V. Kuznetsov, L. Kay, P. Sikk, T. Tiivel, L. Tranqui, J. Olivares, K. Winkler, F. Wiedemann, and W. S. Kunz. 1998. 'Permeabilized cell and skinned fiber techniques in studies of mitochondrial function in vivo', *Mol Cell Biochem*, 184: 81-100.

Samant, S. A., H. J. Zhang, Z. Hong, V. B. Pillai, N. R. Sundaresan, D. Wolfgeher, S. L. Archer, D. C. Chan, and M. P. Gupta. 2014. 'SIRT3 deacetylates and activates OPA1 to regulate mitochondrial dynamics during stress', *Mol Cell Biol*, 34: 807-19.

Santamaria, A., M. E. Jimenez-Capdeville, A. Camacho, E. Rodriguez-Martinez, A. Flores, and S. Galvan-Arzate. 2001. 'In vivo hydroxyl radical formation after quinolinic acid infusion into rat corpus striatum', *Neuroreport*, 12: 2693-6.

Santel, A., and M. T. Fuller. 2001. 'Control of mitochondrial morphology by a human mitofusin', *J Cell Sci*, 114: 867-74.

Sas, K., E. Szabo, and L. Vecsei. 2018. 'Mitochondria, Oxidative Stress and the Kynurenine System, with a Focus on Ageing and Neuroprotection', *Molecules*, 23.

Schaper, J., E. Meiser, and G. Stammler. 1985. 'Ultrastructural morphometric analysis of myocardium from dogs, rats, hamsters, mice, and from human hearts', *Circ Res*, 56: 377-91.

Schwarcz, R., J. P. Bruno, P. J. Muchowski, and H. Q. Wu. 2012. 'Kynurenines in the mammalian brain: when physiology meets pathology', *Nat Rev Neurosci*, 13: 465-77.

Sebastian, D., E. Sorianello, J. Segales, A. Irazoki, V. Ruiz-Bonilla, D. Sala, E. Planet, A. Berenguer-Llergo, J. P. Munoz, M. Sanchez-Feutrie, N. Plana, M. I. Hernandez-Alvarez, A. L. Serrano, M. Palacin, and A. Zorzano. 2016. 'Mfn2 deficiency links age-related sarcopenia and impaired autophagy to activation of an adaptive mitophagy pathway', *EMBO J*, 35: 1677-93.

Shalwala, M., S. G. Zhu, A. Das, F. N. Salloum, L. Xi, and R. C. Kukreja. 2014. 'Sirtuin 1 (SIRT1) activation mediates sildenafil induced delayed cardioprotection against ischemia-reperfusion injury in mice', *PLoS One*, 9: e86977.

Sharp, W. W., Y. H. Fang, M. Han, H. J. Zhang, Z. Hong, A. Banathy, E. Morrow, J. J. Ryan, and S. L. Archer. 2014. 'Dynamin-related protein 1 (Drp1)-mediated diastolic dysfunction in myocardial ischemia-reperfusion injury: therapeutic benefits of Drp1 inhibition to reduce mitochondrial fission', *FASEB J*, 28: 316-26.

Shimizu, M., M. Tropak, R. J. Diaz, F. Suto, H. Surendra, E. Kuzmin, J. Li, G. Gross, G. J. Wilson, J. Callahan, and A. N. Redington. 2009. 'Transient limb ischaemia remotely preconditions through a humoral mechanism acting directly on the myocardium: evidence suggesting cross-species protection', *Clin Sci (Lond)*, 117: 191-200.

Shirakabe, A., P. Zhai, Y. Ikeda, T. Saito, Y. Maejima, C. P. Hsu, M. Nomura, K. Egashira, B. Levine, and J. Sadoshima. 2016. 'Drp1-Dependent Mitochondrial Autophagy Plays a Protective Role Against Pressure Overload-Induced Mitochondrial Dysfunction and Heart Failure', *Circulation*, 133: 1249-63.

Sloth, A. D., M. R. Schmidt, K. Munk, R. K. Kharbanda, A. N. Redington, M. Schmidt, L. Pedersen, H. T. Sorensen, H. E. Botker, and Condi Investigators. 2014. 'Improved long-term clinical outcomes in patients with ST-elevation myocardial infarction undergoing remote ischaemic conditioning as an adjunct to primary percutaneous coronary intervention', *Eur Heart J*, 35: 168-75.

Smirnova, E., D. L. Shurland, S. N. Ryazantsev, and A. M. van der Bliek. 1998. 'A human dynamin-related protein controls the distribution of mitochondria', *J Cell Biol*, 143: 351-8.

Smith, R. M., N. Suleman, L. Lacerda, L. H. Opie, S. Akira, K. R. Chien, and M. N. Sack. 2004. 'Genetic depletion of cardiac myocyte STAT-3 abolishes classical preconditioning', *Cardiovasc Res*, 63: 611-6.

Song, M., A. Franco, J. A. Fleischer, L. Zhang, and G. W. Dorn, 2nd. 2017. 'Abrogating Mitochondrial Dynamics in Mouse Hearts Accelerates Mitochondrial Senescence', *Cell Metab*, 26: 872-83 e5.

Song, M., K. Mihara, Y. Chen, L. Scorrano, and G. W. Dorn, 2nd. 2015. 'Mitochondrial fission and fusion factors reciprocally orchestrate mitophagic culling in mouse hearts and cultured fibroblasts', *Cell Metab*, 21: 273-86.

Spiegel, R., A. Saada, P. J. Flannery, F. Burte, D. Soiferman, M. Khayat, V. Eisner, E. Vladovski, R. W. Taylor, L. A. Bindoff, A. Shaag, H. Mandel, O. Schuler-Furman, S. A. Shalev, O. Elpeleg, and P. Yu-Wai-Man. 2016. 'Fatal infantile mitochondrial encephalomyopathy, hypertrophic cardiomyopathy and optic atrophy associated with a homozygous OPA1 mutation', *J Med Genet*, 53: 127-31.

Staat, P., G. Rioufol, C. Piot, Y. Cottin, T. T. Cung, I. L'Huillier, J. F. Aupetit, E. Bonnefoy, G. Finet, X. Andre-Fouet, and M. Ovize. 2005. 'Postconditioning the human heart', *Circulation*, 112: 2143-8.

Stazka, J., P. Luchowski, M. Wielosz, Z. Kleinrok, and E. M. Urbanska. 2002. 'Endothelium-dependent production and liberation of kynurenic acid by rat aortic rings exposed to L-kynurenine', *Eur J Pharmacol*, 448: 133-7.

Stone, T. W., and L. G. Darlington. 2002. 'Endogenous kynurenines as targets for drug discovery and development', *Nat Rev Drug Discov*, 1: 609-20.

———. 2013. 'The kynurenine pathway as a therapeutic target in cognitive and neurodegenerative disorders', *Br J Pharmacol*, 169: 1211-27.

Stone, T. W., M. N. Perkins, J. F. Collins, and K. Curry. 1981. 'Activity of the enantiomers of 2-amino-5-phosphono-valeric acid as stereospecific antagonists of excitatory aminoacids', *Neuroscience*, 6: 2249-52.

Sun, M. S., H. Jin, X. Sun, S. Huang, F. L. Zhang, Z. N. Guo, and Y. Yang. 2018. 'Free Radical Damage in Ischemia-Reperfusion Injury: An Obstacle in Acute Ischemic Stroke after Revascularization Therapy', *Oxid Med Cell Longev*, 2018: 3804979.

Sundaresan, N. R., M. Gupta, G. Kim, S. B. Rajamohan, A. Isbatan, and M. P. Gupta. 2009. 'Sirt3 blocks the cardiac hypertrophic response by augmenting Foxo3a-dependent antioxidant defense mechanisms in mice', *J Clin Invest*, 119: 2758-71.

Szijarto, A., Z. Czigany, Z. Turoczi, and L. Harsanyi. 2012. 'Remote ischemic perconditioning--a simple, low-risk method to decrease ischemic reperfusion injury: models, protocols and mechanistic background. A review', *J Surg Res*, 178: 797-806.

Taguchi, N., N. Ishihara, A. Jofuku, T. Oka, and K. Mihara. 2007. 'Mitotic phosphorylation of dynamin-related GTPase Drp1 participates in mitochondrial fission', *J Biol Chem*, 282: 11521-9.

Tamareille, S., V. Mateus, N. Ghaboura, J. Jeanneteau, A. Croue, D. Henrion, A. Furber, and F. Prunier. 2011. 'RISK and SAFE signaling pathway interactions in remote limb ischemic perconditioning in combination with local ischemic postconditioning', *Basic Res Cardiol*, 106: 1329-39.

Tan, L., J. T. Yu, and L. Tan. 2012. 'The kynurenine pathway in neurodegenerative diseases: mechanistic and therapeutic considerations', *J Neurol Sci*, 323: 1-8.

Thevandavakkam, M. A., R. Schwarcz, P. J. Muchowski, and F. Giorgini. 2010. 'Targeting kynurenine 3-monooxygenase (KMO): implications for therapy in Huntington's disease', *CNS Neurol Disord Drug Targets*, 9: 791-800.

Thibault, H., C. Piot, P. Staat, L. Bontemps, C. Sportouch, G. Rioufol, T. T. Cung, E. Bonnefoy, D. Angoulvant, J. F. Aupetit, G. Finet, X. Andre-Fouet, J. C. Macia, F. Raczka, R. Rossi, R. Itti, G. Kirkorian, G. Derumeaux, and M. Ovize. 2008. 'Long-term benefit of postconditioning', *Circulation*, 117: 1037-44.

Tilokani, L., S. Nagashima, V. Paupe, and J. Prudent. 2018. 'Mitochondrial dynamics: overview of molecular mechanisms', *Essays Biochem*, 62: 341-60.

Truban, D., X. Hou, T. R. Caulfield, F. C. Fiesel, and W. Springer. 2017. 'PINK1, Parkin, and Mitochondrial Quality Control: What can we Learn about Parkinson's Disease Pathobiology?', *J Parkinsons Dis*, 7: 13-29.

Turski, W. A., J. B. Gramsbergen, H. Traitler, and R. Schwarcz. 1989. 'Rat brain slices produce and liberate kynurenic acid upon exposure to L-kynurenine', *J Neurochem*, 52: 1629-36.

Varanita, T., M. E. Soriano, V. Romanello, T. Zaglia, R. Quintana-Cabrera, M. Semenzato, R. Menabo, V. Costa, G. Civiletto, P. Pesce, C. Viscomi, M. Zeviani, F. Di Lisa, M. Mongillo, M. Sandri, and L. Scorrano. 2015. 'The OPA1-dependent mitochondrial cristae remodeling pathway controls atrophic, apoptotic, and ischemic tissue damage', *Cell Metab*, 21: 834-44.

Varma, C., and S. Brecker. 2001. 'Predictors of mortality in acute myocardial infarction', *Lancet*, 358: 1473-4.

Vasquez-Trincado, C., I. Garcia-Carvajal, C. Pennanen, V. Parra, J. A. Hill, B. A. Rothermel, and S. Lavandero. 2016. 'Mitochondrial dynamics, mitophagy and cardiovascular disease', *J Physiol*, 594: 509-25.

Vecsei, L., L. Szalardy, F. Fulop, and J. Toldi. 2013. 'Kynurenines in the CNS: recent advances and new questions', *Nat Rev Drug Discov*, 12: 64-82.

Wai, T., J. Garcia-Prieto, M. J. Baker, C. Merkwirth, P. Benit, P. Rustin, F. J. Ruperez, C. Barbas, B. Ibanez, and T. Langer. 2015. 'Imbalanced OPA1 processing and mitochondrial fragmentation cause heart failure in mice', *Science*, 350: aad0116.

Wai, T., and T. Langer. 2016. 'Mitochondrial Dynamics and Metabolic Regulation', *Trends Endocrinol Metab*, 27: 105-17.

Wakabayashi, J., Z. Zhang, N. Wakabayashi, Y. Tamura, M. Fukaya, T. W. Kensler, M. Iijima, and H. Sesaki. 2009. 'The dynamin-related GTPase Drp1 is required for embryonic and brain development in mice', *J Cell Biol*, 186: 805-16.

Walczak, K., W. A. Turski, and G. Rajtar. 2014. 'Kynurenic acid inhibits colon cancer proliferation in vitro: effects on signaling pathways', *Amino Acids*, 46: 2393-401.

Walker, M. A., and R. Tian. 2018. 'Raising NAD in Heart Failure: Time to Translate?', *Circulation*, 137: 2274-77.

Wang, B., and A. Xu. 2019. 'Aryl hydrocarbon receptor pathway participates in myocardial ischemia reperfusion injury by regulating mitochondrial apoptosis', *Med Hypotheses*, 123: 2-5.

Wang, H., P. Song, L. Du, W. Tian, W. Yue, M. Liu, D. Li, B. Wang, Y. Zhu, C. Cao, J. Zhou, and Q. Chen. 2011. 'Parkin ubiquitinates Drp1 for proteasome-dependent degradation: implication of dysregulated mitochondrial dynamics in Parkinson disease', *J Biol Chem*, 286: 11649-58.

Wang, J., N. Simonavicius, X. Wu, G. Swaminath, J. Reagan, H. Tian, and L. Ling. 2006. 'Kynurenic acid as a ligand for orphan G protein-coupled receptor GPR35', *J Biol Chem*, 281: 22021-8.

Wang, Q., D. Liu, P. Song, and M. H. Zou. 2015. 'Tryptophan-kynurenine pathway is dysregulated in inflammation, and immune activation', *Front Biosci (Landmark Ed)*, 20: 1116-43.

Wang, X. D., F. M. Notarangelo, J. Z. Wang, and R. Schwarcz. 2012. 'Kynurenic acid and 3-hydroxykynurenine production from D-kynurenine in mice', *Brain Res*, 1455: 1-9.

Wang, X., S. Hu, and L. Liu. 2017. 'Phosphorylation and acetylation modifications of FOXO3a: Independently or synergistically?', *Oncol Lett*, 13: 2867-72.

Wang, X. X., X. L. Wang, M. M. Tong, L. Gan, H. Chen, S. S. Wu, J. X. Chen, R. L. Li, Y. Wu, H. Y. Zhang, Y. Zhu, Y. X. Li, J. H. He, M. Wang, and W. Jiang. 2016. 'SIRT6 protects cardiomyocytes against ischemia/reperfusion injury by augmenting FoxO3alpha-dependent antioxidant defense mechanisms', *Basic Res Cardiol*, 111: 13.

Wang, Y., R. Branicky, A. Noe, and S. Hekimi. 2018. 'Superoxide dismutases: Dual roles in controlling ROS damage and regulating ROS signaling', *J Cell Biol*, 217: 1915-28.

Waterham, H. R., J. Koster, C. W. van Roermund, P. A. Mooyer, R. J. Wanders, and J. V. Leonard. 2007. 'A lethal defect of mitochondrial and peroxisomal fission', *N Engl J Med*, 356: 1736-41.

Wei, H., G. Fiskum, R. E. Rosenthal, and D. C. Perry. 1997. 'Global cerebral ischemia and reperfusion alters NMDA receptor binding in canine brain', *Mol Chem Neuropathol*, 30: 25-39.

Wilding, J. R., F. Joubert, C. de Araujo, D. Fortin, M. Novotova, V. Veksler, and R. Ventura-Clapier. 2006. 'Altered energy transfer from mitochondria to sarcoplasmic reticulum after cytoarchitectural perturbations in mice hearts', *J Physiol*, 575: 191-200.

Wirthgen, E., A. Hoeflich, A. Rebl, and J. Gunther. 2017. 'Kynurenic Acid: The Janus-Faced Role of an Immunomodulatory Tryptophan Metabolite and Its Link to Pathological Conditions', *Front Immunol*, 8: 1957.

Yamamoto, T., J. Byun, P. Zhai, Y. Ikeda, S. Oka, and J. Sadoshima. 2014. 'Nicotinamide mononucleotide, an intermediate of NAD+ synthesis, protects the heart from ischemia and reperfusion', *PLoS One*, 9: e98972.

Yang, J. Y., and M. C. Hung. 2009. 'A new fork for clinical application: targeting forkhead transcription factors in cancer', *Clin Cancer Res*, 15: 752-7.

Yang, X. C., Y. Liu, L. F. Wang, L. Cui, T. Wang, Y. G. Ge, H. S. Wang, W. M. Li, L. Xu, Z. H. Ni, S. H. Liu, L. Zhang, H. M. Jia, J. Vinten-Johansen, and Z. Q. Zhao. 2007. 'Reduction in myocardial infarct size by postconditioning in patients after percutaneous coronary intervention', *J Invasive Cardiol*, 19: 424-30.

Yang, Y., and A. A. Sauve. 2016. 'NAD(+) metabolism: Bioenergetics, signaling and manipulation for therapy', *Biochim Biophys Acta*, 1864: 1787-800.

Yellon, D. M., and G. F. Baxter. 1999. 'Reperfusion injury revisited: is there a role for growth factor signaling in limiting lethal reperfusion injury?', *Trends Cardiovasc Med*, 9: 245-9.

Yellon, D. M., and D. J. Hausenloy. 2007. 'Myocardial reperfusion injury', *N Engl J Med*, 357: 1121-35.

Yingzhong, C., C. Lin, and W. Chunbin. 2016. 'Clinical effects of cyclosporine A on reperfusion injury in myocardial infarction: a meta-analysis of randomized controlled trials', *Springerplus*, 5: 1117.

Yonashiro, R., S. Ishido, S. Kyo, T. Fukuda, E. Goto, Y. Matsuki, M. Ohmura-Hoshino, K. Sada, H. Hotta, H. Yamamura, R. Inatome, and S. Yanagi. 2006. 'A novel mitochondrial ubiquitin ligase plays a critical role in mitochondrial dynamics', *EMBO J*, 25: 3618-26.

Youle, R. J., and A. M. van der Bliek. 2012. 'Mitochondrial fission, fusion, and stress', *Science*, 337: 1062-5.

Youn, H. S., T. G. Kim, M. K. Kim, G. B. Kang, J. Y. Kang, J. G. Lee, J. Y. An, K. R. Park, Y. Lee, Y. J. Im, J. H. Lee, and S. H. Eom. 2016. 'Structural Insights into the Quaternary Catalytic Mechanism of Hexameric Human Quinolinate Phosphoribosyltransferase, a Key Enzyme in de novo NAD Biosynthesis', *Sci Rep*, 6: 19681.

Yu, W., B. Gao, N. Li, J. Wang, C. Qiu, G. Zhang, M. Liu, R. Zhang, C. Li, G. Ji, and Y. Zhang. 2017. 'Sirt3 deficiency exacerbates diabetic cardiac dysfunction: Role of Foxo3A-Parkin-mediated mitophagy', *Biochim Biophys Acta Mol Basis Dis*, 1863: 1973-83.

Yung, M. M., D. W. Chan, V. W. Liu, K. M. Yao, and H. Y. Ngan. 2013. 'Activation of AMPK inhibits cervical cancer cell growth through AKT/FOXO3a/FOXM1 signaling cascade', *BMC Cancer*, 13: 327.

Zhang, H., P. Wang, S. Bisetto, Y. Yoon, Q. Chen, S. S. Sheu, and W. Wang. 2017. 'A novel fission-independent role of dynamin-related protein 1 in cardiac mitochondrial respiration', *Cardiovasc Res*, 113: 160-70.

Zhang, J., X. Wang, V. Vikash, Q. Ye, D. Wu, Y. Liu, and W. Dong. 2016. 'ROS and ROS-Mediated Cellular Signaling', *Oxid Med Cell Longev*, 2016: 4350965.

Zhao, P., H. Sharir, A. Kapur, A. Cowan, E. B. Geller, M. W. Adler, H. H. Seltzman, P. H. Reggio, S. Heynen-Genel, M. Sauer, T. D. Chung, Y. Bai, W. Chen, M. G. Caron, L. S. Barak, and M. E. Abood. 2010. 'Targeting of the orphan receptor GPR35 by pamoic acid: a potent activator of extracellular signal-regulated kinase and beta-arrestin2 with antinociceptive activity', *Mol Pharmacol*, 78: 560-8.

Zhao, T., X. Huang, L. Han, X. Wang, H. Cheng, Y. Zhao, Q. Chen, J. Chen, H. Cheng, R. Xiao, and M. Zheng. 2012. 'Central role of mitofusin 2 in autophagosome-lysosome fusion in cardiomyocytes', *J Biol Chem*, 287: 23615-25.

Zhao, Z. Q., J. S. Corvera, M. E. Halkos, F. Kerendi, N. P. Wang, R. A. Guyton, and J. Vinten-Johansen. 2003. 'Inhibition of myocardial injury by ischemic postconditioning during reperfusion: comparison with ischemic preconditioning', *Am J Physiol Heart Circ Physiol*, 285: H579-88.

Zweier, J. L. 1988. 'Measurement of superoxide-derived free radicals in the reperfused heart. Evidence for a free radical mechanism of reperfusion injury', *J Biol Chem*, 263: 1353-7.

UNIVERSITE BIOLOGIE BRETAGNE SANTE LOIRE

université angers

Titre : Implication de la dynamique mitochondriale et de la voie de la kynurénine dans la cardioprotection au cours de l'infarctus du myocarde

Mots clés : ischémie/reperfusion myocardique, cardioprotection, dynamique mitochondriale, kynurénine, acide kynurénique

Résumé : L'infarctus du myocarde reste une des principales causes de mortalité dans les pays développés. Bien que la reperfusion soit indispensable au sauvetage du myocarde ischémique, la taille finale de l'infarctus est due à la fois aux lésions d'ischémie mais aussi de reperfusion. La cardioprotection consiste à activer des voies de signalisation endogène de protection pour réduire les lésions d'ischémie/reperfusion (I/R). Il a été montré que la fission mitochondriale augmentait après une ischémie. Nous avons donc étudié l'impact d'un déficit en protéine de la dynamique mitochondriale dans des modèles de souris. Les souris DRP1$^{+/-}$ déficientes en fission mitochondriale présentaient un infarctus d'une taille réduite par rapport aux souris WT, réduction potentiellement liée à une augmentation de la mitophagie. Une déficience simultanée en protéines de fusion et de fission mitochondriales (Drp1$^{+/-}$ Opa1$^{+/-}$) n'a pas d'influence sur la morphologie et la fonction cardiaque à l'état basal. De plus, Les souris Drp1$^{+/-}$ Opa1$^{+/-}$ présentaient une taille d'infarctus comparable à celle des souris WT. Ensuite, nous avons montré l'importance de la voie de la kynurénine dans la cardioprotection. Une étude récente menée dans notre laboratoire a montré que la kynurénine était augmentée après un conditionnement ischémique à distance. La kynurénine est un métabolite de la voie de la kynurénine, la principale voie de dégradation du tryptophane. Nous avons montré que la kynurénine et l'acide kynurénique, un sous-produit de la kynurénine, pouvaient médier une cardioprotection dans un modèle d'I/R myocardique chez le rat. La cardioprotection était associée à la stimulation de la mitophagie et du système de défense anti-oxydant. Cependant, une meilleure compréhension des voies de signalisation associées à la cardioprotection est nécessaire pour pouvoir identifier des cibles thérapeutiques.

Title: Implication of mitochondrial dynamics and kynurenine pathway in cardioprotection after myocardial infarction

Keywords : myocardial ischemia/reperfusion, cardioprotection, mitochondrial dynamics, kynurenine, Kynurenic acid

Abstract: Myocardial infarction remains a leading cause of mortality in developed countries. Although timely reperfusion is indispensable for ischemic myocardium salvage, final infarct size is due to both ischemia and reperfusion injuries. Cardioprotection consists of activating endogenous signaling protective pathways to decrease ischemia/reperfusion (I/R) injuries. Mitochondrial fission has been shown increased after ischemia, thus we studied the impact of mitochondrial dynamics proteins deficiency in mice models. Mitochondrial fission deficient DRP1$^{+/-}$ mice, exhibited a smaller infarct size compared to WT due to a potential increase in mitophagy. Simultaneous deficiency in mitochondrial fusion and fission proteins (*Drp1$^{+/-}$ Opa1$^{+/-}$*) did not influence cardiac morphology and function at baseline and infarct size was comparable to WT. Next, We showed an importance of kynurenine pathway in cardioprotection. A recent study conducted in our laboratory showed that kynurenine, was increased after remote ischemic conditioning. Kynurenine is a metabolite of the kynurenine pathway which is the main tryptophan degradation route. We showed that kynurenine and kynurenic acid, a byproduct of kynurenine, mediated cardioprotection in a rat myocardial I/R model. Cardioprotection was associated to stimulation of mitophagy and anti-oxidant defense system. However a better understanding of associated signaling pathways is necessary to identify therapeutic targets.